The paraventricular nucleus of the thalamus:

a hub in the neural network for fear and anxiety

By

Xinwen Dong

A thesis submitted to the Faculty of Graduate Studies of

The University of Manitoba

In partial fulfillment of the requirements of the degree of

DOCTOR OF PHILOSOPHY

Department of Oral Biology

Dr. Gerald Niznick College of Dentistry

Rady Faculty of Health Science

University of Manitoba

Winnipeg, Manitoba

Abstract

The paraventricular nucleus of the thalamus (PVT) is a part of a group of the midline and intralaminar thalamic nuclei. The PVT receives and sends projections to brain regions essential for fear and anxiety indicating that the PVT may be a critical hub in the brain's fear and anxiety network. This thesis presents a series of studies investigating the involvement of the PVT and its projection in fear and anxiety. The first study showed that lesions of the PVT attenuated the expression of conditioned fear while blocking orexin receptors in the PVT had no effect on fear but reduced anxiety. These findings can be potentially viewed as evidence that the PVT regulates different defensive responses independently via unique groups of neurons that project to different basal forebrain nuclei. The second study used a dual-retrograde-tracing strategy to determine whether the PVT contains distinct subpopulations of neurons that project to the shell of the nucleus accumbens (NAcSh), the dorsolateral part of the bed nucleus of the stria terminalis (BSTDL), and the lateral part of the central nucleus of the amygdala (CeL). This study revealed that most neurons in the PVT innervate the NAcSh and that many neurons project to more than one brain region. In addition, PVT neurons that project to the NAcSh, BSTDL, or CeL did not appear to be activated differentially when rats were exposed to footshocks or an open field. The third study examined the involvement of the PVT-NAcSh projection in fear and anxiety using an intersectional chemogenetic technique. The result showed that selective inhibition of PVT neurons that innervate NAcSh reduced footshock-induced social anxiety but not conditioned fear in stress-susceptible rats. In summary, studies in this thesis demonstrate that the PVT contributes to conditioned fear and stress-induced anxiety and point to the possibility that the PVT may coordinate defensive responses by acting on the NAcSh, BSTDL, and CeL.

Acknowledgements

I would like to thank my mentor and thesis advisor Dr. Gilbert Kirouac for his kindly support and patient guidance for my experiments and thesis and his generous support for my attendance in international conferences. His knowledge and work ethics have also influenced me deeply.

I would like to thank my committee members Dr. Rajinder Bhullar, Dr. Jean-Eric Ghia, and Dr. Michael Jackson for their guidance and comments. I would like to thank my external examiner Dr. Gavan McNally for reviewing my thesis and his comments and questions at the oral examination.

I would like to thank Dr. Sa Li for her help for my experiments. She provided me patient guidance in stereotaxic surgery and many other techniques. I would like to thank Dr. Yonghui Li for his support and encouragement. Experiments in Chapter 2 were done under the guidance of Dr. Yonghui Li and Dr. Kirouac. Dr. Yonghui Li and Dr. Sa Li completed most of the work of *Experiment 1* in Chapter 2. Dr. Yonghui Li is the primary author of the paper for that experiment.

I would like to thank my previous lab member and roommate Dr. Huiying Wang for her help for my experiments. I would like to thank the people in the Department of Oral Biology and Central Animal Care Services in University of Manitoba and Institute of Psychology in Chinese Academy of Sciences for their help and support. I would also like to thank Research Manitoba for offering me two terms of Graduate Studentship.

I would like to thank my friends in Winnipeg and Beijing for their help and encouragement. I would like to thank my parents for their love and support.

Dedication

To the rats used and sacrificed for the experiments that were done to complete the research that makes up this thesis.

Publications and Contributions

Li, Y., Dong, X., Li, S., & Kirouac, G. J. (2014). Lesions of the posterior paraventricular nucleus of the thalamus attenuate fear expression. Frontiers in Behavioral Neuroscience, 8(March), 94. https://doi.org/10.3389/fnbeh.2014.00094

Y. Li and G. Kirouac designed research; Y. Li, S. Li, X. Dong performed experiments; Y. Li, S. Li and G. Kirouac analyzed data; Y. Li and G. Kirouac wrote the paper. This work was supported by the Canadian Institutes of Health Research (CIHR; MOP89758 to Gilbert J. Kirouac); Natural Sciences and Engineering Council of Canada (NSERC; 261739- 2008 to GJK); Chinese Academy of Sciences (KSCX2-EW-Q-18, KJ2D-EW-L04 to YL); and the National Natural Science Foundation (31070911 to YL).

Dong, X., Li, Y., & Kirouac, G. J. (2015). Blocking of orexin receptors in the paraventricular nucleus of the thalamus has no effect on the expression of conditioned fear in rats. Frontiers in Behavioral Neuroscience, 9(June), 161. https://doi.org/10.3389/fnbeh.2015.00161

X. Dong, Y. Li and G. Kirouac designed the research; X. Dong performed experiments; X. Dong, Y. Li and G. Kirouac analyzed data; X. Dong and G. Kirouac wrote the paper. This work was supported by the Canadian Institutes of Health Research (CIHR; MOP89758 to GJK); and the National Key Technology Research and Development Program of China (2013BAI08B02 to YL).

Dong, X., Li, S., & Kirouac, G. J. (2017). Collateralization of projections from the paraventricular nucleus of the thalamus to the nucleus accumbens, bed nucleus of the stria terminalis, and central nucleus of the amygdala. Brain Structure and Function, 222(9), 3927–3943. https://doi.org/10.1007/s00429-017-1445-8

X. Dong, S. Li and G. Kirouac designed research; X. Dong and S. Li performed the experiment; X. Dong, S. Li and G. Kirouac analyzed data; X. Dong and G. Kirouac wrote the paper. This work was supported by the Canadian Institutes of Health Research (CIHR; MOP89758 to GJK).

Table of Contents

List of Figures

List of Tables

Abbreviations

AAV	adeno-associated virus
ANOVA	analysis of variance
BLA	basolateral nucleus of amygdala
BST	bed nucleus of stria terminalis
BSTDL	bed nucleus of stria terminalis, dorsolateral
CART	cocaine- and amphetamine-related transcript
CeC	central nucleus of amygdala, capsular
CeL	central nucleus of amygdala, lateral
CeM	central nucleus of amygdala, medial
CR	conditioned response
CRF	corticotropin releasing factor
CS	conditioned stimulus
CTb	cholera toxin subunit B
D1R	type 1 dopamine receptor
D2R	type 2 dopamine receptor
DAB	diaminobenzidine tetrachloride
DIO	double-floxed inverted open reading frame

DOR	delta opioid receptor
DORA	dual orexin receptor antagonist
DREADDs	Designer Receptor Exclusively Activated by Designer Drugs
DYN	dynorphin
ENK	enkephalin
EPM	elevated plus maze
GABA	γ-amino butyric acid
HR	high-responder
i.p.	intraperitoneally
ITI	intertrial interval
KOR	kappa opioid receptor
LR	low-responder
mPFC	medial prefrontal cortex
MSN	medium-sized spiny neuron
NAc	nucleus accumbens
NAcC	nucleus accumbens, core
NAcSh	nucleus accumbens, shell
dmNAcSh	nucleus accumbens, shell, dorsomedial

vmNAcSh	nucleus accumbens, shell, ventromedial
NS	nonshocked
PBS	phosphate buffered saline
PKCδ	protein kinase C delta
PR	progressive ratio
PTSD	post-traumatic stress disorder
PVT	paraventricular nucleus of thalamus
aPVT	paraventricular nucleus of thalamus, anterior
pPVT	paraventricular nucleus of thalamus, posterior
s.c.	subcutaneously
SAA	social approach-avoidance
SOM	somatostatin
UR	unconditioned response
US	unconditioned stimulus
VI	variable interval

Chapter 1 Introduction and research objectives

1.1 A general introduction of fear, anxiety, and neural mechanism of emotion

The emotions that we experience every day are important for our physical health and social well-being. At the same time, strong negative emotions can be a source of distress with negative effects on cognitive ability and psychological health (Arnsten, 2009; Burgdorf & Panksepp, 2006; Eysenck, Derakshan, Santos, & Calvo, 2007; Stein, Scott, de Jonge, & Kessler, 2017). An important goal of behavioral neurosciences is to understand how different regions of the brain work together as a network to produce emotional states. The overall goal of this research is to learn how to reduce the negative impact of negative emotions in individuals who suffer from mental illnesses where a disruption in emotions forms a central component of these illnesses (Gross & Muñoz, 1995; Insel & Quirion, 2005; Ressler & Mayberg, 2007).

1.1.1 Fear, anxiety, and related psychiatric disorders

Fear and anxiety are negative emotions in response to threatening situations. Although both emotions contain subjective experience of distress, fear and anxiety are usually regarded as beneficial states because they enable the organism to avoid or reduce harm and maximize its chance of survival (LeDoux, 2012; Steimer, 2002). Failure or errors in the detection of a threat or in the selection of an appropriate emotional response can result in increased risk, distress, and loss of limited energy store (Steimer, 2002; Tovote, Fadok, & Lüthi, 2015). Fear- and anxiety-related psychiatric disorders are the most common mental illnesses in North America. A survey conducted by Government of Canada in 2013 found that an estimated of 3-million Canadian adults (11.6%) reported that they had a mood and/or anxiety disorder (Pearson, Janz, & Ali, 2013). An epidemiological investigation in the United States estimated the prevalence of

anxiety-related disorders (Kessler et al., 2005). It reported that the lifetime prevalence of specific phobia and social phobia are more than 10% respectively while post-traumatic stress disorder (PTSD), generalized anxiety disorder, and panic disorder are around 5%. This report concluded that anxiety disorders are the most prevalent class of psychiatric disorders with a lifetime prevalence of 28.8%, higher than mood disorders and substance use disorders.

Anxiety disorders cause unpleasant feelings, physical symptoms, reduced cognitive functions, and decreased work productivity (Eysenck et al., 2007; Stein et al., 2017). As a common mental illness, it is a burden on individuals and society. It is essential that we get a better understanding of the neural mechanism that produces fear and anxiety to develop effective treatments and to improve the mental health of sufferers.

1.1.2 Neural mechanism of emotion

Behavioral neuroscientists largely conceptualize emotion as a stimulus-response process where a stimulus (or a group of stimuli in the environment) with specific survival value, along with the internal physiological state that accompany this stimulus, triggers a series of responses composed of behavioral, physiological, endocrine, autonomic reactions, and the associated subjective experience (Adolphs, 2013; Anderson & Adolphs, 2014; Panksepp, 1998a; Steimer, 2002). The stimulus can be instinctual, or a neutral stimulus can become fear-producing because the organism has learned that it is predictive of a painful or unpleasant outcome through an associative learning process (LeDoux, 2012; Panksepp, 1998b; Tovote et al., 2015).

The generation of an emotion can be dissected into four basic steps: stimulus detection, interpretation, evaluation, and response initiation (Calhoon & Tye, 2015; Swanson, 2000). As presented in Figure 1-1, each step has its specific mechanism involving unique neural substrates in the central nervous system. At the beginning, sensory information is detected and relayed by

the sensory cortex and thalamus. The perceived information is transmitted to limbic cortices which are the cortical areas lying along the boundary between neocortex and subcortical structures (Mesulam, 2000). The limbic cortices include the olfactory cortex, the hippocampus, medial prefrontal cortex (mPFC), lateral prefrontal cortex (insular cortex), and the basolateral amygdala complex (Heimer & Van Hoesen, 2006). The limbic cortices form a highly interconnected network that interprets the meaning of sensory stimuli according to individual's previous experience. The information is then transmitted to the basal forebrain nuclei for further evaluation based on the expected outcome of a potential response along with other competing motivational states (Calhoon & Tye, 2015). Evaluation here refers to a process of weighing and integrating the information from various sources rather than a conscious process. Nuclei in the basal forebrain integrate information from these cortical areas to select an appropriate response by sending signals to effectors in the hypothalamus and brainstem (Panksepp, 1998a; Swanson, 2000). Effectors here refers to specialized nuclei or circuits that have a direct control over a specific behavioral, autonomic, or other type of reaction. The research on the neural mechanism of emotions usually focuses largely on the interpretation and evaluation steps and less on the detection or execution steps. A basic schematic for the functional and anatomical organization of the emotional circuit is shown in Figure 1-1.

Figure 1-1 A scheme of the neural circuit for emotion with four basic steps

A proposed schematic diagram for the basic organization of the neural circuit for emotion underlying a stimulus-response process with four basic steps: stimulus detection, interpretation, evaluation, and response initiation.

Abbreviations: BLA, basolateral nucleus of amygdala; BST, bed nucleus of stria terminalis; CeA, central nucleus of amygdala; Hip, hippocampus; IC, insular cortex; mPFC, medial prefrontal cortex; NAc, nucleus accumbens.

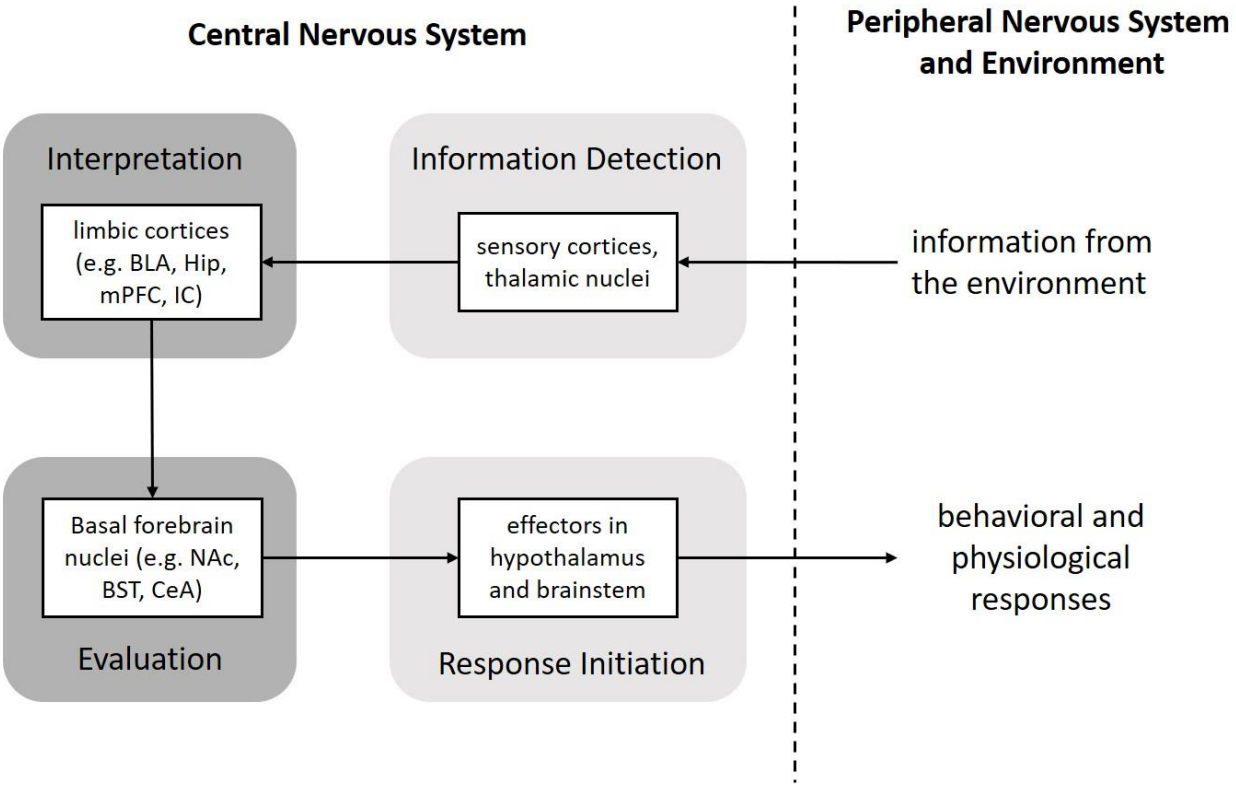

The neural pathways involved in emotional expression can be viewed as descending pathways from cortex to nuclei in basal forebrain similar to the framework associated with the neural circuitry for voluntary motor control (Swanson, 2000; Figure 1-2). The principal neurons of the cortex are glutamatergic pyramidal neurons that send excitatory projections to the basal forebrain nuclei and to effectors in the lower brain (Swanson, 2000). By contrast, the principal neurons in the basal forebrain nuclei contain the inhibitory γ-amino butyric acid (GABA) as the main neurotransmitter. The nuclei in the basal forebrain can be further divided into two main types with distinct features. First, the striatum and other striatum-like structures are characterized by medium-sized spiny neurons (MSNs) that receive direct cortical inputs and send massive outputs to the globus pallidus or other pallidum-like structures in the basal forebrain nuclei. Second, pallidum-like structures are composed of aspiny neurons which are larger neurons that receive striatal afferents and project to effectors in the lower brain and the thalamus (de Olmos & Heimer, 1999; Swanson, 2000). Similar as the neural network for voluntary motor behavior, the cortico-striato-pallidal descending projection system for emotional responses is topographically organized with specific cortical regions having unique projections and influence on distinct regions in striatum-like and pallidum-like areas (de Olmos & Heimer, 1999; Heimer, Van Hoesen, Trimble, & Zahm, 2008). Compared to the neural circuit for voluntary motor behavior, the circuit that mediate emotion is composed of a group of rather primitive brain structures with less specificity in their projections and functions (Mesulam, 2000). The cortical structures in the limbic area, represented by the hippocampus (allocortex) and the mPFC (transitional cortical area), have less than six layers (one to five) and primitive cytoarchitectonic characteristics. Similarly, the striatum-like and pallidum-like structures of the emotional pathway usually have vague or unrecognizable borders and extensive interconnection between regions at the same level

(Mesulam, 2000). Therefore, the information processing mode in the limbic regions is more like a network with multiple nodes than a serial cascade.

Figure 1-2 A simplified model of the cortico-striato-pallidal descending projection

Abbreviations: Glu, glutamate; GABA, γ-amino butyric acid; +, excitatory; −, inhibitory.

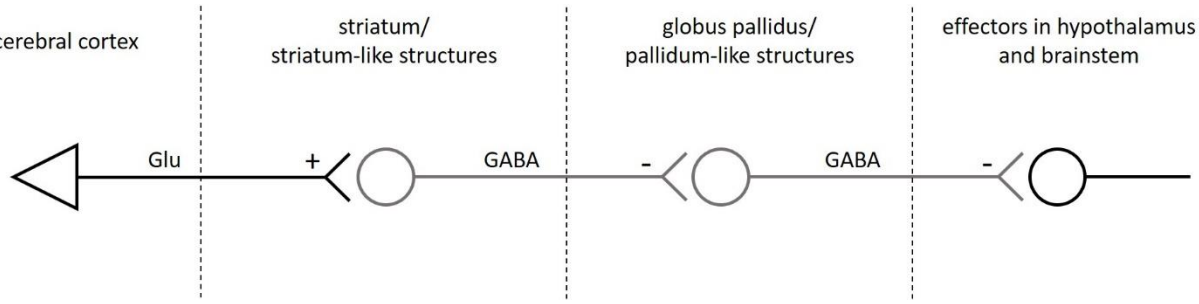

In addition to the cortico-striato-pallidal descending pathway, the neural network for emotion also contains a diencephalic component. Specifically, the midline and intralaminar thalamic nuclei receive information from the hypothalamus and brainstem and provide an intense innervation to the striatum-like structures (van der Werf, Witter, & Groenewegen, 2002; Vertes, Linley, & Hoover, 2015). The function of this thalamo-striatal pathway has been traditionally considered as playing a role in the regulation of arousal (Groenewegen & Berendse, 1994; Groenewegen & Witter, 2004). The paraventricular nucleus of the thalamus (PVT) of the midline thalamus has particularly received a surge of interest in research of emotion because the PVT preferentially innervates specific striatum-like regions that are considered as the critical nodes in the neural circuitry for fear and anxiety (Kirouac, 2015; Li & Kirouac, 2008, 2012; van der Werf et al., 2002; Vertes & Hoover, 2008). The connectivity suggests that the PVT may have a potent

influence on the integration and evaluation process of fear and anxiety (Kirouac, 2015; Li & Kirouac, 2008). The purpose of this thesis is to examine the function of the PVT in fear and anxiety. I will review the neural circuitry for fear and anxiety briefly and introduce how the PVT fits within this network as part of the introduction and present experimental evidence to discuss the organization of PVT output and its function in fear and anxiety in the later chapters.

1.2 The neural circuit for fear

1.2.1 Fear-evoking stimuli and threat-imminence theory

Fear and anxiety are often considered and studied as a unitary emotional response. However, it is beneficial to distinguish them from each other based on the conditions that evoke the emotions and the behavioral and physiological reactions associated with them (Perusini & Fanselow, 2015). According to a threat-imminence theory, different types of threats and emotional reactions fall along a threat-imminence continuum (Fanselow, 1980, 2018). In other words, distant or close threats will trigger different types of emotional responses. Specifically, animal will show panic to direct contact with a predator or other types of life-threatening events. The common reactions to such situation include changes in the autonomic system and attempts at getting away. When the threat is imminent and impending, individuals will be in the state of fear with a highly activated sympathetic system, a suppressed parasympathetic system, and freezing behavior (shutting down any on-going movement to prevent detection by a predator). In contrast, anxiety is evoked when an individual detects some vague or potential threats. An anxious state is associated with increased vigilance, avoidance, and decreased foraging (Fanselow, 2018; Steimer, 2002).

In contrast with anxiety, fear has explicit triggers and produces a series of relatively consistent behavioral responses. The threat(s) that induces fear can be dangerous stimuli/situations or neutral stimuli/situations that were previously associated with harmful events. The first type of threat induces innate fear response while the second type induces experience-dependent fear or learned fear. The terminology used in Pavlovian fear conditioning experiments refers to the unconditioned stimulus (US) as an innately aversive stimulus/situation; the unconditioned response (UR) as an innate emotional response to a US; the conditioned stimulus (CS) as a neutral stimulus that is associated with the US; and the conditioned response (CR) as an emotional response produced by a learned association between the CS and the US. A conditioned emotional response involves the neural mechanism of learning and memory (reviewed in Fendt & Fanselow, 1999; LeDoux, 2000; Maren, 2001; Tovote et al., 2015). The neural circuit underlying US-UR response is comprised of more primitive brain structures while the neural circuit underlying CS-CR association involves cortical components (reviewed in Herry & Johansen, 2014; LeDoux, 2012; Tovote et al., 2015). The neural mechanism of learned fear has received more interest because it is more closely related to fear-related psychiatric disorders. For example, specific phobia that usually develops after a traumatic experience features excessive fear towards stimuli which have little potential for causing harm (Fyer, 1998; LeDoux, 1998; Öhman & Mineka, 2001). Fear conditioning is also a good model to study the neural mechanism of learning and memory (LeDoux, 1998). I will present a brief review of the neural circuit processing innate fear and the neural circuit for learned fear as a background knowledge to understand how the PVT connects to brain regions regulating innate and learned fear.

1.2.2 The neural circuit for innate fear

The neural circuit for innate fear contains four basic units underlying the four steps of emotional processing: stimulus detection, interpretation, evaluation, and response initiation. Some researchers propose that the pathways which mediate innate fear induced by different types of threats are comprised of the same functional units but different anatomical structures, especially the brain regions contributing to interpretation and evaluation (Gross & Canteras, 2012; Silva, Gross, & Gräff, 2016). In other words, there are parallel neural pathways processing innate fear to different types of threats (Figure 1-3). For example, the circuit mediating fear to predators is different from the circuit mediating fear to aggressive conspecifics (Silva et al., 2013). Briefly, odor of predator is processed by the main and accessory olfactory bulb (Breer, Fleischer, & Strotmann, 2006; Isogai et al., 2011), directly or through the piriform cortex (Kondoh et al., 2016), to the posteroventral part of the medial nucleus and basomedial nucleus of the amygdala for interpretation (Martinez, Carvalho-Netto, Ribeiro-Barbosa, Baldo, & Canteras, 2011; Motta et al., 2009). The two amygdalar regions in turn project to the anterior hypothalamic nucleus and dorsomedial portion of the ventromedial hypothalamus for evaluation (Canteras, Simerly, & Swanson, 1995; Petrovich, Risold, & Swanson, 1996). These nuclei then project to effectors in the hypothalamus and brainstem to induce defensive responses to predator such as flight mediated by the dorsal part of periaqueductal gray (Canteras, 2002; Cezario, Ribeiro-Barbosa, Baldo, & Canteras, 2008; Sukikara, Mota-Ortiz, Baldo, Felicio, & Canteras, 2010).

The neural substrates mediating the detection of aggressive conspecifics overlap with those for predator threats (Ben-Shaul, Katz, Mooney, & Dulac, 2010). Olfactory cue of aggressive conspecifics is conveyed through the main and accessory olfactory bulb and piriform cortex (Gross & Canteras, 2012; Kollack-Walker, Don, Watson, & Akil, 1999). In contrast, this type of

threat information is then directed to the posterodorsal part of the medial amygdala which in turn projects to the medial preoptic nucleus and ventrolateral regions of the ventromedial hypothalamus (Motta et al., 2009; Silva et al., 2016, 2013) for interpretation and evaluation. The brain structures for conspecific threat interpretation and evaluation do not overlap with those responding to predator threat (Silva et al., 2016).

The neural substrates mediating fear induced by painful stimuli such as footshock are different from the structures processing predator or social fear (Gross & Canteras, 2012; Figure 1-3). The nociceptive information or pain is relayed from spinal dorsal horn to the basolateral amygdalar complex and insular cortex via the periaqueductal gray and the parabrachial nucleus in the midbrain and pons (Fendt & Fanselow, 1999; Neugebauer, Galhardo, Maione, & Mackey, 2009). The amygdala and insular cortex interpret the nociceptive signals and relay these signals to the central nucleus of the amygdala and bed nucleus of the stria terminalis (BST) for evaluation. The central nucleus of the amygdala and BST project directly to multiple effectors in the hypothalamus and brainstem which can initiate specific defensive responses including the ventrolateral part of the periaqueductal gray that regulates freezing and the dorsal motor nucleus of the vagus nerve and the parabrachial nucleus that regulate autonomic nervous system (Bandler & Shipley, 1994; Hopkins & Holstege, 1978). Many studies using advanced technology revealed how the microcircuits within each nucleus regulate fear in a conditioned fear memory model (see Section 1.2.4) and it is generally accepted that the same local microcircuit is also involved in innate fear.

Figure 1-3 A simplified scheme of parallel neural pathways mediating innate fear to different types of threats

A diagram presents neural pathways which mediate innate fear induced by different types of threats with an emphasis on four basic functional steps of a stimulus-response process. Arrows indicate information flows rather than actual neural connections.

Abbreviations: AHN, anterior hypothalamic nucleus; AOB, accessory olfactory bulb; BLA, basolateral nucleus of amygdala; BMA, basomedial nucleus of amygdala; BST, bed nucleus of stria terminalis; CeA, central nucleus of amygdala; DMV, dorsal motor nucleus of the vagus nerve; dmVMH, dorsomedial part of ventromedial hypothalamic nucleus; dPAG, dorsal part of periaqueductal gray; IC, insular cortex; MOB, main olfactory bulb; MPN, medial preoptic nucleus; PAG, periaqueductal gray; PB, parabrachial nucleus; pdMeA, posterodorsal part of medial nucleus of amygdala; pvMeA, posteroventral part of medial nucleus of amygdala; vlPAG, ventrolateral part of periaqueductal gray; vlVMH, ventrolateral part of ventromedial hypothalamic nucleus.

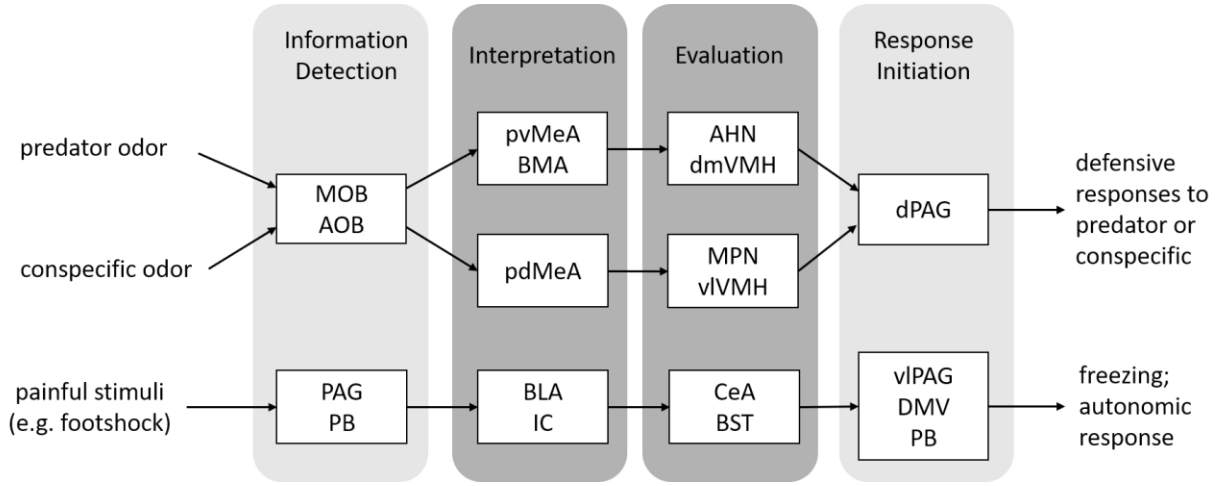

1.2.3 Pavlovian fear conditioning as a model to study learned fear

Pavlovian or classical fear conditioning is the most commonly used paradigm to study learned fear (LeDoux, 2000; Tovote et al., 2015). Fear conditioning is a model with distinguishable phases of emotional associative memory. The first phase is the memory acquisition. At this stage, fear is elicited by the US (usually a series of footshocks) with the CS (usually a distinct auditory tone). During the acquisition process, an associative memory between the US and CS is formed. After the association is learned, the CS itself can evoke a fear response (CR) with freezing commonly used as the behavioral measure of fear (Bouton & Bolles, 1980; Fanselow, 1980). After acquisition of conditioned fear, repeated presentation of the CS alone starts a new learning process called extinction (Myers & Davis, 2007). At the end of the extinction process, CS alone does not induce freezing indicating that a new associative memory has been formed that the CS is no longer a threat.

1.2.4 Conditioned fear and the amygdala

The amygdala complex is an essential brain structure for processing fear (Janak & Tye, 2015; LeDoux, 2003; Figure 1-4). The amygdala complex can be divided into two major parts: a cortical-like basolateral part and a striato-pallidal-like central part (McDonald, 2006; Swanson, 2003). The similarity between the basolateral amygdalar complex and cerebral cortex has been confirmed by anatomical and histochemical evidence (Carlsen & Heimer, 1988). In contrast, the central part of amygdala, including the capsular (CeC), lateral (CeL) and medial central nucleus (CeM), contains GABAergic principal neurons. The structure of CeC and CeL resembles the ventral striatum in many perspectives while the CeM has pallidal-like features (Cassell, Freedman, & Shi, 1999; de Olmos & Heimer, 1999). GABAergic projection neurons in CeC and CeL have a high density of dendritic spines and resemble the medium-sized spiny neurons in the

striatum (McDonald, 2006). These neurons express a variety of neuropeptides and neuropeptide receptors such as corticotropin releasing factor (CRF), neurotensin, and opioid peptides (McDonald, 2006). In contrast, neurons in CeM resemble the principal neurons in the globus pallidus which are GABAergic neurons with less spines and neuropeptides (Cassell et al., 1999; de Olmos & Heimer, 1999).

Figure 1-4 A simplified scheme of the neural pathway mediating conditioned fear

A diagram presents a simplified model of the neural pathway which mediates conditioned fear with an emphasis on four basic functional steps of a stimulus-response process. Arrows indicate information flows rather than actual neural connections.

Abbreviations: CeL, lateral part of central nucleus of amygdala; CeM, medial part of central nucleus of amygdala; DMV, dorsal motor nucleus of the vagus nerve; Hip, hippocampus; IC, insular cortex; IL, infralimbic cortex; MGN, medial geniculate nucleus; PAG, periaqueductal gray; PB, parabrachial nucleus; PL, prelimbic cortex; vlPAG, ventrolateral part of periaqueductal gray.

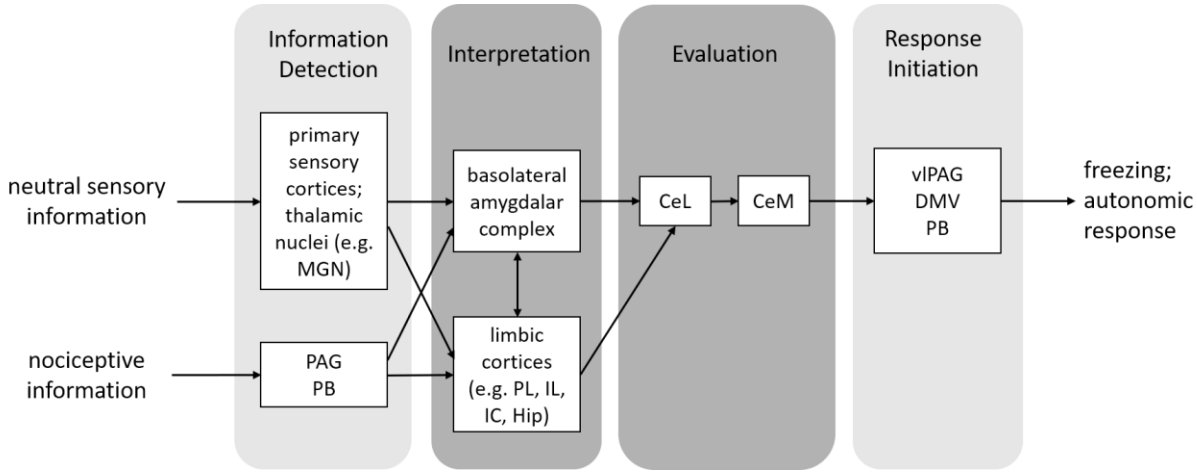

The basolateral amygdalar complex receives sensory inputs from the thalamus and cerebral cortex and projects to the CeC, CeL (Figure 1-4) as well as many other striatal-like structures such as the nucleus accumbens (NAc) and BST (McDonald, 1991b). It also interconnects with other limbic cortices including the prefrontal, hippocampal, and perirhinal, entorhinal cortices (McDonald, 1991a, 2006). The distribution of inputs and outputs of the basolateral amygdalar complex suggests that this area is an important node in the neural network integrating information from different sensory modalities and regulating the association between sensory information and adaptive behaviors. It is known from research in rodents, primates, and humans that the basolateral amygdalar complex is necessary for fear learning and expression (reviewed in Janak & Tye, 2015). In addition, the basolateral amygdalar complex is postulated to be the place that the stimuli with affective values get associated with neutral signals through mechanisms involving synaptic plasticity mediated by NMDA and AMPA receptors (Pape & Paré, 2010). Therefore, the basolateral amygdalar complex is necessary for the acquisition and expression of conditioned fear as well as other types of associative learning.

The CeC and CeL are striatal-like structures in the cortico-striato-pallidal pathway. The CeC and CeL have some differences in their cell density, immunoreactivity, and connectivity (Cassell et al., 1999; van den Burg & Stoop, 2019). In this thesis they will be viewed together as the lateral portion of the central amygdala and referred as CeL. The CeL receives cortical afferents from the lateral nucleus and basolateral nucleus (BLA) in the basolateral amygdalar complex (McDonald, 1998). It also receives cortical inputs from the mPFC and agranular insular cortex (McDonald, 1998; Figure 1-4). The CeL also receives diencephalic afferent from the PVT (Li & Kirouac, 2008). The CeL is intensely interconnected with the lateral portion of the BST (de Olmos & Heimer, 1999; Dong & Swanson, 2004b; Swanson, 2003). In fact, the CeL and the

lateral part of the dorsal BST are viewed as a continuum which forms the central extended amygdala (Alheid, 2003; de Olmos & Heimer, 1999). The concept of the central extended amygdala will be introduced in Section 1.3.4.

The CeL contains subpopulations of GABAergic neurons identified by distinctive molecular makers (Haubensak et al., 2010; Kim et al., 2017). These neurons form an intricate local microcircuit with reciprocal inhibitory connections. Recent technological developments in electrophysiology and optogenetics have expanded our understanding of how the microcircuit in the CeL regulates fear (Ciocchi et al., 2010; Fadok et al., 2017; Haubensak et al., 2010; Haohong Li et al., 2013). For example, neurons expressing protein kinase C delta (PKCδ) are inhibited by the CS (Ciocchi et al., 2010), and inhibition of the PKCδ+ neurons in CeL enhances conditioned fear (Haubensak et al., 2010). In contrast, somatostatin-expressing (SOM+) interneurons in the CeL are activated by the CS and provide a potent inhibition on PKCδ+ neurons locally to promote the expression of fear (Haohong Li et al., 2013). The CeL also contains a subgroup of CRF-expressing neurons that do not overlap with the subgroups of PKCδ+ or SOM+ neurons (Fadok et al., 2017). A recent study found that the CRF+ neurons and SOM+ neurons mutually inhibit each other and a stimulation of the CRF+ neurons initiates escape while a stimulation of the SOM+ subgroup initiates freezing (Fadok et al., 2017).

The microcircuit in the CeL synthesizes converging information and sends an inhibitory projection to the CeM (Ciocchi et al., 2010; Fadok, Markovic, Tovote, & Lüthi, 2018; McDonald, 1991b, 2006; Figure 1-4). As the pallidal structure of the pathway, the CeM sends widespread GABAergic projections to effectors in the lower brain to regulate the behavioral, autonomic, and neuroendocrine responses associated with fear (McDonald, 2006; Tovote et al., 2015; Viviani et al., 2011). For example, the CeM innervates the ventrolateral part of

periaqueductal gray which mediates freezing (LeDoux, Iwata, Cicchetti, & Reis, 1988; Rizvi, Ennis, Behbehani, & Shipley, 1991) and dorsal vagal complex which regulates autonomic responses (Danielsen, Magnuson, & Gray, 1989). It should be noted that the CeL–CeM pathway is not only involved in fear but also other adaptive processes such as anxiety (Botta et al., 2015) and reward-seeking (Kim et al., 2017).

1.2.5 A top-down control of conditioned fear expression

The mPFC plays a key role in conditioned fear expression through its reciprocal connection with the basolateral amygdalar complex (Quirk, Garcia, & González-Lima, 2006; Quirk, Likhtik, Pelletier, & Paré, 2003; Figure 1-4). The prelimbic cortex located in the dorsal part of the mPFC (Heidbreder & Groenewegen, 2003) receives direct excitatory innervation from neurons in the BLA that are activated during fear response (Senn et al., 2014). Experiments using cFos (a marker of neuronal activation) and single unit recording showed that local neuronal activity in the prelimbic cortex is increased after fear conditioning and during fear expression (Burgos-Robles, Vidal-Gonzalez, & Quirk, 2009; Do-Monte, Quiñones-Laracuente, & Quirk, 2015; Morrow, Elsworth, Inglis, & Roth, 1999). However, lesions or inhibition of the prelimbic cortex neural activity during the conditioning process have no effect on conditioned fear acquisition (performance during the conditioning) or expression (fear response to CS alone after acquisition) (Corcoran & Quirk, 2007; Lacroix, Spinelli, Heidbreder, & Feldon, 2000; Rosen et al., 1992). This suggests that the prelimbic cortex may not be necessary for the acquisition of conditioned fear. In contrast, pharmacological or optogenetic inactivation of the prelimbic cortex during the conditioned fear test reduces fear (Corcoran & Quirk, 2007; Do-Monte, Quiñones-Laracuente, et al., 2015; Morgan, Romanski, & LeDoux, 1993). The prelimbic cortex has no direct projection to the CeL (McDonald, 1998) but innervates the basal amygdalar complex and

the PVT which both in turn send glutamatergic projections to the CeL (Heidbreder & Groenewegen, 2003; Vertes, 2004).

The infralimbic cortex forms the ventral part of the mPFC. The infralimbic cortex is not involved in fear conditioning or expression but plays a key role in fear extinction (Do-Monte, Manzano-Nieves, Quiñones-Laracuente, Ramos-Medina, & Quirk, 2015; Knapska & Maren, 2009; Milad & Quirk, 2002; Sotres-Bayon & Quirk, 2010; Thompson et al., 2010). The neural activity in the infralimbic cortex increases during extinction learning and extinction retrieval (Barrett, Shumake, Jones, & Gonzalez-Lima, 2003; Herry & Mons, 2004; Milad & Quirk, 2002). Silencing the infralimbic cortex impairs the retrieval of an extinction memory (Do-Monte, Manzano-Nieves, et al., 2015; Sierra-Mercado, Padilla-Coreano, & Quirk, 2011). The BLA contains distinct subpopulations of neurons selectively targeting the prelimbic and infralimbic cortex (Senn et al., 2014). BLA neurons whose activity positively correlates with fear selectively project to the prelimbic cortex whereas BLA neurons that are activated during extinction specifically project to the infralimbic cortex (Senn et al., 2014). In addition, the activity of these two subpopulations of BLA neurons is balanced by local microcircuit mechanisms (Senn et al., 2014). Meanwhile, the prelimbic cortex can influence the infralimbic cortex activity by direct innervation (Heidbreder & Groenewegen, 2003). The organization of the BLA-mPFC connectivity may underlie the regulation of fear response during fear expression and extinction. Moreover, a group of neurons in the medial part of intercalated cell masses located between the BLA and CeL send inhibitory projection to the CeM (Paré & Smith, 1993; Royer, Martina, & Paré, 1999). A postulated circuit for fear extinction is that the infralimbic cortex projects to a subpopulation of BLA neurons which send excitatory projection to neurons in the medial part of

intercalated cell masses which in turn provides a feedforward inhibition to neurons in the CeM (Duvarci & Pare, 2014; Tovote et al., 2015).

The infralimbic cortex receives a strong input from the ventral hippocampus which may convey contextual information to the infralimbic cortex during extinction learning (Heidbreder & Groenewegen, 2003; Hoover & Vertes, 2007). A recent study found that the ventral hippocampus preferentially innervates the parvalbumin-expressing interneurons in the infralimbic cortex which have local inhibitory synaptic connection with pyramidal neurons that project to the amygdala (Marek et al., 2018). In that study, activation of ventral hippocampus-infralimbic cortex projection impaired fear extinction retrieval whereas silencing the same pathway blocked fear renewal (renewal is the re-emergence of an extinguished conditioned fear when the tone is present in a context different from the context for extinction training). This study along with evidence from the contextual fear conditioning model (Maren, Phan, & Liberzon, 2013; Xu et al., 2016) suggest that the ventral hippocampus may be important for processing contextual information related to conditioned fear.

1.2.6 Summary of the circuit for conditioned fear

The neural circuit comprising the mPFC, basolateral amygdalar complex, and the CeL undertakes the interpretation and evaluation steps of conditioned fear response (Figure 1-4). It is arbitrary to define the activity in a few neural substrates as “interpretation” or “evaluation”, but the neural connectivity and activity of these substrates during fear help us postulate potential roles of these brain regions in fear. For example, the CeL contains different subpopulations of neurons receiving inputs with varied sources and neurochemical identities (de Olmos & Heimer, 1999; Kim et al., 2017; McDonald, 2006). The microcircuit formed by these neurons integrates information and sends output to the CeM which directly innervates multiple effectors to initiate

the responses associated with fear (Fadok et al., 2018). It suggests that the CeL and CeM, compared to cortical or cortical-like regions that provide input to them, are downstream parts of the circuit processing fear response and have a more direct influence on response. In contrast, the limbic cortices show functional specificity at different phases of conditional fear memory. Specifically, the lateral nucleus of the amygdala is postulated to be the place where the CS obtains its valence (pleasant or aversive value of a stimulus) during associative memory acquisition; the prelimbic cortex may store the information of emotional cues which drive the expression of conditioned responses; the infralimbic cortex in contrast may drive the inhibitory effect of cues on conditioned responses obtained during extinction learning; the ventral hippocampus may process the contextual discriminative information of cues (reviewed in Fendt & Fanselow, 1999; Marek, Sun, & Sah, 2019; Tovote et al., 2015).

The functional characteristics of these limbic regions are not only reflected in the regulation of conditional fear response but also in the appetitive behavioral model with reward-seeking as its typical response (Heimer & Van Hoesen, 2006; Salamone & Correa, 2018). In contrast, there is almost no overlapping in their downstream brain regions with more direct control over emotional responses (Fendt & Fanselow, 1999; Salamone & Correa, 2018). It indicates that the function of the neural network for information interpretation is not limited to a certain type of emotional behavior but influences a variety of behaviors via different downstream pathways. Section 1.3.3 will discuss how the neural network comprised of the same brain regions acts for the interpretation of anxiety. By definition, anxiety is a state induced by vague and distal threatening stimuli. This essential feature of anxiety-inducing stimuli makes it difficult to distinguish unconditioned versus conditioned stimuli, so as the innate versus conditioned

response, or any phases of associative memory. As a result, it is difficult to show any functional specificity of different brain regions in the interpretation process of anxiety.

It is also worth mentioning that, in addition to the tone-freezing model, there are other behavioral models with more complicated stimulus or response to study conditioned fear memory. For example, footshock can be delivered with a tone in an operant box where an association between bar-press and sucrose-delivery has been formed (e.g., Corcoran & Quirk, 2007). The level of fear is reflected by the suppression degree of bar-pressing behavior during tone after footshock. Another model uses the alteration in the amplitude of startle reflex, a basic reflex induced by a loud and abrupt auditory stimulus, to indicate fear level (e.g., Lee & Davis, 1997). In this fear-potentiated startle model, a light stimulus (CS) is paired with footshock during the acquisition session. The light stimulus alone then can increase the amplitude of startle reflex in the expression session. The neural circuits of conditioned fear postulated from such models may differ from the one based on the tone-freezing model because their behavioral measurements reflect the relationship between two behaviors, such as the trade-off between bar-pressing and freezing or the enhancement of startle reflex caused by fear-induced hypertonia. Such models may be more closely related to specific symptoms in fear-related psychiatric disorders, but they add difficulty to the research of neural mechanism of fear because the behaviors in these models are more complex. The anxiety behavioral model described below has a similar shortcoming in that it does not use a model with a simple stimulus-response association like the tone-freezing model. It is difficult to study a complex neural network distributed over a large brain area which processes polymodal information and projects to a group of effectors.

1.3 Neural circuitry of anxiety

1.3.1 Anxiety-generating situations

Anxiety is an emotion evoked by vague or potential threats (Grupe & Nitschke, 2013; Perusini & Fanselow, 2015). This threat could be a novel and spacious open area, an enclosed space with no supply of life essentials, or an unfamiliar conspecific which could be aggressive. An anxiety-generating situation can evoke defensive behaviors but will not completely suppress other adaptive behaviors such as food intake and parental behaviors (Neumann & Slattery, 2016; Petrovich, 2013). Unlike fear, anxiety-related behaviors do not have a top priority over other types of behaviors. Therefore, a strategy for behavioral measurement of anxiety is to compare two conflicting behavioral intentions in an environment with potential threat (Cryan & Holmes, 2005).

1.3.2 Anxiety measurement in rodents

The most commonly used anxiety tests in rodents are the open field test and elevated plus maze test (EPM) (Cryan & Holmes, 2005). In the open field test, rodents are placed into a novel context of circular or square shape for a few minutes. In such a situation, anxious animals spend less time exploring the center of the arena but stay close to the wall (Litvin, Pentkowski, Pobbe, Blanchard, & Blanchard, 2008). In the EPM test, rodents are placed on an elevated cross-shaped maze with two open arms and two arms enclosed by walls. Anxious animals spend less time exploring the open arms where they may fall off but spend more time in the walled arms where they are more secured (Litvin et al., 2008; Pellow, Chopin, File, & Briley, 1985). These two tests and other less commonly used tests like social approach-avoidance and light-dark box are designed to reflect the conflict between approach and avoidance motivational tendencies (Calhoon & Tye, 2015).

Because the operational definition of anxiety is based on motivational conflicts, the neural mechanism for anxiety postulated based on such models may involve a component as inhibition of other adaptive behaviors. Another feature of the current anxiety models is the presence of poorly defined threats in the test situation (Perusini & Fanselow, 2015). As mentioned earlier, it is difficult to distinguish between innate and learned anxiety based on the definition or the test situation of anxiety. Similarly, the commonly used anxiety models to study the neural substrates for anxiety do not distinguish any phases of associative memory.

1.3.3 The neural network for anxiety – cortical components

It is difficult to provide an overview of the neural network for anxiety because functional studies usually demonstrate how a single brain area or pathway regulates anxiety. Nevertheless, we can improve our understanding of the neural network for anxiety by sorting the experimental evidence according to the cortico-striato-pallidal scheme. Functionally, cortical components in the anxiety network are proposed to interpret external and internal information, while the striato-pallidal components integrate the information and select appropriate responses by descending projections to effectors in the lower brain (Figure 1-5).

Almost all the limbic cortical areas have been shown to mediate anxiety (reviewed in Calhoon & Tye, 2015; Tovote, Fadok, & Lüthi, 2015). On one hand, limbic cortices including the basolateral amygdalar complex, ventral hippocampus, mPFC, and agranular insular cortex, receive different combinations of information which reflect potential threats from different perspectives (Figure 1-5). On the other hand, these regions are highly interconnected and converge on the same group of subcortical structures.

Figure 1-5 A simplified scheme of the neural pathway mediating conditioned fear

A diagram presents a simplified model of the neural pathway which mediates anxiety with an emphasis on four basic functional steps of a stimulus-response process. Arrows indicate information flows rather than actual neural connections.

Abbreviations: BS, brainstem; BSTDL, dorsolateral part of bed nucleus of stria terminalis; BSTM, medial part of bed nucleus of stria terminalis; CeL, lateral part of central nucleus of amygdala; CeM, medial part of central nucleus of amygdala; HYP, hypothalamus; IC, insular cortex; IL, infralimbic cortex; LS, lateral septum; NAc, nucleus accumbens; PB, parabrachial nucleus; PL, prelimbic cortex; vHip, ventral hippocampus; VP, ventral pallidum.

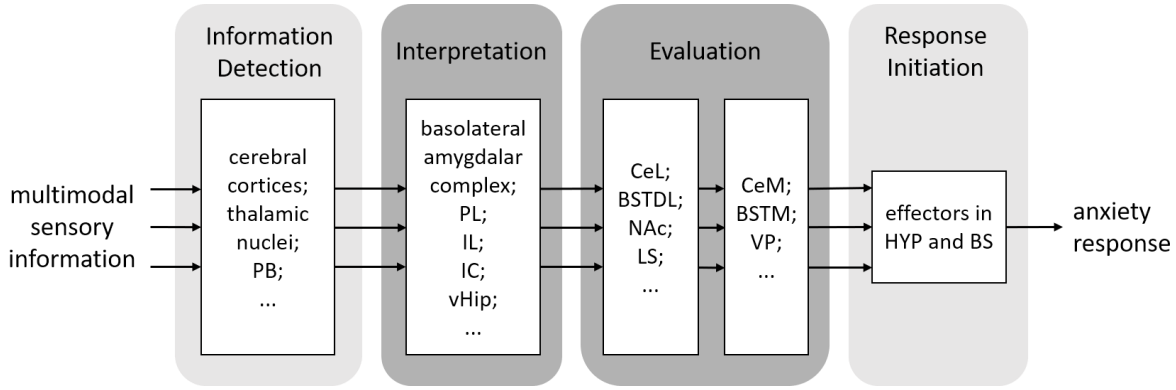

The basolateral amygdalar complex is considered a critical component for not only the fear circuit but also the anxiety circuit (Adhikari, 2014; Calhoon & Tye, 2015). It has been proposed that the cortico-like part of the amygdala integrates multimodal sensory information and establishes association between these stimuli (Fernando, Murray, & Milton, 2013). Functional studies showed that the neural activity in the BLA is positively correlated with anxiety level (Wang et al., 2011) and photoactivation of the BLA increases anxiety-like behavior in the EPM and open field test (Felix-Ortiz et al., 2013; Tye et al., 2011). As stated in Section 1.2.4, the basolateral amygdalar complex does not preferentially innervate the CeL over other regions but sends robust projections to many subcortical striatal-like structures that influence anxiety, including the NAc and BST (McDonald, 1991b, 2006). Whether the basolateral amygdalar complex regulates anxiety via any specific output or by broadcasting signals to multiple areas is not known.

The ventral hippocampus, comprised of the ventral CA1 and ventral subiculum, receives massive inputs from the perirhinal and postrhinal (analogue of the parahippocampal in primates) cortices where information from all sensory modalities is converged (Risold & Swanson, 1996; van Strien, Cappaert, & Witter, 2009; Witter, Doan, Jacobsen, Nilssen, & Ohara, 2017). The ventral hippocampus is distinctive from the dorsal hippocampus by the fact that it receives strong inputs from the olfactory and gustatory areas of the brain (Ranganath & Ritchey, 2012). The ventral hippocampus sends descending projections to striatal-like subcortical nuclei including the lateral septum, BST, CeL, and NAc (Fanselow & Dong, 2010; Groenewegen, der Zee, te Kortschot, & Witter, 1987), which in turn innervate effectors in the hypothalamus and brainstem. The ventral hippocampus also issues direct projections to the medial and periventricular zones of the hypothalamus and medial preoptic area where nuclei regulate neuroendocrine, autonomic and

behavioral responses to threats (Cenquizca & Swanson, 2006). The ventral hippocampus is also reciprocally connected to the basolateral amygdalar complex, mPFC, and agranular insular cortex (Hoover & Vertes, 2007; Ranganath & Ritchey, 2012). The connectivity of the ventral hippocampus implicates a role in the regulation of anxiety as well as other emotional responses. Lesions of the ventral hippocampus or disruption of the activity of the ventral hippocampus to the lateral septum projection increase exploration in the EPM and open field test (Anthony et al., 2014; Kjelstrup et al., 2002; Padilla-Coreano et al., 2016; Trent & Menard, 2010) indicating an anxiolytic effect. There is also evidence showing that chemogenetic activation of ventral hippocampus neurons that project to the lateral septum reduced anxiety whereas inhibition of these neurons produced an anxiogenic effect (Parfitt et al., 2017). The function of the projection from the ventral hippocampus to the BST, CeL, and NAc in anxiety has not been studied adequately.

The mPFC, especially the ventral part of the mPFC, is not connected to primary or associative sensory cortices but receives highly integrated information from the basolateral amygdalar complex, ventral hippocampus, agranular insular cortex and perirhinal cortex (Heidbreder & Groenewegen, 2003). The mPFC also projects back to these limbic cortical areas directly or indirectly, forming a reciprocal connection pattern (Groenewegen, Wright, & Uylings, 1997; Heidbreder & Groenewegen, 2003). The dorsal mPFC contains the medial precentral cortex, the anterior cingulate cortex, and the dorsal part of the prelimbic cortex; the ventral mPFC contains the infralimbic cortex and the ventral part of the prelimbic cortex. The functional difference of prelimbic and infralimbic cortex is demonstrated in conditioned fear memory expression (see Section 1.2.5), which may provide an explanation for the conflicting evidence about the effect of pharmacological manipulation in the mPFC on anxiety-like behaviors

(Covington et al., 2010; Pati, Sood, Mukhopadhyay, & Vaidya, 2018; Shah, Sjovold, & Treit, 2004). The prelimbic and infralimbic cortex may have opposite effects on anxiety by preventing or permitting the anxiogenic activity through the projection to the basolateral amygdalar complex or ventral hippocampus (reviewed in Adhikari, 2014; Calhoon & Tye, 2015). For example, some studies reported that blocking $GABA_A$ receptor in the infralimbic cortex increased the excitability there and produced more anxiety-like behaviors (Berg, Eckardt, & Masseck, 2019; Bi et al., 2013) while another study found that optogenetic activation of the prelimbic cortex reduced anxiety (Wang et al. 2015). The mPFC may also influence anxiety level via the descending projection to the NAc, BST, CeL, or lateral septum. The mPFC projects heavily to the shell of NAc (NAcSh) while much less to the BST, CeL, and lateral septum (Groenewegen et al., 1997). Although there is no direct evidence confirming the involvement of the mPFC to NAcSh pathway in anxiety, it will be of interest for future neural circuitry studies since substantial evidence demonstrating that the NAcSh regulates defensive responses including anxiety.

The insular cortex, especially the agranular insular cortex at the ventral side, receives prominent visceral sensory inputs from the parabrachial nucleus directly or via the ventroposterior parvicellular nucleus of the thalamus (Saper & Stornetta, 2015). The agranular insular cortex projects to the lateral hypothalamus, parabrachial nucleus, nucleus of the solitary tract, periaqueductal gray, ventral tegmental area, and CeL, BST, substantia innominata, NAc (Barrett & Simmons, 2015). Functional studies support the idea that the insular cortex mediates anxiety. Human neuroimaging studies found hyperactivity in the anterior insula (analogue of the agranular insular cortex in rodents) in PTSD patients (Etkin & Wager, 2007) and reduced volume of the insular cortex in social anxiety patients (Kawaguchi et al., 2016) and late-life

depression patients with severe anxiety symptoms (Laird et al., 2019) suggesting that anxiety symptoms are related with dysfunction in the insular cortex. Studies in rodents further addressed this idea by showing that inhibition of the insular cortex reduces anxiety level while activation increases anxiety in the EPM and open field test (Hui Li, Chen, Li, Wang, & Zhai, 2014; Méndez-Ruette et al., 2019; Shi et al., 2018). A recent study using optogenetic methods reported that inhibition of the insular projection to the CeL has an anxiolytic effect in the EPM test and activation of this pathway increases anxiety (Gehrlach et al., 2019). In contrast, manipulations of the insular projection to the core of the NAc had no effect on anxiety in the EPM test but interrupted feeding and drinking (Gehrlach et al., 2019). It should be noted that disruption of consummatory behaviors is associated with a state of high vigilance and anxiety. Tracing studies showed that the agranular insular cortex also reciprocally connects to the basolateral amygdalar complex, ventral mPFC, and ventral hippocampus (Allen, Saper, Hurley, & Cechetto, 1991; Hurley, Herbert, Moga, & Saper, 1991; Saper, 1982; Vertes, 2004). The cortical outputs from the insular cortex have been traditionally considered to convey integrated visceral sensory information for further interpretation (Saper, 1982; Saper & Stornetta, 2015). There has been no direct evidence to decipher the function of cortical interconnection between the insular cortex and other limbic cortices in anxiety yet.

The limbic cortices may regulate anxiety by direct projections to their preferential subcortical targets. More likely, these cortical regions may synchronize their activity via their intense interconnection. Rodent *in vivo* recordings of local field potentials showed that increased theta-frequency synchronization between the mPFC, ventral hippocampus, and the basolateral amygdalar complex correlates with a higher level of anxiety-like behaviors (Adhikari, Topiwala, & Gordon, 2010; Likhtik et al., 2014). In addition, disruption of the synchronization between

ventral hippocampus and mPFC reduces innate anxiety (Schoenfeld et al., 2014). The synchrony between different limbic cortices during anxiety indicates that any source of anxiogenic information can activate these highly interconnected cortical areas and thereafter activate the whole neural network for anxiety.

1.3.4 Subcortical components of the anxiety network

The cortical network interprets information that reflects threatening stimuli from various perspectives and sends signals to striatal structures for integration and evaluation to generate emotional responses (Figure 1-5). These striatal structures, represented by the dorsolateral part of BST (BSTDL) and the CeL, can be viewed as a continuum because of the similarity in their cytoarchitecture and neurochemistry as well as the fact that they are intensively interconnected (de Olmos & Heimer, 1999). This continuum is the striatal-like part, or lateral part, of a structure named the central division of the extended amygdala. The central extended amygdala also contains a pallidal-like part on the medial side. The striatal-like part of central extended amygdala consists of the BSTDL, CeL, and structures connecting BSTDL and CeL which are the interstitial nucleus of the posterior limb of the anterior commissure and the dorsolateral portions of sublenticular substantia innominata (de Olmos & Heimer, 1999; McDonald, 2006). The NAc can be viewed as the rostral extension of the lateral portion of the central extended amygdala because it is anatomically similar and adjacent to the anterior BST and interstitial nucleus of posterior limb of anterior commissure (de Olmos & Heimer, 1999; Zahm, 2000, 2006). However, the NAc is not interconnected with the rest of the lateral portion of the central extended amygdala and the NAc is not usually viewed as a part of central extended amygdala (Zahm, 1998).

The CeL is the most caudal part of the lateral portion of the central extended amygdala. The function of the CeL in conditioned fear has been studied thoroughly, but how it is involved in anxiety has not received as much attention. A study has identified distinct neuronal populations in the CeL activated by stimuli with positive or negative valences (Xiu et al., 2014) suggesting that the CeL may be an important site in the neural network for anxiety that coordinates both approach and avoidance. In addition, selective manipulation of subpopulations of neurons in the CeL produces effects on anxiety. For example, activation of the excitatory BLA axonal terminals in the CeL has an anxiolytic effect (Tye et al., 2011); optogenetic activation of PKCδ+ neurons reduces anxiety in the EPM and open field test (Cai, Haubensak, Anthony, & Anderson, 2014); increasing the excitability of SOM+ neurons in the CeL induces a higher anxiety level in the EPM and open field test (Ahrens et al., 2018); benzodiazepines execute an anxiolytic effect in part by inhibiting SOM+ neurons and in turn result in a reduced suppression on the PKCδ+ neurons in the CeL (Griessner et al., 2018). There is also conflicting evidence showing that specific subpopulations of neurons in the CeL have opposite behavioral effects. For example, optogenetic activation of PKCδ+ neurons in the CeL promoted anxiety-like behavior (Botta et al., 2015; Kim et al., 2017); activation of the SOM+ neurons there promoted appetitive behaviors while had no effect on defensive behaviors (Kim et al., 2017). Studies targeting the CRF+ neurons in the microcircuit found that chemogenetic inhibition of CRF+ neurons in the CeL reduces anxiety triggered by immobilization stress (Pomrenze et al., 2019) or footshock (Asok et al., 2018). This effect is probably mediated by local PKCδ+ neurons because these neurons express CRF1 receptor and promote anxiety (Kim et al., 2017; Sanford et al., 2017). It should be noted that optogenetic activation with specific stimulation parameters may create artifacts because it disrupts the homeostasis in the neural network of anxiety (Bass et al., 2013).

The BSTDL has been studied as a major subcortical area regulating anxiety (reviewed in Davis, Walker, Miles, & Grillon, 2010). Some early studies treated the BST as one functional entity disregarding the fact that subnuclei are interconnected via inhibitory projections (Dong, Petrovich, & Swanson, 2000; Dong, Petrovich, Watts, & Swanson, 2001; Dong & Swanson, 2004a, 2004b, 2006). Recent evidence with specific subregion-targeting methods found that the optogenetic inactivation of the BSTDL reduced anxiety level while inactivation of the anterodorsal BST increased anxiety (Kim et al., 2013). There is no direct evidence addressing how the microcircuit in the BSTDL regulates anxiety. Nevertheless, an anatomical study analyzed the cell-type specific microcircuits in the BSTDL and CeL and found parallel circuits (Ye & Veinante, 2019). Specifically, this research shows that PKCδ+ cells are concentrated in the BSTDL and CeL and receive glutamatergic inputs from the BLA and insular cortex. In contrast, the SOM+ cells are found at all subdivisions of the BST and the central nucleus of the amygdala (CeL and CeM), sending long-range projections to effectors in the lower brain, such as the parabrachial nucleus and periaqueductal gray. Within each area, PKCδ+ and SOM+ cells have mutual inhibitory connections. The similarity in the local microcircuits of BSTDL and CeL suggests that the local neural mechanism of threat evaluation in the BSTDL may be like the mechanism mediating fear in the CeL. It also supports the idea that the central extended amygdala is a structural and functional continuum.

The NAc is a striatal-like structure ventral to the caudate putamen and rostral to the anterior BST in rodent brain. It is known as the major component of the ventral striatum (Alheid & Heimer, 1988). There is evidence from clinic studies showing that the activity of the NAc is positively correlated with the anxiety level (Hasler et al., 2007; Levita, Hoskin, & Champi, 2012; Wacker, Dillon, & Pizzagalli, 2009) suggesting that the NAc regulates anxiety. In addition, deep

brain stimulation in the NAc attenuates anxiety in treatment-resistant depression patients (Bewernick et al., 2010; Bewernick, Kayser, Sturm, & Schlaepfer, 2012). The rodent literature also provides evidence supporting a causal relationship that inhibition of the NAc by infusion of $GABA_A$ receptor agonist or glutamatergic AMPA receptor antagonist in the NAc reduces anxiety-like behavior (da Cunha et al., 2008; Lopes et al., 2012; Reynolds & Berridge, 2001, 2002). However, studies focusing on the NAc and anxiety are much less than a massive volume of evidence emphasizing the contribution of the NAc in reward and goal-direct behaviors. A more general idea on the function of the NAc is that it serves as an interface integrating cognitive and affective information and biasing the direction and intensity of behavioral responses when appropriate action is ambiguous and uncertain (Floresco, 2015). From this perspective, it can be proposed that the function of the NAc in anxiety is to bias the behavioral intention toward defensive response in a situation with uncertain threats. Interestingly, the NAc is emerging as a brain area critical for social interaction where disruption of normal signaling contributes to social avoidance, a key facet of many anxiety disorders (Gunaydin et al., 2014; Steinman, Duque-Wilckens, & Trainor, 2019).

The NAc is a heterogeneous brain area with two primary segments: a core region around the anterior limb of the anterior commissure and a shell region at the medial and ventral side of the core in the rat brain (Heimer et al., 1997; Zahm & Brog, 1992). The shell of the NAc (NAcSh), especially the medial portion, is demonstrated to be more likely a critical node in the neural network of anxiety while the NAc core shares more features of cytoarchitecture, connectivity, and function with the dorsal striatum (reviewed in Castro & Bruchas, 2019). This section will only discuss the potential role of the NAcSh in anxiety.

The NAcSh has two major cell types. The principal projection neurons, accounting for 90-95% of all neurons in the striatum, are GABAergic MSNs. These neurons send long-range projections to the ventral pallidum, the lateral hypothalamus, the ventral tegmental area and other areas in the lower brain (Heimer et al., 1997; Zahm & Heimer, 1993). The other 5-10% neurons are the local interneurons with three subpopulations characterized by parvalbumin-expressing, somatostatin-expression, and acetylcholine-releasing (Kawaguchi, 1993; Tepper et al., 2018). Another perspective on the classification of neurons in NAc is based on the specific expression of endogenous opioid peptides. The MSNs in the NAc are composed of two distinct groups: one group that expresses dynorphin (DYN), substance P (not an opioid peptide), and type 1 dopamine receptor (DYN-MSNs or D1R-MSNs); another group that expresses enkephalin (ENK) and type 2 dopamine receptor (ENK-MSNs or D2R-MSNs) (Zhou, Furuta, & Kaneko, 2003). These two groups of neurons have comparable size and total amount (Castro & Bruchas, 2019; Zhou et al., 2003). The DYN-MSNs directly innervate both the ventral pallidum and midbrain areas while the ENK-MSNs only project to the ventral pallidum (Zhou et al., 2003). DYN and ENK can selectively activate kappa opioid receptor (KOR) and delta opioid receptor (DOR) respectively. The KORs are expressed on most MSNs in the NAc and on presynaptic terminals of glutamate, serotonin, and dopamine projections in the NAc (Al-Hasani et al., 2015; Meshul & McGinty, 2000; Minami et al., 1993). The DORs are preferentially expressed on the cholinergic interneurons (Bertran-Gonzalez, Laurent, Chieng, Christie, & Balleine, 2013) and ENK-MSNs (Banghart, Neufeld, Wong, & Sabatini, 2015). Some recent functional studies found that the DYN-KOR and ENK-DOR systems in NAcSh are involved in the regulation of aversive behavior. A study reported that optogenetic stimulation on DYN-MSNs increased local release of DYN and local infusion of KOR antagonist blocked the behavioral effect induced by

optogenetic stimulation (Al-Hasani et al., 2015). Interestingly, activation of DYN-MSNs in the dorsal part of the NAcSh induced a real-time place preference while activation in the ventral part of NAcSh induced a real-time place avoidance (Al-Hasani et al., 2015). The opposite functions of DYN-MSNs at dorsal and ventral part of the NAcSh suggest that neurons in different subregions may have distinct neural connectivity. In addition, stimulation of DYN-MSNs does not only increase DYN release in the NAcSh locally but also regulates neural activity in the ventral pallidum and midbrain. A recent study reported that real-time place avoidance induced by optogenetic stimulation of the DYN-MSNs in the NAcSh was blocked by KOR antagonist infusion in the ventral tegmental area (Soares-Cunha et al., 2019). The ENK-DOR system in NAcSh has also been shown to mediate aversive states. A study found that reduced ENK levels in the NAc was associated with higher social anxiety while local infusion of DOR agonist in the NAc had an anxiolytic effect in social interaction test after social defeat stress (Nam et al., 2019).

The NAcSh receives cortical afferents from limbic cortices including the mPFC, insular cortex, ventral hippocampus, and the basolateral amygdalar complex, and subcortical afferents from the midline thalamus and the ventral tegmental area (Brog, Salyapongse, Deutch, & Zahm, 1993; Zahm, 2000). It also receives inputs to a less extent from the ventral pallidum, sublenticular substantia innominata, lateral septum, BST, medial amygdala, preoptic area, lateral hypothalamus, parabrachial nucleus, dorsal and median raphe, locus coeruleus and a few nuclei in brainstem. Inputs from different sources may have distinct preferential target zones or cell types (Groenewegen, Wright, Beijer, & Voorn, 1999; Wright & Groenewegen, 1995). For example, the ventral mPFC projects to a band-like region in the medial part of the shell (Berendse, Galis-de Graaf, & Groenewegen, 1992); the agranular insular cortex prefers more lateral part of the shell (Wright & Groenewegen, 1996); the diencephalic afferents from the PVT

avoid cholinergic interneuron (Ligorio, Descarries, & Warren, 2009). The output of the NAcSh is mostly descending along the medial forebrain bundle and the density declines in more posterior regions (Zahm, 2000). The complexity in the neural connectivity within NAcSh makes it possible for the NAcSh to integrate information from different sources to select and orchestrate behavioral reactions. A major difference between NAcSh and the core and the dorsal striatum is the direct projection from the NAcSh to the lateral hypothalamus and preoptic area (Zahm, 2000). The connectivity of the NAcSh resembles the one of the lateral portion of the central extended amygdala suggesting that outputs from the NAcSh and BSTDL, CeL may converge on effectors in hypothalamus and brainstem (Figure 1-5) and they collectively evaluate interpreted information and select appropriate behavior at the presence of uncertain threats.

The lateral septum is a striatal-like structure extending along the medial edge of the lateral ventricle (Alheid & Heimer, 1988; Zahm, 2006). The lateral septum receives dense cortical innervation from the hippocampus and projects to the preoptic area and rostral hypothalamus which contain sparsely spiny neurons that project to other areas of the hypothalamus and the brainstem (Risold & Swanson, 1997; Zahm, 2006). Local inhibition of the lateral septum or disruption of the ventral hippocampus-lateral septum projection produces an anxiolytic effect (Menard & Treit, 1996; Trent & Menard, 2010). There is evidence showing that pharmacological or optogenetic activation of CRF type 2 receptor on the GABAergic projection neurons in the lateral septum increases anxiety-like behaviors (Anthony et al., 2014; Radulovic, Rühmann, Liepold, & Spiess, 1999). A study further showed that the projection neurons in the lateral septum in turn inhibit cells in the rostral lateral hypothalamus which sends an inhibitory projection to the paraventricular nucleus of the hypothalamus and the periaqueductal gray (Anthony et al., 2014). This circuit-targeting study showed a pathway by which the lateral

septum activates effectors in the lower brain and triggers neuroendocrine and behavioral reactions of anxiety.

1.3.5 Summary of the circuit for anxiety

The brief review of the neural network of anxiety emphasizes the interaction between multiple descending pathways. Within this highly interconnected network, information from different sources or modalities could trigger similar responses via different descending pathways converging on the same group of effectors in the hypothalamus and brainstem (Figure 1-5). Functional redundancy in multiple pathways improves the sensitivity of processing ambiguous information and lowers the probability of failure in reaction toward threatening stimuli (Calhoon & Tye, 2015). However, this interconnected structure makes studying the anxiety circuitry difficult because a disruption at any node of this network may result only in a mild reduction in one of the behavioral responses associated with anxiety. On the other hand, almost all the brain areas associated with anxiety have been shown to contribute to approach and appetitive behavior (Klumpers & Kroes, 2019). Accordingly, it is difficult to distinguish whether there is a distinct neural circuit that mediates defensive behavior or a complex neural circuit that controls the balance between defensive and approach behaviors.

Functional redundancy is one explanation for the experimental evidence showing that anxiety is processed in a distributed network. Another explanation is that the current behavioral model is too simplistic to show the functional differences between brain regions. New behavioral models based on clinical symptoms of different anxiety disorders will be needed to identify functional difference in brain circuits and to discover new therapeutic targets. In this thesis, an anxiety model related to clinical anxiety of PTSD is used to study the long-lasting increase in the level of anxiety after a traumatic/intense stress experience (Chen, Li, Li, & Kirouac, 2012). In

this model, anxiety-like responses are induced by stimuli and conditions which are not directly associated with the stressful experience.

1.3.6 A thalamic component of the anxiety circuit

Decades of research on the neural substrates underlying anxiety supports a hierarchical model of anxiety. A robust thalamic afferent to the striatal regions has not received much attention as the cortical afferent. Anatomical studies have demonstrated that the midline and intralaminar thalamic nuclei provide an intense innervation to the NAc, BST, and CeL (Berendse & Groenewegen, 1990; Groenewegen & Witter, 2004). The projections and function of the midline and intralaminar thalamic nuclei were considered to be nonspecific in that these nuclei had been presumed to provide widespread projections to the frontal cortex and relay general arousal information (Groenewegen & Berendse, 1994; van der Werf et al., 2002). However, recent studies on the anatomical and functional features of different nuclei in the midline and intralaminar thalamus revealed distinctive patterns of connectivity and functions (Groenewegen & Berendse, 1994; Vertes, Linley, & Hoover, 2015). For example, the PVT preferentially innervates the NAcSh, BSTDL, and CeL over other regions and reciprocally connects with the ventral mPFC, ventral subiculum, and agranular insular cortex (reviewed in Kirouac, 2015; Vertes, Linley, & Hoover, 2015; see Figure 1-7). The connectivity suggests that the PVT may have a direct influence on the integration process of anxiety. Functional studies also find that the PVT gets activated by a variety of stressors, and lesions or inhibition of the PVT lead to reduction in anxiety or fear response (see Section 1.4.4). The evidence supports the involvement of the PVT in the regulation of defensive behaviors including anxiety and fear.

1.4 The PVT as a hub in the neural circuitry for fear and anxiety

The PVT is a member of the midline and intralaminar group of nuclei in the dorsal thalamus. Nuclei in the dorsal thalamus can be divided into three groups according to their organization of connections: the relay nuclei, the association nuclei, and nonspecific nuclei (Groenewegen & Witter, 2004; Vertes, Linley, Groenewegen, & Witter, 2015). The relay nuclei receive specific sensory or motor information through ascending pathways and project to discrete regions of the cerebral cortex. The association nuclei reciprocally connect to associational areas of the cortex. Nonspecific nuclei located in the midline and intralaminar thalamus receive information from brainstem and hypothalamus and send projections to subcortical regions like the basal forebrain nuclei in addition to their reciprocal connection with a broad area of the limbic cortices. The subcortical efferent is one of the major differences between the midline and intralaminar thalamus and other parts of the dorsal thalamus. The function of the midline and intralaminar thalamus had been traditionally postulated as nonspecific regulation of arousal and attention according to their "nonspecific" connectivity. However, recent anatomical studies have shown that nuclei in this region of the thalamus innervate unique and confined cortical and subcortical regions, and each member in this thalamic nuclei group has its distinct function (reviewed in Vertes, Linley, & Hoover, 2015). For example, the nucleus reuniens, in contrast to other parts of the midline thalamus, has few subcortical outputs but sends a strong projection to the hippocampus and probably is a critical node in the neural circuit regulating spatial memory. In contrast, the PVT is a midline thalamic nucleus sending the most prominent projection to the NAc and central extended amygdala and receiving more peptidergic fiber innervation compared to other midline and intralaminar thalamic nuclei (reviewed in Kirouac, 2015; Vertes, Linley, & Hoover, 2015). The anatomical features of the PVT have led to a surge of interest in its function

in defensive behaviors and reward-seeking behaviors. This section will introduce the involvement of the PVT in fear and anxiety.

1.4.1 Neurons in the PVT

The PVT is the dorsal most nucleus of the midline thalamus. It lies directly ventral to the dorsal part of the third ventricle (Figure 1-6). The anterior-posterior extension of the PVT is relatively long (Figure 1-6B), about 3 mm in the rat brain and 2 mm in the mouse brain. The PVT has usually been assigned into the anterior PVT (aPVT) and posterior PVT (pPVT) based on the difference in their connectivity and functions. In contrast, the morphological, electrophysiological, and neurochemical properties of the PVT neurons have minor variations along the anterior-posterior axis (reviewed in Kolaj, Zhang, Hermes, & Renaud, 2014). Neurons in the PVT are primarily excitatory neurons expressing vesicular glutamate transporter 2 (Myers, Mark Dolgas, Kasckow, Cullinan, & Herman, 2014; Papp et al., 2012). The PVT and other midline thalamic nuclei in rodent brain do not contain GABAergic interneuron (Arcelli, Frassoni, Regondi, Biasi, & Spreafico, 1997; Bentivoglio, Balercia, & Kruger, 1991; Christie, Summers, Stephenson, Cook, & Beart, 1987). The reticular nucleus of the thalamus provides a major GABAergic input to the midline and medial thalamus (Chen & Su, 1990; Li & Kirouac, 2012; Vertes, Linley, Groenewegen, et al., 2015). The cell bodies of PVT neurons range from 12 to 20 μm while their dendrites extend widely to a field of ~200 μm in diameter (Richter, 2005; Unzai, Kuramoto, Kaneko, & Fujiyama, 2017; Zhang, Renaud, & Kolaj, 2009). The PVT neuron usually has a long axon with many collaterals (branches of axon) that bifurcates extensively in the terminal regions (Unzai et al., 2017). The distribution and functional consideration of PVT axon collaterals will be discussed in Section 1.4.4.3.

Figure 1-6 Location of the PVT in rat brain

Location of the PVT (highlighted by red dash line) in a rat brain from a coronal view (**A**) and a sagittal view (**B**). Figures are adapted from http://brainmaps.org (see also Mikula et al. 2007).

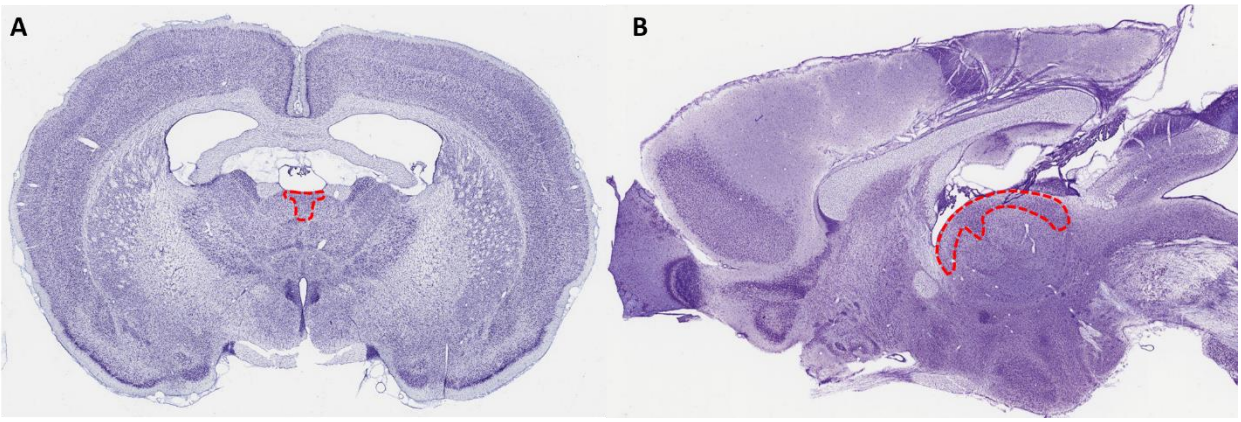

1.4.2 Inputs to the PVT

The PVT receives projections from many nuclei in the brainstem and the hypothalamus. A major characteristic of the PVT afferents compared to other midline and intralaminar thalamic nuclei is that the PVT receives heavy projections from almost all the regions in the hypothalamus including various peptidergic innervations (Li & Kirouac, 2012; Risold, Thompson, & Swanson, 1997; Vertes, Linley, Groenewegen, et al., 2015; Vertes, Linley, & Hoover, 2015). Another main source of inputs to the PVT is the limbic cortices (Li & Kirouac, 2012). The PVT also receives thalamic GABAergic inputs from the reticular nucleus of the thalamus which also sends GABAergic projection to all components of the midline and intralaminar thalamus (Li & Kirouac, 2012; Chen & Su, 1990). Some minor inputs are from the septal area, the BST, and the parasubthalamic nucleus (Li & Kirouac, 2012).

The inputs to the PVT are not the main focus of this thesis. Nevertheless, the following sections will briefly review the PVT afferents from the brainstem, hypothalamus, and cortex to postulate the type of information that the PVT provides to the neural network regulating fear and anxiety.

1.4.2.1 Inputs from the brainstem and hypothalamus

The PVT is innervated by many brainstem regions associated with arousal and visceral functions (reviewed in Kirouac, 2015). For example, the periaqueductal gray, parabrachial nucleus, and nucleus of the solitary tract are likely to relay visceral and nociceptive sensory information to the forebrain regions including the PVT (Krout & Loewy, 2000a, 2000b). Most of these ascending projections from the brainstem project to many members in the midline and intralaminar thalamic nuclei group and do not innervate the PVT exclusively (Krout, Belzer, & Loewy, 2002; Vertes, Linley, & Hoover, 2015). The ascending pathway relaying arousal and visceral information to the forebrain is traditionally proposed to regulate general arousal level (Krout et al., 2002; van der Werf et al., 2002). However, lesion studies reported that lesions of the PVT or the complete midline and intralaminar thalamus have no effect on sleep-wake cycle (Ebling, Maywood, Humby, & Hastings, 1992; Nakahara, Fukui, & Murakami, 2004) implying that the arousal information transmitted by the midline and intralaminar thalamus may not contribute to the sleep-wake cycle but other arousal-related functions such as the elevated vigilance associated with anxiety.

The hypothalamus is another major source of inputs to the PVT. A prominent characteristic of the hypothalamic afferents to the PVT is that many regions of the hypothalamus project to the PVT compared to other midline and intralaminar thalamic nuclei which receive inputs from more restricted number of areas in the hypothalamus (Risold et al., 1997). The hypothalamic afferent

fibers contain a large number of neuropeptides. For example, the PVT receives fibers containing cholecystokinin from the dorsomedial nucleus (Otake, 2005), fibers containing arginine vasopressin and gastrin-releasing peptide from the suprachiasmatic nucleus (Mikkelsen, Larsen, O'Hare, & Wiegand, 1991; Sofroniew & Weind, 1978; Watts & Swanson, 1987), fibers containing cocaine- and amphetamine-related transcript (CART) from the arcuate nucleus mostly (Kirouac, Parsons, & Li, 2006). In particular, the PVT receives fibers containing orexins from lateral and perifornical hypothalamus which are denser in the PVT region compared to other nuclei in the thalamus (Kirouac, Parsons, & Li, 2005; Parsons, Li, & Kirouac, 2006).

Orexins, also known as hypocretins, are a family of neuropeptides synthesized and released by orexinergic neurons located exclusively in the lateral and perifornical hypothalamus (de Lecea et al., 1998; Sakurai et al., 1998). There are two bioactive forms of orexins, orexin-A and orexin-B, which are derived from the same precursor prepro-orexin. The orexins bind to two G-protein coupled receptors which are the orexin-1 receptor and the orexin-2 receptor (de Lecea et al., 1998; Sakurai et al., 1998). The orexin-1 receptor has a greater affinity for orexin-A than orexin-B whereas the orexin-2 receptor has similar affinity for both orexin-A and orexin-B (Sakurai et al., 1998). Orexin receptors have been shown to be able to couple to at least three G-protein families (Gq, Gi/o, Gs; reviewed in detail in Kukkonen and Leonard, 2014). Activation of orexin receptors leads to depolarization of the postsynaptic neurons via opening of nonselective cation channels and/or closing of K^+ channels (reviewed in Kolaj et al., 2014). Orexinergic neurons in the hypothalamus send widespread projections throughout the brain including many regions in the hypothalamus, locus coeruleus and many other nuclei in the brainstem and midbrain, lateral septum, BST, CeL, PVT, central medial nucleus of the thalamus, and cerebral cortex with less prominent projections (Nambu et al., 1999; Peyron et al., 1998).

Similarly, orexin receptors are distributed in brain regions with orexin fibers (Marcus et al. 2001). Of all the thalamic nuclei, the PVT is especially notable for its very dense orexin innervations and receptor expression of both the orexin-1 receptor and the orexin-2 receptor on the soma and dendrites of PVT neurons (Kirouac et al., 2005; Marcus et al., 2001; Parsons et al., 2006). Electrophysiological recording in rat brain slices showed that exogenous orexins application induces slowly rising and prolonged membrane depolarizations in PVT neurons and alters their firing patterns (Kolaj, Doroshenko, Yan Cao, Coderre, & Renaud, 2007). The orexin signaling system has been demonstrated to regulate a number of adaptive behaviors: orexin is named from its role in promoting food consumption (Sakurai et al., 1998); orexin is engaged in arousal and that genetic ablation of prepro-orexin produces disruption in the maintenance of arousal and narcolepsy (e.g. Chemelli et al., 1999); orexin is also involved in the modulation of reward seeking (e.g. Aston-Jones et al., 2010) and stress-induced behavioral and neuroendocrine responses (e.g. Bonnavion, Jackson, Carter, de Lecea, 2015; Chang et al., 2007). The Kirouac group has first launched a series of studies on the behavioral effect of orexin signaling in the PVT in fear and anxiety: local infusion of orexins at the PVT increases anxiety-like behavior while blocking orexin receptors in the PVT has an anxiolytic effect (Li, Li, Sui, & Kirouac, 2009; Li et al., 2010a, 2010b; see Section 1.4.4.1 and Chapter 2 for more details). The evidence suggests that orexins can potently act on the PVT neurons and probably amplify their effect via the PVT outputs to other brain regions that mediate anxiety-like response. Therefore, the PVT is postulated to be the node in the thalamus by which the orexins transmission influence anxiety.

The PVT also contains dopamine fibers originated from dopaminergic neurons scattered in the hypothalamus and the periaqueductal gray (S. Li, Shi, & Kirouac, 2014; Otake & Ruggiero, 1995). The function of dopaminergic transmission in the PVT has not been addressed

adequately. One study showed that overexpression of D2Rs in the PVT attenuated cocaine locomotor sensitization whereas had no effect on acquisition or expression of conditioned fear, or anxiety-like behaviors in the EPM or open field test (Clark et al., 2017).

1.4.2.2 Inputs from the cerebral cortex

The limbic cortex is one of the main sources of inputs to the PVT. Retrograde tracing studies demonstrated that neurons in the layer 6 of the mPFC and the agranular insular cortex innervate the PVT (Li & Kirouac, 2012). The ventral subiculum also innervates the PVT (Chen & Su, 1990; Li & Kirouac, 2012). Noticeably, the distribution of the cortical inputs to the PVT has a topographic difference along the anterior-posterior extent of the PVT that the ventral subiculum primarily projects to the aPVT while the insular cortex and the ventral mPFC provide a more robust innervation to the pPVT than aPVT (Li & Kirouac, 2012). In contrast, the distribution of fiber terminals from the brainstem and hypothalamus show little difference between the aPVT and pPVT. The functional implications of the topographic organization of the cortical inputs to the PVT should be considered along with the distribution of the neuronal outputs from the aPVT and pPVT.

1.4.3 Outputs from the PVT

One major difference between the midline thalamus and intralaminar thalamus is that the midline thalamus innervates many limbic forebrain structures while the output of the intralaminar thalamus is almost restricted to sensorimotor structures (Groenewegen & Witter, 2004). The output of PVT is more strongly weighted to subcortical limbic structures whereas other midline nuclei predominantly innervate limbic areas of the cortex (Vertes, Linley, Groenewegen, et al., 2015; Vertes, Linley, & Hoover, 2015). Specifically, the PVT sends heavy projections to a basal forebrain continuum that extends from the NAc and ventral regions of the

caudate putamen, to the BST, interstitial nucleus of posterior limb of anterior commissure, and ends in the central nucleus of the amygdala (Li & Kirouac, 2008; Vertes & Hoover, 2008). In particular, the NAcSh, BSTDL, and CeL, which are the striatal structures that appear to be a prominent part of the neural circuits for fear and anxiety, receive the most intense PVT innervation (Li & Kirouac, 2008). In contrast, the PVT projects relatively weakly to the limbic cortices including the mPFC, agranular insular cortex, ventral subiculum, and basolateral amygdalar complex (Li & Kirouac, 2008; Vertes & Hoover, 2008). The PVT also send weak projections to the suprachiasmatic, arcuate, dorsomedial and ventromedial nuclei of the hypothalamus, the medial amygdala, and the lateral septum (Li & Kirouac, 2008; Vertes & Hoover, 2008).

This section will review the distribution of the PVT outputs with an emphasis on the projection to the NAc, BSTDL, and CeL. Functional indications of the different projection patterns of the aPVT and pPVT, and the organization of axon collaterals will also be discussed briefly.

1.4.3.1 The PVT projection to NAc

It has been confirmed by many tracing studies that the NAc receives a dense innervation from the PVT (Berendse & Groenewegen, 1990; Brog et al., 1993; Li & Kirouac, 2008; Otake & Nakamura, 1998; Su & Bentivoglio, 1990; Vertes & Hoover, 2008). In particular, the medial NAcSh is more densely innervated than the lateral shell and the core of the NAc (Li & Kirouac, 2008; Otake & Nakamura, 1998; Vertes & Hoover, 2008). Single-neuron tracing of a small number of cells in the PVT showed that the axons innervating NAc give off collaterals throughout large portions of the NAc and bifurcate extensively there (Unzai et al., 2017). Anterograde tracing studies found that both the aPVT and pPVT innervate the NAcSh heavily

while the pPVT also sends relatively dense projections to the core of the NAc and ventromedial part of the caudate putamen (Li & Kirouac, 2008). Retrograde tracing studies with tracers injected in the NAcSh found that a large number of neurons were labeled in both the aPVT and pPVT (Li & Kirouac, 2008; Otake & Nakamura, 1998). These results suggest that both the aPVT and pPVT project densely to the NAcSh while the distribution of fibers innervating regions adjacent to the NAcSh are slightly different.

The midline thalamus, mPFC, basolateral amygdalar complex, and ventral hippocampus are the major sources of glutamatergic inputs of the NAc (Brog et al., 1993). The PVT provides the densest projection to the NAc among the midline thalamic nuclei (Berendse & Groenewegen, 1990). Groenewegen and colleagues have published a series of studies describing the distribution of afferents in the NAcSh from different sources (Berendse et al., 1992; Groenewegen et al., 1999; Wright, Beijer, & Groenewegen, 1996; Wright & Groenewegen, 1995, 1996). They found that the distribution of PVT afferents in the NAc overlaps with that of the inputs from the infralimbic cortex and ventral subiculum while avoids the regions innervated by the basolateral amygdalar complex. The anatomical and functional subregions of the NAc have not been studied adequately and further discoveries related with subregional specialization may probably provide novel insights on how different neural pathways regulate adaptive behaviors.

Many studies have reported that the PVT is activated by stressful and aversive conditions (reviewed in Kirouac, 2015). Accordingly, a PVT projection to the NAc may mediate stress-induced behavioral effects on approach and avoidance because of the prominent role of the NAc in these motivational behavioral tendencies. Optogenetic activation of the PVT neurons that project to the NAc induces real-time place aversion (Do-Monte, Minier-Toribio, Quiñones-Laracuente, Medina-Colón, & Quirk, 2017; Zhu, Wienecke, Nachtrab, & Chen, 2016) suggesting

that the activation of this pathway is associated with aversive behavioral responses. There is some experimental evidence showing that the PVT-NAc projection also mediates social avoidance induced by chronic social defeat (Christoffel et al., 2015) and conditioned avoidance induced by morphine withdrawal (Zhu et al., 2016). The activity of the PVT-NAcSh projection is also related to inhibition of approach behaviors. For example, a study showed that optogenetic activation of the neurons in the aPVT that project to the NAc abolished food seeking behavior while inhibition of the aPVT-NAc projection increased food seeking (Do-Monte et al., 2017). Interestingly, the aPVT-NAc pathway inhibition only enhanced food seeking when the food reward was omitted while had no effect when reward was available. The author explained this effect by postulating that reward omission triggers frustration with the PVT being recruited under such negative conditions (Do-Monte et al., 2017). In summary, the PVT provides a dense projection to the NAcSh through which the PVT may influence anxiety by promoting avoidance and suppressing approach.

1.4.3.2 The PVT projection to central extended amygdala

A dense projection from the PVT to the CeL and BSTDL is one of the reasons that the PVT receives attention for its role in fear and anxiety. Anterograde studies have shown that the PVT provides moderate to dense projections to several subcortical areas that belong to the central extended amygdala, including the BSTDL, CeL, and some transitional area between them (Li & Kirouac, 2008; Moga, Weis, & Moore, 1995; Otake & Nakamura, 1998; Vertes & Hoover, 2008). Fibers from the aPVT to these regions are weak and relatively evenly distributed in both the medial and lateral portion of the central extended amygdala. In contrast, anterograde tracers injected in the pPVT resulted in densely labeled fibers in the BSTDL and CeL (Li & Kirouac, 2008), which belong to the lateral portion of the central extended amygdala. Retrograde tracing

result also confirmed that the pPVT contains more cells innervating the BSTDL and CeL compared to the aPVT (Li & Kirouac, 2008).

The BSTDL and CeL are striatal-like structures having GABAergic medium-sized spiny neurons labeled by different molecular markers (see Section 1.3.4). Evidence from an anterograde tracing study has shown that the fiber terminals labeled by tracer injected in the PVT are located close to the CRF immunopositive neurons (Li & Kirouac, 2008) indicating potential contacts with CRF+ neurons in the BSTDL and CeL. This hypothesis is consistent with an observation from a recent study showing that CRF+ neurons in the CeL are more likely to respond to optogenetic stimulation of neural fibers originated from the PVT than SOM+ and PKCδ+ neurons in the CeL (Pliota et al., 2020). Another study using a retrograde monosynaptic tracing method showed that the PVT neurons synapse on both PKCδ+ neurons and SOM+ neurons in the CeL with a higher proportion of PVT neurons that innervate SOM+ neurons (Penzo et al., 2015). Since a study found that these three types of GABAergic neurons in the CeL are merely overlapped (Fadok et al., 2017), the selectivity of PVT innervation needs more evidence to address.

1.4.3.3 The PVT projection to cortex

The PVT projects to a few cortical and cortical-like regions including the ventral mPFC (ventral prelimbic, infralimbic, and dorsal peduncular cortices), dorsal and ventral agranular insular cortex, ventral subiculum, and basolateral amygdala complex (Li & Kirouac, 2008; Moga et al., 1995; Su & Bentivoglio, 1990; Vertes & Hoover, 2008). Only the aPVT innervates the ventral subiculum (Li & Kirouac, 2008). Compared to the projection to subcortical regions, the PVT projection to the cortex is weaker and the proportion of PVT neurons innervating cortex is lower. A single-neuron axon tracing study reported the axonal trajectory of a few PVT neurons

(Unzai et al., 2017). They found that single PVT neuron can innervate both subcortical and cortical areas while the axonal arborization (extent of bifurcating) of the axon branch innervating the cortex is much lower than that of the branch innervating striatal-like structures. There is no evidence supporting that the PVT contains neurons that exclusively project to the cortex.

1.4.4 The PVT and the neural network for anxiety and fear

The neural connection of the PVT can be summarized into three points: 1) the PVT receives neurochemically diverse projections from the brainstem and hypothalamus conveying internal state information; 2) the PVT provides robust innervation to the NAcSh, BSTDL, and CeL which mediate adaptive behaviors including anxiety and fear; 3) the PVT reciprocally connects with some limbic cortical areas (mPFC, agranular insular cortex, and ventral subiculum) which also project to NAcSh and central extended amygdala (see Figure 1-7).

Figure 1-7 A diagram of the basic organization of the neural connectivity of the PVT

A diagram summarizes the connectivity of the PVT based on rodent studies. The PVT receives neurochemically diverse projections from the brainstem and hypothalamus conveying visceral and arousal related information. In turn, the PVT provides robust innervation to a continuum that includes the NAc and central extended amygdala which mediates adaptive behaviors including anxiety and fear. The PVT is also reciprocally connected with some limbic cortical areas which also project to the NAc and central extended amygdala.

Abbreviations: AI, insular cortex, agranular; BSTDL, bed nucleus of stria terminalis, dorsolateral; CeL, central nucleus of amygdala; IL, infralimbic cortex; NAcSh, nucleus accumbens, shell; PL, prelimbic cortex; PVT, paraventricular nucleus of thalamus; vSub, subiculum, ventral.

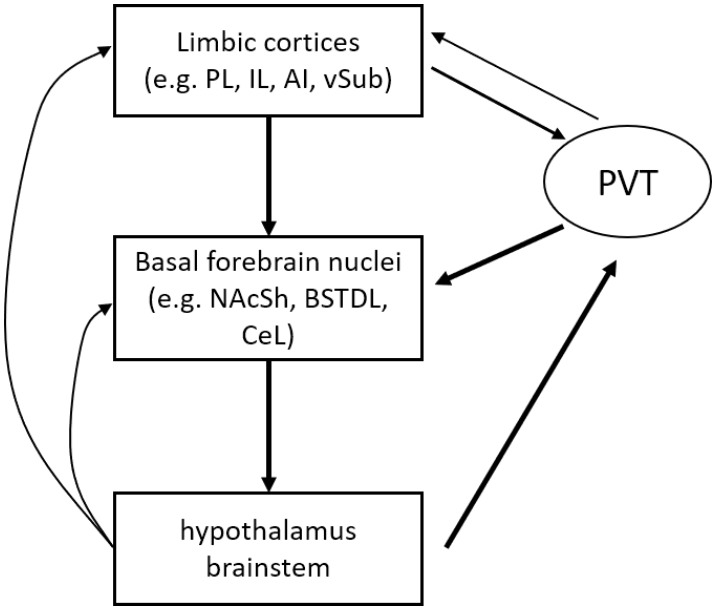

The connectivity of the PVT indicates that the PVT is a part of the neural circuitry for anxiety and fear for a few reasons. First, the limbic cortices form an interconnected network interpreting threat-related information (Calhoon & Tye, 2015). The PVT is reciprocally connected with almost every component of this limbic cortical network. Second, the PVT and these limbic cortices converge on the same striatal-like structures mediating many behaviors related with anxiety and fear. Third, the brain regions in the brainstem and hypothalamus which provide inputs to the PVT receive and process not only visceral and homeostatic sensation but also threat-related nociceptive information (Saper & Stornetta, 2015). In addition, these areas also project directly to the effectors as well as the limbic and striatal-like regions. For example, the lateral part of the parabrachial nucleus projects to the paraventricular nucleus of the hypothalamus, the agranular insular cortex, the BSTDL, and CeL (Alden, Besson, & Bernard, 1994; Bernard, Alden, & Besson, 1993; Jasmin, Granato, & Ohara, 2004; Sarhan, Freund-Mercier, & Veinante, 2005). Taken together, the PVT may act as a hub in the neural circuitry for anxiety and fear which integrates and relays the threat-related sensory information with internal state information from the lower brain into the striatal-like components in the circuitry as well as amplify or modulate the cortical influence on the striatal-like structures by interacting with limbic cortices and cortical afferents in the NAcSh and central extended amygdala.

The idea that the PVT relays internal state information to the neural circuit regulating negative emotions like fear and anxiety can be translated into specific experimental hypotheses. Here I would like to list some specific functional assumptions along with experimental evidence about whether and how the PVT contributes to innate fear or anxiety responses to direct threats (unconditioned response) and how the PVT is involved in learned response (conditioned fear response).

1.4.4.1 PVT and innate fear and anxiety

The PVT receives strong projections from the brainstem and hypothalamus conveying viscerosensory information associated with nociception and it is hypothesized that the PVT can function as an emotional arousal center (Kirouac, 2015; van der Werf et al., 2002). This hypothesis is supported by many studies that reported an increased number of cFos-positive cells in the PVT following exposure to stressful conditions including aversive visceral stimulation (Yasoshima, Scott, & Yamamoto, 2007), food deprivation (Timofeeva & Richard, 2001), and footshock (Beck & Fibiger, 1995; Yasoshima et al., 2007). Most of these stressors can induce fear- and anxiety-like response in rodent models. The above evidence suggests that the PVT is sensitive to threatening and aversive conditions regardless of the sensory modality and may be involved in a variety of stress-induced behavioral responses.

The Kirouac group has launched a series of studies focusing on how the PVT mediates innate fear and anxiety after the observation of intense projection from the PVT to the NAcSh, BSTDL, and CeL. We have been interested in the orexinergic innervation from orexin neurons in the lateral hypothalamus to the PVT because orexins regulate arousal levels involved in responses to stress (España, Valentino, & Berridge, 2003; Furlong, Vianna, Liu, & Carrive, 2009), and orexin fibers are expressed much more densely in the PVT region compared to other areas in the midline thalamus (Kirouac et al., 2005). Previous studies from the Kirouac group found that local infusion of orexin-A or orexin-B in the PVT in rats reduces exploration and produces freezing in a novel environment (Li et al., 2009) and has an anxiogenic effect in the EPM test (Li et al., 2010b). Furthermore, blocking orexin-2 receptors in the PVT by local infusion of orexin-2 receptor antagonist TCSOX229 attenuates anxiety produced by exposure to footshocks in rats while local infusion of orexin-1 receptor antagonist SB334867 had no effect

on anxiety (Li et al., 2010b). These findings suggest that the PVT may act as a relay site which receives stress-related signals from the orexinergic system and activates brain areas which have a more direct control over defensive responses.

1.4.4.2 PVT and conditioned fear

In addition to a robust bottom-up innervation from the hypothalamus and brainstem, the PVT also receives a strong top-down cortical innervation. There is accumulating evidence showing that the mPFC is activated by conditioned stimuli which are associated with an aversive event (reviewed in Courtin et al., 2013). In addition, a few studies reported that the cFos expression is increased in the PVT after exposure to footshock cue or context (conditioned stimuli) (Beck & Fibiger, 1995; Park & Chung, 2019; Yasoshima et al., 2007). Both prelimbic and infralimbic cortices send a projection to the PVT (Li & Kirouac, 2012; Vertes, 2004) by which the mPFC may activate the PVT at the presence of conditioned stimuli. Therefore, it can be hypothesized that this cue-related signal activates PVT neurons which in turn influence the neural activity in the microcircuit formed by inhibitory neurons in the CeL to mediate conditioned fear (Y. Li, Dong, Li, & Kirouac, 2014; Do-Monte, Quiñones-Laracuente, et al., 2015).

1.4.4.3 Axon collaterals and PVT outputs

Any postulated functions of the PVT based on its anatomical features should consider whether PVT neurons project to more than one target via axon collaterals. One neuron has only one axon, but the axon may bifurcate into several branches and single neuron can innervate multiple targets directly via axon collaterals (Parent et al., 2000; Prensa, Giménez-Amaya, Parent, Bernácer, & Cebrián, 2009). For example, an MSN in the NAcSh can project to the

ventral pallidum, lateral hypothalamus, midbrain areas, and its neighboring area in the NAcSh via collaterals (Tripathi, Prensa, Cebrían, & Mengual, 2010).

A single-neuron tracing study has shown that all the traced PVT neurons (n = 5) provided collaterals that innervated more than three areas in the basal forebrain nuclei and limbic cortices (Unzai et al., 2017). Although there is currently no overall estimation of the level of collateralization or the topographic organization of collaterals from PVT neurons, such information can provide important insights on how the PVT functions in fear and anxiety. Specifically, if a low level of collateralization is observed, it could suggest that the PVT may contain subpopulations of neurons with specific downstream targets by which the PVT can independently mediates certain types of behavioral responses. For example, PVT neurons innervating the CeL could selectively mediate the regulation of conditioned fear response while PVT neurons innervating the BSTDL could mediate anxiety. From this perspective, the PVT would be working as a sorter that collects and integrates information from the hypothalamus, brainstem, and limbic cortices and assigns them into different striatal-like nuclei in the basal forebrain nuclei to modulate different types of adaptive behaviors. In contrast, if a high level of collateralization is observed, it could suggest that PVT neurons regulate the activity in multiple downstream targets simultaneously. From this perspective, the PVT would be working as a broadcaster which mediates a general factor of stress, fear, anxiety, and other types of emotional response. The PVT may also be composed of neurons which exhibit variable amounts of collaterals. For example, some neurons may influence one target preferentially and other neurons may influence multiple targets simultaneously via collaterals.

1.5 Objectives and hypotheses

The objective of this thesis is to explore the involvement of the PVT in fear and anxiety. The experiments presented are a continuation and closely related to previously published findings from the Kirouac group. All data were collected in rat models.

The objective of experiments in Chapter 2 is to determine the role of PVT in conditioned fear. The specific hypotheses were: 1) lesions of the pPVT reduce the acquisition and expression of conditioned fear memory; 2) blocking of orexin receptors in the pPVT attenuates conditioned fear expression.

The objective of experiments in Chapter 3 is to identify the collateralization of PVT projection. The specific hypotheses were: 1) the PVT projections to the NAcSh, BSTDL, CeL originate from distinct subpopulations of neurons; 2) the projection-specific subpopulations of PVT neurons respond differently to stress events.

The objective of the experiment in Chapter 4 is to determine the role of the PVT-NAcSh pathway in stress-induced fear and anxiety. The hypothesis was that inhibition of the PVT-NAcSh pathway attenuates stress-induced conditioned fear and anxiety-like responses in stress-susceptible individuals.

Chapter 2 The PVT mediates conditioned fear expression

The experiments presented in Chapter 2 were published in the following two papers:

Li, Y., Dong, X., Li, S., & Kirouac, G. J. (2014). Lesions of the posterior paraventricular nucleus of the thalamus attenuate fear expression. Frontiers in Behavioral Neuroscience, 8(March), 94. https://doi.org/10.3389/fnbeh.2014.00094

Dong, X., Li, Y., & Kirouac, G. J. (2015). Blocking of orexin receptors in the paraventricular nucleus of the thalamus has no effect on the expression of conditioned fear in rats. Frontiers in Behavioral Neuroscience, 9(June), 161. https://doi.org/10.3389/fnbeh.2015.00161

These experiments were done as part of an ongoing collaboration between the Dr. Kirouac's laboratory at the University of Manitoba and Dr. Li's laboratory at the Institute of Psychology, Chinese Academy of Sciences. The introduction of this chapter will review the background knowledge at the time when the research was carried out. After the dissemination of the findings of these experiments at conferences and journals, other research groups confirmed our findings and provided further evidence that the PVT mediates conditioned fear via a projection to the CeL (Do-Monte, Quiñones-Laracuente, et al., 2015; Penzo et al., 2015).

2.1 Introduction

The PVT is in a unique position to influence fear through its direct projection to the CeL (Li & Kirouac, 2008; Moga et al., 1995; Vertes & Hoover, 2008). In addition, the PVT also receives inputs from the prelimbic and infralimbic cortex (Chen & Su, 1990; Li & Kirouac,

2012) which are activated by the CS previously associated with fear-inducing footshocks. There is evidence showing that the PVT can be activated by footshocks and contextual cues previously associated with footshocks (Beck & Fibiger, 1995; Yasoshima et al., 2007). The activation of the PVT after footshocks as well as other types of stress could be mediated by a type of neuropeptide called orexins which are synthesized exclusively in the neurons in the hypothalamus (de Lecea et al., 1998; Sakurai et al., 1998). The orexin peptides play a key role in maintaining aroused state and regulating the behavioral responses to stressful conditions (España et al., 2003; Furlong et al., 2009; Winsky-Sommerer et al., 2004). Of all the thalamic nuclei, the PVT is especially notable for its very dense orexin innervations and receptor expression of both orexin-1 receptor and the orexin-2 receptor on the soma and dendrites of PVT neurons (Kirouac et al., 2005; Marcus et al., 2001; Parsons et al., 2006). Indeed, our research group was the first to show that administrations of orexin-A or orexin-B in the PVT produced an anxiogenic effect (Li et al., 2009, 2010a, 2010b). Furthermore, we found that the mRNA of orexin peptides' precursor prepro-orexin was upregulated and correlated with anxiety-like behavior at one to two weeks after footshock exposure indicating an increase in the baseline activity of orexin neurons following footshock stress, and blocking orexin-1 and orexin-2 receptors by systemic infusion of a dual orexin receptor antagonist reduced fear- and anxiety-like responses in shocked rats at two weeks after footshock (Chen, Wang, et al., 2014). Another study from our group found that blocking of orexin-2 receptors but not orexin-1 receptors in the PVT attenuated the increase in anxiety produced by exposure of rats to a series of footshocks (Li et al., 2010b) indicating that footshock stress leads to an enhanced activity of orexin neurons and possibly the release of orexins in the PVT where they promote anxiety-like behavioral responses. However, the

contribution of the PVT to conditioned fear including the contribution of orexins in the PVT had not been investigated prior to this study.

This chapter reports on experiments in which the effect of lesions or blocking orexin receptors in the posterior portion of the PVT (pPVT) on the acquisition and expression of conditioned fear response was examined. The pPVT instead of the whole PVT was targeted because this part sends a dense projection to the CeL, the area most associated with conditioned fear. In *Experiment 1*, we examined if electrolytic lesions confined to the pPVT interfered with the acquisition, expression, and extinction session of conditioned fear memory. In *Experiment 2 and 3*, we microinfused a dual orexin receptor antagonist (DORA) in the pPVT to determine if orexin receptors contribute to conditioned fear associated with an auditory tone (*Experiment 2*) and conditioned fear associated with the shock context (*Experiment 3*). We also examined whether DORA had an anxiolytic effect to further characterize the role of orexin receptors in the PVT.

2.2 Methods

2.2.1 *Experiment 1*: effect of pPVT lesions on conditioned fear expression and acquisition

2.2.1.1 Animals and housing

A total of 37 adult male Sprague-Dawley rats (Vital River Laboratory Animal Technology Co. Ltd., Beijing, China) were used for *Experiment 1*. The rats weighing 260–280 g at the time of arrival were housed individually in cages kept in a room maintained on a 12 h/12 h light/dark cycle (lights on at 07:00) with controlled temperature (20–24°C) and humidity (40–70%). All the rats had free access to food and water. Rats were handled for 2 min on alternate days during a 7-

day adaptation period. All the behavioral training and tests were done in the light cycle of the day (09:00–17:00). All procedures were conducted according to the National Institutes of Health Guide for the Care and Use of Laboratory Animals. The protocols were approved by the Research Ethics Committee of Institute of Psychology, Chinese Academy of Sciences.

2.2.1.2 Experimental procedure and timeline

Fear conditioning was conducted in a standard operant conditioning chamber (MED Associates, St. Albans, VT, USA). Bar-pressing for palatable food was trained as an operant behavior before fear conditioning (the suppression ratio of bar-pressing along with freezing time were used as indicators of fear level in the subsequent fear expression test). A food restriction schedule was adopted for the subsequent bar-pressing training for palatable food. After 7 days from the start of the food restriction schedule, the bar-pressing training with a variable interval (VI) schedule started. It took 7 to 10 days to establish a stable bar-pressing response in the operant chamber. Then we did the first fear conditioning session. One day later we did stereotaxic surgery to conduct electrolytic lesion in the midline thalamus. After 7 days of recovery, the ability to bar press for sucrose pellet was re-trained for one or two days to restore pre-surgical level.

An important part of this experiment was the series of behavioral tests on conditioned fear memory listed below. We examined conditioned fear expression and conducted fear extinction in the same behavioral session by repeatedly presenting CSs. One day later we tested the retrieval of extinction memory. Two days later the second fear conditioning session was conducted in a novel chamber with a different tone. The chamber for the second fear conditioning did not have a bar or food magazine. Two days later we used a progressive ratio (PR) schedule for bar-pressing to measure the motivation for food. One day later, we started a 24-hour food deprivation and

measured the motivation for food with PR schedule again. The timeline of behavioral procedures is also presented in Table 2-1.

Table 2-1 Timetable of the major procedures of *Experiment 1* in Chapter 2

Timepoint	Behavioral session
Day 1	Food restriction started (lasting one month)
Day 8-17	Bar-pressing training with VI schedule
Day 18	1st Fear conditioning
Day 19	Midline thalamus lesion surgery
Day 26	Restoration of bar-pressing
Day 28	Conditioned fear expression test and extinction learning
Day 29	Extinction memory retrieval test
Day 31	2nd Fear conditioning
Day 33	Motivation test with PR schedule in non-deprived rats
Day 35	Motivation test with PR schedule in deprived rats

2.2.1.3 Food Restriction

After one week of adaptation, the animals were placed on a food restriction schedule which lasted throughout the behavioral procedures. During the food restriction, rats were given 10–15 g of regular chows per day until they reached 85% of their free-feeding weights. After they reached the criterion, the size of daily meal was adjusted to maintain their reduced body weight. During behavioral procedures, chow food was given after test.

2.2.1.4 Bar-Pressing Training

Rats were trained to bar press for palatable food using a standard operant conditioning chamber (MED Associates, St. Albans, VT, USA). The chamber consisted of a stainless-steel grid floor for the delivery of footshocks, a lever on one wall for bar-pressing, and a speaker

mounted to the ceiling of the chamber for the delivery of tones. The chamber was housed in a sound-attenuating box to reduce ambient noise to 60 dB. A standard sugar pellet (45 mg per pellet, Bio-Serv, Frenchtown, NJ, USA) was used as the food reward for bar-pressing. Pellet delivery was controlled by a computer running the software MED-PC (MED associates, St. Albans, VT, USA). The rats were trained to bar press for sugar pellets during 30-min sessions using a variable interval (VI) schedule. The initial reinforcement ratio was VI2 (one pellet was available as a reward for bar press every 2 s on average) and the ratio was increased gradually (VI5, VI10, VI30, VI60) until rats reached a minimum of 15 presses per minute (7–10 days of training).

2.2.1.5 1st Fear conditioning

The CS was a 30 s tone (4 kHz at 80 dB) and the US was a scrambled footshock (0.65 mA, 1.0 s) that co-terminated with the tone. Rats were exposed to five habituation trials of the tone alone followed by ten conditioning trials (tones paired with footshocks, intertrial interval (ITI) = 60–180 s). The presence of a conditioned fear response was assessed using percent freezing time and suppression of bar-pressing. The activity of the rats was recorded using a digital camera suspended in the ceiling of the chamber. The amount of freezing during the tone presentation was quantified by the software Ethovision (Noldus, Wageningen, Netherland) with freezing defined as the complete lack of movement except for those related to breathing. Freezing time percentage was defined as the proportion of freezing time during a tone (freezing time during CS/30 s × 100%). The number of bar presses during a tone and 30 s prior to the tone (pre-CS) was used to calculate the conditioned suppression ratio [responses during CS/(responses during pre-CS + responses during CS)]. Consequently, a suppression ratio of 0.5 is an indication of a lack of fear whereas a suppression ratio of 0 is indicative of intense fear.

2.2.1.6 Stereotaxic surgery and midline thalamus lesions

Lesions of the midline thalamus were done 24 h after fear conditioning. Rats were anesthetized with equithesin (0.3 ml/100 g, i.p.) and placed in a Stoelting stereotaxic frame (Stoelting Co. Wood Dale, IL, USA). Bilateral electrolytic lesions of the pPVT were done using bipolar stainless-steel electrodes (RH SNE-100 × 50 mm, David Kopf Instruments, CA, USA) that were lowered in the brain at a 10° angle from the midline on one side of the sagittal sinus. The coordinates were 3.1 mm posterior to bregma, 0.7 mm and 1.2 mm lateral to the midline (for contralateral and ipsilateral lesions, respectively), and 5.3 mm ventral to the skull (incisor bar at 3.3 mm below intra-aural line). The lesions were made using anodal constant direct current (25 μA, 120 s). The sham lesion animals were exposed to the same procedure except that no electrical current was passed through the electrode. There was a 7-day recovery period before examining the effects of the lesions on conditioned fear.

2.2.1.7 Conditioned fear expression and extinction

The ability of rats to bar press was examined at one week after the lesions were made. One or two bar-pressing training sessions were done to recover the bar-pressing response in rats that performed below the baseline criterion of 15 presses per min. Fear expression and extinction were assessed the next day by presenting 15 conditioning tones to the rats placed in the conditioning chamber. Locomotion and freezing were assessed in the periods before the first tone presentation (pre-CS, 180 s) to exclude the non-specific effect of lesion on movement. The recall of the extinction memory was examined the next day by presenting the tones five more times.

2.2.1.8 2nd Fear conditioning in a novel context

Two days later, the rats were placed in a novel plastic chamber with black walls and white lid and no bar or food magazine (MacroAmbition S&T Development Co., Ltd., Beijing, China)

in a different room for fear conditioning to a new tone. In this case, the CS was a 2 kHz pure tone lasting 30 s (80 dB) that co-terminated with footshocks (1.0 mA, 1.0 s). The rats were placed into the chamber and allowed to explore the novel context for 2 min before receiving three CS-US pairings (ITI = 60–180 s). Freezing during the tone presentation was quantified as described above.

2.2.1.9 Motivation test with progressive ratio schedule

Two days after the second fear conditioning procedure, experiments were done to determine if pPVT lesions interfered with the motivation of rats to bar press for food when they were exposed to a PR procedure. The response requirement for getting a food pellet was incremental as derived from a PR equation (Richardson & Roberts, 1996). The PR session lasted 60 min with the last rewarded bar press defined as the breakpoint. The rats were food deprived for 24 h and were re-exposed to the same PR schedule to evaluate their motivation for food in a food deprived state.

2.2.1.10 Lesion verification

Rats were anesthetized with chloral hydrate (40 mg/kg) and perfused with heparinized saline followed by ice cold 4.0% paraformaldehyde in 0.1 M phosphate buffer (pH 7.4). Coronal sections of the posterior thalamus were obtained at 100 µm using a vibratome which were subsequently stained for Nissl substance using Cresyl Violet. The lesions were mapped to identify rats with lesions that were restricted to the pPVT and those with lesions that involved the pPVT as well as parts of the mediodorsal and intermediodorsal nuclei.

2.2.1.11 Data analysis

Data for freezing time percentage and the suppression ratio were averaged over three tone presentations (five test blocks). The data for each test block was used for all subsequent

statistical tests involving fear expression (first test block) and extinction (all five test blocks). Data from the first test block (first three trials) were used for statistical analysis of the extinction memory expression test. The breakpoint (highest PR reached) was calculated for each animal and used to assess the motivation for food. Statistical analysis was done using two-way and one-way ANOVA as appropriate (with repeated measure for the extinction data). Post-hoc LSD tests were used to compare group differences. A value of $p < 0.05$ was considered to be significant and the data were presented as mean ± SEM.

2.2.2 *Experiment 2*: effect of blocking orexin receptors in the pPVT on cued conditioned fear expression

2.2.2.1 Animals and Housing

A total of 53 adult male Sprague-Dawley rats were used for *Experiment 2*. All the rats had free access to food and water through the experiment. Housing conditions were the same as *Experiment 1*.

2.2.2.2 Experimental procedure and timeline

After adaptation, we did stereotaxic surgery to implant a guide cannula into the PVT. After 7 days of recovery, rats were exposed to a cued fear conditioning with footshocks paired with an auditory tone. One day later, we infused DORA in the PVT and 30 minutes later measured conditioned fear expression and conducted fear extinction in one behavioral session. One day later, we tested the retrieval of extinction memory without drug infusion. The timeline of behavioral procedures is also presented in Table 2-2.

Table 2-2 Timetable of the major procedures of *Experiment 2* in Chapter 2

Timepoint	Behavioral session
Day 1	Cannula implantation surgery
Day 8	Fear conditioning
Day 9	Orexin receptor antagonist infusion; conditioned fear expression test and extinction learning
Day 10	Extinction memory retrieval test

2.2.2.3 Stereotaxic surgery and cannula implantation

Rats were anesthetized with sodium pentobarbital (60 mg/kg, 2 ml/kg, i.p.; Sigma-Aldrich) and placed in a stereotaxic frame (RWD Life Science Co., Ltd., Shenzhen, Guangdong, China). Stainless steel guide cannulas (23 gauge, RWD Life Science Co., Ltd.) were unilaterally implanted into the pPVT (3.1 mm posterior to bregma, 1.3 mm lateral to the midline, and 4.0 mm ventral to the skull, angled at 10° with the incisor bar set at 3.3 mm below intraaural line). The guide cannulas were secured with three small screws attached to the skull and dental cement. Capped stylets were inserted into the guide cannulas and all rats were treated with penicillin (80,000 units) to prevent infection. There was a 7-day recovery period before subsequent behavioral procedures.

2.2.2.4 Fear conditioning

Footshocks were given in an acrylic black chamber (30 × 30 × 27 cm) with a grid floor (MacroAmbition S&T Development Co., Ltd., Beijing, China) which was illuminated at 200–300 lux. The rats were acclimated to the shock chamber for 180 s and then exposed to eight 30 s tones (4 kHz, 75 dB) that co-terminated with a 0.5 s shock of 0.65 mA (ITI = 60–180 s). The rats were assigned to four homogeneous groups based on their freezing time during fear learning.

2.2.2.5 Drugs and microinjections

A dual orexin receptor antagonist (DORA) called N-biphenyl-2-yl-1-[(1-methyl-1H-benzimidazol-2yl) sulfanyl] acetyl-L-prolinamide (TCS-1102) was dissolved in poly-ethylene glycol 200 (PEG200, Beijing Chemical Works, Beijing, China). TCS-1102 blocks both orexin type 1 receptor and orexin type 2 receptor and has been shown to be effective in blocking orexin-mediated behaviors for up to 4 h (Bergman et al., 2008; Winrow et al., 2010). The rats received DORA of 0.1, 1.0, and 10 nmol or the vehicle. The drug and vehicle were microinjected into the PVT (0.5 μl) through an injector cannula (28 gauge, RWD Life Science Co., Ltd.) which protrudes 2.0 mm below the guide cannula. Infusions were delivered with a 5.0 μl Hamilton microsyringe connected to the injector cannula with polyethylene tubing and an infusion pump was used to deliver the drug at the rate of 0.2 μl/min over 2.5 min. The injector cannula was kept in the guide cannula for another minute to prevent backflow before the stylet was placed back into the guide cannula. The rat was returned to its home cage for 30 minutes and then put into the shock chamber for the fear expression test.

2.2.2.6 Conditioned fear expression and extinction

The fear expression and extinction session were started at 24 hr after fear conditioning. Each rat was exposed to the tone 20 times (ITI = 30–60 s). Fear extinction recall was examined 24 h later by exposing the rats to 10 tones in the shock chamber. The purpose of the extinction recall experiment was to examine if DORA interfered with the consolidation processes of the extinction memory. The freezing response was recorded by the software XeyeFCs (MacroAmbition S&T Development Co., Ltd., Beijing, China).

2.2.2.7 Cannula Verification

Rats were deeply anesthetized with chloral hydrate (50 mg/kg) prior to decapitation. The brains were removed, post-fixed overnight in 4% paraformaldehyde and subsequently cryoprotected in 30% sucrose solution in 0.1 M phosphate buffer at 4°C. Serial coronal sections (60 μm) were cut using a freezing microtome and subsequently stained for Nissl substance using Cresyl Violet. Three cases with misplaced cannulas were excluded from behavioral data analysis.

2.2.2.8 Data analysis

The freezing responses during the presentation of the tone for the expression, extinction and extinction recall sessions were analyzed using an ANOVA with repeated-measures. Freezing for each trial consisting of two consecutive tone presentations.

2.2.3 *Experiment 3*: effect of blocking orexin receptors in the PVT on contextual conditioned fear expression

2.2.3.1 Animals and Housing

A total of 42 adult male Sprague-Dawley rats were used for *Experiment 3*. All the rats had free access to food and water through the experiment. Housing conditions were the same as *Experiment 1*.

2.2.3.2 Experimental procedure and timeline

After adaptation, we did stereotaxic surgery to implant the guide cannula into the PVT. After 7 days of recovery, we did a contextual fear conditioning in which footshock was delivered alone in a shock chamber. One day later, we infused DORA to the PVT and 30 minutes later measured conditioned fear expression in the shock chamber. Fourteen days later, we tested the

effect of DORA on anxiety in the open field test and social approach-avoidance (SAA) test. The timeline of behavioral procedures is also presented in Table 2-3.

Table 2-3 Timetable of the major procedures of *Experiment 3* in Chapter 2

Timepoint	Behavioral session
Day 1	Cannula implantation surgery
Day 8	Fear conditioning
Day 9	Orexin receptor antagonist infusion; conditioned fear expression test
Day 23	Orexin receptor antagonist infusion; open field test; SAA test

2.2.3.3 Stereotaxic surgery and cannula implantation

The surgery and cannula implantation of *Experiment 3* were the same as *Experiment 2*.

2.2.3.4 Fear conditioning

A contextual fear conditioning protocol was used in *Experiment 3*. Rats were exposed to five 5 s footshocks of 1.5 mA (ITI = 90–150 s) and returned to their home cages 60 s after the last footshock. The choice to use more intense footshocks for the contextual conditioning experiment was based on previous evidence that exposure of 1.5 mA footshocks produces an orexin-mediated fear and anxiety (Chen, Wang, et al., 2014). For example, exposure of rats to footshocks of this intensity has been shown to produce long-lasting increases in prepro-orexin mRNA as well as contextual fear and anxiety that are attenuated by systemic injections of a DORA (Chen, Wang, et al., 2014).

2.2.3.5 Drug and microinjections

The drug, doses, and microinjection procedures were the same as *Experiment 2*.

2.2.3.6 Conditioned fear expression

Fear expression was examined at 24 h after fear conditioning. The rats were placed into the shock chamber at 30 min after DORA microinjections in the PVT region. Freezing behavior was measured in the expression test for 10 minutes.

2.2.3.7 Anxiety tests

Fourteen days after footshocks, the animals were reassigned to four groups randomly, and microinjections of one of three different doses of DORA or the vehicle were made in the PVT region. Thirty minutes later, the rats were placed in a circular open field (100 cm in diameter, 50 cm high, with 15–20 lux illumination) for 5 min. The activity of the rats was recorded by the video tracking system for subsequent analysis of locomotor activity, latency to the center area, and time spent in the center area. After the open field test, the rats were transferred to another room for the SAA test. The apparatus and procedure were designed and performed based on the previous studies (Chen et al., 2012; Chen, Wang, et al., 2014; Haller & Bakos, 2002). The test was conducted in a black rectangle open field (100 × 60 ×50 cm, 5–10 lux illumination). A stimulus rat (male rat weighing 450–500 g) was put into a small mesh box (25 × 12.5 × 25 cm) in a corner of the arena, and the test rat was placed in an enclosed compartment located in the opposite corner. After a 2 min habituation period, the sliding door of the enclosed box was opened, allowing the test rat to move freely in the arena for 5 min. The time spent in the social interaction zone (20 × 30 cm zone immediately adjacent to the target rat compartment) and the latency to come out of the box was recorded by the video tracking system.

2.2.3.8 Cannula Verification

The cannula verification procedures were the same as *Experiment 2*. Six cases with misplaced cannulas were excluded from behavioral data analysis.

2.2.3.9 Data analysis

The freezing time in the shock chamber were analyzed using an ANOVA with repeated-measures. Each data point represented the average in a 2.5-min time period. The total amount of freezing in the shock chamber, locomotion in the open field and time spent in social zone were analyzed by one-way ANOVA with Bonferroni post-hoc tests used for multiple comparisons. The latency in the open field test and in the social interaction test were analyzed by Kruskal-Wallis one-way analysis of variance by ranks followed by Mann-Whitney test.

2.3 Results

2.3.1 *Experiment 1*: the pPVT lesions attenuated conditioned fear expression but not acquisition or extinction.

The animals were grouped according to the size and location of lesions. Figure 2-1 shows a typical lesion largely restricted to the pPVT (Figure 2-1A) and a larger lesion involving more of the midline thalamus (pPVT and surrounding area; Figure 2-1B). Subjects were assigned to the pPVT lesion group (pPVT only; $n = 13$; Figure 2-2A), midline lesion group (pPVT and parts of the mediodorsal and intermediodorsal nuclei; $n = 7$; Figure 2-2B), non-pPVT lesion (no visible lesion because the electrode was placed in the third ventricle or small lesions that were dorsolateral to the pPVT in the medial habenula; $n = 12$) and sham lesion group ($n = 5$) based on the location of the lesions. Data from the sham group and non-pPVT lesion group were pooled together (control lesion group; $n = 17$) since both groups had similar fear levels and extinction rates as assessed by the suppression ratio ($F_{(4,60)} = 1.049$, $p = 0.39$, for interaction effect; and $F_{(1,15)} = 0.799$, $p = 0.386$, for group differences) and freezing ($F_{(4,60)} = 0.678$, $p = 0.61$, for interaction effect; $F_{(1,15)} = 0.033$, $p = 0.857$, for group differences) expressed over the 15 tone

presentations of the expression/extinction phase of the tests. A similar amount of fear to the tone as measured by freezing ($F_{(2,34)} = 0.182$, $p = 0.835$; Figure 2-3A) or the suppression ratio ($F_{(2,34)} = 0.097$, $p = 0.908$; Figure 2-4A) was displayed by the pPVT, midline and control lesion groups during fear conditioning (before the lesion surgery).

Figure 2-1 Examples of lesions of the pPVT

A. An example from the pPVT lesion group with complete lesions limited to the pPVT. **B.** An example from the midline lesion group with complete lesion of the pPVT and surrounding area including the mediodorsal and intermediodorsal nuclei.

Abbreviations: 3V, third ventricle; IMD, intermediodorsal nucleus of thalamus; LHb, lateral habenular nucleus; mHb, medial habenular nucleus; MD, mediodorsal nucleus of thalamus; pPVT, paraventricular nucleus of thalamus, posterior.

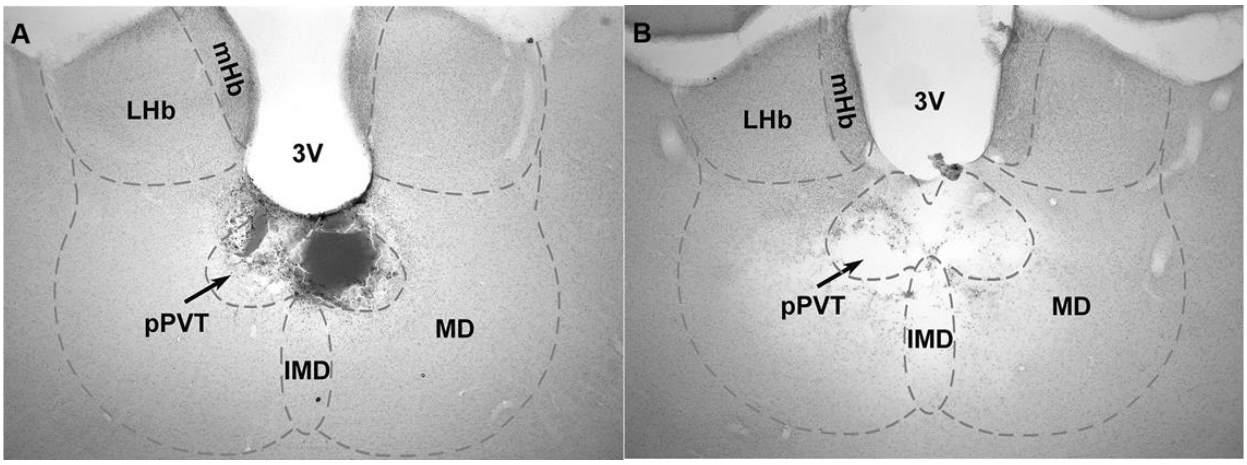

Figure 2-2 Drawings showing the location of midline thalamic lesions

A. Sections of subjects that were assigned to the pPVT lesion group. **B.** Subjects that were assigned to the midline lesion group. Numbers represent the distance from bregma.

Abbreviations: CM, central medial nucleus of thalamus; fr, fasciculus retroflexus; Hb, habenular nucleus; IMD, intermediodorsal nucleus of thalamus; MD, mediodorsal nucleus of thalamus; PF, parafascicular nucleus of thalamus; pPVT, paraventricular nucleus of thalamus, posterior.

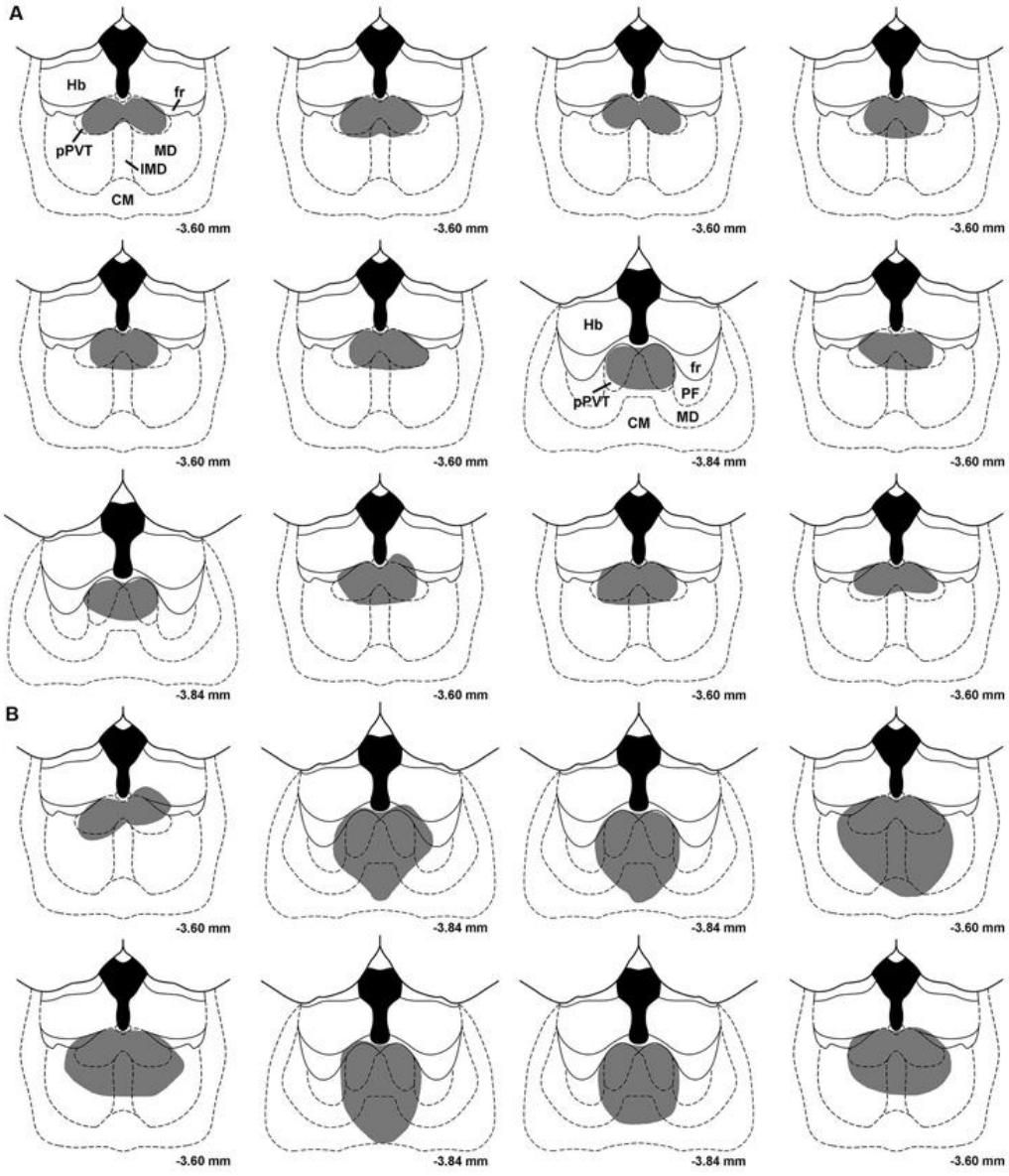

Figure 2-3 Effect of pPVT lesions on freezing to fear-conditioning tones

A. Different experimental groups displayed similar amounts of freezing prior to electrolytic lesions of the pPVT. In contrast, freezing was attenuated in groups of rats that had pPVT and midline lesions when they were compared to the control lesion group. **B.** The different groups showed similar extinction of freezing behavior over subsequent presentations of the tone. **C.** Lesions of the pPVT or the midline thalamus had no effect on recall of the extinguished fear memory. *$p < 0.05$; **$p < 0.01$.

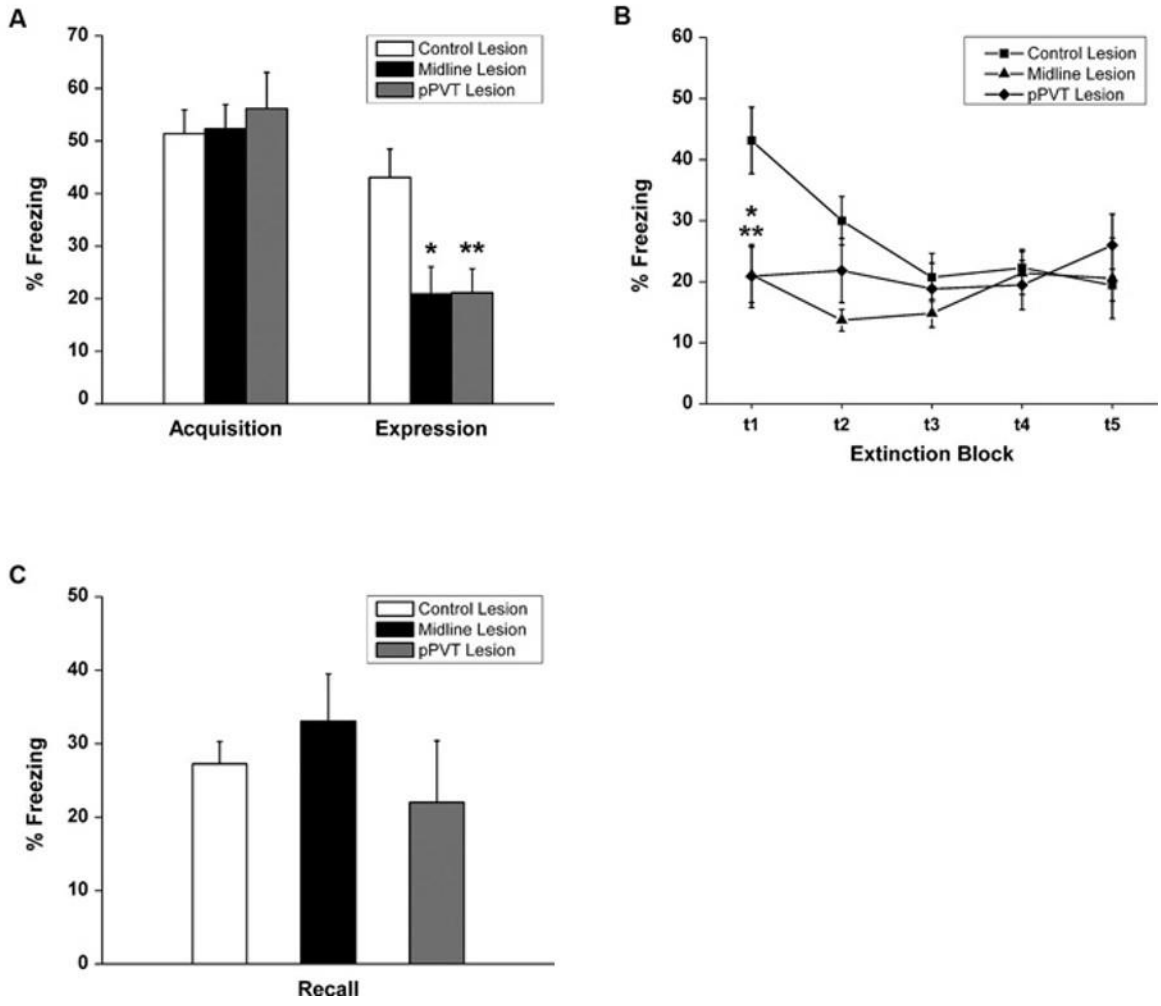

Animals with lesion in the pPVT or the dorsal midline thalamus showed attenuated conditioned fear expression with less freezing and lower suppression ratio. There was a significant group difference in freezing during the fear expression test ($F_{(2,34)} = 5.83$, $p = 0.007$; Figure 2-3A). Compared to the control lesion group, the pPVT lesion group ($p = 0.004$) and the midline lesion group ($p = 0.018$) showed significant decreases in freezing. There was also a significant difference between groups on the suppression ratio during the expression test ($F_{(2,34)} = 4.215$, $p = 0.023$; Figure 2-4A). Compared to the control lesion group, the pPVT lesion group ($p = 0.022$) and the midline lesion group ($p = 0.023$) showed significant decreases in the suppression ratio. The one-way ANOVA indicated no group differences in locomotion ($F_{(2,34)} = 0.161$, $p = 0.852$; Figure 2-5C) or freezing ($F_{(2,34)} = 0.198$, $p = 0.821$, data not shown) during the pre-CS period.

The pPVT or dorsal midline thalamus lesion did not affect fear extinction, fear acquisition, or motivation on bar press for food. There was a significant interaction effect between the test blocks and lesions on freezing ($F_{(8,136)} = 4.99$, $p < 0.001$) in the extinction learning process. Simple effect analysis was done to confirm that only the control group showed a significant extinction effect ($F_{(4,136)} = 15.81$, $p < 0.001$; Figure 2-3B). The pPVT and midline lesion groups showed no extinction using freezing as a measure because fear expression was already inhibited to extinction levels in the first test block. In contrast, lesions had no effect on the extinction of fear memory as measured by suppression ratio as specified by the two-way ANOVA analysis showing a lack of a main effect for lesions ($F_{(2,34)} = 1.89$, $p = 0.167$; Figure 2-4B) or an interaction effect between lesions and test blocks ($F_{(8,136)} = 1.55$, $p = 0.144$; Figure 2-4B). The one-way ANOVA reveled no difference between lesion groups in recall test for extinction memory as assessed by freezing ($F_{(2,34)} = 0.331$, $p = 0.720$; Figure 2-3C) or suppression ratio

($F_{(2,34)} = 0.193$, $p = 0.826$; Figure 2-4C). The effect of lesions of the pPVT on the acquisition of novel fear was also examined. Rats acquired a novel fear within three trials ($F_{(2,68)} = 36.525$, $p < 0.001$; Figure 2-5A). However, pPVT or midline lesions had no effect on fear acquisition ($F_{(4,68)} = 1.015$, $p = 0.406$ for the interaction between lesion and trial; $F_{(2,34)} = 0.297$, $p = 0.745$ for group differences; Figure 2-5A). Finally, neither the pPVT lesions or the midline lesions had any effect on the motivation to bar press in non-deprived or in food deprivation rats ($F_{(2,34)} = 0.276$, $p = 0.360$ for the interaction between lesion and deprivation state; $F_{(2,34)} = 0.446$, $p = 0.646$ for group differences; Figure 2-5B).

Figure 2-4 Effect of pPVT lesions on suppression of bar-pressing to fear-conditioning tones

A. Different experimental groups displayed similar amounts of bar-pressing prior to electrolytic lesions of the pPVT. In contrast, bar-pressing was attenuated in groups of rats that had pPVT and midline lesions when they were compared to the control lesion group. **B.** The different groups showed similar extinction of bar-pressing over subsequent presentations of the tone. **C.** Lesions of the pPVT or the midline thalamus had no effect on recall of the extinguished fear memory. *$p < 0.05$.

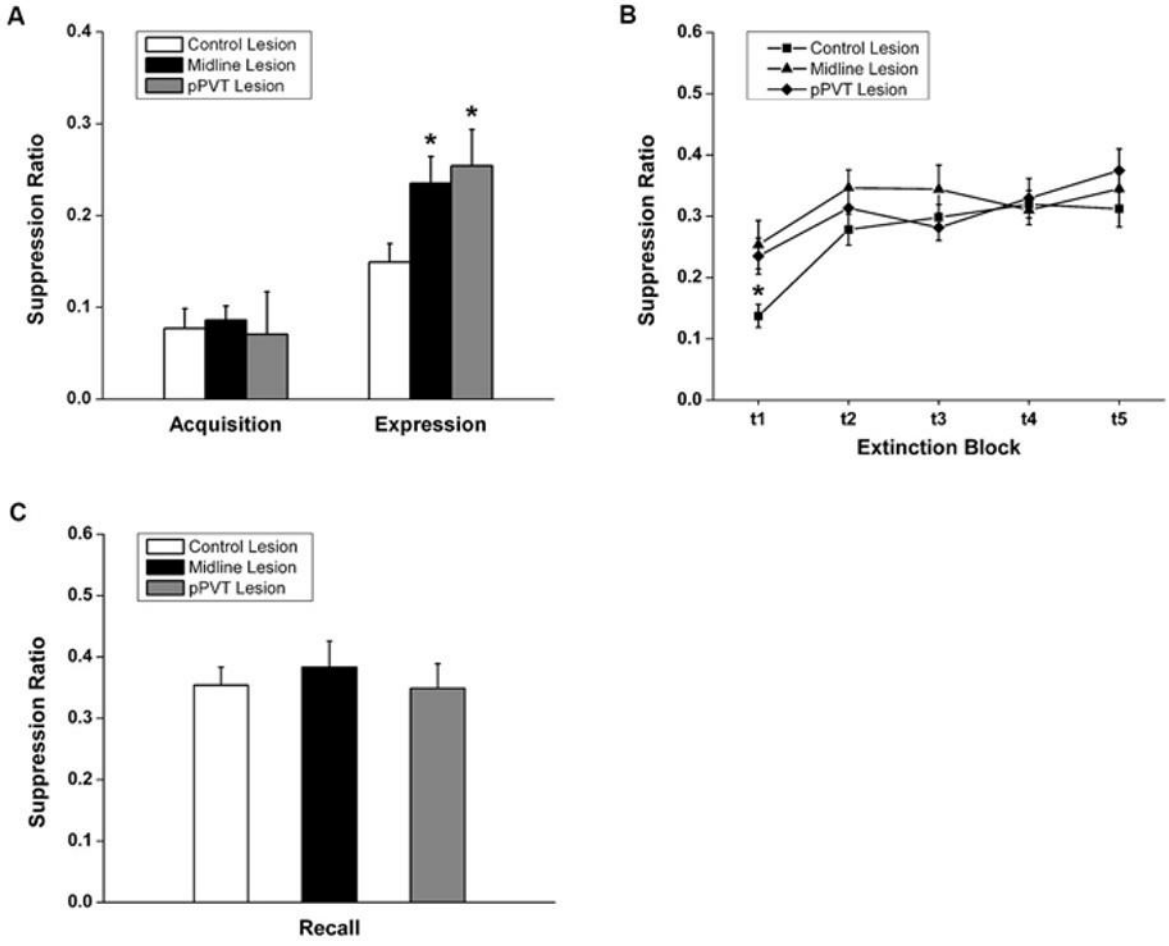

Figure 2-5 Effect of pPVT lesions on the acquisition of a novel fear, motivation for food reward, and locomotor activity.

A. Lesions of the pPVT or the midline thalamus had no effect on the freezing displayed in rats exposed to a new fear conditioning protocol. **B.** Lesions of the pPVT or the midline thalamus did not affect the breakpoint in food deprived or non-deprived rats. **C.** Lesions of the pPVT did not affect the amount of locomotor activity displayed by rats during the pre-CS period of expression test.

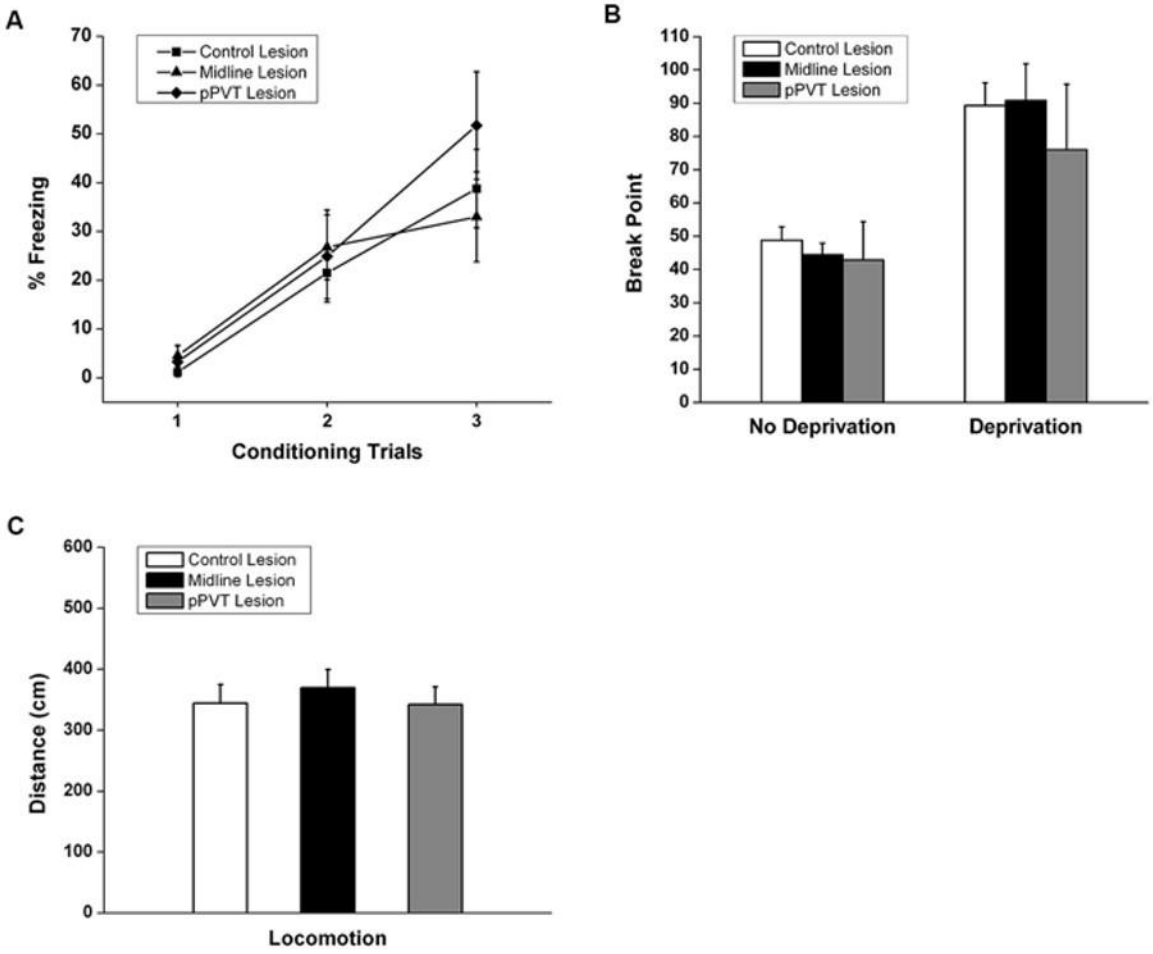

2.3.2 *Experiment 2*: blocking of orexin receptors in the PVT did not affect cued conditioned fear expression.

Two examples of cannula placement are shown in Figure 2-6A. The locations for all cases in *Experiment 2* and *Experiment 3* are shown in Figure 2-6B.

Figure 2-6 The location of injector tips in the thalamus.

A. Pictures show two examples of placements of the injector tip (arrows) in the region of the PVT as verified from histological sections. Scale bar, 0.5 mm. **B.** The diagram shows the location of the injector tips in the region of the PVT as verified from histological sections. The numbers correspond to distance from bregma.

Abbreviations: CM, central medial nucleus of thalamus; IMD, intermediodorsal nucleus of thalamus; Hb, habenular nucleus; MD, mediodorsal nucleus of thalamus; PVT, paraventricular nucleus of thalamus.

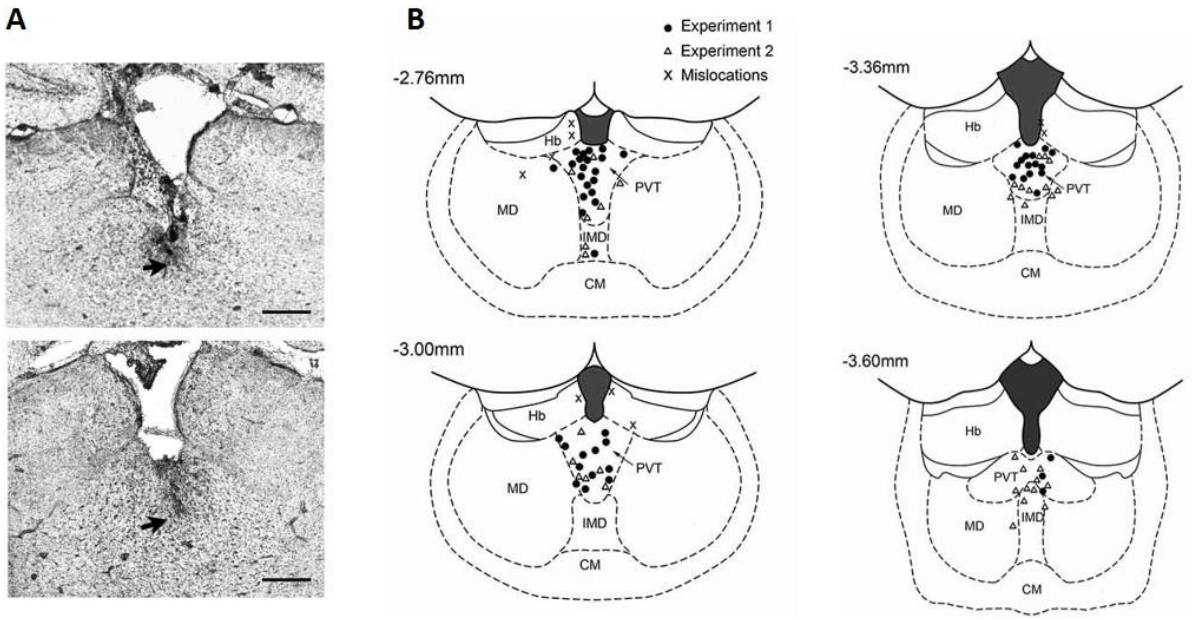

Exposure of rats to tones paired with footshocks resulted in increasing amounts of freezing with conditioning trials ($F_{(3,138)} = 68.3$, $p < 0.001$; Figure 2-7, Day1). Repeated presentation of the conditioning tone produced a significant extinction effect (main effect of extinction in repeated-measures ANOVA $F_{(9,414)} = 13.3$, $p < 0.001$; Figure 2-7, Day 2) and the three doses of DORA infusion (0.1 nmol, 1 nmol, or 10 nmol) did not affect fear expression during the first tone presentation ($F_{(3,46)} = 0.51$, $p = 0.66$; Figure 2-7, Day 2; vehicle n = 14, 0.1 nmol n = 13, 1.0 nmol n = 12, 10 nmol n = 11) nor the fear extinction in the extinction trials that followed ($F_{(3,46)} = 1.68$, $p = 0.18$). There was no interaction between the trials and DORA doses ($F_{(27,414)} = 1.13$, $p = 0.30$; Figure 2-7). The pre-tone baseline level of freezing in the chamber was unaffected by DORA (vehicle 21.7%, 0.1 nmol 26.9%, 1.0 nmol 21.2%, and 10 nmol 20.7%; $F_{(3,46)} = 0.17$, $p = 0.92$). There were no group differences in the recall of the extinction memory 24 h after the extinction phase ($F_{(3,46)} = 1.512$, $p = 0.22$; Figure 2-7), nor any interaction between doses of DORA and the trials ($F_{(12,184)} = 0.70$, $p = 0.75$; Figure 2-7).

Figure 2-7 Effect of injections of a DORA in the region of the PVT on freezing in cued fear conditioning.

Rats were fear conditioned on Day 1 and freezing to the tone was examined on Day 2 following injections of the vehicle or one of the 0.1, 1.0, and 10 nmol concentrations of DORA. The drug had no effect on fear expression or fear extinction. In addition, the drug treatment on Day 2 had no effect on the extinction recall on Day 3.

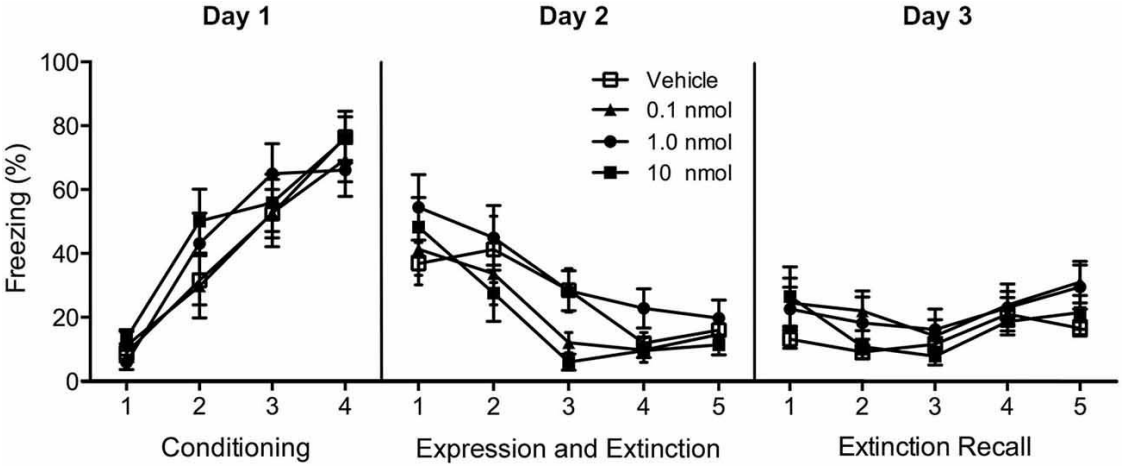

2.3.3 *Experiment 3*: blocking of orexin receptors in the PVT did not affect contextual conditioned fear expression but reduced anxiety.

We used a contextual fear conditioning paradigm based on previous studies which produced an orexin-mediated fear and anxiety (Chen, Wang, et al., 2014) to investigate the role of orexin receptors in the PVT in fear and anxiety. In terms of the contextual fear expression 24 h after fear conditioning, DORA had no effect on fear to the shock chamber (freezing in four 2.5 min time periods $F_{(3,32)} = 0.72$, $p = 0.55$; interaction between time and DORA doses, $F_{(9,96)} = 0.15$, $p = 0.99$; total freezing for the 10 min in the shock chamber, $F_{(3,32)} = 1.01$, $p = 0.40$; Figure 2-8A; vehicle n = 9, 0.1 nmol n = 7, 1.0 nmol n = 10, 10 nmol n = 10). However, in the SAA test, the Kruskal-Wallis one-way ANOVA indicated a main effect for DORA ($\chi^2_{(3)} = 11.78$, $p = 0.008$; Figure 2-8B; rats were re-assigned to groups with different doses of DORA injection, vehicle n = 9, 0.1 nmol n = 10, 1.0 nmol n = 7, 10 nmol n = 10) with the 1.0 nmol ($p = 0.038$) and 10 nmol ($p = 0.003$) doses decreasing the latency to enter the social interaction zone. The time spent in the social zone was not significantly increased in groups with DORA ($F_{(3,32)} = 1.47$, $p = 0.24$; Figure 2-8B). In the open field test, DORA had no effect on the latency to go to the center ($\chi^2_{(3)} = 5.55$, $p = 0.14$; Figure 2-8C) but the one-way ANOVA revealed a main effect of drug dose on locomotion ($F_{(3,32)} = 3.27$, $p = 0.034$; Figure 2-8C) with the highest dose significantly increasing locomotion ($p = 0.024$). In summary, DORA had an anxiolytic effect but had no effect on contextual fear expression.

Figure 2-8 Effect of injections of a DORA in the PVT region on contextual fear expression and anxiety-like behaviors

A. Rats were exposed to footshock and the amount of freezing to the shock chamber was examined on Day 2 following injections of the vehicle or one of the 0.1, 1.0, and 10 nmol concentration of DORA. The drug had no effect on fear expression. **B.** The 1.0 and 10 nmol concentrations of DORA decreased the latency for rats to enter the social zone in the social interaction test while the same doses did not significantly affect the time spent in the social zone. **C.** Injections of DORA did not have a significant effect on the latency to enter the center of the open field while the 10 nmol concentration increased the amount of locomotion. Note that injections of DORA were made in the PVT prior to exposing the rats consecutively to the open field and social interaction tests. *$p < 0.05$; **$p < 0.01$.

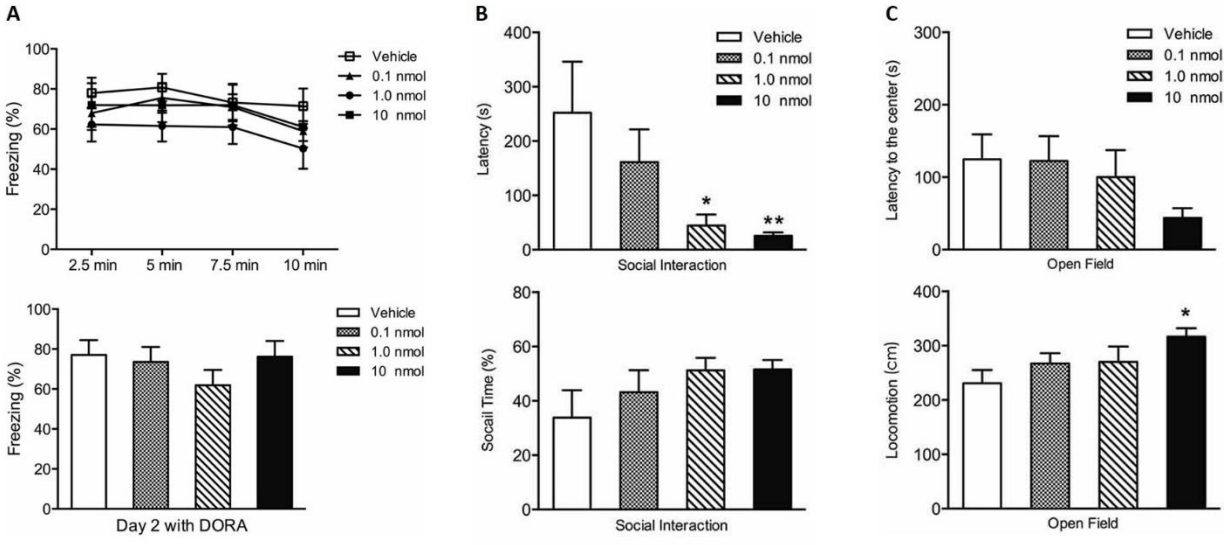

2.4 Discussion

This study showed that lesions of the pPVT attenuated conditioned fear expression while had no effect on extinction nor acquisition of conditioned fear to a novel tone. Microinjections of a dual orexin receptor antagonist in the PVT did not attenuate the conditioned fear expressed following exposure of rats to cued and contextual fear conditioning paradigms.

The result that lesions of the PVT reduce conditioned fear expression is consistent with evidence from other research groups showing that lesions of the mediodorsal nucleus and midline thalamic nuclei interfere with fear expression to the shock context (Li, Inoue, Nakagawa, & Koyama, 2004) and that inhibition of the dorsal midline thalamus by GABA receptor agonist prevents fear to a tone previously associated with footshocks but has no effect on the acquisition or the extinction (Padilla-Coreano, Do-Monte, & Quirk, 2012). The previous studies involved lesions or inhibition of large areas of the dorsal midline thalamus that include a number of nuclei besides the PVT. Our results established that small lesions entirely restricted to the pPVT was sufficient to attenuate conditioned fear expression. However, it is possible that damaged fibers passing through the pPVT could be responsible for the effects observed from the lesions in the pPVT.

The PVT may regulate conditioned fear expression via activation of its projection to the CeL. Indeed, another study showed that cFos expression level was increased in the CeL but reduced in the CeM following inhibition of the midline thalamus in the fear expression test (Padilla-Coreano et al., 2012). This suggests that in fear conditioned rats, neurons in the dorsal midline thalamus exert inhibitory influence on a population of CeL neurons that in turn inhibit neurons in the CeM. A possible mechanism is that the PVT modulates fear expression via

excitation of neurons in the CeL which exerts a tonic inhibitory influence on another subpopulation of neurons in the CeM that project to effectors of fear response in the lower brain.

The results of the current study along with previous studies on the midline thalamus also showed that the midline thalamus and the pPVT are not necessary for forming a shock-tone association. It is possible that the PVT is selectively involved in the retrieval of conditioned fear memory. The prelimbic cortex has been reported as a critical brain area which may drive the expression of learned fear (Burgos-Robles et al., 2009; Corcoran & Quirk, 2007). The prelimbic cortex sends a strong projection to the PVT (Li & Kirouac, 2012; Vertes, 2004) by which the prelimbic cortex may activated the PVT during memory retrieval which in turn influences the neural activity in the microcircuit formed by inhibitory neurons in the CeL.

In addition to the glutamatergic input from the prelimbic cortex which may activate the PVT during fear expression, we proposed that the orexinergic input from hypothalamus may also contribute to the conditioned stimulus induced activation. This hypothesis was based on findings from our group that blocking of orexin type 2 receptors in the PVT selectively decreased anxiety in rats which were exposure to one 2.0 mA footshock for 10 s 2 days earlier (Li et al., 2010b). However, the results of the current experiments indicate that orexin receptors in the PVT are not necessary for the expression of cued or contextual fear memory. The anxiety tests in *Experiment 3* were conducted to verify that the microinjections of DORA blocked orexin receptors in the PVT. Indeed, the moderate and high doses of DORA had anxiolytic effects. As such, the negative results in the fear conditioning experiments in *Experiment 2 and 3* are unlikely due to inadequate antagonism of orexin receptors in the PVT. These results indicate that conditioned fear response and anxiety-like behaviors induced by the same stress event may be regulated

independently and orexin signaling in the PVT may be only involved in modulating anxiety which is closely related to elevated arousal level.

Chapter 3 Distribution of PVT output collaterals

Experiment 1 presented in Chapter 3 was published in the following paper:

Dong, X., Li, S., & Kirouac, G. J. (2017). Collateralization of projections from the paraventricular nucleus of the thalamus to the nucleus accumbens, bed nucleus of the stria terminalis, and central nucleus of the amygdala. Brain Structure and Function, 222(9), 3927–3943. https://doi.org/10.1007/s00429-017-1445-8

3.1 Introduction

The PVT has been postulated to mediate emotional behavioral responses because it innervates many brain regions in the limbic cortex and basal forebrain nuclei that are critical for emotional behaviors including the NAc, BST, CeL, and mPFC (reviewed in Section 1.4.2, 1.4.3). Experimental evidence demonstrates that the PVT can influence a broad range of behaviors including reward seeking (e.g., Otis et al., 2017; Zhang & van den Pol, 2017), conditioned place avoidance (e.g., Li et al., 2011; Zhu et al., 2016), anxiety-like behavior, and conditioned fear expression (reviewed in Section 1.4.4). As shown in Chapter 2, we found that lesions of the PVT attenuated conditioned fear expression while blocking orexin receptors in the PVT reduced anxiety but had no effect on conditioned fear expression (Dong, Li, & Kirouac, 2015; Y. Li, Dong, Li, & Kirouac, 2014), suggesting that the PVT may modulate conditioned fear and anxiety independently. A possible neural mechanism by which the PVT could modulate these different behavioral responses is that the PVT may contain subpopulations of neurons which are selectively connected to the neural substrates that regulate fear or anxiety.

The question of whether the PVT consists of subpopulations of neurons with unique projections can be addressed by determining if subpopulation of PVT neurons preferentially innervate certain targets involved in different behavioral responses. In contrast, it is possible that the same neurons provide collateral innervation of multiple targets indicating a less specialized role for the PVT. Collaterals are fiber projections that emanate from a major axon that serve to innervate multiple targets (e.g., Reichard et al., 2017). Previous studies have estimated the extent that PVT neurons innervate more than one target via collaterals by injecting two different retrograde tracers in two selected targets of the PVT. Most of these studies indicate that despite being largely intermingled, neurons that project to the subcortical areas like NAc and CeL are mostly separate from those that project to cortical or cortical-like areas including the prefrontal cortex, ventral subiculum of the hippocampus and the basolateral amygdala (Deutch, Bubser, & Young, 1998; Penzo et al., 2015; Su & Bentivoglio, 1990). While it appears that projections to the cortical and subcortical regions may be issued from different populations of PVT neurons, the extent that PVT neurons project to the different subcortical areas has not been addressed adequately.

Experiments in this chapter focus on the question of whether, or to what extent, neurons in the PVT that project to its main subcortical targets are from distinct subpopulations. To address this issue, we injected two different fluorescent retrograde tracers into different pairs of subcortical targets most densely innervated by the PVT. The brain areas to be targeted by tracer injection were selected based on a comprehensive study of the PVT projections showing that the NAcSh, CeL, and BSTDL are the most densely innervated regions by the PVT (Li & Kirouac, 2008). Detailed maps of the location and counts of labeled neurons in the PVT were carried out to determine the extent of segregation and colocalization of neurons that make up these PVT

projections. In addition, we combined dual retrograde tracing with cFos staining to investigate if subpopulations of PVT neurons respond differentially to emotional responses associated with fear and anxiety. The hypotheses were that the projection to the NAcSh, BSTDL, CeL originate from distinct subpopulations of PVT neurons, and these PVT output pathways are activated differentially by stress events that can induce fear and anxiety.

3.2 Methods

3.2.1 *Experiment 1*: collateralization of projections from the PVT to NAcSh, BSTDL, and CeL

3.2.1.1 Animals and housing

A total of 61 male Sprague–Dawley rats (University of Manitoba vivarium) weighing 300 ± 10 g were used for *Experiment 1*. Twenty-four rats were used to generate the figures and data presented in this study. Animals were housed individually in cages kept in a room maintained on a 12 h/12 h light/dark cycle (lights on at 07:00) with controlled temperature (20–24°C) and humidity (40–70%). All the rats had free access to food and water through the experiment. The experimental procedures were in compliance with the Canadian Council on Animal Care and the experimental protocol was approved by Research Ethics Review Board of the University of Manitoba.

3.2.1.2 Stereotaxic surgery and tracer injection

Rats were anesthetized with 2–3% isoflurane and given meloxicam (2 mg/kg, s.c.) for post-surgery pain management. Rats were placed in a Stoelting stereotaxic frame and a hand drill was used to expose the brain surface above the target sites. Pressure injections of retrograde tracers

were done using a pressure injection device (Picospritzer, Park Hannifin, Hollis, NH, USA) connected to glass pipettes with outer diameter of tips of approximately 40 μm. Injections of tracers were done in the following areas using coordinates derived from a stereotaxic atlas of the rat brain (Paxinos & Watson, 2007): NAcSh, 1.5 mm anterior, 1.0 mm lateral, 7.2 mm ventral; dorsomedial NAcSh (dmNAcSh), 1.5 mm anterior, 0.9 mm lateral, 6.0 mm ventral; ventromedial NAcSh (vmNAcSh), 1.5 mm anterior, 1.1 mm lateral, 7.5 mm ventral; core of the nucleus accumbens (NAcC), 1.5 mm anterior, 1.8 mm lateral, 6.5 mm ventral; BSTDL, 0.3 mm anterior, 1.6 mm lateral, 6.0 mm ventral; CeL, 2.1 mm posterior, 4.2 mm lateral, 7.5 mm ventral; basolateral amygdala (BLA), 2.5 mm posterior, 4.9 mm lateral, 7.8 mm ventral (all coordinates are relative to bregma and the dural surface of the brain). The retrograde tracer cholera toxin subunit B conjugated to Alexa Fluor-488 (CTb-AF488; catalogue No. C22841, Invitrogen, Calsbad, CA, USA) and Alexa Fluor-594 (CTb-AF594; catalogue No. C22842, Invitrogen) were dissolved in 0.06 M neutral phosphate buffer at 0.5% concentration and 50 nl of the tracer was injected over 10–15 min using the picospritzer into one of the two regions of interest in the same hemisphere of the brain. Four cases of each combination were used for analysis: NAcSh and CeL; NAcSh and BSTDL; BSTDL and CeL; CeL and BLA; NAcSh and NAcC; dmNAcSh and vmNAcSh. The pipette was kept in place for another 10 min before removal to prevent leakage. The scalp incisions were sutured, and rats were returned to their home cages for recovery.

3.2.1.3 Histology

Rats were deeply anesthetized with 10% chloral hydrate (600 mg/kg, i.p.) and transcardially perfused with 200 ml heparinized saline followed by 500 ml ice-cold 4% paraformaldehyde in 0.1 M phosphate buffer (pH 7.4) 7 to 9 days after tracer injections (Conte, Kamishina, & Reep, 2009). The brains were removed and post-fixed in the same fixative for 4–5

h, and cryoprotected in 20% sucrose with 10% glycerin over 2 days at 4 °C. Coronal sections of the brain containing the injection sites and the PVT were taken at 50 μm and sections at every 200 μm were mounted on slides for subsequent examination under a fluorescent microscope. The sections were dehydrated through a series of graded alcohol solutions, cleared with CitriSolv (Fisher Scientific, ON, Canada), and coverslipped with mounting medium.

Alternate brain sections containing the injected areas or the PVT region were selected for NeuN staining. The immunohistochemical reactions were carried out at room temperature on free-floating sections. Primary and secondary antibodies were diluted in blocking solution containing 0.1% sodium azide, 0.3% Triton X-100, and 5% normal donkey serum in 0.1 M phosphate buffered saline (PBS). Brain sections were pre-incubated in the blocking solution for 1 h and then incubated in primary mouse anti-NeuN antibody (1:1000; catalogue No. MAB377, Chemicon, Temecula, CA, USA) overnight. After 3 rinses in PBS, sections were transferred into a biotinylated donkey anti-mouse (1:500; Jackson Immunoresearch, West Grove, PA, USA) antiserum for 1 h. Then sections were rinsed thoroughly and incubated with an avidin–biotin complex solution (Elite ABC kit; Vector Laboratories, Burlingame, CA, USA) for 1 h. After three more rinsing steps, sections were reacted with diaminobenzidine tetrachloride (DAB) with nickel intensification (Vector DAB Kit) to produce a black reaction product. The DAB reaction was terminated by rinsing the sections with PBS and the sections were mounted on slides, air dried and coverslipped with mounting medium.

3.2.1.4 Data analysis

Brain sections were examined and photographed using an Olympus BX51 microscope equipped with a digital camera (SPOT RT Slicer, Diagnostic Instruments Inc, Sterling Heights, MI, USA). Injection sites were drawn based on photos taken under 40× magnification and the

distribution of fluorescent labeled cells in the PVT were drawn based on merged sets of images taken at 200× magnification. The stereotaxic levels chosen for these illustrations were those that are representative of the distribution of labeled cells in the PVT and adjacent thalamic nuclei. The NeuN-stained sections were used in combination with a stereotaxic atlas to identify and draw the anatomical demarcations of brain regions (Paxinos & Watson, 2007). Calibration bars were inserted using SPOT software (Version 3.2, Diagnostic Instruments) and the images were transferred to Adobe Photoshop CS4 to optimize light and contrast levels.

The total numbers of NeuN and fluorescent labeled cells in the PVT were counted on sections 200 μm apart starting at the level of the aPVT (1.08 mm posterior to bregma) to the pPVT (3.96 mm posterior to bregma) according to a standard atlas of the rat brain (Paxinos & Watson, 2007). The presence of fluorescent labeled neurons in the PVT was examined under appropriate filters and counts of single-labeled neurons were made under 200× magnification. Double-labeled neurons were identified under 200× magnification and always verified under 400× magnification and by focusing through the labeled neurons. The data represent the mean of the cell counts done independently by two experimenters. The count data for all the sections analyzed were subdivided into aPVT and pPVT levels (eight sections each) with stereotaxic level 2.5 mm posterior to bregma as the divide. Likewise, the number of NeuN-stained neurons in the PVT was counted in four cases on the sections corresponding to the approximate stereotaxic levels used for counting the number of fluorescent labeled neurons. The total number of NeuN-stained neurons for these sections was divided in half since the retrogradely labeled neurons were found only on the ipsilateral side of the injection sites. The mean of the NeuN labeled cells was used to estimate the proportion of CTb-labeled cells in the PVT in all the cases (CTb-labeled cells/NeuN-labeled cells × 100%). A two-way ANOVA was used to analyze the proportion of

labeled cells with levels (aPVT vs pPVT) and tracer target sites as independent variables. Bonferroni post hoc test was used for further comparison.

3.2.2 *Experiment 2*: activation of different PVT output neurons to fear and anxiety

3.2.2.1 Animals and Housing

A total of 40 adult male Sprague-Dawley rats were used for *Experiment 2*. Housing conditions were the same as *Experiment 1*.

3.2.2.2 Stereotaxic surgery and tracer injection

The surgery and tracer injection procedure of *Experiment 2* were the same as *Experiment 1*. Two combinations of injection sites were used in *Experiment 2*: dmNAcSh and CeL, and BSTDL and CeL.

3.2.2.3 Behavioral procedures

The behavioral experiment was designed to examine whether projection-specific neurons in the PVT are activated to fear and anxiety associated with stressful events. The first stressful condition was exposure to a series of footshocks which can induce unconditioned fear. One week after surgery, a group of rats (n = 6) were placed into a shock chamber (MED Associates, St. Albans, Vermont, USA) for a total of 5 min. After a 2 min acclimation period, each rat received 5 footshocks (1.5 mA, 2 s, ITI = 10–50 s). The rats were kept in the chamber for 1 min after last footshock and then returned to their home cage. A control group of rats (n = 6) were placed in the shock chamber for the same amount of time but received no shock. Ninety minutes after leaving the shock chamber, rats were deeply anesthetized and perfused transcardially. The second stressful condition was exposure to a context where they received footshock previously

(conditioned fear expression). This group of rats (n = 6) received 5 footshocks (1.5 mA, 2 s, same procedure as the first stressful event) in the shock chamber. One day later the rats were placed into the shock chamber for 5 min without shock. The amount of freezing displayed in the shock chamber was measured to determine if footshocks and shock context re-exposure induced conditioned fear expression in the rats that received the footshocks. A nonshocked (NS) group of rats (n = 6) was also placed in the shock chamber in two consecutive days but received no shock at the first or second time. Rats were perfused 90 min after being removed from the shock chamber and returned to their home cages. A combination of tracer injections was made in the dmNAcSh and CeL for rats exposed to the first or the second stressful conditions. The third stressful condition was exposure to a novel open field which induces anxiety. The open field test was done in an open Plexiglas box (80 × 80 × 40 cm) with 1-100 lux of illuminance. The rats (n = 12) were randomly assigned to four conditions involving different levels of illuminance (1, 5, 40, or 100 lux) in the open field. Rats were placed in a corner of the open field and allowed to explore for 5 min. Their behaviors in the open field were videotaped by a camera mounted on the ceiling. The time spent in the center area (35 × 35 cm) and the total distance traveled were analyzed by a software Ethovision (Noldus, Wageningen, Netherland). The time spent immobile in the open field was quantified manually. An immobile state was defined as no movement on four limbs. A control group of rats (n = 4) involved placing rats in the test room but kept in the cage used for the transfer from the colony to the test room for 5 min. Rats were perfused 90 min after being returned to their home cages in the colony room. The tracer injection sites were BSTDL and CeL animals in rats that were exposed to the third stressful condition.

3.2.2.4 Histology

Rats were perfused 90 min after the behavioral tests using the same procedure of perfusion and collection of brain sections as done for *Experiment 1*. Brain sections containing the PVT region were pre-incubated in the blocking solution for 1 h and then incubated in primary rabbit anti-cFos antibody (1:2000; catalogue No. ABE457, Millipore, Temecula, CA, USA) overnight. After 3 rinses in PBS, sections were transferred into a secondary donkey anti-rabbit conjugated to Alexa Fluor 647 (1:1000; catalogue No. A31573, Invitrogen, Calsbad, CA, USA) antiserum for 2 h. After three more rinsing steps, sections were mounted, dehydrated, and coverslipped as described in *Experiment 1*.

3.2.2.5 Data analysis

Behavioral data in the contextual fear expression test and the open field test were presented as mean ± SEM. Anxiety level in the open filed test were estimated by three behavioral measures: the time spent in the center, distance traveled, and the time of immobility. Each rat was given an ordinal rank for each measure. The average rank of three measures for each rat was used to assign the rats into high- and low-anxiety groups. The high-anxiety group consisted of rats with higher ranks (n = 6) and the low-anxiety group consisted of rats with lower ranks (n = 6).

Brain sections were examined using a Zeiss Axio Observer Z1 fluorescent microscope equipped with Axiocam 503 mono camera. The total numbers of cFos and CTb labeled cells in the PVT were counted on sections 400 µm apart starting at the level of the aPVT (1.30 mm posterior to bregma) to the pPVT (3.70 mm posterior to bregma) according to a standard atlas of the rat brain (Paxinos & Watson, 2007). The presence of fluorescent labeled neurons in the PVT was examined and photographed under appropriate filters. Single-, double-, and triple-labeled

neurons were counted on images taken under 20× magnification in software ZEN 2 from Zeiss. The count data for all the sections analyzed were subdivided into aPVT and pPVT levels (three sections each). The proportion of CTb-labeled cells in the PVT were estimated based on the mean number of NeuN-labeled cells in the PVT from *Experiment 1*. In addition, *Experiment 2* used cFos labeling to evaluate whether a PVT neuron was activated during behavioral test. All sections were analyzed using the same level of fluorescent brightness and a set of fixed settings in the software for image taking and viewing to determine whether a cell was cFos-positive. The proportion of neurons in the PVT expressing cFos was estimated based on the mean number of NeuN-labeled cells in the PVT from *Experiment 1*. The proportion of cFos-positive nuclei in CTb-labeled cells in the PVT was used to indicate the extent of activation of PVT neurons that projecting to a specific area. Students *t*-test was used to compare the expression levels of cFos between stressed group and control group in the aPVT or pPVT. A two-way ANOVA was used to analyze the proportion of cFos-labeled cells in PVT neurons that labeled by CTb tracers under different behavioral treatments or anxiety levels. Tukey's post-hoc test and simple effect test were used for further comparison.

3.3 Results

3.3.1 *Experiment 1*: collateralization of the main subcortical outputs from the PVT.

Four cases for each pair were selected based on the criteria that the injections were restricted to targeted regions and were of approximately the same size in terms of the diffusion of tracer. The cases discarded were those with an injection off target or that had injections that were visibly smaller than the typical injection site selected for the study. Figure 3-1 shows one representative case with injection sites in the NAcSh and CeL as well as the retrograde labeling

in the aPVT and pPVT resulted from these injections. The dense cores of the tracers were largely confined to the medial NAcSh and the CeL. The pattern of fluorescent labeling observed was consistent to that observed in a previous study using immunohistochemical staining with DAB (Li & Kirouac, 2008). Regions around the dense cores also contained more diffuse CTb. However, it is unlikely that fibers to areas of diffuse CTb produce observable retrograde transport in the PVT (Luppi, Fort, & Jouvet, 1990). The pairs of injection sites selected for analysis are schematically illustrated in Figure 3-2. For the combinations of NAcSh and CeL, NAcSh and BSTDL, NAcSh and NAcC, the injections to the NAcSh were confined to the medial region of the shell.

Figure 3-1 Images and drawings of one representative case showing the tracer injection sites in NAcSh and CeL and retrogradely labeled cells in aPVT and pPVT

A. CTb injection sites with demarcation (dashed line) identified based on adjacent sections with NeuN staining. **B, C**. Images of aPVT (**B**) and pPVT (**C**) section showing AF-CTb-488-labeled (green), AF-CTb-594-labeled (red) and double-labeled (merged; yellow) PVT neurons. Drawing of the same section on the right shows labeled neurons with demarcation of the midline thalamus adapted from a stereotaxic atlas (Paxinos & Watson, 2007). Double-labeled neurons are identified as black asterisk in the drawing. Each symbol represents the position of a single neuron and the numbers at the bottom of each picture represent the approximate distance from bregma. **D.** High magnification images of the same aPVT section in b (white frame) showing single- and double-labeled cells of the aPVT, the inset shown in the last panel was taken at a higher magnification. Scale bars **A** 250 μm; **B**, **C** 100 μm; **D** 25 μm and the inset 10 μm.

Abbreviations: 3V, third ventricle; aca, anterior commissure, anterior limb; BLA, basolateral nucleus of amygdala; CeC, central nucleus of amygdala, capsular; CeL central nucleus of amygdala, lateral; CeM, central nucleus of amygdala, medial; CPu, caudate putamen; Hb, habenular nucleus; ic, internal capsular; IMD, intermediodorsal nucleus of thalamus; MD, mediodorsal nucleus of thalamus; NAcC, nucleus accumbens, core; NAcSh, nucleus accumbens, shell; opt, optic tract; PT, paratenial nucleus of thalamus; aPVT, paraventricular nucleus of thalamus, anterior; pPVT, paraventricular nucleus of thalamus, posterior.

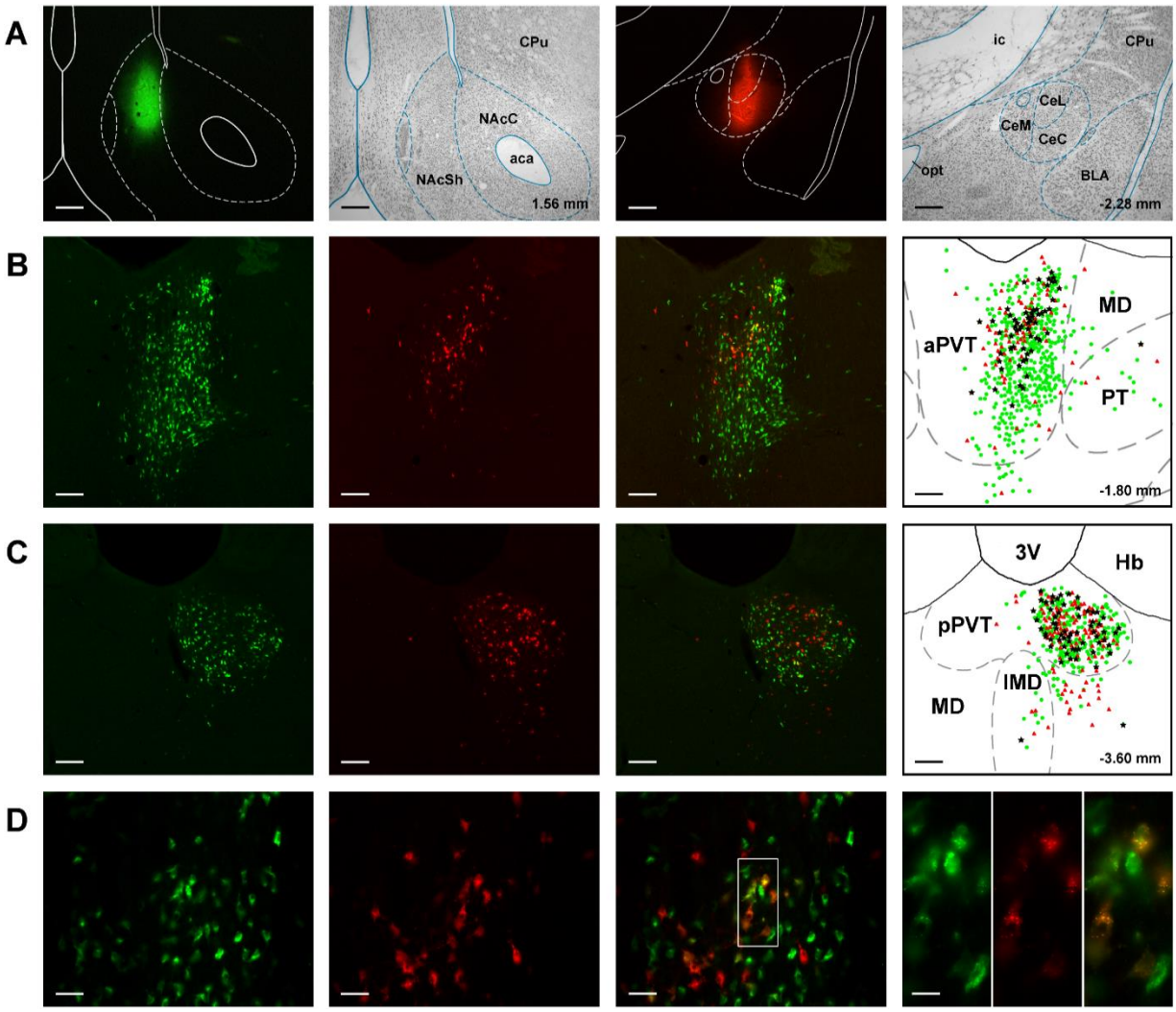
A
CPu
NAcC
aca
NAcSh
1.56 mm
ic
CPu
CeL
CeM
CeC
opt
BLA
-2.28 mm
B
MD
aPVT
PT
-1.80 mm
C
3V
Hb
pPVT
lMD
MD
-3.60 mm
D

Figure 3-2 Schematic representations of paired CTb-AF488 (green) and CTb-AF594 (red) injection sites in different cases

Injections were grouped as NAcSh + CeL; NAcSh + BSTDL; BSTDL + CeL; CeL + BLA; NAcSh + NAcC, and dmNAcSh + vmNAcSh. Numbers at the bottom of each drawing represent the approximate distance from bregma. Scale bar: 250 μm.

Abbreviations: ac, anterior commissure; aca, anterior commissure, anterior limb; BLA, basolateral nucleus of amygdala; BLP, basolateral nucleus of amygdala, posterior; BSTDL, bed nucleus of stria terminalis, dorsolateral; BSTM, bed nucleus of stria terminalis, medial; CeC, central nucleus of amygdala, capsular; CeL central nucleus of amygdala, lateral; CeM, central nucleus of amygdala, medial; CPu, caudate putamen; ic, internal capsular; NAcC, nucleus accumbens, core; NAcSh, nucleus accumbens, shell.

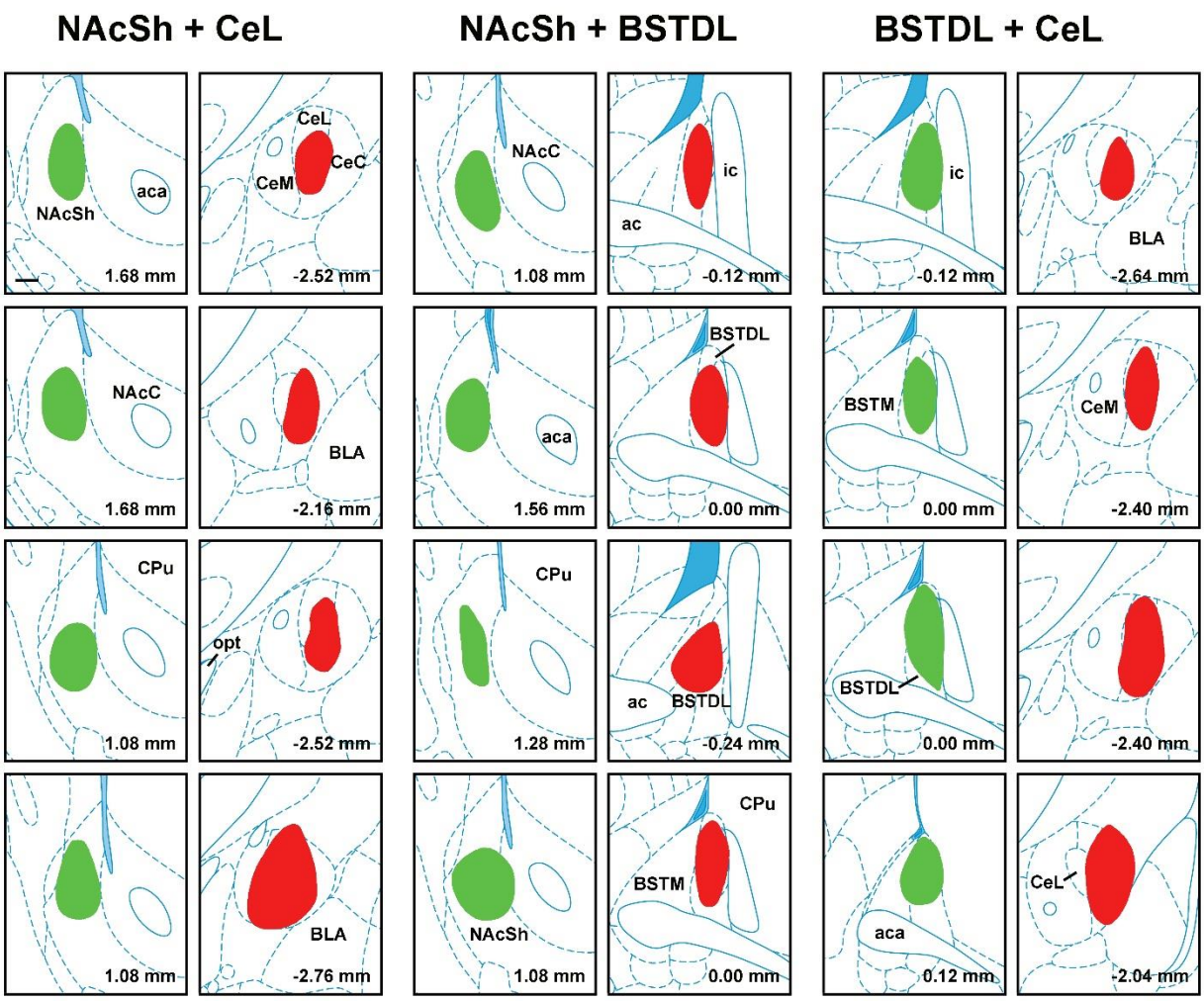
NAcSh + CeL
NAcSh + BSTDL
BSTDL + CeL
NAcSh
aca
1.68 mm
CeL
CeC
CeM
-2.52 mm
NAcC
1.08 mm
ic
ac
-0.12 mm
-0.12 mm
BLA
-2.64 mm
NAcC
1.68 mm
BLA
-2.16 mm
aca
1.56 mm
BSTDL
0.00 mm
BSTM
0.00 mm
CeM
-2.40 mm
CPu
1.08 mm
opt
-2.52 mm
CPu
1.28 mm
ac
BSTDL
-0.24 mm
BSTDL
0.00 mm
-2.40 mm
1.08 mm
BLA
-2.76 mm
NAcSh
1.08 mm
CPu
BSTM
0.00 mm
aca
0.12 mm
CeL
-2.04 mm

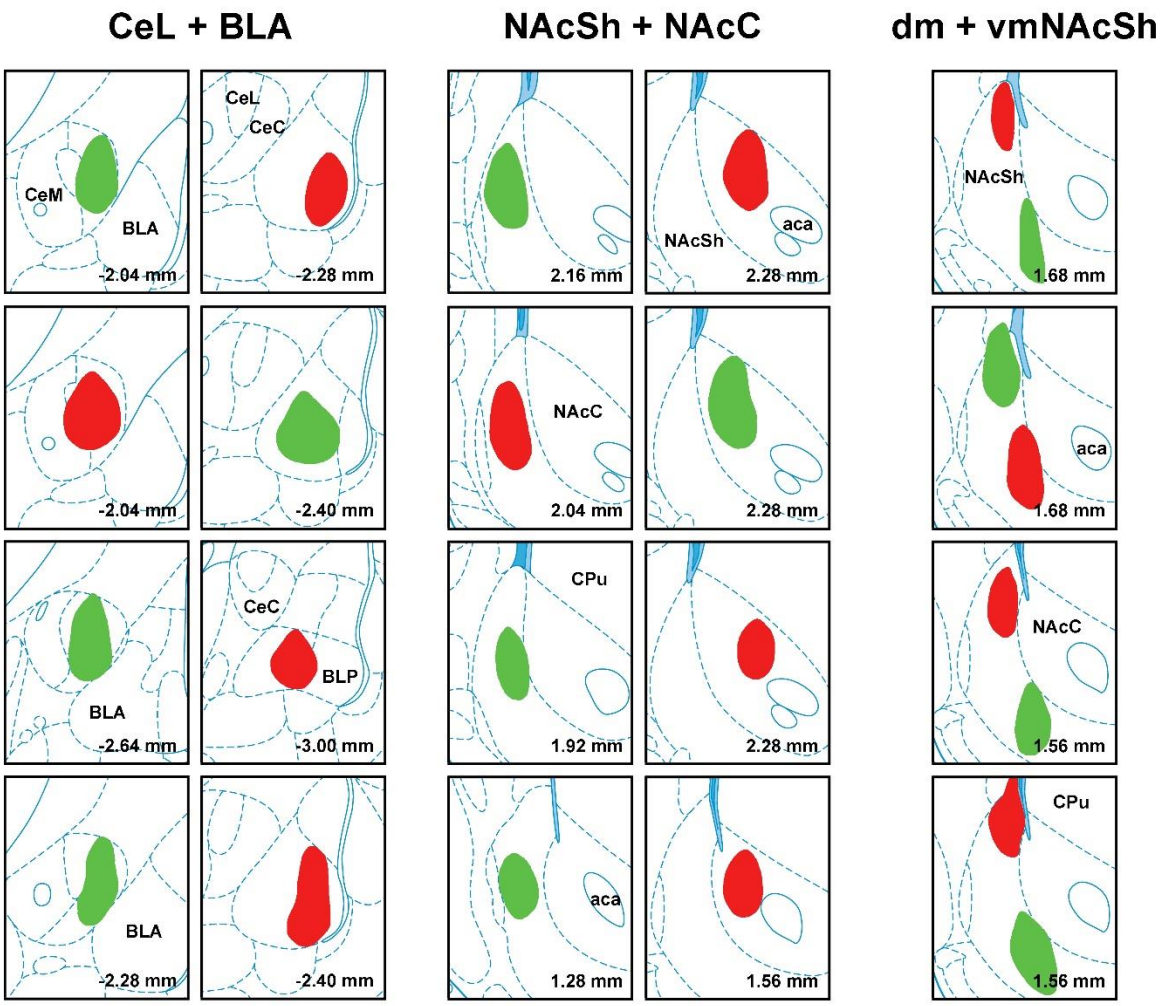
CeL + BLA
NAcSh + NAcC
dm + vmNAcSh
CeM
BLA
-2.04 mm
CeL
CeC
-2.28 mm
2.16 mm
NAcSh
aca
2.28 mm
NAcSh
1.68 mm
-2.04 mm
-2.40 mm
NAcC
2.04 mm
2.28 mm
aca
1.68 mm
BLA
-2.64 mm
CeC
BLP
-3.00 mm
CPu
1.92 mm
2.28 mm
NAcC
1.56 mm
BLA
-2.28 mm
-2.40 mm
aca
1.28 mm
1.56 mm
CPu
1.56 mm

The fluorescent conjugate of CTb used was reversed in some of the injections to evaluate the uptake and transport of the different conjugates (see Figure 3-2 for placement of different conjugates in the same regions). For example, the number of labeled neurons in the PVT in cases with CTb-AF594 injections in the BSTDL (2217 ± 385, n = 4) was very close to the number counted when CTb-AF488 was injected to the BSTDL (2221 ± 331, n = 4). Similarly, the number of labeled neurons in the PVT in cases with CTb-AF594 injections in the CeL (1354 ± 176; n = 7) was comparable to the number when CTb-AF488 was injected to the CeL (1272 ± 233; n = 3).

The purpose of this study is to provide a map of the location and an estimation of the number of neurons in the PVT that project to two different subcortical targets. The distributions of retrogradely labeled cells (single- and double-labeled neurons) are shown in four anterior–posterior levels of the PVT (e.g. Figure 3-4). The proportion of labeled cells was estimated from the number of NeuN-stained neurons counted on the same levels used to count the fluorescent labeled neurons (Figure 3-3). The average numbers of NeuN-stained neurons for the aPVT (7412 ± 379) and pPVT (5854 ± 274) were applied to all cases to estimate the proportion of CTb-labeled cells in the PVT that project to the different subcortical targets.

Figure 3-3 NeuN-stained cells in PVT coronal sections at different anterior-posterior levels

A. Images showing the location of the aPVT and pPVT in the midline thalamus histochemically immunoreacted for NeuN. **B**. Numbers of NeuN-stained cells at different anterior–posterior levels of the PVT. Cells were counted bilaterally at 16 levels (1–16, anterior to posterior) in four animals. Values are shown as mean ± SEM in **B**. Scale bar, 250 μm.

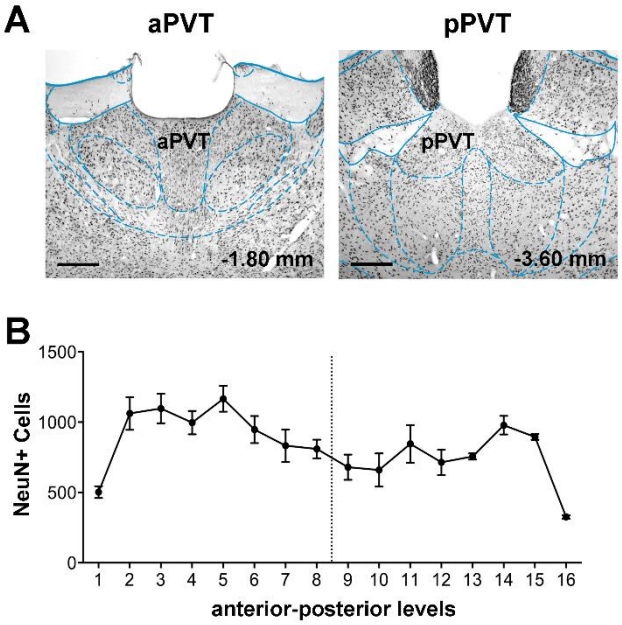

3.3.1.1 Combined injections into the NAcSh and CeL

The dense cores of the injection were located in the medial portion of the NAcSh and the CeL (Fig. 3-2). Figure 3-1 shows the anterior–posterior retrograde labeling observed in one representative case (the first case of the left column in Figure 3-2). The NAcSh-projecting cells were located throughout the PVT on the ipsilateral side of the injection (Figure 3-1, 3-4). Labeled cells were also found in other midline and intralaminar nuclei, including the paratenial, paracentral, and more sparsely in the central medial, mediodorsal and intermediodorsal thalamic nuclei. The CeL-projecting cells were distributed sporadically in the more anterior sections of the PVT, but progressively increased in more posterior sections to numbers that are comparable to that of the NAcSh-projecting cells. The estimated percentages of single- and double-labeled cells in the aPVT and the pPVT for this case are shown in the lower right corner of Figure 3-4 while the average proportions for the four cases are shown in Figure 3-11A. Significantly more neurons in the aPVT projected to the NAcSh compared to the numbers of neurons projecting to the CeL ($F_{(1,3)} = 16.68$, $p = 0.027$; Figure 3-11A). In contrast, there was no difference in the proportions of the pPVT neurons that projected to these two areas ($F_{(1,3)} = 0.94$, $p = 0.405$; Figure 3-11A). A proportion of cells was found to project to both the NAcSh and the CeL with 7.0 and 8.6% of the total number of neurons in aPVT and pPVT, respectively. It is noteworthy that nearly half of the aPVT neurons that projected to the CeL also projected to the NAcSh, whereas approximately 30% of the pPVT neurons that projected to the CeL projected to the NAcSh (Figure 3-11A). Finally, the one case that involved a larger injection of CTb in the CeL (100 nl, last case in Figure 3-2 left column) produced more labeled cells in the PVT, but the pattern of distribution and the proportion of doubled-labeled cells remained similar to the other cases (data not shown).

Figure 3-4 A representative case with combined injections in the NAcSh and CeL

Drawings of labeled cells are from four anterior–posterior levels with the approximate distance from bregma shown as numbers at the bottom of each drawing. Cells projecting to the NAcSh are in green (dot), CeL are in red (triangle), and the double-labeled neurons are in black (asterisk). Each symbol represents the position of a single neuron and the numbers at the bottom of each picture represent the approximate distance from bregma. The estimated percentages of single- and double-labeled neurons to the total number of NeuN+ cells in the aPVT vs the pPVT are shown in the bar graphs at the lower right corner. Scale bars, 250 μm for injection sites, 150 μm for drawings.

Abbreviations: 3V, third ventricle; aca, anterior commissure, anterior limb; CeC, central nucleus of amygdala, capsular; CeL central nucleus of amygdala, lateral; CeM, central nucleus of amygdala, medial; CM, central medial nucleus of thalamus; DB, double-labeled; IMD, intermediodorsal nucleus of thalamus; MD, mediodorsal nucleus of thalamus; NAcSh, nucleus accumbens, shell; PT, paratenial nucleus of thalamus; PVT, paraventricular nucleus of thalamus; aPVT, paraventricular nucleus of thalamus, anterior; pPVT paraventricular nucleus of thalamus, posterior.

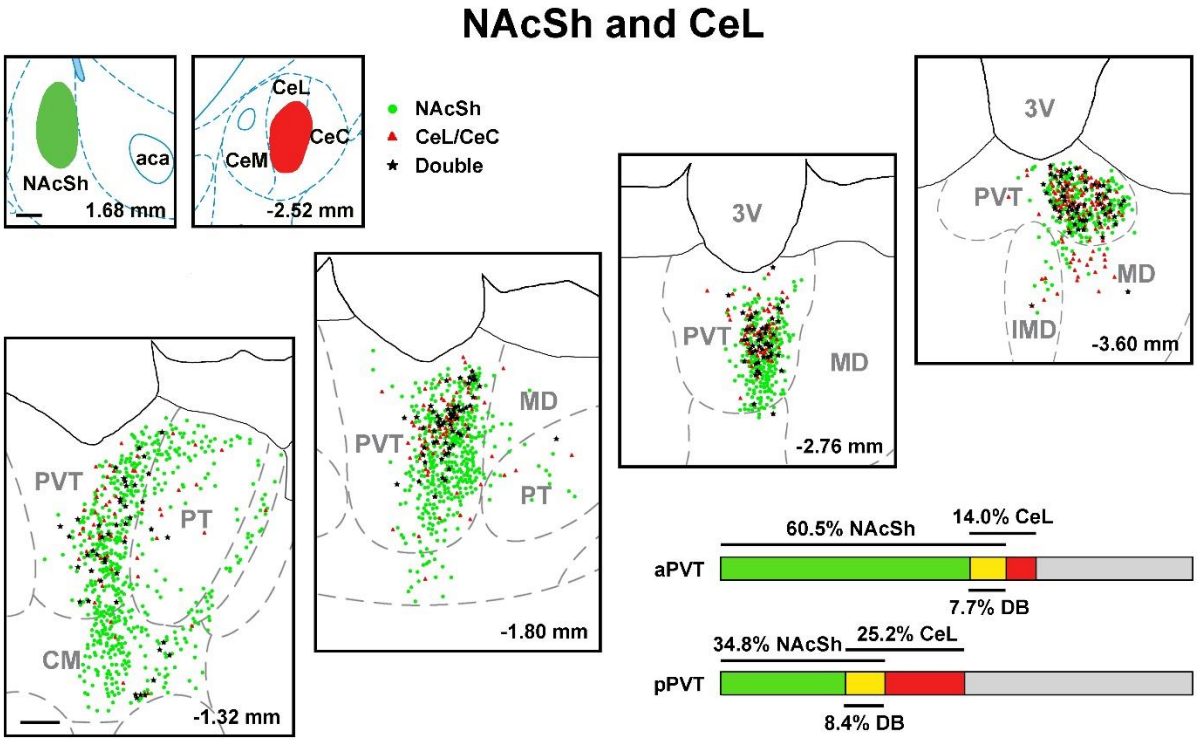
NAcSh and CeL
NAcSh
aca
1.68 mm
CeL
CeC
CeM
-2.52 mm
NAcSh
CeL/CeC
Double
3V
PVT
MD
-2.76 mm
3V
PVT
MD
IMD
-3.60 mm
PVT
MD
PT
-1.80 mm
PVT
PT
CM
-1.32 mm
60.5% NAcSh
14.0% CeL
aPVT
7.7% DB
34.8% NAcSh
25.2% CeL
pPVT
8.4% DB

3.3.1.2 Combined injections into the NAcSh and BSTDL

The BSTDL- and NAcSh-projecting cells were distributed throughout the dorsal–ventral and anterior–posterior extent of the PVT (Figure 3-5). A large number of BSTDL-projecting cells were also found in other midline thalamic nuclei. More neurons in the aPVT projected to the NAcSh compared to the numbers of neurons projecting to the BSTDL ($F_{(1,3)} = 181.98$, $p = 0.001$; Figure 3-11B). However, there was no difference in the proportions of the pPVT neurons that projected to these two areas ($F_{(1,3)} = 8.03$, $p = 0.066$; Figure 3-11B). A proportion of cells was found to project to both the NAcSh and the BSTDL with 16.0 and 17.4% of the total number of neurons in aPVT and pPVT, respectively. In this combination, almost a half of the BSTDL-projecting cells were found to also project to the NAcSh (Figure 3-11B). It is clear from a qualitative perspective that a larger proportion of NAcSh-projecting cells also projected to the BSTDL (aPVT 28%, pPVT 40%) than to the CeL (aPVT 14%, pPVT 22%).

Figure 3-5 A representative case with combined injections in the NAcSh and BSTDL

Cells projecting to the NAcSh are in green (dot), BSTDL are in red (triangle), and the double-labeled neurons are in black (asterisk). Each symbol represents the position of a single neuron and the numbers at the bottom of each picture represent the approximate distance from bregma. The estimated percentages of single- and double-labeled neurons to the total number of NeuN+ cells in the aPVT vs the pPVT are shown in the bar graphs at the lower right corner. Scale bars, 250 μm for injection sites, 150 μm for drawings.

Abbreviations: 3V, third ventricle; aca, anterior commissure, anterior limb; BSTDL, bed nucleus of stria terminalis, dorsolateral; CM, central medial nucleus of thalamus; DB, double-labeled; Hb, habenular nucleus; ic, internal capsular; IMD, intermediodorsal nucleus of thalamus; MD, mediodorsal nucleus of thalamus; NAcSh, nucleus accumbens, shell; PC, paracentral nucleus of thalamus; PT, paratenial nucleus of thalamus; PVT, paraventricular nucleus of thalamus; aPVT, paraventricular nucleus of thalamus, anterior; pPVT paraventricular nucleus of thalamus, posterior.

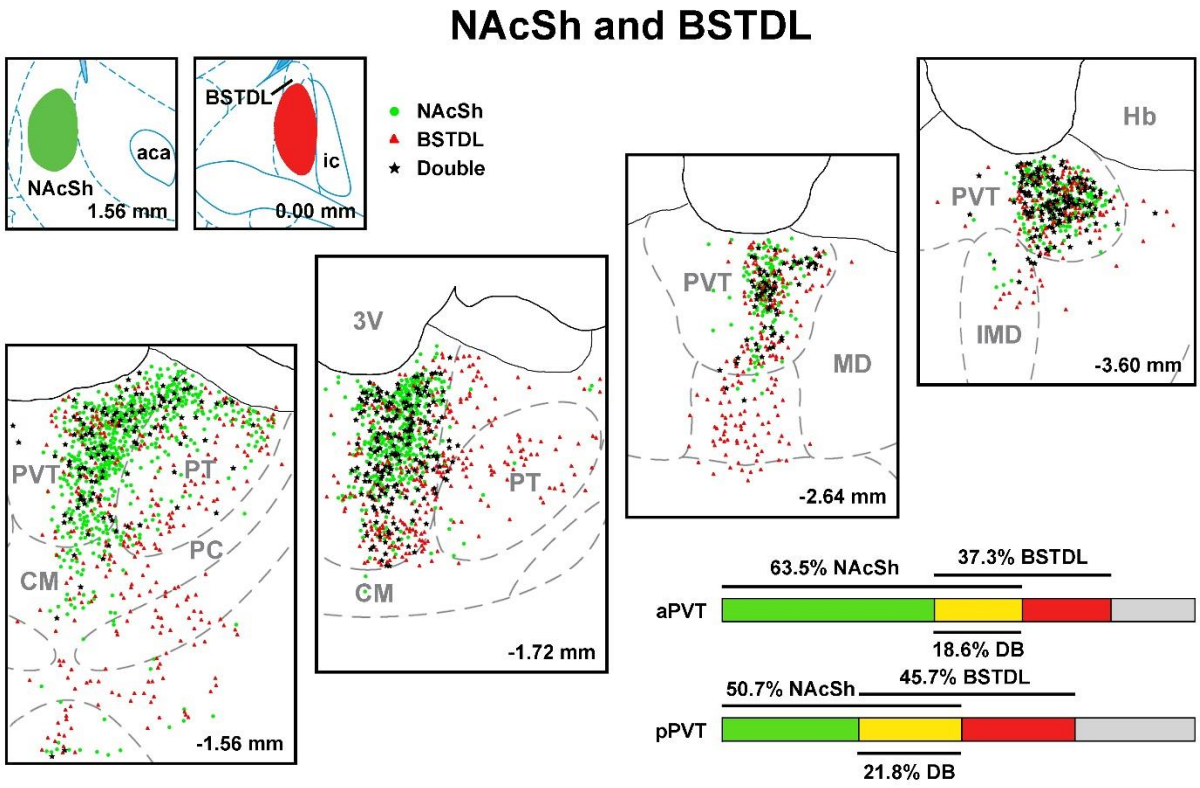
NAcSh and BSTDL
NAcSh
1.56 mm
aca
BSTDL
ic
0.00 mm
NAcSh
BSTDL
Double
Hb
PVT
IMD
-3.60 mm
PVT
MD
-2.64 mm
3V
PT
CM
-1.72 mm
PVT
PT
PC
CM
-1.56 mm
63.5% NAcSh
37.3% BSTDL
aPVT
18.6% DB
50.7% NAcSh
45.7% BSTDL
pPVT
21.8% DB

3.3.1.3 Combined injections into the BSTDL and CeL

The distribution of BSTDL-projecting cells (Figures 3-6) was comparable to the previous combination (Figure 3-5) with large numbers of cells found throughout the anterior to posterior extent of the PVT and surrounding nuclei in the midline thalamus. The pattern of CeL-projecting cells (Figures 3-6) was also similar to the case in Figure 3-4 with labeled cells being largely confined to the PVT. Figure 3-7 shows the labeled PVT neurons in one representative case. No difference was found in the proportions of neurons that projected to these two areas at either aPVT ($F_{(1,3)} = 8.26$, $p = 0.064$; Figure 3-11C) or pPVT ($F_{(1,3)} = 1.74$, $p = 0.279$; Figure 3-11C). The proportion of double-labeled cells projecting to both the BSTDL and CeL was 5.9 and 12.5% of the total number of neurons in aPVT and pPVT, respectively.

Figure 3-6 A representative case with combined injections in the BSTDL and CeL

Cells projecting to the BSTDL are in green (dot), CeL are in red (triangle), and the double-labeled neurons are in black (asterisk). Each symbol represents the position of a single neuron and the numbers at the bottom of each picture represent the approximate distance from bregma. The estimated percentages of single- and double-labeled neurons to the total number of NeuN+ cells in the aPVT vs the pPVT are shown in the bar graphs at the lower right corner. Scale bars, 250 μm for injection sites, 150 μm for drawings.

Abbreviations: 3V, third ventricle; ac, anterior commissure; AM, anteromedial nucleus of thalamus; BSTDL, bed nucleus of stria terminalis, dorsolateral; CeC, central nucleus of amygdala, capsular; CeL central nucleus of amygdala, lateral; CeM, central nucleus of amygdala, medial; CM, central medial nucleus of thalamus; DB, double-labeled; ic, internal capsular; IAM, interanteromedial nucleus of thalamus; IMD, intermediodorsal nucleus of thalamus; MD, mediodorsal nucleus of thalamus; PT, paratenial nucleus of thalamus; PVT, paraventricular nucleus of thalamus; aPVT, paraventricular nucleus of thalamus, anterior; pPVT paraventricular nucleus of thalamus, posterior; Re, nucleus reuniens of thalamus.

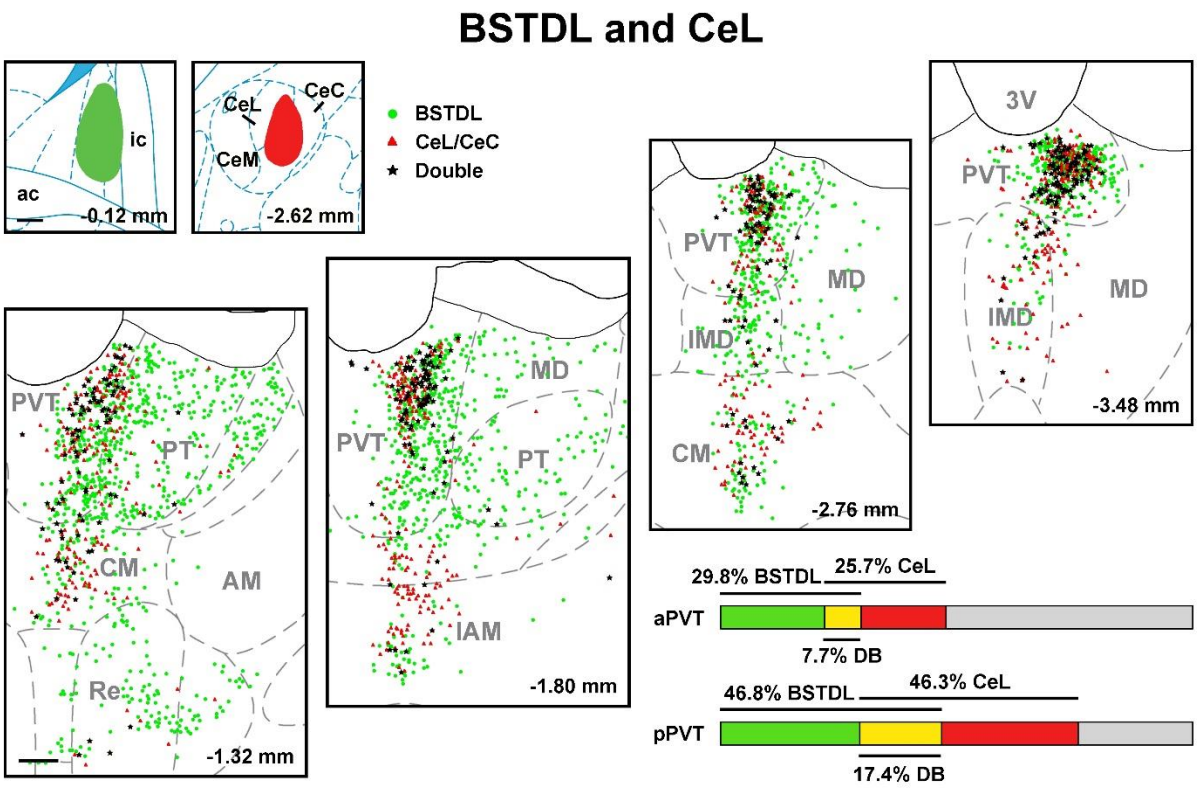
BSTDL and CeL
ic
ac
-0.12 mm
CeL
CeC
CeM
-2.62 mm
BSTDL
CeL/CeC
Double
3V
PVT
MD
IMD
-3.48 mm
PVT
MD
IMD
CM
-2.76 mm
PVT
PT
CM
AM
Re
-1.32 mm
MD
PVT
PT
IAM
-1.80 mm
29.8% BSTDL
25.7% CeL
aPVT
7.7% DB
46.8% BSTDL
46.3% CeL
pPVT
17.4% DB

Figure 3-7 Images and drawings of one representative case showing the tracer injection sites in BSTDL and CeL and retrogradely labeled cells in aPVT and pPVT

A. CTb injection sites with demarcation (dashed line) identified based on adjacent sections with NeuN staining. **B, C.** Images of aPVT (**B**) and pPVT (**C**) section showing AF-CTb-488-labeled (green), AF-CTb-594-labeled (red) and double-labeled (merged; yellow) PVT neurons. Drawing of the same section on the right shows labeled neurons with demarcation of the midline thalamus adapted from a stereotaxic atlas (Paxinos & Watson, 2007). Double-labeled neurons are identified as black asterisk in the drawing. Each symbol represents the position of a single neuron and the numbers at the bottom of each picture represent the approximate distance from bregma. **D.** High magnification images of the same pPVT section in **C** (white frame) showing single- and double-labeled cells of the pPVT, the inset shown in the last panel was taken at a higher magnification. Scale bars, **A** 250 μm; **B**, **C** 100 μm; **D** 25 μm, inset 10 μm. Abbreviations: ac, anterior commissure; BLA, basolateral nucleus of amygdala; BSTDL, bed nucleus of stria terminalis, dorsolateral; BSTM, bed nucleus of stria terminalis, medial; CeC, central nucleus of amygdala, capsular; CeL central nucleus of amygdala, lateral; CeM, central nucleus of amygdala, medial; CPu, caudate putamen; ic, internal capsular; IMD, intermediodorsal nucleus of thalamus; MD, mediodorsal nucleus of thalamus; opt, optic tract; PT, paratenial nucleus of thalamus; aPVT, paraventricular nucleus of thalamus, anterior; pPVT, paraventricular nucleus of thalamus, posterior.

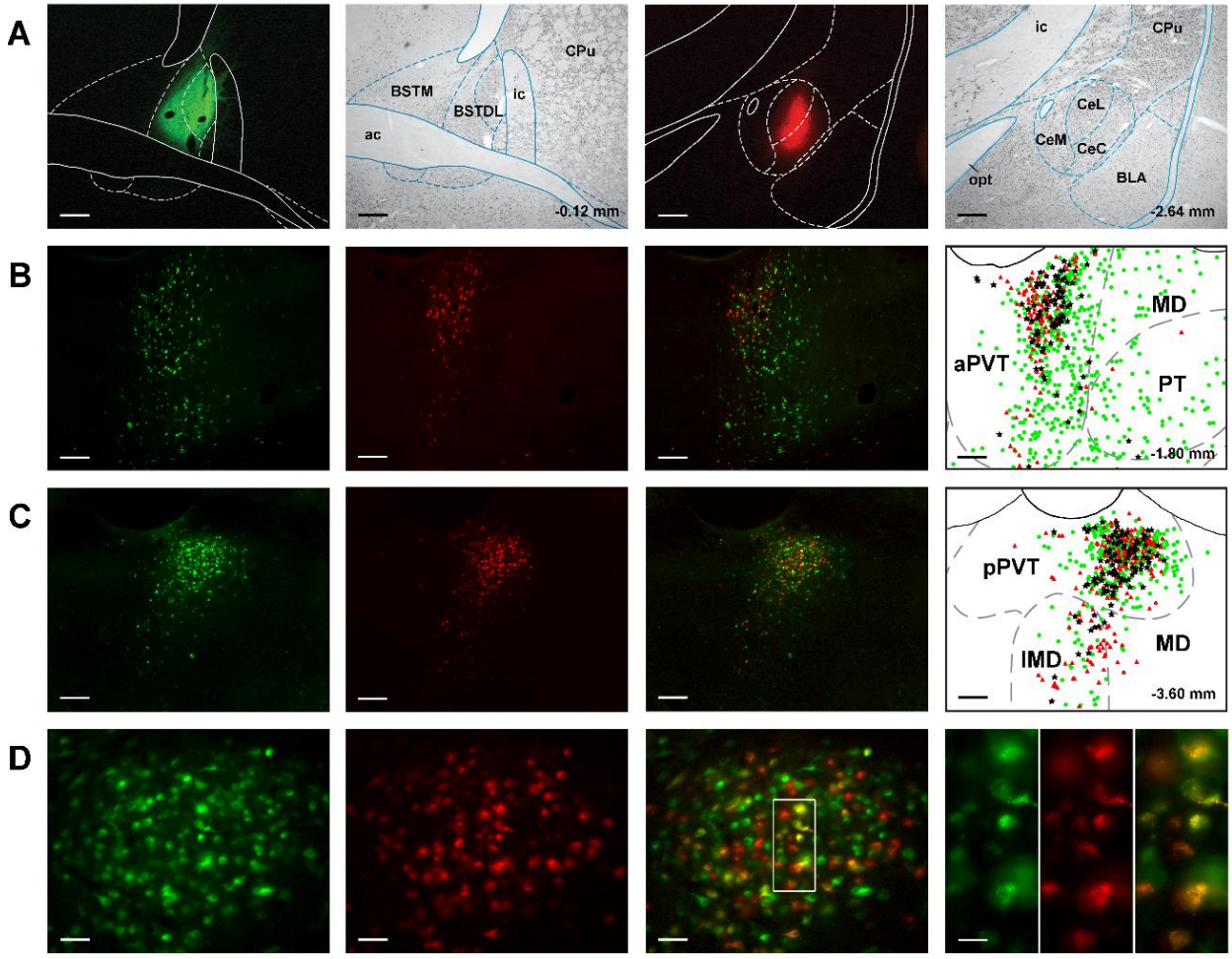
A
CPu
BSTM
BSTDL
ic
ac
-0.12 mm
ic
CPu
CeL
CeM
CeC
opt
BLA
-2.64 mm
B
MD
aPVT
PT
-1.80 mm
C
pPVT
MD
lMD
-3.60 mm
D

3.3.1.4 Combined injections into the CeL and BLA

The distribution of CeL-projecting cells in this combination (Figure 3-8) was similar to the case shown in Figure 3-4. The BLA-projecting cells were scattered in the more anterior sections of the PVT and other midline thalamic nuclei while their numbers progressively increased in more posterior sections of the PVT in a pattern that was similar to the CeL-projecting cells in the pPVT. The CeL- and BLA-projecting cells were largely intermingled throughout the PVT region and there was no appearance of topographical segregation of subpopulation that was projection specific for CeL or BLA. There was significantly more CeL-projecting neurons than BLA-projecting neurons in both aPVT ($F_{(1,3)} = 10.67$, $p = 0.047$; Figure 3-11D) and pPVT ($F_{(1,3)} = 17.39$, $p = 0.025$; Figure 3-11D). The proportion of double-labeled cells projecting to both the CeL and BLA was 1.9 and 7.1% of the total number of neurons in aPVT and pPVT, respectively.

Figure 3-8 A representative case with combined injections in the CeL and BLA

Cells projecting to the CeL are in green (dot), BLA are in red (triangle), and the double-labeled neurons are in black (asterisk). Each symbol represents the position of a single neuron and the numbers at the bottom of each picture represent the approximate distance from bregma. The estimated percentages of single- and double-labeled neurons to the total number of NeuN+ cells in the aPVT vs the pPVT are shown in the bar graphs at the lower right corner. Scale bars, 250 μm for injection sites, 150 μm for drawings.

Abbreviations: 3V, third ventricle; BLA, basolateral nucleus of amygdala; CeL central nucleus of amygdala, lateral; CeM, central nucleus of amygdala, medial; CM, central medial nucleus of thalamus; DB, double-labeled; Hb, habenular nucleus; IMD, intermediodorsal nucleus of thalamus; MD, mediodorsal nucleus of thalamus; PC, paracentral nucleus of thalamus; PT, paratenial nucleus of thalamus; PVT, paraventricular nucleus of thalamus; aPVT, paraventricular nucleus of thalamus, anterior; pPVT paraventricular nucleus of thalamus, posterior.

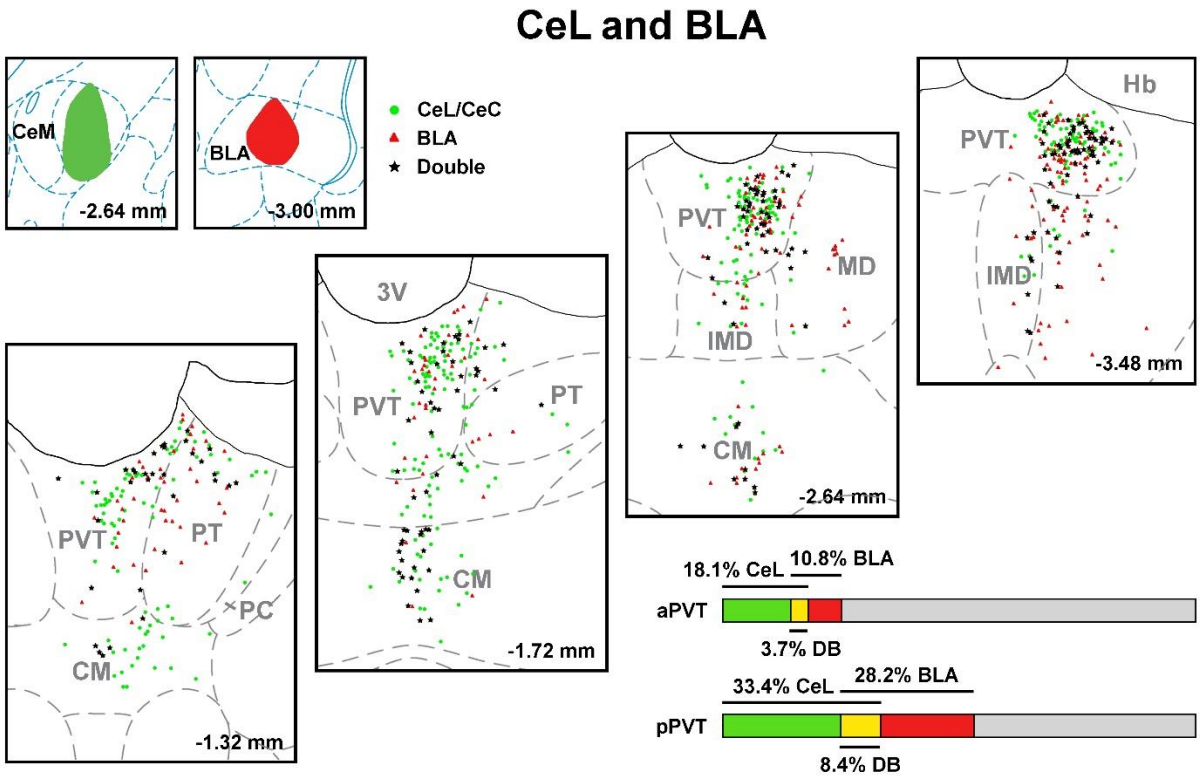
CeL and BLA
CeM
-2.64 mm
BLA
-3.00 mm
CeL/CeC
BLA
Double
3V
PVT
PT
CM
-1.72 mm
PVT
PT
PC
CM
-1.32 mm
PVT
MD
IMD
CM
-2.64 mm
Hb
PVT
IMD
-3.48 mm
18.1% CeL
10.8% BLA
aPVT
3.7% DB
33.4% CeL
28.2% BLA
pPVT
8.4% DB

3.3.1.5 Combined injections into the NAcSh and NAcC

The NAcC-projecting cells were found throughout the anterior–posterior extent of the PVT and intermingled with NAcSh-projecting cells (Figure 3-9). The number of labeled NAcC-projecting PVT cells was lower than the NAcSh-projecting cells while more NAcC-projecting cells were found in the paratenial, paracentral, central medial, and intermediaodorsal nucleus of the thalamus. The core-projecting cells were found more in the lateral and ventral part of the PVT when compared to shell-projecting cells. More neurons in the aPVT were found to project to the shell compared to neurons projecting to the core ($F_{(1,3)} = 26.89$, $p = 0.014$; Figure 3-11E). No difference was found in the proportions of the pPVT neurons that projected to these two areas ($F_{(1,3)} = 0.85$, $p = 0.428$; Figure 3-11E). A proportion of double-labeled cells was found with 15.8 and 13.9% of the total number of neurons in aPVT and pPVT, respectively. However, it should be pointed out that 38–49% of the neurons that were found to project to the NAcC were also found to project to the NAcSh.

Figure 3-9 A representative case with combined injections in the NAcSh and NAcC

Cells projecting to the NAcSh are in green (dot), NAcC are in red (triangle), and the double-labeled neurons are in black (asterisk). Each symbol represents the position of a single neuron and the numbers at the bottom of each picture represent the approximate distance from bregma. The estimated percentages of single- and double-labeled neurons to the total number of NeuN+ cells in the aPVT vs the pPVT are shown in the bar graphs at the lower right corner. Scale bars, 250 μm for injection sites, 150 μm for drawings.

Abbreviations: 3V, third ventricle; aca, anterior commissure, anterior limb; CPu, caudate putamen; CM, central medial nucleus of thalamus; DB, double-labeled; Hb, habenular nucleus; IMD, intermediodorsal nucleus of thalamus; MD, mediodorsal nucleus of thalamus; NAcC, nucleus accumbens, core; NAcSh, nucleus accumbens, shell; PC, paracentral nucleus of thalamus; PT, paratenial nucleus of thalamus; PVT, paraventricular nucleus of thalamus; aPVT, paraventricular nucleus of thalamus, anterior; pPVT paraventricular nucleus of thalamus, posterior.

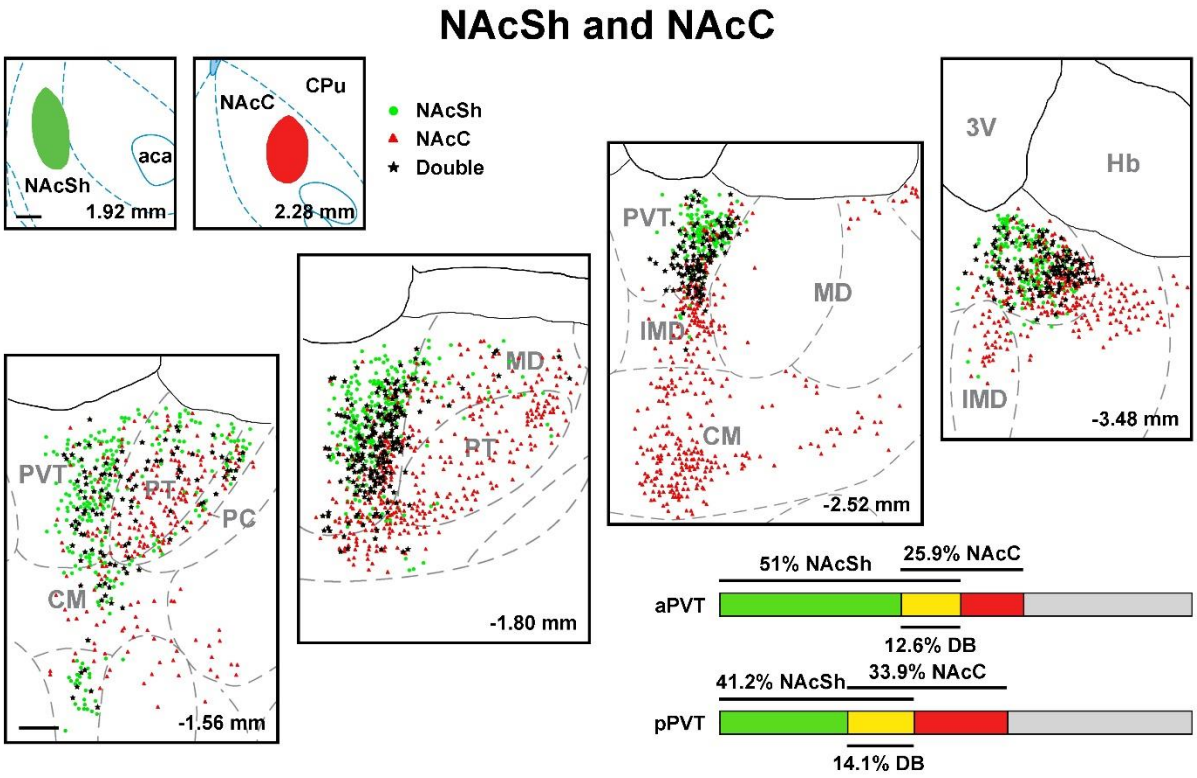
NAcSh and NAcC
NAcSh
aca
1.92 mm
NAcC
CPu
2.28 mm
NAcSh
NAcC
Double
PVT
PT
PC
CM
-1.56 mm
MD
PT
-1.80 mm
PVT
MD
IMD
CM
-2.52 mm
3V
Hb
IMD
-3.48 mm
51% NAcSh
25.9% NAcC
aPVT
12.6% DB
41.2% NAcSh
33.9% NAcC
pPVT
14.1% DB

3.3.1.6 Combined injections into the vmNAcSh and dmNAcSh

The distribution of vmNAcSh-projecting cells in the midline thalamus was different from the pattern of dmNAcSh-projecting cells (Figure 3-10). The posterior levels of the PVT contained a larger number of vmNAcSh-projecting cells than anterior-most sections of the PVT. In fact, the pPVT contained more vmNAcSh-labeled cells than it did following injection of the tracer in the medial NAcSh (see Figures 3-4, 3-5, 3-9). There were also a relatively large number of vmNAcSh-projecting cells in the paratenial and paracentral nucleus of the thalamus. The dmNAcSh-projecting cells were found throughout the dorsoventral extent of the aPVT, whereas fewer of these projection-specific cells were found in the pPVT where they were mostly located in the dorsal most region of the pPVT. Few dmNAcSh-projecting cells were found in other midline thalamic nuclei. There was no difference in the proportions of the aPVT neurons that project to dmNAcSh or vmNAcSh ($F_{(1,3)} = 0.63$, $p = 0.485$; Figure 3-11F), but more neurons in the pPVT projected to the vmNAcSh ($F_{(1,3)} = 34.26$, $p = 0.010$; Figure 3-11F). A relatively small proportion of PVT neurons was found to project to both the vmNAcSh and the dmNAcSh with 10.3 and 7.5% of the total number of neurons in aPVT and pPVT, respectively.

Figure 3-10 A representative case with combined injections in the vmNAcSh and dmNAcSh

Cells projecting to the vmNAcSh are in green (dot), dmNAcSh are in red (triangle), and the double-labeled neurons are in black (asterisk). Each symbol represents the position of a single neuron and the numbers at the bottom of each picture represent the approximate distance from bregma. The estimated percentages of single- and double-labeled neurons to the total number of NeuN+ cells in the aPVT vs the pPVT are shown in the bar graphs at the lower right corner. Scale bars, 250 μm for injection sites, 150 μm for drawings.

Abbreviations: aca, anterior commissure, anterior limb; AM, anteromedial nucleus of thalamus; DB, double-labeled; IMD, intermediodorsal nucleus of thalamus; MD, mediodorsal nucleus of thalamus; NAcC, nucleus accumbens, core; NAcSh, nucleus accumbens, shell; PT, paratenial nucleus of thalamus; PVT, paraventricular nucleus of thalamus; aPVT, paraventricular nucleus of thalamus, anterior; pPVT paraventricular nucleus of thalamus, posterior.

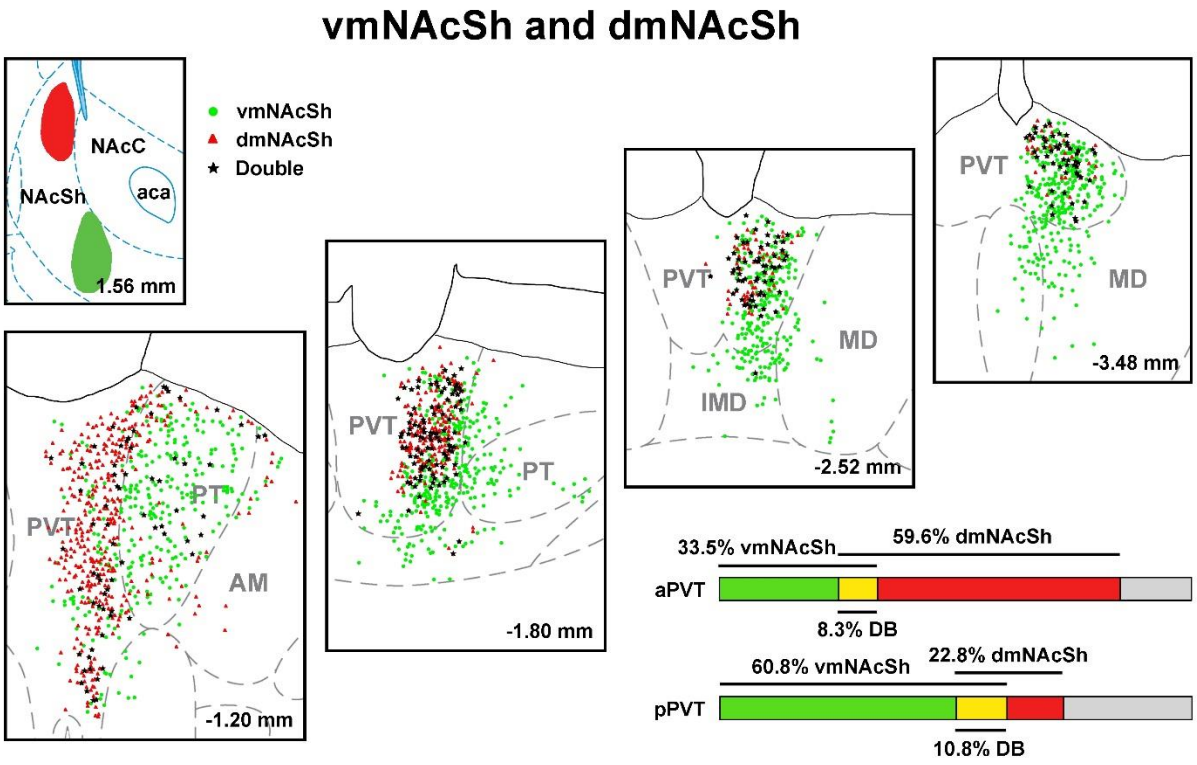
vmNAcSh and dmNAcSh
vmNAcSh
dmNAcSh
Double
NAcC
NAcSh
aca
1.56 mm
PVT
PT
AM
-1.20 mm
PVT
PT
-1.80 mm
PVT
MD
IMD
-2.52 mm
PVT
MD
-3.48 mm
33.5% vmNAcSh
59.6% dmNAcSh
aPVT
8.3% DB
60.8% vmNAcSh
22.8% dmNAcSh
pPVT
10.8% DB

Figure 3-11 The average proportions of single- and double-labeled neurons in the aPVT and pPVT in all six injection combinations in *Experiment 1*.

A. NAcSh + CeL; **B.** NAcSh + BSTDL; **C.** CeL + BSTDL; **D**. CeL + BLA; **E.** NAcSh + NAcC; **F.** vmNAcSh + dmNAcSh. Each combination contains four cases. Values are shown as mean − SEM. Error bars represent the SEMs of the proportions of the PVT neurons that project to one of the injection sites or both.

Abbreviations: BSTDL, bed nucleus of stria terminalis, dorsolateral; CeL central nucleus of amygdala, lateral; DB, double-labeled; NAcC, nucleus accumbens, core; NAcSh, nucleus accumbens, shell; dmNAcSh, nucleus accumbens, shell, dorsomedial; vmNAcSh, nucleus accumbens, shell, ventomedial; aPVT, paraventricular nucleus of thalamus, anterior; pPVT paraventricular nucleus of thalamus, posterior.

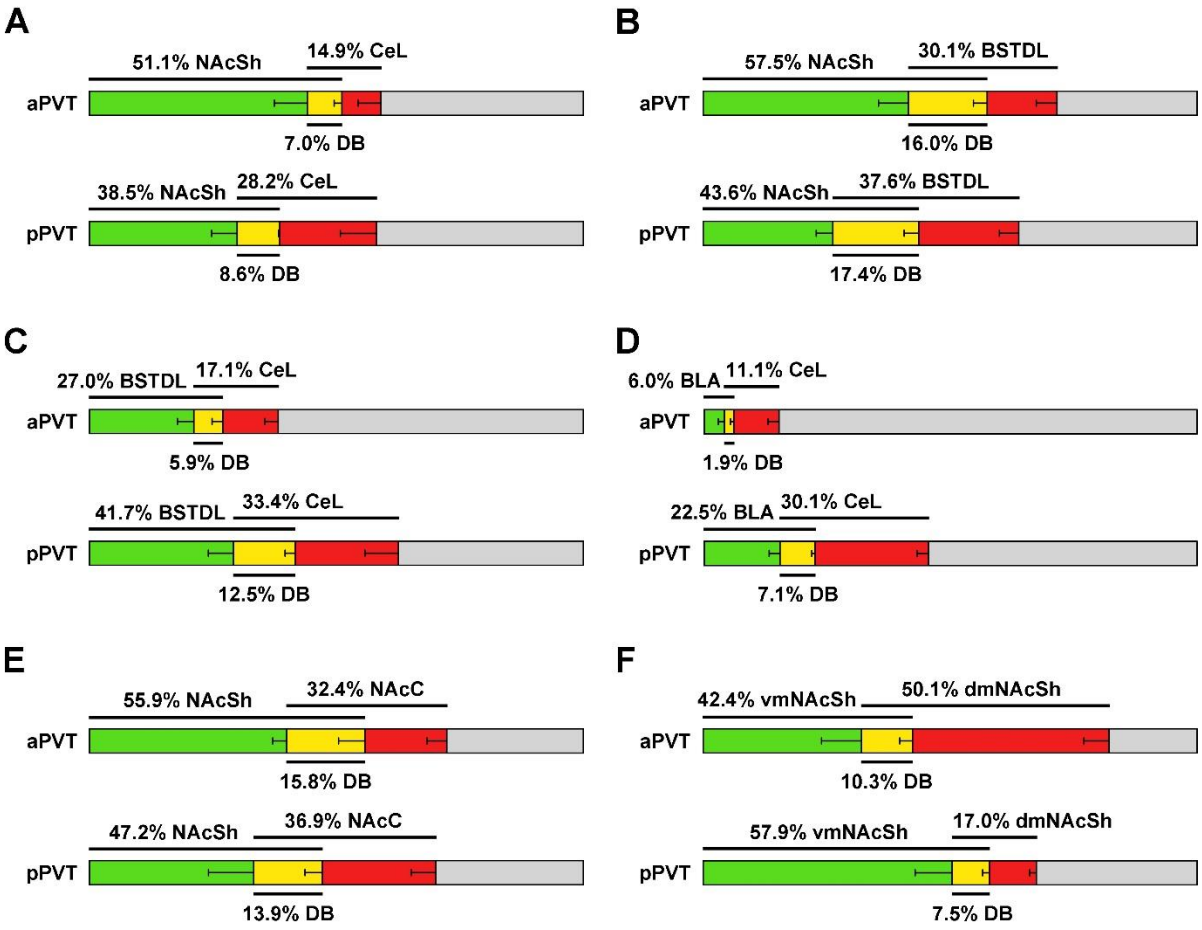
A
51.1% NAcSh
14.9% CeL
aPVT
7.0% DB
38.5% NAcSh
28.2% CeL
pPVT
8.6% DB
B
57.5% NAcSh
30.1% BSTDL
aPVT
16.0% DB
43.6% NAcSh
37.6% BSTDL
pPVT
17.4% DB
C
27.0% BSTDL
17.1% CeL
aPVT
5.9% DB
41.7% BSTDL
33.4% CeL
pPVT
12.5% DB
D
6.0% BLA
11.1% CeL
aPVT
1.9% DB
22.5% BLA
30.1% CeL
pPVT
7.1% DB
E
55.9% NAcSh
32.4% NAcC
aPVT
15.8% DB
47.2% NAcSh
36.9% NAcC
pPVT
13.9% DB
F
42.4% vmNAcSh
50.1% dmNAcSh
aPVT
10.3% DB
57.9% vmNAcSh
17.0% dmNAcSh
pPVT
7.5% DB

3.3.2 *Experiment* 2: activation of different PVT outputs during fear and anxiety.

Combined injections of retrograde tracers resulted in a similar labeling pattern of PVT neurons as the ones shown in *Experiment 1* (Figure 3-12).

Figure 3-12 The average proportions of single- and double-labeled neurons in the aPVT and pPVT in two combinations of retrograde tracer injections in *Experiment 2*

A. dmNAcSh + CeL (n = 24); **B**. BSTDL + CeL (n = 16). Values are shown as mean − SEM. Error bars represent the SEMs of the proportions of the PVT neurons that project to one of the injection sites or both.

Abbreviations: BSTDL, bed nucleus of stria terminalis, dorsolateral; CeL central nucleus of amygdala, lateral; DB, double-labeled; dmNAcSh, nucleus accumbens, shell, dorsomedial; aPVT, paraventricular nucleus of thalamus, anterior; pPVT paraventricular nucleus of thalamus, posterior.

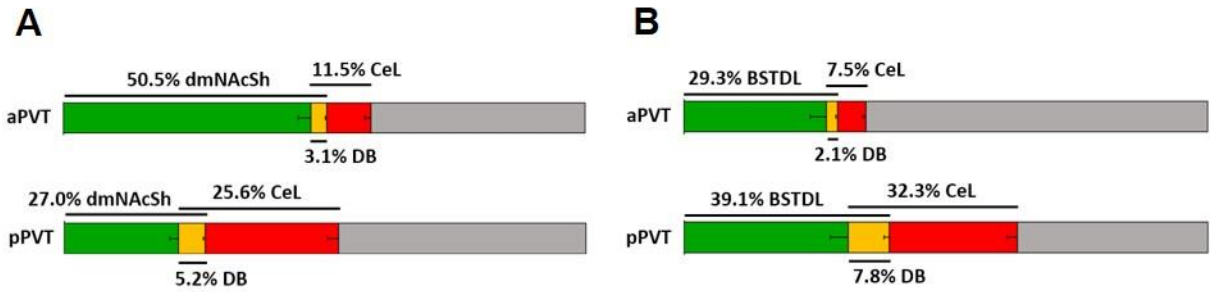

We immunolabled and counted cFos-positive PVT neurons in rats with tracers injected in the dmNAcSh and CeL to compare the activation of these PVT neurons in rats that received footshock or expressed conditioned fear. Data is presented as the total number of neurons in the aPVT and pPVT that expressed cFos in the different conditions and as proportions of neurons that project to a particular area labeled with CTb that express cFos (i.e., double-labeled neurons). The amount of triple-labeled neurons (labeled by two tracers and cFos) was very low in all cases and the statistical results for these neurons are not shown.

Rats that had received footshocks showed a higher level of cFos expression in the aPVT compared to the control group that had no footshock in the chamber (Figure 3-13A, aPVT, $t_{(10)} = 3.32$, $p = 0.008$). The proportions of cFos labeled neurons in the pPVT showed a similar trend but the difference between the shocked and nonshocked groups was not statistically significant (Figure 3-13A, pPVT, $t_{(10)} = 2.15$, $p = 0.057$). The proportions of cFos-labeled neurons in all tracer-labeled neurons in the aPVT or pPVT in rats that received footshocks were higher than that of the nonshocked rats (aPVT: Figure 3-13B, main effect of footshock, $F_{(1,10)} = 11.52$, $p = 0.007$; pPVT: Figure 3-13C, $F_{(1,10)} = 8.51$, $p = 0.015$). The proportion of aPVT or pPVT neurons that project to the dmNAcSh that were labeled with cFos was significantly greater in rats exposed to footshocks compared to the nonshocked rats (aPVT, Figure 3-13B, $p = 0.003$; pPVT, Figure 3-13C, $p = 0.020$) whereas the proportion of aPVT or pPVT neurons that project to the CeL that were labeled with cFos was not different between shocked and nonshocked rats (aPVT, Figure 3-13B, $p = 0.164$; pPVT, Figure 3-13C, $p = 0.052$). The results of the footshock experiment indicate that projection-specific neurons in the PVT are activated by footshocks in a nonspecific manner. Figure 3-13D shows cFos- and tracer-labeled cells in a representitive section of the PVT.

Figure 3-13 The percentatge of cFos-positive neurons in the aPVT and pPVT after footshock

A. The percentage of cFos-positive cells in the aPVT and pPVT after footshocks. **B.** The percentage of cFos-positive cells in aPVT neurons that project to the dmNAcSh or CeL after footshocks. **C.** The percentage of cFos-positive cells in pPVT neurons that project to the dmNAcSh or CeL after footshocks. **D.** A representitive PVT section showing CTb and cFos double-labeled neurons is included to show the appearance of multiple fluorescent signals in the PVT from the experiments described. Scale bar, 50 µm. * p< 0.05.

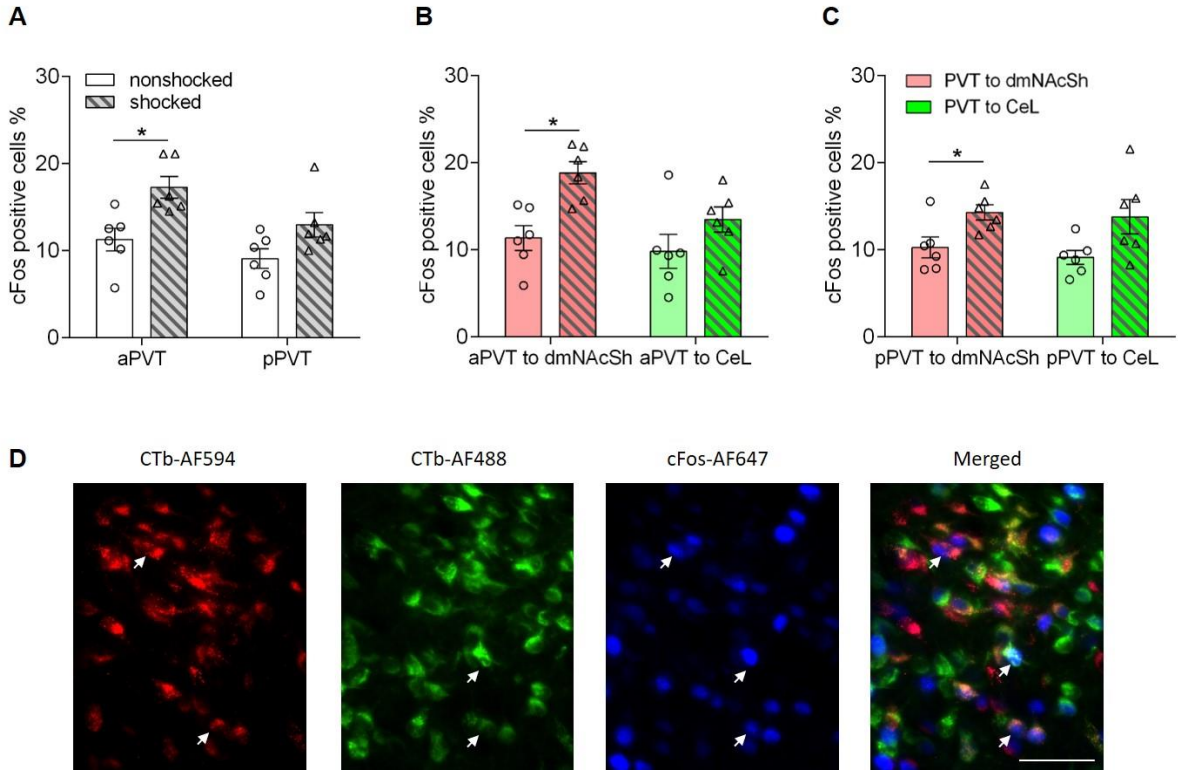

Rats that had received footshocks showed more time spent freezing when re-exposed to the shock chamber compared to the NS rats (percentage of freezing during the 5-min test, shocked group: 84.4 ±7.0 %; NS group: 1.1 ± 1.2%). There was a higher proportion of neurons labeled with cFos in the aPVT in the shocked rats than the NS rats (Figure 3-14A, aPVT, $t_{(10)} = 2.80$, $p = 0.019$) but not in the pPVT (pPVT, $t_{(10)} = 0.827$, $p = 0.225$). There were also some projection-specific differences observed in the shock context re-exposure experiment. The proportion of aPVT neurons that project to the dmNAcSh that were labeled with cFos was higher in rats re-exposed to shock context compared to the NS rats (Figure 3-14B, main effect of footshock, $F_{(1,10)} = 1.937$, $p = 0.194$; interaction between footshock and tracer injected sites, $F_{(1,10)} = 7.846$, $p = 0.019$; simple effect, shocked vs nonshocked in aPVT neurons that project to dmNAcSh, $p = 0.002$) whereas the proportion of aPVT neurons that project to the CeL that were labeled by cFos in the shocked rats was not significantly different from that of the NS rats (Figure 3-14B, $p = 0.64$). The proportions of cFos-labeled neurons in pPVT neurons that project to the dmNAcSh or CeL were not statistically different between groups with footshock experience or not (Figure 3-14C, main effect of footshock, $F_{(1,10)} = 0.022$, $p = 0.885$; interaction, $F_{(1,10)} = 0.881$, $p = 0.37$). The results of the shock context re-exposure experiment indicate that aPVT neurons that project to the dmNAcSh are preferentially activated after re-exposure to the shock context.

Figure 3-14 The percentatge of cFos-positive neurons in the aPVT and pPVT after shock context re-exposure

A. The percentage of cFos-positive cells in the aPVT and pPVT after shock context re-exposure. **B**. The percentage of cFos-positive cells in aPVT neurons that projecting to the dmNAcSh or CeL after shock context re-exposure. **C**. The percentage of cFos-positive cells in pPVT neurons that projecting to the dmNAcSh or CeL after shock context re-exposure. * p< 0.05.

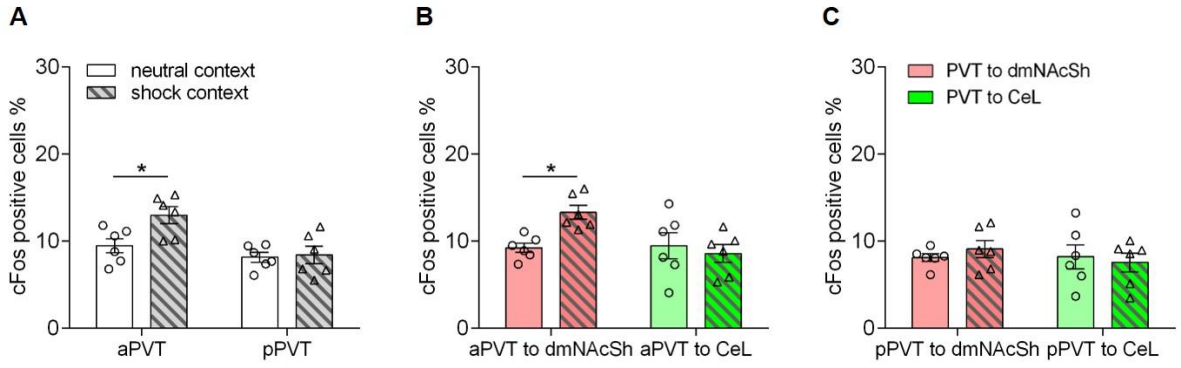

Rats with injections of the retrograde tracers in the BSTDL and CeL were placed in an open field to trigger anxiety-like responses. These rats were then grouped as low- and high-anxiety rats based on three behavioral measures for anxiety: percentage of time spent in the center (low-anxiety 5.4 ± 0.6%, high-anxiety 3.1 ± 1.4%); percentage of time spent immobile (low-anxiety 4.4 ± 1.7%, high-anxiety 10.9 ± 2.8%); distance traveled (low-anxiety 3053 ± 270 cm; high-anxiety 2486 ± 273 cm). A control group with inejctions of tracers in the same areas but not exposed to the open field was used to measure the baseline level of cFos expression in the PVT in non-anxious rats. Figure 3-15A shows the proportion of cFos-labeled neurons in the PVT after the open field test. A higher proportion of cFos-labeled neurons was found in both the aPVT and pPVT after rats were placed in the open field test (Figure 3-15A, main effect of test, aPVT, $F_{(2,13)} = 5.864$, $p = 0.015$; pPVT, $F_{(2,13)} = 5.113$, $p = 0.023$). When considering the extent that the open field generated an anxiety-like behavioral response elicited cFos expression, the proportion of cFos-labeled neurons in the high-anxiety and low-anxiety groups were significantly (or showed a trend towards being significantly) higher in aPVT (Figure 3-15A, *post-hoc* test, high-anxiety vs control, $p = 0.005$; low-anxiety vs control, $p = 0.023$) and pPVT (Figure 3-15A, *post-hoc* test, high-anxiety vs control, $p = 0.007$; low-anxiety vs control, $p = 0.055$) when compared to rats not placed in the open field. In contrast, the proportion of cFos-labeled neurons in the high-anxiety group was not different from the low-anxiety group for both the aPVT and pPVT (Figure 3-15A, *post-hoc* test, high- vs low-anxiety, aPVT, $p = 0.662$; pPVT, $p = 0.473$). In the aPVT, both the high-anxiety and low-anxiety groups showed a higher proportion of cFos-labeled neurons in neurons that project to the BSTDL (Figure 3-15B, *post-hoc* test, high-anxiety vs control, $p = 0.039$; low-anxiety vs control, $p = 0.013$), whereas no difference was found between the control and high-anxiety or low-anxiety groups in the

proportion of cFos-labeled neurons in aPVT neurons that project to the CeL (Figure 3-15B, *post-hoc* test, high-anxiety vs control, $p = 0.23$; low-anxiety vs control, $p = 0.15$). For the tracer-labeled cells in the pPVT, the high-anxiety group showed a higher proportion of cFos-labeled neurons in the pPVT-BSTDL projecting or pPVT-CeL projecting neurons than the control group while the low-anxiety group did not (Figure 3-15C, *post-hoc* test, high-anxiety vs control, $p = 0.025$; low-anxiety vs control, $p = 0.12$). No difference was found between the high-anxiety group and the low-anxiety group. In summary, a higher proportion of cFos labeled cells was found in both the aPVT and pPVT after exposure to an open field but this was apparently independent from whether these neurons projected to the BSTDL or CeL and the level of anxiety expressed by these rats.

Figure 3-15 The percentatge of cFos-positive neurons in the aPVT and pPVT after exposure to a novel open field

A. The percetage of cFos-positive cells in the aPVT and pPVT after exposure to a novel open field. **B**. The percentage of cFos-positive cells in aPVT neurons that projecting to the dmNAcSh or CeL after exposure to a novel open field. **C**. The percentage of cFos-positive cells in pPVT neurons that projecting to the dmNAcSh or CeL after exposure to a novel open field. * $p < 0.05$.

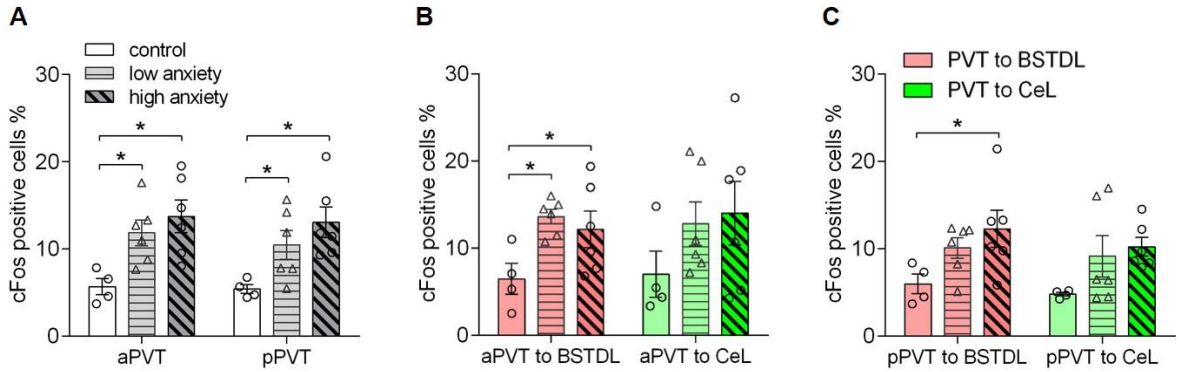

3.4 Discussion

This chapter describes the projections from the PVT to the NAcSh, NAcC, BSTDL and amygdala using a dual retrograde tracing method. A key finding of *Experiment 1* is that most neurons in the PVT appear to innervate the NAcSh and that a significant portion of these NAcSh-projecting neurons give off collaterals to the BSTDL and CeL. The study suggests that most neurons in the PVT exert an extensive influence on the NAcSh and at the same time these neurons also likely exert a broad influence on a large continuum of subcortical structures that includes both the BSTDL and CeL. Along the same line, differences in the pattern of projections from the aPVT and pPVT are suggestive of potential functional differences in terms of its ability to bias efferent influence toward different subregions of the NAcSh, BSTDL, and CeL in an anterior to posterior gradient manner. *Experiment 2* measured cFos protein expression to determine if PVT neurons that project to different areas are activated during fear or anxiety. As a whole, the results of these experiments suggest that stressful and arousing events like footshocks or exposure to a novel environment activated PVT neurons that project to the dmNAcSh, CeL, or BSTDL in a largely nonspecific manner with the possible exception of an apparent activation of aPVT neurons that project to the dmNAcSh by retrieval and expression the contextual fear memory associated with the footshock chamber. This suggests that the PVT may broadly transmit stress- or arousal-related signals to the NAcSh, BSTDL, and CeL but that a projection to the dmNAcSh may have some function related to the behavioral responses associated with contextual fear. For example, this projection could promote freezing or could inhibit food-seeking responses.

It is important to recognize that the methods used in the present study could generate an under-estimation of the proportion of PVT neurons that project to the two areas because the

number of labeled neurons was determined from injections of tracers that involved only a portion of a larger region (Li and Kirouac, 2008). While great care was taken to restrict the retrograde tracers in the anatomically and functionally distinct areas of BSTDL and CeL that are most densely innervated by the PVT, injections in the NAcSh were broadly directed to the NAcSh which appears to be composed of subregions with poorly defined anatomical and functional differences (Al-Hasani et al., 2015; Berridge & Kringelbach, 2015; Reed et al., 2015; Reynolds & Berridge, 2008). Indeed, when injections were made in the dmNAcSh and vmNAcSh, up to 80% of the neurons in the PVT were labeled despite the small volume of injected tracers. Consequently, it is very likely that the number of neurons that project to both the NAcSh and BSTDL or CeL would be much greater than the observation with the combination of injections made in this study. Consistent with this view, a single cell reconstruction study also reported that all the neurons traced (n = 5) from the PVT innervated the NAcSh and provided variable amount of collaterals to a number of subcortical targets including the BSTDL and CeL (Unzai et al., 2017). This single cell reconstruction study also reported that PVT neurons give off extensive collaterals throughout large portions of the NAc, which can explain that in our experiment a small injection in the medial NAcSh labeled more than 50% of PVT neurons.

Our results showed that in many of the combinations, the proportion of PVT neurons labeled by a single tracer from injections in either the NAcSh, BSTDL, or CeL was similar to the proportion of double labeled neurons in the PVT neurons labeled by another tracer injected in another area. For example, in the group with tracers in the BSTDL and CeL, tracer in the BSTDL labeled about 30% of all PVT neurons and also labeled about 30% of PVT neurons that were labeled by the tracer injected in the CeL. This type of distribution suggests that PVT neurons innervate the two regions independently. Put another way, the result does not support the idea

that a subpopulation of PVT neurons specifically innervates one or a group of targets and avoids other targets.

It was unexpected that the number of double-labeled cells in the cases with combined injections in the dmNAcSh and vmNAcSh was relatively low (<10%) considering that the combination resulted in up to 80% of all the cells in the PVT being labeled by these two injections. In addition, there were some notable topographical differences in the location of cells innervating the dmNAcSh and vmNAcSh. For example, the anterior-most part of the PVT contains a large number of dmNAcSh-projecting cells. There was a progressive decrease in the number of dmNAcSh-projecting cells in the most posterior part of the PVT with these cells occupying the dorsal region of the pPVT. The distribution of dmNAcSh-projecting cells in the PVT is consistent with a previous report with a retrograde tracer injection in the septal pole of the NAcSh (Deutch et al., 1998). The location of the NAcC-projecting cells was also topographically organized in the PVT with NAcC-projecting cells found in greater numbers in the more lateral aspects of the PVT as well as areas lateral and ventral to the PVT. The general pattern of labeling observed in the midline thalamus following injections of the retrograde tracer CTb reported here is consistent with previous anterograde tracing studies (Berendse & Groenewegen, 1990; Li & Kirouac, 2008; Vertes & Hoover, 2008).

In *Experiment 2*, data was presented demonstrating that neurons in the PVT were activated in rats exposed to a stressful event as evidence by involving fear- or anxiety-like behaviors. Of note, the proportions of cFos labeled neurons of all the PVT neurons appears similar to the proportion of cFos labeled neurons of projection-specific neurons in various combinations of retrograde tracer injections. This result does not support our hypothesis that PVT neurons that project to specific brain regions are selectively activated under specific emotional or stressful

conditions. From this perspective, the PVT might be regarded as a site that relays nonspecific stress- or emotion-related signals to the NAcSh, BSTDL, and CeL and not as a relay for signals that carry unique information associated with different emotional responses. One possible exception to this general conclusion of non-specificity was the finding that a larger proportion of aPVT neurons that project to the dmNAcSh labeled with cFos in shocked rats re-exposed to the shock chamber. Future research will be needed to determine if the aPVT-dmNAcSh projection contributes to contextual fear conditioning memory retrieval or expression.

In summary, we interpreted the results of the experiments presented in this chapter as evidence that most neurons in the PVT project to the NAcSh with many of these neurons also sending collaterals that innervate the BSTDL and CeL. The results also support the view that PVT neurons may be non-specifically activated by stress or emotionally significant events, and that these neurons relay signals to the NAcSh, BSTDL, and CeL in a manner that is largely nonspecific relative to the type of emotional response.

Chapter 4 Chemogenetic inhibition of the PVT projection to the NAcSh attenuates stress-induced anxiety

4.1 Introduction

Many studies have reported that the PVT can be activated by stressful and aversive conditions (reviewed in Kirouac, 2015) including *Experiment 2* in Chapter 3. Anatomical tracing studies suggest that the PVT may be activated by afferents from nuclei in the hypothalamus and brainstem that have viscerosensory functions. The PVT may relay signals to the NAc, BST, and CeL where these signals could influence behavioral responses (see section 1.4.3). In Chapter 3, analysis of the axonal collateral projections from the PVT to the NAcSh, BSTDL, and CeL indicated that the output of PVT neurons to these three areas is broadly and mostly nonspecifically distributed across the three areas with a higher number of neurons sending fibers to the NAcSh (Dong, Li, & Kirouac, 2017). The findings of the retrograde tracing experiments presented in this thesis are consistent with previous anterograde tracing experiments showing that the fiber density provided to the NAcSh are clearly denser than those provided to the BSTDL and CeL (Li & Kirouac, 2008). The robust projection from the PVT to the NAcSh suggests that this pathway is likely to contribute significantly to the behavioral effect of stress mediated by the PVT.

Recent studies using optogenetic or chemogenetic projection-specific intervention have reported that the PVT projection to the NAcSh mediates stress-related behaviors including social avoidance produced by social defeat (Christoffel et al., 2015), conditioned place avoidance elicited by morphine withdrawal (Zhu et al., 2016), and compulsive drug-seeking elicited by food restriction (Chisholm et al., 2019). Other evidence suggests that the PVT-NAcSh pathway

may be important for selecting approach or avoidance responses in situations involving a motivational conflict (Choi et al., 2019; Choi & McNally, 2017; Do-Monte et al., 2017). It has been proposed that clinical anxiety involves shifting the balance between the motivation for approach and avoidance towards an exaggerated avoidance tendency (Hofmann & Hay, 2018; Steimer, 2002) and previous work by our group (Li et al., 2009, 2010a, 2010b) and experiments in Chapter 2 (Dong, Li, & Kirouac, 2015; Y. Li et al., 2014) demonstrate that the PVT contributes to stress-induced anxiety. In the present study, we further investigated whether chemogenetic inhibition of the PVT projection to the NAcSh attenuates stress-induced anxiety. This study used a PTSD animal model developed by our laboratory to measure stress-induced anxiety and fear responses. This model can induce persistent high anxiety and distinguish between stress-susceptible and stress-resilient individuals (Chen et al., 2012; Chen, Wang, et al., 2014).

4.2 Methods

4.2.1 Animals and housing

A total of 81 adult male Sprague-Dawley rats (University of Manitoba vivarium) were used in the experiment, of which 73 rats were used to generate the figures and data, 8 rats were used as a social stimulus in social approach-avoidance (SAA) test. Animals were pair-housed in cages kept in a room maintained on a 12 h/12 h light/dark cycle (lights on at 07:00) with controlled temperature (20–24°C) and humidity (40–70%). All the rats had free access to food and water through the experiment. All the rats were handled for 2 min on alternate days during a 7-day adaptation period. All the behavioral training and tests were done in the light cycle of the day (09:00–17:00). The experimental procedures were in compliance with the Canadian Council on

Animal Care and the experimental protocol was approved by Research Ethics Review Board of the University of Manitoba.

4.2.2 Experimental procedure and timeline

After adaptation to handling, viral vectors were microinjected into the NAcSh and PVT according to coordinates stated below. The approach involved an intersectional strategy which results in the expression of the inhibitory Designer Receptors Exclusively Activated by Designer Drugs (DREADDs) hM4Di (abbreviated as hM4Di for this chapter) in PVT neurons that project to the NAcSh (Figure 4-1). After 7 days of recovery, rats received a series of footshocks. One day later, rats were placed in a novel environment (a small rectangular open field) and assigned to either high-responder (HR) group or low-responder (LR) group according to the amount of time they spent immobile, which is indicative of an acute fear response to novelty. Thirteen days later, we tested the effect of activation of hM4Di with the agonist clozapine (i.e., chemogenetic inhibition of PVT neurons that project to the NAcSh) in rat exposed to the SAA test. Two days later, we tested the effect of hM4Di activation in rats placed in a large open field. Two days later, we re-examined the effect of hM4Di activation in a second SAA test (rats were reassigned to different treatment with animals treated with clozapine earlier receiving saline injection this time and vice versa). Ninety minutes after the SAA test, the rats were placed into the shock chamber for a conditioned fear expression test (no shock given) followed by perfusion with fixative for subsequent histological analysis of cFos expression in PVT neurons expressing hM4Di following exposure to the SAA test. The timeline of behavioral procedures is also presented in Table 4-1.

Figure 4-1 A schematic of the intersectional strategy to express hM4Di in PVT neurons that project to the NAcSh

AAV8-DIO-hM4Di-mCherry was injected in both the aPVT and pPVT; AAVrg-Cre was injected in the NAcSh bilaterally.

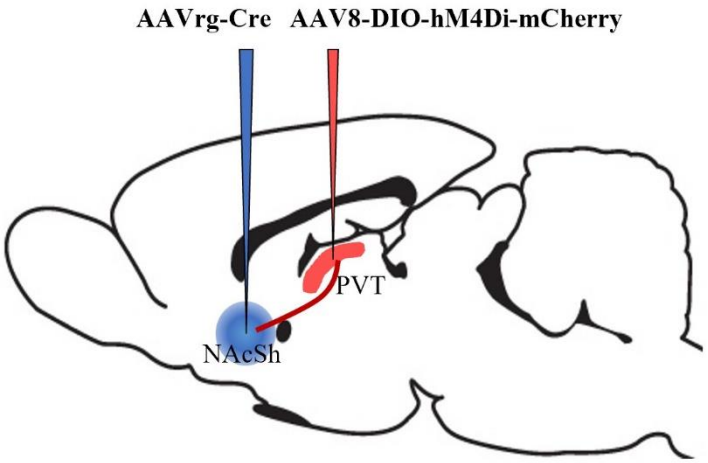

Table 4-1 Timetable of the major procedures of the experiment in Chapter 4

Timepoint	Behavioral session
	Surgery for microinjection of viral vectors
Day 0	Footshock exposure
Day 1	Novel environment test (in a small rectangular open field)
Day 14	hM4Di activation; social approach-avoidance test
Day 16	hM4Di activation; open field test
Day 18	hM4Di activation; social approach-avoidance test; shock chamber re-exposure; perfusion

4.2.3 Stereotaxic surgery and viral vectors injections

Animals were anesthetized with 2–3% isoflurane and given meloxicam (2 mg/kg, s.c.) for post-surgery pain management. Animals were placed in a Stoelting stereotaxic frame and a hand drill was used to expose the brain surface above the target sites. Pressure injections of viral vectors were done using pressure injection device (Picospritzer, Park Hannifin, Hollis, NH, USA) connected to glass pipettes with an outer diameter of tips of approximately 40 μm. Injections of viral vectors were done in the following areas using coordinates derived from a stereotaxic atlas of the rat brain (Paxinos & Watson, 2007): NAcSh, 1.5 mm anterior, 0.9 mm bilateral, 7.2 mm ventral; aPVT 1.8 mm posterior, 1.05 mm lateral, 5.9 mm ventral; pPVT 3.1 mm posterior, 1.0 mm lateral, 5.8 mm ventral. All coordinates were relative to skull surface and bregma. Injection into the aPVT and pPVT were done using a pipette holder at a 10° angle from the midline on the right side of the sagittal sinus. During the same surgery, rats were injected with 350 nl of viral vector AAV2-retro-Syn1-EBFP-Cre (2.9×10^{13} vg/ml, catalogue No. 51507-AAVrg, AddGene, Cambridge, MA, USA) in the NAcSh bilaterally, and 670 nl of viral vector AAV8-hSyn-DIO-hM4Di-mCherry (1.4×10^{13} vg/ml, catalogue No. 44362-AAV8, AddGene) or AAV8-hSyn-DIO-mCherry (1.6×10^{13} vg/ml, catalogue No. 50459-AAV8, AddGene) in the aPVT and pPVT at a rate of 80 nl/minute. The pipette was kept in the brain for another 10 min before removal to prevent leakage along the pipette tract. The scalp incisions were sutured, and rats were returned to their home cages for recovery. The use of this intersectional viral strategy results in the expression of the inhibitory receptor hM4Di (Roth, 2016; Urban & Roth, 2015) in a Cre-dependent manner in PVT neurons that send collateral projections to the NAcSh.

4.2.4 Footshock stress

Rats were transferred one at a time to a brightly illuminated room (400–500 lx) dedicated exclusively for the delivery of footshocks in commercially constructed shock chamber (MED Associates, St. Albans, Vermont, USA) with a grid floor. After a 2 min acclimation period, each rat received 5 footshocks (1.5 mA, 2 s, ITI = 10–50 s). The rats were kept in the chamber for another 60 s before they were returned to their home cages. Nonshocked (NS) rats were placed in the shock chamber for the same amount of time. The shock chamber was cleaned with alcohol (10 %) and the bedding under the grid floor was changed after exposure of each rat.

4.2.5 Acute response to a novel environment

Twenty-four hours after the shock exposure, rats were placed in a rectangular open field (65 × 40 × 50 cm; illuminated at 3–5 lx) for 6 min. A novel tone was presented at 3^{rd} – 6^{th} min (9 kHz, 75 dB). Immobility, defined as no movement on four limbs, was measured based on the video taken by a camera on the ceiling. We used immobility to indicate a reduced tendency to explore a novel environment. The percentage of the total immobility during the 6-min test was used to assign the animals into HR and LR groups. A cut-off criterion at 50% of immobility time was selected in the present study as this cut-off effectively produces groups with low and high levels of anxiety lasting for up to 4 weeks post-shock (Chen et al., 2012; Chen, Wang, et al., 2014).

4.2.6 Drug injection

Clozapine (catalogue No. 0444, Tocris, Minneapolis, MN, USA) was dissolved into distilled water (pH = 4, adjusted by a few drops of 1 M acetic acid) as 3 mM stock solution. On the test day, the stock solution was dissolved with 0.9% sterile saline into 30 µM solution and

administered i.p. at a dose of 0.01 mg/kg. Saline was used as vehicle in the vehicle groups. Clozapine or saline injection was conducted 30 min before behavioral tests.

4.2.7 Social approach-avoidance (SAA) test

Social anxiety was conducted in a black rectangle open field (65 × 40 × 50 cm, 3–5 lux illumination; Figure 4-2). A stimulus rat (male rat weighing 450–500 g) was put into a compartment of the open field with a mesh wall facing the interaction zone (15 × 40 × 50 cm, Compartment A). The test rat was placed in an enclosed compartment (20 × 40 × 50 cm, Compartment B) located in the opposite side of the open field. Compartment B had a sliding door (10 × 10 cm) on the wall facing the middle zone (30 × 40 × 50 cm) located between the two compartments. The test procedure was performed as described before (Chen et al., 2012; Chen, Wang, et al., 2014; Haller & Bakos, 2002). After a 3-min habituation period, the sliding door was open allowing the test rat to move freely in the arena for 10 min. The behavior was recorded by a video camera mounted on the ceiling and analyzed manually for the amount of time spent in the social zone (15 × 40 cm zone immediately adjacent to Compartment A) and data tabulated for 5-min time bins.

Figure 4-2 The apparatus for social approach-avoidance test

An unfamiliar male rat as the stimulus rat was placed in Compartment A with a meshed wall on the right side. The test rat was placed in Compartment B which had a sliding door on the wall (left side of Compartment B in the figure). At the beginning the sliding door was closed and the test rat stayed in Compartment B for 3 minutes. Then the sliding door was opened allowing the test rat to move freely in the middle area and Compartment B for 10 min. A region adjacent to the meshed wall was viewed as a social zone.

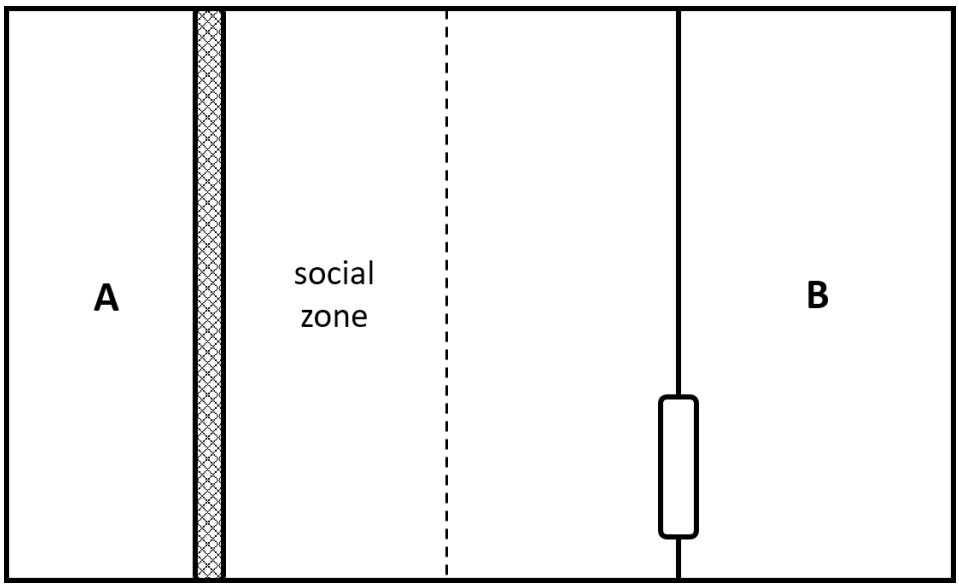

4.2.8 Open field test

The open field test was done in a square open field (80 × 80 × 40 cm) with a black floor which was illuminated at 3-5 lx. The rat was placed into one corner of the open field and allowed to freely explore the open field for 5 min. The time spent in the center of the open field (35 × 35 cm) and the behavior in the whole open field was recorded by the video tracking system Ethovision (Noldus, Wageningen, Netherland). The total amount of time spent in the center of the open field and distance traveled in the whole open field were analyzed by Ethovision. The total time the rat spent immobile was quantified by two experimenters.

4.2.9 Shock context re-exposure

The shock context re-exposure (conditioned fear expression) test was done at 90 min after the second SAA test and immediately before perfusion. The rats were placed into the shock chamber for 5 min and the total time of freezing behavior was quantified by two experimenters from the video of behaviors. The expression of protein product of *cfos* gene peaks at approximately 90 min (Dragunow & Faull, 1989) and was used to determine if activation of hM4Di had inhibited PVT neurons during the SAA test.

4.2.10 Histology

After exposure to the second SAA test and the shock chamber, rats were deeply anesthetized with 10% chloral hydrate (600 mg/kg, i.p.) and transcardially perfused with 200 ml heparinized saline followed by 500 ml ice-cold 4% paraformaldehyde in 0.1 M phosphate buffer (pH 7.4). The brains were removed and post-fixed in the same fixative for 24 h followed by cryoprotection in 20% sucrose with 10% glycerin over 2 days at 4 °C. Coronal sections of the brain containing the NAcSh and the PVT were taken at 50 μm. Brain sections containing the PVT region and every 300 μm were selected for the cFos staining. Brain sections were pre-

incubated in the blocking solution for 1 h and then incubated in primary rabbit anti-cFos antibody (1:2000; catalogue No. ABE457, Millipore, Temecula, CA, USA) and mouse anti-mCherry antibody (1:3000; catalogue No. 632543, Takara Bio, Mountain View, CA, USA) overnight. After 3 rinses in PBS, sections were transferred into a secondary donkey anti-rabbit conjugated to Alexa Fluor 488 (1:1000; catalogue No. A21206, Invitrogen, Calsbad, CA, USA) and donkey anti-mouse conjugated to Cy3 (1:500; catalogue No. 715-165-151, Jackson Immunoresearch, West Grove, PA, USA) antiserum for 2 h. After three more rinsing steps, sections were mounted, dehydrated, and coverslipped with fluorescent protectant mounting medium Fluoromount-G (SouthernBiotech, Birmingham, AL, USA) for subsequent examination.

4.2.11 Data analysis

Brain sections were examined and photographed using a Zeiss Axio Observer Z1 fluorescent microscope equipped with Axiocam 503 mono camera. Single- and double-labeled neurons were manually marked by examining merged color channels of the images taken under 20× magnification and counted using the ZEN 2 software (Zeiss). The proportions of double-labeled/cFos-labeled cells in the PVT were calculated and compared among different treatment groups. One-way ANOVA was used to analyze the main effect of clozapine injection on cFos expression in hM4Di-expressing PVT neurons.

Behavioral data including immobility time, freezing time, and time spent in social zone, time spent in the center of the open field, are presented as percentage of the total test period time. There were three chemogenetic conditions: 1) hM4Di and clozapine injection (chemogenetic inhibition); 2) hM4Di and saline injection (control for clozapine injection); 3) mCherry and clozapine injection (control for hM4Di). A decision to not include a mCherry alone and saline injection group was taken because the critical factors required to interpret the results were well-

controlled. Two-way ANOVA was used for analyzing the behavioral effect of inhibiting PVT neurons that project to the NAcSh and post-hoc by Tukey HSD adjustment and simple effect test by Sidak adjustment were used to compare group differences. Statistic analyses were conducted in GraphPad Prism 6.0 (GraphPad Software, San Diego, CA, USA). A value of $p < 0.05$ was considered to be significant and the data were presented as mean ± SEM.

4.3 Results

Experimental groups consisted of rats with hM4Di or mCherry. The shocked group was further divided into HR and LR based on their immobility time percentages at 24 hr after footshock exposure (Figure 4-3). Rats in NS, LR, and HR groups were further assigned to three chemogenetic conditions (mCherry-NS-clozapine, $n = 6$; hM4Di-NS-saline, $n = 7$; hM4Di-NS-clozapine, $n = 6$; mCherry-LR-clozapine, $n = 8$; hM4Di-LR-saline, $n = 11$; hM4Di-LR-clozapine, $n = 10$; mCherry-HR-clozapine, $n = 7$; hM4Di-HR-saline, $n = 9$; hM4Di-HR-clozapine, $n = 9$) which would receive different treatments before behavioral tests at two weeks post-shock.

Figure 4-3 Immobility in a novel context at Day 1 and the assignment of groups

Rats displayed a wide range of immobility time when placed in a novel context at 24 hr after footshock exposure while the nonshocked (NS) rats displayed low immobility in this test. Shocked rats were subdivided into a low responder (LR) group and a higher responder (HR) group based on their immobility time.

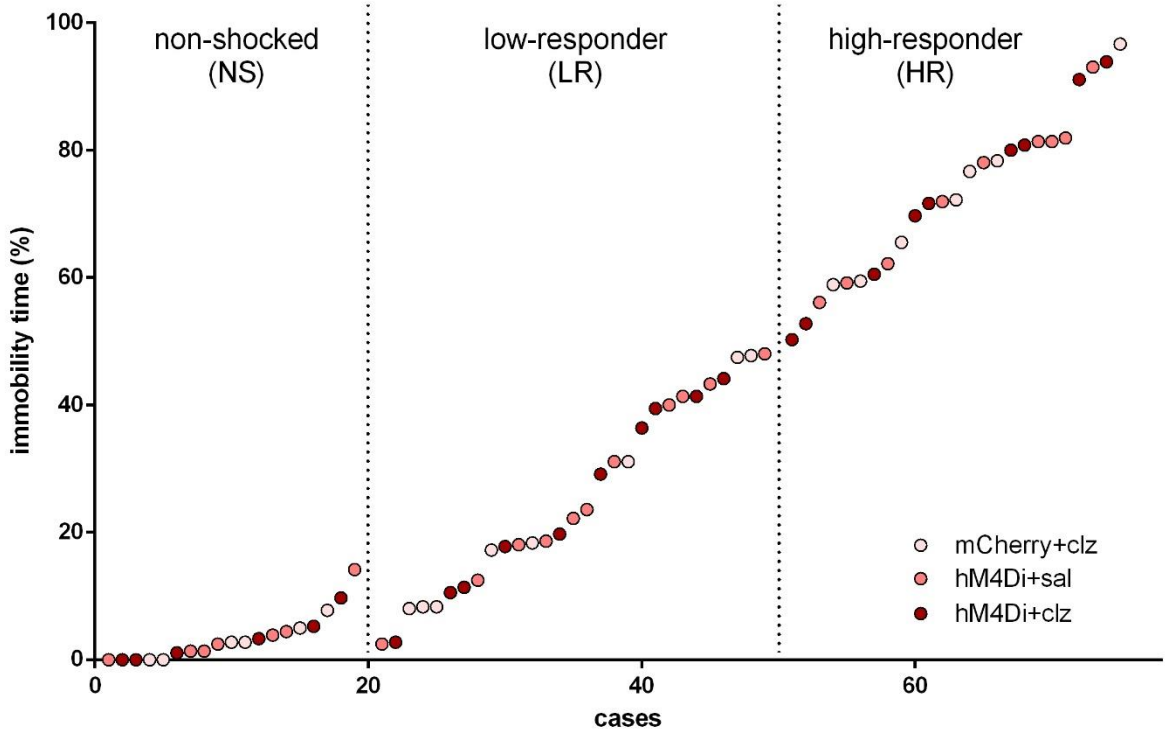

In the first SAA test (Day 14), there was a significant difference in the amount of time that rats in NS, LR, and HR groups spent in the social zone during the first 5 min (0-5 min, Figure 4-4A, main effect of early response, $F_{(2,64)} = 27.77$, $p < 0.001$) and the second 5 min (5-10 min, Figure 4-4B, $F_{(2,64)} = 3.96$, $p = 0.024$). *Post-hoc* tests indicate that HR spent less time in the interaction zone compared to NS and LR during the 0-5 min (Figure 4-4A, HR vs NS: $p < 0.001$; HR vs LR: $p < 0.001$) and 5-10 min periods (Figure 4-4B, HR vs NS: $p = 0.054$; HR vs LR: $p = 0.043$). More specifically, saline-treated HR with hM4Di spent significantly less time in the social zone compared to saline-treated NS with hM4Di during the 0-5 min ($p = 0.002$) and 5-10 min periods ($p = 0.036$). The social zone time of saline-treated HR with hM4Di was also lower than that of saline-treated LR with hM4Di during the 0-5 min ($p < 0.001$) and 5-10 min periods ($p = 0.017$). The saline-treated LR with hM4Di showed no difference with the saline-treated NS with hM4Di (0-5 min: $p = 0.826$, 5-10 min: $p = 0.999$). The chemogenetic conditions showed an effect on social zone time only in 5-10 min (Figure 4-4B, main effect of chemogenetic conditions, $F_{(2,64)} = 5.904$, $p = 0.004$) but not 0-5 min period (Figure 4-4A, $F_{(2,64)} = 1.58$, $p = 0.214$). *Post-hoc* comparison showed that clozapine-treated rats with hM4Di spent more time in the social zone than clozapine-treated rats with mCherry ($p = 0.005$) while there was no significant difference between clozapine and saline-treated rats with hM4Di ($p = 0.118$) in the 5-10 min period. More specifically, clozapine-treated HR with hM4Di showed significantly increased social zone time in the 5-10 min period compared to saline-treated HR with hM4Di ($p = 0.030$). In contrast, no difference was found between clozapine-treated LR with hM4Di and clozapine-treated NS with hM4Di ($p = 0.998$), nor clozapine-treated LR with mCherry and clozapine-treated NS with mCherry ($p = 0.430$). The result indicates that chemogenetic inhibition of the PVT neurons that project to the NAcSh selectively reduced social anxiety in HR rats.

Figure 4-4 Chemogenetic inhibition of NAcSh-projecting PVT neurons increased social time in social approach-avoidance (SAA) test in higher-responder (HR) rats at Day 14 and Day 18 post-shock.

The percentages of time spent in the social zone in 0-5 min and 5-10 min periods of the SAA test at Day 14 and Day 18 post-shock. **A**. HR rats spent less time in social zone time compared to nonshocked (NS) or low-responder (LR) rats in the 0-5 min period of the SAA test at Day 14. **B**. Clozapine(clz)-treated HR rats with hM4Di in PVT-NAcSh projecting neurons showed an increased time spent in the social zone compared to saline(sal)-treated HR with hM4Di in the 5-10 min period of the SAA test at Day 18. **C**. No difference was found in the time spent in the social zone of rats in NS, LR, and HR groups nor different chemogenetic conditions in the 0-5 min period of the SAA test at Day 18. **D**. Clz-treated HR rats with hM4Di spent more time in the social zone than sal-treated HR with hM4Di and clz-treated HR with mCherry at the 5-10 min period of the SAA test at Day 18. Data are presented as mean ± SEM. * $p < 0.05$. clz, clozapine; sal, saline.

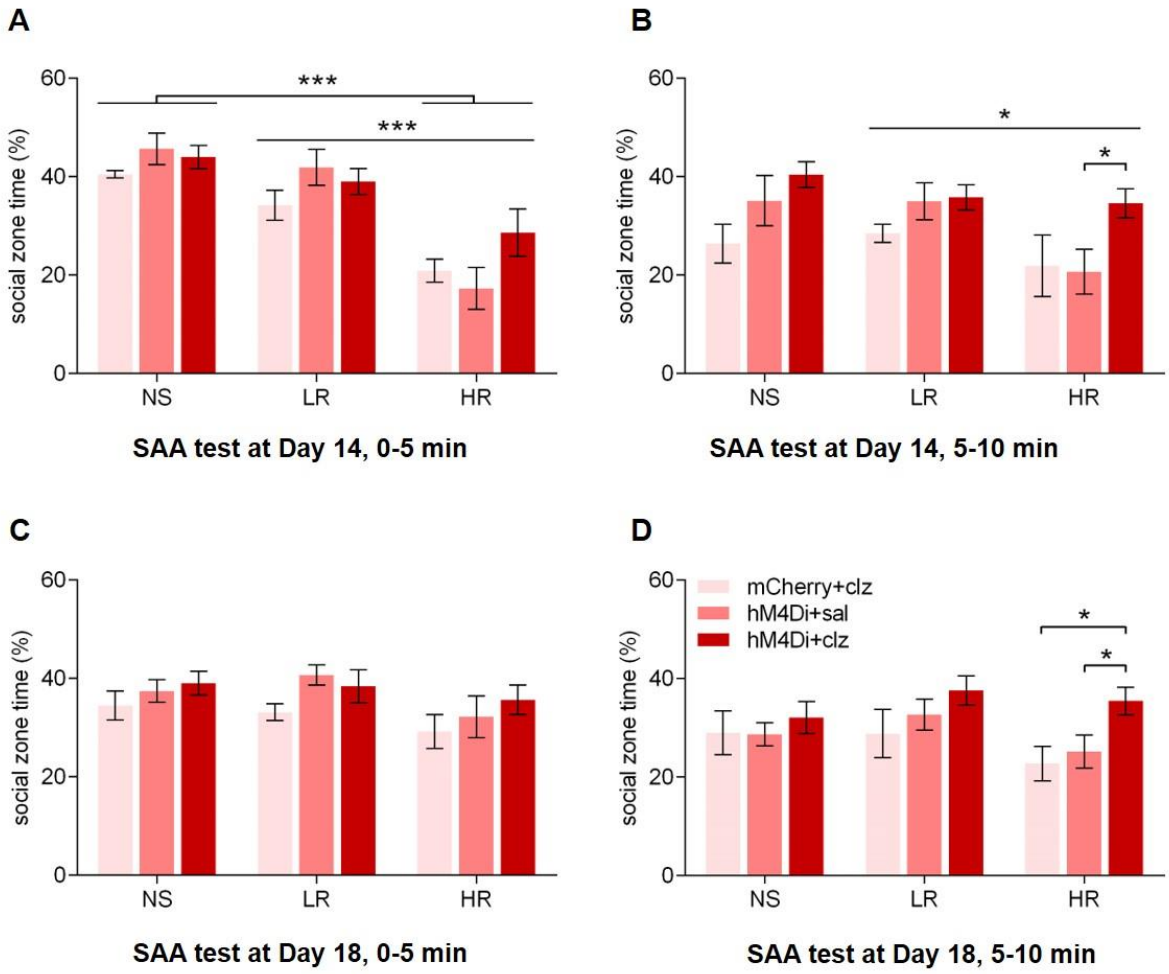
A
B
C
D
social zone time (%)
60
40
20
0
NS
LR
HR
***
***
*
*
*
*
mCherry+clz
hM4Di+sal
hM4Di+clz
SAA test at Day 14, 0-5 min
SAA test at Day 14, 5-10 min
SAA test at Day 18, 0-5 min
SAA test at Day 18, 5-10 min

In the second SAA test (Day 18), no difference was found in the time spent in the social zone between rats in NS, LR, and HR groups in 0-5 min period (Figure 4-4C, main effect of early response, $F_{(2,64)} = 2.562$, $p = 0.085$) or 5-10 min period (Figure 4-4C, main effect of early response, $F_{(2,64)} = 1.864$, $p = 0.163$), whereas rats under different chemogenetic conditions showed different amounts of time in the social zone in the 5-10 min period (Figure 4-4C, 0-5 min, main effect of chemogenetic conditions, $F_{(2,64)} = 2.440$, $p = 0.0952$; Figure 4-4D, 5-10 min, main effect of chemogenetic conditions, $F_{(2,64)} = 4.452$, $p = 0.0155$). The *post-hoc* tests indicated that clozapine-treated rats with hM4Di spent more time in the interaction zone compared to the clozapine-treated rats with mCherry during the 5-10 min period ($p = 0.011$). Further simple effect analysis showed that clozapine-treated HR with hM4Di spent more time in the social zone than saline-treated HR with hM4Di ($p = 0.032$) and clozapine-treated HR with mCherry ($p = 0.014$) at the 5-10 min period. The result in the second SAA test with groups rearranged in a way that the rats received a different treatment (clozapine vs saline) than in the first SAA test also demonstrates an anxiolytic effect of chemogenetic inhibition of the PVT neurons that project to the NAcSh in the HR group (consistent with the result of the first SAA test).

In the open field test (Day 16), footshock reduced locomotion in the HR and LR groups (Figure 4-5A, $F_{(2,64)} = 27.51$, $p < 0.001$; *post-hoc* test: HR vs NS, $p < 0.001$, LR vs NS, $p = 0.039$), and the locomotion of the HR group was also lower than the LR (*post-hoc* test: HRs vs LRs, $p < 0.001$). Similarly, the HR also showed more immobility in the open field than the NS and LR (Figure 4-5B, main effect of early response, $F_{(2,64)} = 37.23$, $p < 0.001$; *post-hoc* tests: HR vs NS, $p < 0.001$, HR vs LR, $p < 0.001$), while the LR was not different from the NS (*post-hoc* test: LR vs NS, $p = 0.21$). Footshocks also had an effect on the time spent in the center of the open field (Figure 4-5C, $F_{(2,64)} = 4.061$, $p = 0.022$). *Post-hoc* analysis showed that the HR spent

less time in the center of the open field compared to the LR ($p = 0.031$), while the difference between HR and NS was not statistically significant ($p = 0.12$). The chemogenetic conditions did not change immobility or time in the center (Figure 4-5B, main effect on immobility, $F_{(2,64)} = 0.486$, $p = 0.617$; Figure 4-5C, main effect on center time, $F_{(2,64)} = 2.379$, $p = 0.101$). A significant main effect of chemogenetic conditions was found on the distance traveled in the open field without significant group differences in *post-hoc* analysis (Figure 4-5A, main effect on locomotion $F_{(2,64)} = 3.72$, p = 0.030; *post-hoc* test: hM4Di + clozapine vs mCherry + clozapine, $p = 0.065$, hM4Di + clozapine vs hM4Di + saline, $p = 0.699$). The ANOVA did not reveal any significant interaction between chemogenetic conditions and footshock experience indicating that chemogenetic inhibition of PVT neurons that project to the NAcSh did not affect anxiety-like behaviors in the open field test.

Figure 4-5 Chemogenetic inhibition of the PVT-NAcSh projecting neurons did not change anxiety-like behaviors in the open field test at Day 16 post-shock.

A. HR rats showed a lower level of distance traveled in the open field compared to the NS and LR rats. **B**. HR rats showed a higher level of time spent immobile in the open field compared to the NS and LR rats. **C**. HR rats spent less time in the center compared with the LR. No difference was found in distance traveled (**A**) immobility time (**B**) and center time (**C**) between groups in different chemogenetic conditions. Data are presented as mean ± SEM. clz, clozapine; sal, saline.

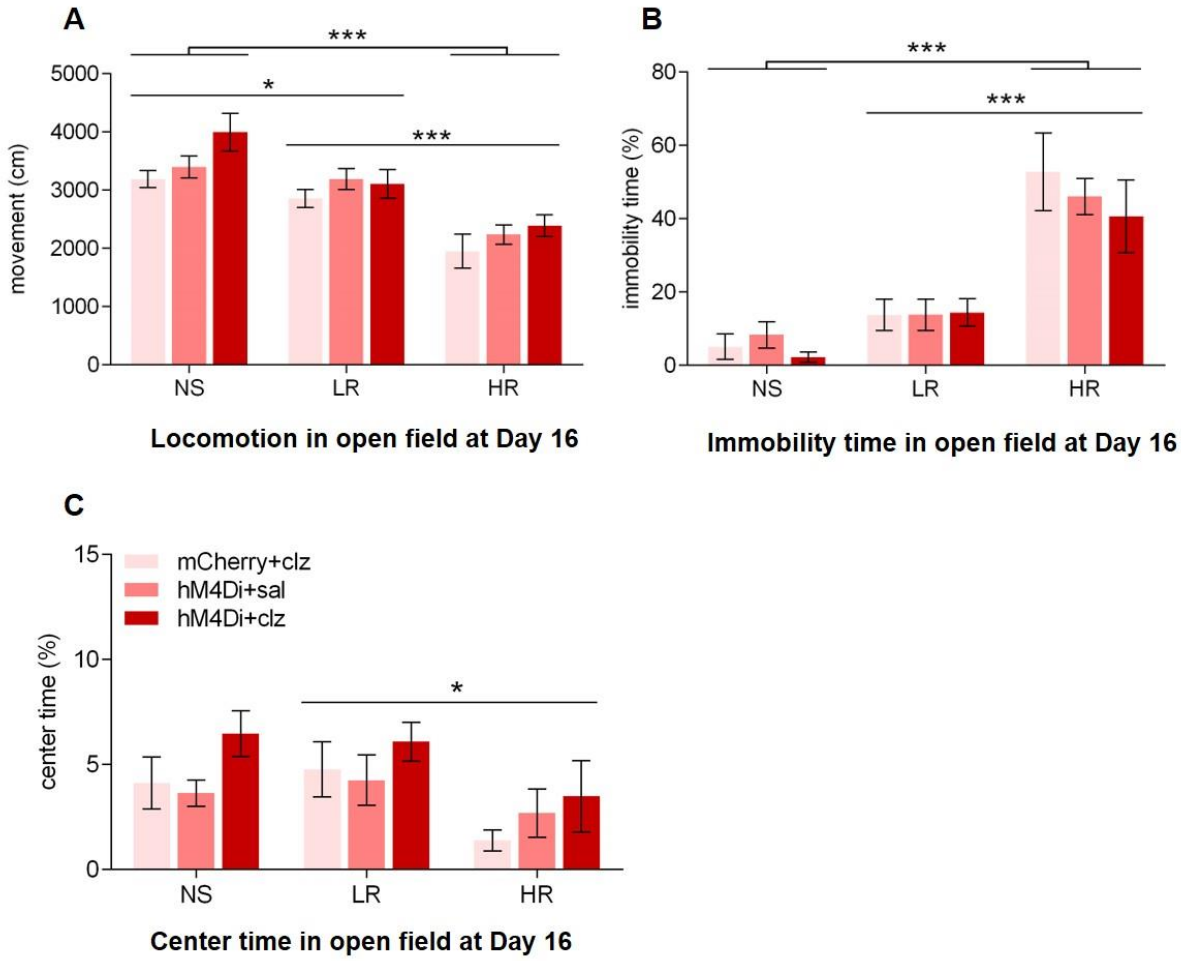

The rats were placed in the shock chamber at 18 days after the shock exposure to examine if they would express fear to the footshock context (expression of contextual fear memory) when the PVT-NAcSh projection was inhibited. Both LR and HR showed a higher level of freezing compared to the NS (Figure 4-6, main effect of early response, $F_{(2,64)} = 45.12$, $p < 0.001$; *post-hoc* test: LR vs NS, $p < 0.001$, HR vs NS, $p < 0.001$). The freezing time of the HR was also higher than the LR (*post-hoc* test: $p = 0.002$). The freezing displayed by NS, LR, and HR groups expressing hM4Di or mCherry and treated with clozapine or saline were not significantly different (Figure 4-6, main effect of chemogenetic conditions, $F_{(2,64)} = 0.319$, $p = 0.728$), indicating that chemogenetic inhibition of PVT neurons that project to the NAcSh had no effect on contextual fear expression.

Figure 4-6 Chemogenetic inhibition of the PVT-NAcSh projecting neurons did not change freezing to the shock context (contextual fear) at Day 18 post-shock.

Both HR and LR rats showed more freezing time in the shock context compared to the NS rats. The HR group also showed a higher level of freezing than the LR group. No difference was found between groups with different chemogenetic conditions. Data are presented as mean ± SEM. clz, clozapine; sal, saline.

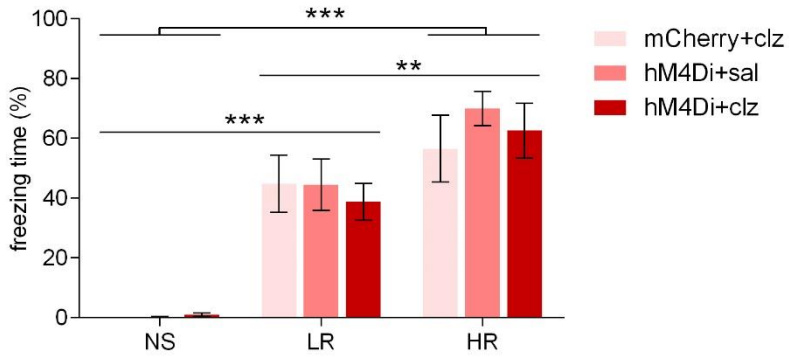

In summary, the HR group showed a higher level of anxiety and conditioned fear compared to the LR or NS groups in a series of behavioral tests conducted at around two weeks after footshock. This observation is consistent with previous reports from our research group (Chen, Li, & Kirouac, 2014; Chen et al., 2012; Chen et al., 2014). The LR group showed significantly more freezing compared to the NS in conditioned fear expression test, but their anxiety levels in the SAA test and the open field test were not different from the NS. Clozapine-treated HR rats with hM4Di showed significantly reduced anxiety-like behavior in the SAA test, while the clozapine-treated LR or NS rats did not. Clozapine injection in rats with hM4Di did not affect anxiety or fear response in the open field test or conditioned fear expression test.

To confirm that the intersectional strategy resulted in selective expression of hM4Di-mCherry or mCherry alone in PVT neurons that project to the NAcSh, we immunolabeled the reporter protein mCherry in sections of the PVT and the NAcSh in all rats used for the experiments. Representative examples are shown in Figure 4-7A and B. Immunofluorescence for hM4Di-mCherry was primarily expressed in PVT neurons and not neurons in other areas of the midline thalamus adjacent to the PVT (note that there are few labeled cells outside the PVT in the mediodorsal, paratenial nuclei). Figure 4-7C shows hM4Di-mCherry expression in the neural fibers in NAcSh and adjacent areas. The dense fiber labeling was noted in the NAcSh consistent with the idea that the PVT neurons that project to the NAcSh were chemogenetically targeted by the intersectional strategy.

Figure 4-7 hM4Di-mCherry expression in PVT neurons and NAcSh

Representative sections showing hM4Di-mCherry expressing in neurons in the aPVT (**A**) and pPVT (**B**); and neural fibers in the NAcSh (**C**). Scale bars: **A**, **B**, 100 µm; **C**, 500 µm. Abbreviations: 3V, third ventricle; ac, anterior commissure; CPu, caudate putamen; Hb, habenula nucleus; LV, lateral ventricle; MD, mediodorsal nucleus of thalamus; NAcC, nucleus accumbens, core; NAcSh, nucleus accumbens, shell; PT, paratenial nucleus of thalamus; aPVT, paraventricular nucleus of thalamus, anterior; pPVT, paraventricular nucleus of thalamus, posterior.

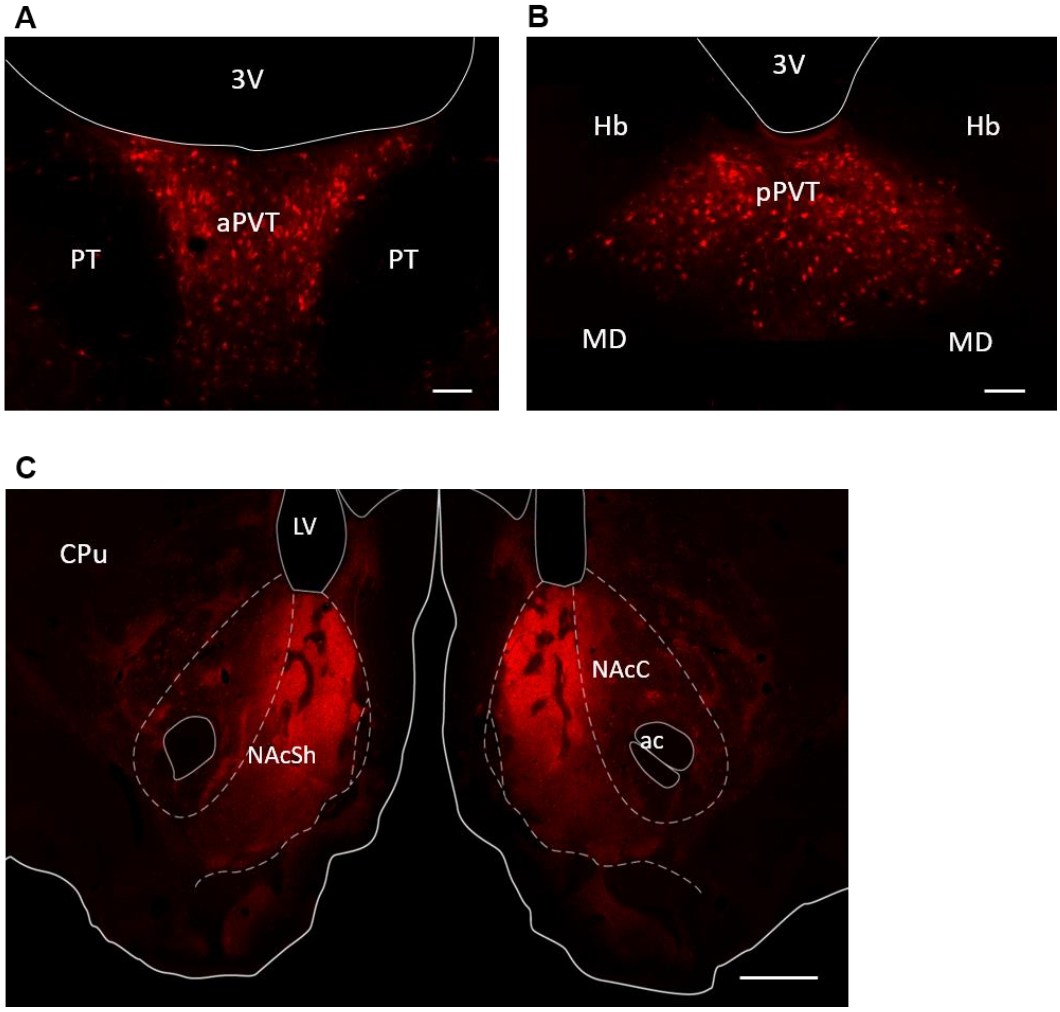

To examine the inhibitory effect of clozapine on hM4Di-expressing neurons, we used immunolabeling of cFos and mCherry on sections of the PVT. Images of the PVT were analyzed to count the number of cFos-expressing neurons and double-labeled neurons (cFos + mCherry) in a number of cases. The comparison was made between three groups: mCherry and clozapine (n = 10), hM4Di and saline (n = 12), and hM4Di and clozapine (n = 12). Figure 4-8A shows cFos- and mCherry-labeled cells in two representative PVT sections from two rats with hM4Di-mCherry after saline or clozapine injection, respectively. The hM4Di and clozapine group showed a significantly lower proportion of double-labeled PVT neurons compared with the hM4Di and saline group, and mCherry and clozapine group (Figure 4-8B, $F_{(2,31)} = 37.34$, $p < 0.001$; *post-hoc* test: hM4Di + clozapine vs hM4Di + saline, $p = 0.004$; hM4Di + clozapine vs mCherry + clozapine, $p < 0.001$) indicating that clozapine injection reduced the number of cFos positive neurons in the PVT that also express hM4Di.

Figure 4-8 Chemogenetic inhibition reduced the expression of cFos in PVT neurons with hM4Di-mCherry.

A. Representative sections showing cFos-labeled (green) and mCherry-labeled (red) cells in the PVT in a saline-treated rat with hM4Di (hM4Di + sal) and a clozapine-treated rat with hM4Di (hM4Di + clz). **B**. Percentages of cFos and mCherry double-labeled neurons in PVT neurons labeled by cFos. Data are presented as mean ± SEM. * $p < 0.05$.

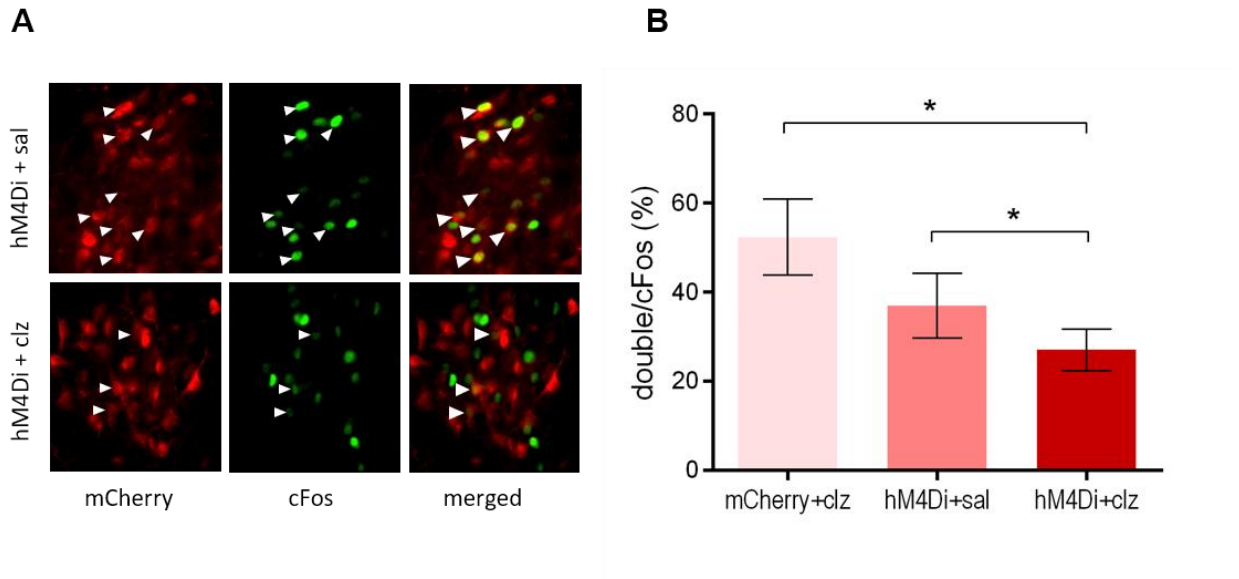

4.4 Discussion

The present study investigated the function of the neuronal projection from the PVT to the NAcSh in anxiety and fear. We used a chemogenetic method to selectively inhibit the PVT neurons that project to the NAcSh and found the inhibition of this pathway reduced social avoidance in susceptible rats in a PTSD behavioral model. At the same time, inhibition of these neurons did not affect anxiety in the open field test or fear response in conditioned fear expression test. The results indicate that the PVT contributes specifically to social avoidance via a projection to the NAcSh.

The involvement of PVT neurons that project to the NAcSh in social avoidance was observed repeatedly in the SAA test done at Day 14 and Day 18 post-shock in rats expressing hM4Di treated with clozapine in a counterbalanced design. Of note, the behavioral effect of pathway inhibition was only found in the 5-10 min period of a 10-min test. One possibility is that social anxiety builds over time and is mixed with anxiety induced by the novelty of a new chamber and/or other unknowable factors. For example, rats in the NS and LR groups showed a trend to spend less time in the social zone in the 5-10 min period compared to the 0-5 min period, which could result from the habituation of this behavioral response or a reduction of exploration of novelty (Hale et al., 2008). Rats in the HR groups treated with either clozapine or saline showed significantly less time in the social zone in the 0-5 min period at Day 14 than the NS or LR groups suggesting that their social approach behaviors could have been suppressed by the fear of novelty (neophobia) strongly induced by the test environment at the beginning of the test (Siegmund & Wotjak, 2007). Inhibition of the PVT-NAcSh projecting neurons did not affect the avoidance produced in the open field. This observation is consistent with its lack of effect on avoidance in the early part of the SAA test when anxiety to open spaces and neophobia was most

likely to contribute to the behavioral avoidance displayed in the test situation. While these behavioral tests appear to be simple, it is not unreasonable to assume that the motivational mechanism that drive avoidance is complex, time-dependent, and modulated by poorly understood learning mechanism. In the second SAA test done four days later, there was no difference in social zone time between the NS, LR, and HR rats as the ANOVA showed. However, inhibition of the PVT-NAcSh projection in HR increased the social zone time in the 5-10 min period, an anxiolytic effect consistent with the observation from the first SAA test. I think that it is reasonable to suggest that neophobia was reduced in the second SAA test because rats had previously been exposed to the test situation. This could explain why group differences in social zone time were not as evident as the first SAA test. Finally, it is important to recognize that we selected a low dose of clozapine to activate hM4Di to prevent potential confounding effects of this compound since it is a serotonin and dopamine receptor antagonist with potentially mild anxiolytic effect (Gomez et al., 2017; Ilg, Enkel, Bartsch, & Bähner, 2018).

The NAc has been shown to mediate social approach and avoidance (Gunaydin & Kreitzer, 2016; Steinman et al., 2019). Specifically, dopaminergic input from the ventral tegmental area, oxytocinergic input from the hypothalamus and a glutamatergic input from the mPFC to the NAcSh have been shown to mediate social approach or the rewarding effect of social stimuli (Gunaydin et al., 2014; Murugan et al., 2017; Nardou et al., 2019). Our result indicates that inhibition of PVT neurons that project to the NAcSh reduces stress-induced social avoidance. This is consistent with another study showing that reduced social interaction in animals experienced chronic social stress is mediated by the projection from the midline and intralaminar thalamus to the NAc (Christoffel et al., 2015). The PVT is one of the major sources of afferents to the NAcSh and the PVT appears to function as a stress-relaying nucleus with the NAcSh being

a major recipient of these signals (Hsu, Kirouac, Zubieta, & Bhatnagar, 2014; Kirouac, 2015). Therefore, the PVT may act as a hub which conveys information from many types of stress events to several downstream areas. The data from the present experiment indicate that the projection to the NAcSh appears to mediate some signals of threat- and stress-related social avoidance. Some recent studies provide evidence and further postulate that the PVT is selectively involved in selecting behaviors in situations involving potential benefits and threats (motivational conflicts) (Choi et al., 2019; Choi & McNally, 2017; Do-Monte et al., 2017; Zhu et al., 2018). From this perspective, the SAA test could be understood as a test situation involving tendencies to approach and to avoid a novel conspecific.

In this experiment we used a pathway-specific intervention to study the contribution of the PVT-NAcSh projection in stress-induced anxiety. As shown in Chapter 3, the PVT contains a great number of neurons innervating the NAcSh with some of them also issuing collaterals to the BSTDL and CeL (Dong et al., 2017; Li & Kirouac, 2008) which are brain areas that have been shown to regulate anxiety and fear (Calhoon & Tye, 2015; Tovote et al., 2015). We injected the hM4Di agonist clozapine systemically to activate hM4Di in PVT neurons that provide fibers to the NAcSh. However, this experimental manipulation would also potentially inhibit some of the fibers innervating the BSTDL and CeL. Although the density of fibers from the PVT in the NAcSh is much greater than that in the BSTDL and CeL, it is still possible that the manipulation used in the present study would have resulted in the inhibition of projections to the BSTDL and CeL in a way that could be responsible for the anxiolytic effect on social avoidance observed here.

Chapter 5 General discussion

We are interested in the role of the PVT in fear and anxiety because the PVT is anatomically connected to brain regions which appear to be critically involved in mediating these emotions. The neural connection of the PVT can be summarized as: 1) neurochemically diverse inputs from neurons located diffusively throughout the hypothalamus and brainstem; 2) robust outputs to the NAcSh and central extended amygdala (BSTDL, CeL, and other regions); 3) reciprocal connection with limbic cortices (prelimbic, infralimbic, agranular insular cortex, and ventral subiculum). Based on the PVT's anatomical connectivity, we proposed that the PVT integrates signals related to potential threats and emotional arousal to energize defensive responses via descending pathways to NAcSh and central extended amygdala.

5.1 Summary of results

Our group had previously reported that the PVT is densely innervated by fibers from orexin neurons in lateral hypothalamus (Kirouac et al., 2005) and that microinfusions of orexins in the PVT increase fear- and anxiety-like behaviors (Li et al., 2009, 2010a, 2010b). More importantly, blocking of orexin receptors in the PVT decreases anxiety in rats pre-exposed to footshocks implicating that the PVT is involved in stress-induced anxiety (Li et al., 2010b). Thereafter, we hypothesized that orexins act on the PVT to promote conditioned fear and experiments presented in this thesis tested this hypothesis. In Chapter 2, we found that lesions of the pPVT attenuated the expression of conditioned fear. However, blocking orexin receptors in the PVT had no effect on the expression of conditioned fear. The results of these experiments indicate that the PVT is involved in fear but that orexin receptors in the PVT do not appear to

contribute to conditioned fear (Y. Li et al., 2014; Dong et al., 2015). In Chapter 3, we studied if the PVT fiber projections to the NAcSh, BSTDL, and CeL originate from distinct subpopulations of projection-specific neurons in the PVT or from neurons that send divergent projections to multiple targets. This was done by injecting combinations of retrograde tracers in two target areas of the brain in the same rat. The tracing experiment revealed that most neurons in the PVT innervate the NAcSh and that many neurons projected to more than one of the NAcSh, BSTDL, and CeL (Dong et al., 2017). The dual retrograde tracing method was also combined with cFos protein immunofluorescence to examine the hypothesis that the projection-specific neurons in the PVT were activated differentially by stressful or aversive events. The results demonstrated that PVT neurons that project to the NAcSh, BSTDL, or CeL do not appear to be activated differentially when rats are exposed to different stressors including footshocks and a novel open field. However, one exception was the observation that contextual fear memory expression caused a greater activation of the PVT-dmNAcSh projecting neurons than the PVT-CeL projecting neurons. This is notable because the dmNAcSh has not been shown to play a role in fear whereas the CeL is well-known for its involvement in fear (Duvarci & Pare, 2014; Janak & Tye, 2015). In Chapter 4, we examined if the PVT contributes to the fear and anxiety produced by exposure of rats to fear-inducing footshocks in a validated model of PTSD. We found that selective chemogenetic inhibition of PVT neurons that innervate NAcSh reduced social anxiety in susceptible rats. In summary, experiments in this thesis provide evidence that the PVT contribute to conditioned fear and anxiety. As will be discussed later, observations from our own experiments as well as those from other research groups suggest that the PVT does not simply control stress-induced fear or anxiety but may potentially contribute to some subtle or general component of both appetitive and aversive behaviors.

5.2 Does the PVT mediate fear or other aspect of stressful events?

Our lab found that local administration of orexins in the PVT in rats placed in an open field triggered freezing indicative of a fear state (Li et al., 2009). In addition, the mRNA for prepro-orexin polypeptide was found to be increased for up to 14 days after intense footshock stress (Chen, Wang, et al., 2014) indicating that an intense stressor can elevate the activity of orexin neurons and the synthesis of orexin peptides. These findings suggested that the release of orexins and the activation of the orexin receptors in the PVT contribute to fear-like responses. As demonstrated in *Experiment1* in Chapter 2, lesions of the PVT did not have an effect on the immediate fear response to footshocks (Y. Li et al., 2014). Similarly, injection of a GABA agonist in the midline thalamus was also reported to have no effect on freezing produced by footshocks (Padilla-Coreano et al., 2012). Consequently, it does not appear that the PVT is required for an innate fear response to occur even though the PVT is important for conditioned fear (a learned fear). However, it is not exactly clear what the PVT contributes to conditioned fear response. Our own results in addition to those in other studies (Do-Monte, Quiñones-Laracuente, et al., 2015; Y. Li et al., 2014; Padilla-Coreano et al., 2012) showed that lesion or inhibition of the PVT did not prevent the acquisition of a conditioned fear response but attenuated its expression. In contrast, another group showed that chemogenetic inhibition of PVT neurons that project to the CeL interfered with the acquisition of a conditioned fear response (Penzo et al., 2015). Another study found that (Zhu et al., 2018). Electrophysiological evidence indicates that the PVT contributes to synaptic plasticity in fear modulating SOM+ neurons of the CeL at 24 hrs but not 3 hrs after footshock-tone pairings (Penzo et al., 2015) indicating a role for the PVT in a relatively late phase of fear memory acquisition. Similarly, another study showed

that inhibition of the PVT did not affect the expression of conditioned fear at 30 min or 6 hrs after the acquisition session but reduced freezing to the tone at 24 hrs or days after acquisition (Do-Monte, Quiñones-Laracuente, et al., 2015). Based on the studies discussed, it is reasonable to postulate that the influence that the PVT has on conditioned fear may depend on the time interval between the acquisition and expression test. Future studies will be needed for a more precise understanding about when and how the PVT regulates conditioned fear and how the time-dependent factors involved.

The neural circuitry by which the PVT mediates conditioned fear is poorly understood. Results from our laboratory suggest that orexin neurotransmission to the PVT is not involved in the expression of conditioned fear (Dong et al., 2015). Do-Monte and colleagues found that optogenetic inhibition of the prelimbic input in the PVT reduced freezing in the expression test (Do-Monte, Quiñones-Laracuente, et al., 2015) indicating that the prelimbic input to the PVT contributes to conditioned fear expression. A number of studies have shown that the CeL contributes to conditioned fear (see section 1.2.4) and our research group postulated that the PVT is involved in fear via its projection to the CeL (Li & Kirouac, 2008). This hypothesis is now supported by evidence from two studies showing that optogenetic or chemogenetic inhibition of the activity of the PVT-CeL projection reduced the expression of conditioned fear (Do-Monte, Quiñones-Laracuente, et al., 2015; Penzo et al., 2015). A basic assumption made in studies involving projection-specific opto- or chemogenetic interventions is that the observed effect is mediated exclusively by neural fibers in the targeted area where received viral vector injection. This assumption may lead to conclusions such as that PVT neurons that project to CeL mediate conditioned fear. However, the result of our dual retrograde tracing study showed that a large proportion of PVT neurons that project to the CeL also project to the NAcSh and BSTDL.

Furthermore, our group has recently completed a detailed anterograde tracing study using the same strategy as the DREADD experiment in Chapter 4 to specifically target AAV-driven expression of GFP in PVT neurons that project to one of the PVT's target areas (NAcSh, BSTDL, and CeL) and quantify the fiber density of these neurons to other areas of the brain (Li, Dong, & Kirouac, 2019). When we targeted the GFP expression in the PVT neurons that project to the CeL, we found that labeled fibers to the NAcSh and BSTDL were as dense as the fibers innervating the CeL indicating that PVT-CeL projecting neurons send equally dense fibers to the NAcSh and BSTDL. One must be cautious when interpreting the effects of manipulating projection-specific neurons in the PVT because of the fact that PVT neurons send divergent projection to the forebrain. Indeed, the experimental effects observed can be potentially mediated by collaterals to other regions than the ones targeted. For example, when the activity of the PVT-CeL neurons are interrupted, the projection from the PVT to other areas including the NAcSh and BSTDL may also be affected. PVT neurons may regulate conditioned fear response by coordinating the activity of multiple brain areas and not just the CeL. Moreover, the hypothesis that only the PVT-CeL projection mediates fear is somewhat suspicious since that we found a higher level of cFos expression in PVT neurons that project to the dmNAcSh than those PVT neurons innervating the CeL during contextual fear expression test. At the very least, the result of these cFos experiments suggests that the PVT-CeL projection may not be the only PVT projection that contributes to fear.

5.3 Which PVT output mediates anxiety?

Our group has reported an anxiogenic effect of local orexins infusion in the PVT in different test conditions (Li et al., 2009, 2010a, 2010b). Recent reports also support the

involvement of the PVT in anxiety by showing that optogenetic activation of the PVT induced real-time avoidance and abolished food seeking (Do-Monte et al., 2017; Zhu et al., 2016). Moreover, we have found that blocking of orexin receptors in the PVT (Dong et al., 2015; Li et al., 2010b) or chemogenetic inhibition of the PVT neurons that project to the NAcSh reduced anxiety in rats pre-exposed to footshocks but not in nonshocked rats indicating that the PVT is required in stress-induced anxiety. The involvement of the PVT in anxiety and fear is similar in that the PVT appears to be especially important after exposure to some form of stressor or threatening situation possibly through a learning process where previous stress experience affects response to related stressful or threatening stimuli or conditions. It is also important to recognize that orexinergic input from the lateral hypothalamus to the PVT regulates footshock-induced anxiety (Dong et al., 2015; Li et al., 2010b) while the prelimbic glutamatergic input regulates the expression of conditioned fear (Do-Monte, Quiñones-Laracuente, et al., 2015). Another study reported that local administration of $GABA_A$ and $GABA_B$ receptors agonists in the PVT of rats produced an anxiogenic effect in EPM and open field test suggesting that a GABAergic input in the PVT may also be involved in the regulation of anxiety behaviors (Barson & Leibowitz, 2015).

Our dual-retrograde tracing experiments in Chapter 3 (Dong et al., 2017) and the aforementioned anterograde tracing study (Li, Dong, & Kirouac, 2019) show that most PVT neurons innervate the NAcSh and send collaterals to a wide range of cortical and subcortical targets. Experimental studies using project-specific intervention of PVT outputs report that intervention of PVT neurons that project to the NAcSh or other targets do not necessarily have the same effects as pharmacological intervention at the whole PVT region. For example, chemogenetic inhibition of the PVT-NAcSh projection reduced social avoidance in stress

susceptible rats (Chapter 4) and another study reported that optogenetic inhibition of the neurons in the midline thalamus that project to the NAc reduced social avoidance after chronic social defeat (Christoffel et al., 2015). However, we did not find any effect on the behavior displayed in the open field when the PVT-NAcSh projecting neurons were chemogenetically inhibited consistent with another study reporting that optogenetic activation of PVT fibers in the NAc did not increase anxiety-like behaviors in the EPM test and to a novel object (Cheng et al., 2018). It is interesting that activation or inhibition of the orexin receptors in the PVT modulated anxiety in spatial anxiety tests like the open field and EPM test (Dong et al., 2015; Heydendael et al., 2011; Li et al., 2009, 2010a, 2010b) whereas activation or inhibition of the PVT neurons that project to the NAc only had effect on the anxiety associated with a social target (Christoffel et al., 2015; Chapter 4). It is possible that the PVT may regulate anxiety-like behaviors induced by novel contexts or objects through its projections to the BSTDL and CeL and not the NAcSh. The BSTDL has been considered as an essential part of the neural circuit mediating anxiety (see Section 1.3.4) but the involvement of the PVT-BSTDL projection in anxiety has not been addressed. The CeL has also been found to mediate anxiety (Ahrens et al., 2018; Botta et al., 2015; Kim et al., 2017). There is one study showing that PVT neurons that project to the CeL may contribute to a decrease in locomotion in the EPM in rat pre-exposed to footshocks (Pliota et al., 2020) but there are other studies reporting that projection-specific optogenetic activation or inhibition of the PVT fibers in the CeL had no effect on behaviors in the EPM or open field test (Chen & Bi, 2018; Do-Monte, Quiñones-Laracuente, et al., 2015).

5.4 Potential function of the PVT in emotional behaviors: "salience" or "conflict"?

The PVT is not only involved in the regulation of aversive behaviors like fear and anxiety but also appetitive and addictive behaviors (e.g., Choudhary et al., 2018; Matzeu et al., 2017; Otis et al., 2017, 2019; Wunsch et al., 2017; Zhang & van den Pol, 2017) and arousal states (e.g., Gao et al., 2020; Herrera et al., 2016; Hua et al., 2018; Ren et al., 2018). Typically, studies only focus on how the PVT regulates one specific behavioral response or a class of behaviors that have either a positive or negative valence. However, accumulating evidence suggests that the PVT may not only mediate specific types of behavior but instead may contribute to a common component that makes up the basis of emotional behaviors in general. This emerging view comes from experiments where the role of the PVT is investigated in experimental conditions in which both appetitive and aversive behavioral responses are examined.

Chen and colleagues (Zhu et al., 2018) proposed that "the PVT gates associative learning by providing a dynamic representation of stimulus salience". They found that both appetitive and aversive stimuli or conditioned stimuli associated with these stimuli elicited robust calcium signals in the PVT indicating that neurons in the PVT are activated by cues and conditions that are emotionally salient. In addition, when both appetitive and aversive stimuli were presented in one task, a switch from mild to strong aversive stimuli resulted in a higher proportion of PVT neurons that responded to the aversive stimuli and a reduced proportion of PVT neurons that responded to the appetitive stimuli. This observation supports their hypothesis that PVT neurons are "tuned" to the salience of sensory stimuli irrespective of their valence. Their study also showed that optogenetic inhibition of the PVT during the presence of the US or CS during learning of a task reduced the behavioral response to the CS indicating that the PVT is required for associative learning. This salience hypothesis is consistent with the hypothesis that the PVT

relays signals related to emotional arousal (Kirouac, 2015). Accordingly, the PVT contributes to both appetitive and aversive behaviors by relaying signals encoding the salience of stimuli or conditions to brain areas involved in mediating the emotional behavioral responses.

McNally and colleagues also reported that unconditioned appetitive and aversive stimuli as well as the CS associated with these stimuli trigger elevated calcium signals in the PVT (Choi et al., 2019). Furthermore, their studies showed that the PVT is particularly involved in a process of balancing appetitive and aversive behavioral tendencies when test conditions offer the possibility of both types of motivations (Choi et al., 2019; Choi & McNally, 2017). They observed that chemogenetic inhibition of the PVT had no effect on the expression of conditioned fear when the rats had been only trained for the association between a tone and footshock. Similarly, inhibition of the PVT did not reduce conditioned reward-seeking behavior in another group of rats that were only trained to bar-press for food to tones that signaled the availability of a food reward. However, when rats had been trained for both appetitive and aversive contingencies, inhibition of the PVT altered the balance between appetitive and aversive behavioral responses. One study (Choi & McNally, 2017) found that chemogenetic inhibition of the PVT reduced freezing in the test session when rats received training for bar-pressing for food at first and a tone-shock pairing later. In contrast, inhibition of the PVT increased freezing in the rats that received tone-shock pairing training before bar-pressing for food training. The result of this study suggests that the sequence of appetitive and aversive conditioning determines the type of behavioral effect that is produced by inhibition of PVT neurons. In another study (Choi et al., 2019), chemogenetic inhibition of the PVT increased freezing in the rats that received appetitive training before aversive training whereas no effect on freezing was reported in the rats that received aversive training before appetitive training. The experimental design of the two experiments are

complicated by a number of experimental factors including whether the tone that signaled the availability of a food reward was the same tone as the one paired with the footshock; whether the two conditioning sessions were carried out in the same context or different context; whether the food reward was available during test; and the length of the interval between two conditioning sessions. However, the very important point highlighted by these studies is that the PVT's influence on behavior is most apparent or measurable when the experimental animals are placed in a situation where both appetitive and aversive contingencies are present (i.e., a situation involving a motivational conflict).

The hypothesis that the PVT is only recruited in situations involving a motivational conflict provides a plausible explanation for the influence that the PVT has in different experimental situations. For example, in *Experiment 1* in Chapter 2, the animals had been first trained to bar-press for sucrose pellet in the same chamber as was used for the subsequent fear conditioning (Y. Li et al., 2014). The attenuated conditioned fear in rats with pPVT lesion could be viewed as a biased behavioral tendency where there was a motivational conflict (the motivation to avoid danger by freezing vs the motivation to bar-press for a food reward). In contrast, *Experiment 2 and 3* in Chapter 2 used another behavioral model where fear conditioning was examined in rats that had not been trained to bar-press for a food reward (i.e., no food-seeking motivation). In this case, blocking of orexin receptors in the PVT did not produce any effect on freezing during conditioned fear expression tests (Dong et al., 2015). The anxiolytic effect of the orexin antagonist in the social approach-avoidance test in Chapter 2 *Experiment 3* and of chemogenetic inhibition of PVT-NAcSh projecting neurons in Chapter 4 could also be viewed as that experimental manipulations on the PVT shifted a motivational tendency towards reward-seeking in a behavioral task with both reward potentials (interacting

with a novel rat) and threats (fear of a physical confrontation with a novel rat) (Toth & Neumann, 2013). The hypothesis that the PVT is especially involved in resolving motivational conflict is also supported by the result of another study showing that omission of a food reward has the effect of suppressing future bar-pressing and that optogenetic inhibition of the PVT only increased bar-pressing when no sucrose pellet was provided (reward omission), an effect not present when pellets were available (Do-Monte et al., 2017; Zhu et al., 2018). Reward omission might also be viewed as a situation with conflicting motivations in that the CS elicited a motivation to seek a reward while the omission of the pellets produced a motivation to avoid the frustration effect of not receiving a food reward after bar-pressing.

5.5 Significance and limitations

Excessive fear and anxiety are primary symptoms of anxiety disorders which are prevalent psychiatric disorders in the modern society. Research on the neural mechanisms of fear and anxiety may provide theoretical basis for developing treatments for related disorders. Accumulating evidence from research on brain mechanisms shows that connections between the limbic cortices and several basal forebrain nuclei form a complex neural circuit for fear and anxiety. The PVT has received increasing research interest for its role in fear and anxiety because of its dense neural connections with many of the components of this neural circuitry. This thesis examined the involvement of the PVT in different phases of fear memory and found that the PVT contributes to the expression of fear memory. We also found that the PVT mediates stress-induced anxiety. These results indicate that the PVT is critical for the development of enhanced fear- or anxiety-like response after exposure to some form of stressor or fear-inducing situation. These findings suggest that the PVT and its connections to components of the fear and

anxiety circuits may be involved in psychiatric disorders like PTSD. We also found that most PVT neurons project to the NAc and a portion of these neurons also innervate the BSTDL and CeL. This suggests that the PVT may coordinate the activity of multiple targets via its highly collateralized output and provides insights for future studies on the function of the PVT.

There are also limitations in this thesis. As discussed in Section 5.4, *Experiment 1* in the Chapter 2 used both freezing and suppression of reward-seeking behavior to indicate fear level, while *Experiment 2 and 3* in Chapter 2 used only freezing. *Experiment 1* showed that animals with lesions in pPVT expressed a higher level of bar-pressing for sucrose and less freezing to CS during fear expression; *Experiment 2 and 3* showed that blocking orexin receptors in the PVT did not reduce freezing. We explained these findings as that the PVT mediates the expression of fear through a non-orexin mediated mechanism. Another plausible explanation may be that the PVT is only involved in biasing behavioral tendencies in the presence of conflicting motivations as the case in the test situation used in *Experiment 1*. This design makes it difficult to distinguish whether the discrepancy described above was the result of the experimental manipulation (lesions vs blocking orexin receptors) or behavioral paradigms used (bar-pressing for reward and tone-shock paring vs tone-shock pairing alone).

The interpretation of the experiments in Chapter 3 and Chapter 4 are limited by the methods used to study axonal collaterals. As discussed in Section 3.4, the dual retrograde tracing method resulted in an inevitable underestimation of the proportion of PVT neurons innervating both areas. In addition, it is difficult to postulate a comprehensive overview of the distribution of the output collaterals of PVT neurons based on results from multiple combinations of retrograde tracing experiments. Another shortcoming of retrograde tracing is that it can only provide evidence that a labeled neuron innervates the area receiving the injection of retrograde tracer and

does not provide direct information about fiber density. Our laboratory conducted an anterograde tracing study to label and estimate the fiber density of axonal collaterals from PVT neurons that innervate a specific brain area to overcome this limitation (Li, et al., 2019; see Section 5.2, 5.3). The result of this anterograde tracing study was consistent with the retrograde tracing experiments and provided further evidence that PVT neurons provide divergent innervation to most of its forebrain targets. Consequently, the findings in Chapter 3 are likely an oversimplification since many or most PVT neurons innervate multiple target areas but the proportions of PVT neurons that innervate different areas as well as fiber density in different target areas vary widely. This makes the design of experiments that attempt to study the function of individual projection a challenge.

The experiment in Chapter 4 used an intersectional strategy to selectively express an inhibitory receptor in PVT neurons that project to the NAcSh. In this case, systemic injection of receptor agonist clozapine inevitably activated receptors expressed on the collaterals that innervating other areas including the BSTDL and CeL. Our laboratory has recently completed an experiment in which the DREADDs agonist was infused locally in the NAcSh through an implanted cannula in this area of the ventral striatum. Results from this fiber DREADDs experiment are entirely consistent with the findings reported in Chapter 4 and these new findings combined with those in Chapter 4 are currently going to be included together as a part of a new manuscript.

5.6 Future directions

This thesis provides evidence that the PVT promotes stress-induced anxiety by a projection to the NAcSh. However, future studies will need to determine if this effect is mediated

exclusively by PVT fibers in the NAcSh or fibers to other areas like the BSTDL and CeL. The broader question of how the PVT modulates appetitive and aversive behaviors will be more difficult to resolve. Considering the involvement of the PVT in both negative and positive emotional behaviors, it is reasonable to propose that future research should focus on how the PVT integrates and simultaneously sends signals to several key subcortical and cortical regions involved in complex emotional behaviors, especially in situations involving conflicting motivations. Classic behavioral models that include motivational conflict such as the extinction, renewal, and reinstatement of positive or negative associative memory may be modified to investigate how the PVT contributes to resolving motivational conflict. The PVT appears to be involved in conditions or factors poorly controlled or largely neglected in classic behavioral tests. For example, it is apparent that the sequence of how appetitive and aversive behaviors are learned (which is learned first) (Choi et al., 2019; Choi & McNally, 2017), the intensity of the US (Zhu et al., 2018), the length of the training session (Choi & McNally, 2017; Zhu et al., 2018), and the length of the interval between the training session and the expression test of a learned behavior (Do-Monte, Quiñones-Laracuente, et al., 2015) all seem to affect in some way how the PVT influences behavioral responding. The development of a sensitive behavioral model will be essential to better understand how the PVT modulates complex emotional behavior. It will also be important to study the neural pathways through which the PVT exerts its behavioral effect. As aforementioned, the limbic cortices that are reciprocally connected to the PVT also project densely to the same striatal-like areas that the PVT projects to (see Section 1.4.4). For example, the prelimbic cortex projects to the NAcSh; the insular cortex projects to the CeL. The cortical and thalamic inputs have been shown to be the two major sources of glutamatergic inputs in striatal-like areas (Groenewegen et al., 1999; Zahm, 2000). Therefore, in

addition to studying the influence of the direct inputs from the PVT and limbic cortices to subcortical areas like the NAcSh, BSTDL, and CeL, the interaction between the PVT and cortical inputs at these subcortical regions will be important to understanding how this complex circuit mediates emotional behaviors. Future research may consider these two sources of inputs at the same time. It could be achieved by the expression of distinct opsins with different action spectrums coupled to different ion channels or G proteins in the terminal regions along with intersectional strategy to target different pathways (Maimon, Sparks, Srinivasan, Zorzos, & Herr, 2018), or distinct reporter proteins that are sensitive to certain ion concentration in neuronal terminals that come from different sources (Beck & Gong, 2019; Oh et al., 2019). Studies for a more comprehensive as well as precise understanding of the PVT's functions will improve the understanding of the mechanism of emotions and motivations and provide insights for the development of potential therapy for emotion- and motivation-related psychiatric disorders.

References

Adhikari, A. (2014). Distributed circuits underlying anxiety. *Frontiers in Behavioral Neuroscience*, *8*(April), 1–6. https://doi.org/10.3389/fnbeh.2014.00112

Adhikari, A., Topiwala, M. A., & Gordon, J. A. (2010). Synchronized Activity between the Ventral Hippocampus and the Medial Prefrontal Cortex during Anxiety. *Neuron*. https://doi.org/10.1016/j.neuron.2009.12.002

Adolphs, R. (2013). The biology of fear. *Current Biology*, *23*(2), R79–R93. https://doi.org/10.1016/j.cub.2012.11.055

Ahrens, S., Wu, M. V., Furlan, A., Hwang, G.-R. R., Paik, R., Li, H., … Li, B. (2018). A central extended amygdala circuit that modulates anxiety. *Journal of Neuroscience*, *38*(24), 5567–5583. https://doi.org/10.1523/JNEUROSCI.0705-18.2018

Al-Hasani, R., McCall, J. G., Shin, G., Gomez, A. M., Schmitz, G. P., Bernardi, J. M., … Bruchas, M. R. (2015). Distinct Subpopulations of Nucleus Accumbens Dynorphin Neurons Drive Aversion and Reward. *Neuron*, *87*(5), 1063–1077. https://doi.org/10.1016/j.neuron.2015.08.019

Alden, M., Besson, J.-M., & Bernard, J.-F. (1994). Organization of the efferent projections from the pontine parabrachial area to the bed nucleus of the stria terminalis and neighboring regions: A PHA-L study in the rat. *The Journal of Comparative Neurology*, *341*(3), 289–314. https://doi.org/10.1002/cne.903410302

Alheid, G. F. (2003). Extended amygdala and basal forebrain. *Annals of the New York Academy of Sciences*, *985*, 185–205. https://doi.org/10.1111/j.1749-6632.2003.tb07082.x

Alheid, G. F., & Heimer, L. (1988). New perspectives in basal forebrain organization of special relevance for neuropsychiatric disorders: The striatopallidal, amygdaloid, and corticopetal components of substantia innominata. *Neuroscience*, *27*(1), 1–39. https://doi.org/10.1016/0306-4522(88)90217-5

Allen, G. V., Saper, C. B., Hurley, K. M., & Cechetto, D. F. (1991). Organization of visceral and limbic connections in the insular cortex of the rat. *Journal of Comparative Neurology*, *311*(1), 1–16. https://doi.org/10.1002/cne.903110102

Anderson, D. J., Adolphs, R. (2014). A framework for studying emotions across species. *Cell 157*(1): 187–200. https://doi.org/10.1016/j.cell.2014.03.003

Anthony, T. E., Dee, N., Bernard, A., Lerchner, W., Heintz, N., & Anderson, D. J. (2014). Control of stress-induced persistent anxiety by an extra-amygdala septohypothalamic circuit. *Cell*, *156*(3), 522–536. https://doi.org/10.1016/j.cell.2013.12.040

Arcelli, P., Frassoni, C., Regondi, M. C., Biasi, S. De, & Spreafico, R. (1997). GABAergic neurons in mammalian thalamus: A marker of thalamic complexity? *Brain Research Bulletin*, *42*(1), 27–37. https://doi.org/10.1016/S0361-9230(96)00107-4

Arnsten, A. F. T. (2009). Stress signalling pathways that impair prefrontal cortex structure and

function. *Nature Reviews Neuroscience*, *10*(6), 410–422. https://doi.org/10.1038/nrn2648

Asok, A., Draper, A., Hoffman, A. F., Schulkin, J., Lupica, C. R., & Rosen, J. B. (2018). Optogenetic silencing of a corticotropin-releasing factor pathway from the central amygdala to the bed nucleus of the stria terminalis disrupts sustained fear. *Molecular Psychiatry*, *23*(4), 914–922. https://doi.org/10.1038/mp.2017.79

Aston-Jones, G., Smith, R. J., Sartor, G. C., Moorman, D. E., Massi, L., Tahsili-Fahadan, P., & Richardson, K. A. (2010). Lateral hypothalamic orexin/hypocretin neurons: A role in reward-seeking and addiction. *Brain research*, *1314*, 74–90. https://doi.org/10.1016/j.brainres.2009.09.106

Bandler, R., & Shipley, M. T. (1994). Columnar organization in the midbrain periaqueductal gray: modules for emotional expression? *Trends in Neurosciences*, *17*(9), 379–389. https://doi.org/10.1016/0166-2236(94)90047-7

Banghart, M. R., Neufeld, S. Q., Wong, N. C., & Sabatini, B. L. (2015). Enkephalin Disinhibits Mu Opioid Receptor-Rich Striatal Patches via Delta Opioid Receptors. *Neuron*, *88*(6), 1227–1239. https://doi.org/10.1016/j.neuron.2015.11.010

Barrett, D., Shumake, J., Jones, D., & Gonzalez-Lima, F. (2003). Metabolic mapping of mouse brain activity after extinction of a conditioned emotional response. *The Journal of Neuroscience : The Official Journal of the Society for Neuroscience*, *23*(13), 5740–5749. https://doi.org/10.1523/jneurosci.23-13-05740.2003

Barrett, L. F., & Simmons, W. K. (2015). Interoceptive predictions in the brain. *Nature Reviews Neuroscience*, *16*(7), 419–429. https://doi.org/10.1038/nrn3950

Barson, J. R., & Leibowitz, S. F. (2015). GABA-induced inactivation of dorsal midline thalamic subregions has distinct effects on emotional behaviors. *Neuroscience Letters*, *609*(4), 92–96. https://doi.org/10.1016/j.neulet.2015.10.029

Bass, C. E., Grinevich, V. P., Gioia, D., Day-Brown, J. D., Bonin, K. D., Stuber, G. D., … Budygin, E. A. (2013). Optogenetic stimulation of VTA dopamine neurons reveals that tonic but not phasic patterns of dopamine transmission reduce ethanol self-administration. *Frontiers in Behavioral Neuroscience*, *7*(November), 173. https://doi.org/10.3389/fnbeh.2013.00173

Beck, C., & Gong, Y. (2019). A high-speed, bright, red fluorescent voltage sensor to detect neural activity. *Scientific Reports*, *9*(1), 1–12. https://doi.org/10.1038/s41598-019-52370-8

Beck, C. H., & Fibiger, H. C. (1995). Conditioned fear-induced changes in behavior and in the expression of the immediate early gene cFos: with and without diazepam pretreatment. *J Neurosci*, *15*(1 Pt 2), 709–720. https://doi.org/10.1523/JNEUROSCI.15-01-00709.1995

Ben-Shaul, Y., Katz, L. C., Mooney, R., & Dulac, C. (2010). In vivo vomeronasal stimulation reveals sensory encoding of conspecific and allospecific cues by the mouse accessory olfactory bulb. *Proceedings of the National Academy of Sciences*, *107*(11), 5172–5177. https://doi.org/10.1073/pnas.0915147107

Bentivoglio, M., Balercia, G., & Kruger, L. (1991). The specificity of the nonspecific thalamus: The midline nuclei. *Progress in Brain Research*, *87*, 53–80. https://doi.org/10.1016/S0079-

6123(08)63047-2

Berendse, H. W., Galis-de Graaf, Y., & Groenewegen, H. J. (1992). Topographical organization and relationship with ventral striatal compartments of prefrontal corticostriatal projections in the rat. *The Journal of Comparative Neurology*, *316*(3), 314–347. https://doi.org/10.1002/cne.903160305

Berendse, H. W., & Groenewegen, H. J. (1990). Organization of the thalamostriatal projections in the rat, with special emphasis on the ventral striatum. *Journal of Comparative Neurology*, *299*(2), 187–228. https://doi.org/10.1002/cne.902990206

Berg, L., Eckardt, J., & Masseck, O. A. (2019). Enhanced activity of pyramidal neurons in the infralimbic cortex drives anxiety behavior. *PLoS ONE*, *14*(1), 1–19. https://doi.org/10.1371/journal.pone.0210949

Bergman, J. M., Roecker, A. J., Mercer, S. P., Bednar, R. A., Reiss, D. R., Ransom, R. W., … Coleman, P. J. (2008). Proline bis-amides as potent dual orexin receptor antagonists. *Bioorganic and Medicinal Chemistry Letters*. https://doi.org/10.1016/j.bmcl.2008.01.001

Bernard, J. -F, Alden, M., & Besson, J. -M. (1993). The organization of the efferent projections from the pontine parabrachial area to the amygdaloid complex: A phaseolus vulgaris leucoagglutinin (PHA-L) study in the rat. *Journal of Comparative Neurology*. https://doi.org/10.1002/cne.903290205

Berridge, K. C., & Kringelbach, M. L. (2015). Pleasure Systems in the Brain. *Neuron*, *86*(3), 646–664. https://doi.org/10.1016/j.neuron.2015.02.018

Bertran-Gonzalez, J., Laurent, V., Chieng, B. C., Christie, M. J., & Balleine, B. W. (2013). Learning-related translocation of δ-opioid receptors on ventral striatal cholinergic interneurons mediates choice between goal-directed actions. *The Journal of Neuroscience : The Official Journal of the Society for Neuroscience*, *33*(41), 16060–16071. https://doi.org/10.1523/JNEUROSCI.1927-13.2013

Bewernick, B. H., Hurlemann, R., Matusch, A., Kayser, S., Grubert, C., Hadrysiewicz, B., … Schlaepfer, T. E. (2010). Nucleus Accumbens Deep Brain Stimulation Decreases Ratings of Depression and Anxiety in Treatment-Resistant Depression. *Biological Psychiatry*, *67*(2), 110–116. https://doi.org/10.1016/j.biopsych.2009.09.013

Bewernick, B. H., Kayser, S., Sturm, V., & Schlaepfer, T. E. (2012). Long-term effects of nucleus accumbens deep brain stimulation in treatment-resistant depression: evidence for sustained efficacy. *Neuropsychopharmacology : Official Publication of the American College of Neuropsychopharmacology*, *37*(9), 1975–1985. https://doi.org/10.1038/npp.2012.44

Bi, L.-L., Wang, J., Luo, Z.-Y., Chen, S.-P., Geng, F., Chen, Y., … Gao, T.-M. (2013). Enhanced excitability in the infralimbic cortex produces anxiety-like behaviors. *Neuropharmacology*, *72*, 148–156. https://doi.org/10.1016/j.neuropharm.2013.04.048

Bonnavion, P., Jackson, A. C., Carter, M. E., & de Lecea, L. (2015). Antagonistic interplay between hypocretin and leptin in the lateral hypothalamus regulates stress responses. *Nature communications*, *6*, 6266. https://doi.org/10.1038/ncomms7266

Botta, P., Demmou, L., Kasugai, Y., Markovic, M., Xu, C., Fadok, J. P., … Lüthi, A. (2015). Regulating anxiety with extrasynaptic inhibition. *Nature Neuroscience*, *18*(10), 1493–1500. https://doi.org/10.1038/nn.4102

Bouton, M. E., & Bolles, R. C. (1980). Conditioned fear assessed by freezing and by the suppression of three different baselines. *Animal Learning & Behavior*, *8*(3), 429–434. https://doi.org/10.3758/BF03199629

Breer, H., Fleischer, J., & Strotmann, J. (2006). Signaling in the Chemosensory Systems. *Cellular and Molecular Life Sciences*, *63*(13), 1465–1475. https://doi.org/10.1007/s00018-006-6108-5

Brog, J. S., Salyapongse, A., Deutch, A. Y., & Zahm, D. S. (1993). The patterns of afferent innervation of the core and shell in the "Accumbens" part of the rat ventral striatum: Immunohistochemical detection of retrogradely transported fluoro-gold. *Journal of Comparative Neurology*, *338*(2), 255–278. https://doi.org/10.1002/cne.903380209

Burgdorf, J., & Panksepp, J. (2006). The neurobiology of positive emotions. *Neuroscience and Biobehavioral Reviews*, *30*(2), 173–187. https://doi.org/10.1016/j.neubiorev.2005.06.001

Burgos-Robles, A., Vidal-Gonzalez, I., & Quirk, G. J. (2009). Sustained conditioned responses in prelimbic prefrontal neurons are correlated with fear expression and extinction failure. *The Journal of Neuroscience : The Official Journal of the Society for Neuroscience*, *29*(26), 8474–8482. https://doi.org/10.1523/JNEUROSCI.0378-09.2009

Cai, H., Haubensak, W., Anthony, T. E., & Anderson, D. J. (2014). Central amygdala PKC-δ+ neurons mediate the influence of multiple anorexigenic signals. *Nature Neuroscience*. https://doi.org/10.1038/nn.3767

Calhoon, G. G., & Tye, K. M. (2015). Resolving the neural circuits of anxiety. *Nature Neuroscience*, *18*(10), 1394–1404. https://doi.org/10.1038/nn.4101

Canteras, N. S. (2002). The medial hypothalamic defensive system: Hodological organization and functional implications. *Pharmacology Biochemistry and Behavior*, *71*(3), 481–491. https://doi.org/10.1016/S0091-3057(01)00685-2

Canteras, N. S., Simerly, R. B., & Swanson, L. W. (1995). Organization of projections from the medial nucleus of the amygdala: A PHAL study in the rat. *The Journal of Comparative Neurology*, *360*(2), 213–245. https://doi.org/10.1002/cne.903600203

Carlsen, J., & Heimer, L. (1988). The basolateral amygdaloid complex as a cortical-like structure. *Brain Research*, *441*(1–2), 377–380. https://doi.org/10.1016/0006-8993(88)91418-7

Cassell, M. D., Freedman, L. J., & Shi, C. (1999). The intrinsic organization of the central extended amygdala. *Annals of the New York Academy of Sciences*, *877*, 217–241. https://doi.org/10.1111/j.1749-6632.1999.tb09270.x

Castro, D. C., & Bruchas, M. R. (2019). A Motivational and Neuropeptidergic Hub: Anatomical and Functional Diversity within the Nucleus Accumbens Shell. *Neuron*, *102*(3), 529–552. https://doi.org/10.1016/j.neuron.2019.03.003

Cenquizca, L. A., & Swanson, L. W. (2006). Analysis of direct hippocampal cortical field CA1 axonal projections to diencephalon in the rat. *The Journal of Comparative Neurology*, *497*(1), 101–114. https://doi.org/10.1002/cne.20985

Cezario, A. F., Ribeiro-Barbosa, E. R., Baldo, M. V. C., & Canteras, N. S. (2008). Hypothalamic sites responding to predator threats - the role of the dorsal premammillary nucleus in unconditioned and conditioned antipredatory defensive behavior. *European Journal of Neuroscience*, *28*(5), 1003–1015. https://doi.org/10.1111/j.1460-9568.2008.06392.x

Chang, H., Saito, T., Ohiwa, N., Tateoka, M., Deocaris, C. C., Fujikawa, T., & Soya, H. (2007). Inhibitory effects of an orexin-2 receptor antagonist on orexin A- and stress-induced ACTH responses in conscious rats. *Neuroscience research*, *57*(3), 462–466. https://doi.org/10.1016/j.neures.2006.11.009

Chemelli, R., Willie, J., Sinton, C., Elmquist, J., Scammell, T., Lee, C., … Yanagisawa, M. (1999). Narcolepsy in orexin Knockout Mice : Molecular Genetics of Sleep Regulation. *Cell*, *98*(4), 437–451. https://doi.org/10.1016/S0092-8674(00)81973-X

Chen, M., & Bi, L. lin. (2018). Optogenetic Long-Term Depression Induction in the PVT-CeL Circuitry Mediates Decreased Fear Memory. *Molecular Neurobiology*. https://doi.org/10.1007/s12035-018-1407-z

Chen, S., & Su, H.-S. (1990). Afferent connections of the thalamic paraventricular and parataenial nuclei in the rat — a retrograde tracing study with iontophoretic application of Fluoro-Gold. *Brain Research*, *522*(1), 1–6. https://doi.org/10.1016/0006-8993(90)91570-7

Chen, X., Li, S., & Kirouac, G. J. (2014). Blocking of corticotrophin releasing factor receptor-1 during footshock attenuates context fear but not the upregulation of prepro-orexin mRNA in rats. *Pharmacology Biochemistry and Behavior*, *120*, 1–6. https://doi.org/10.1016/j.pbb.2014.01.013

Chen, X., Li, Y., Li, S., & Kirouac, G. J. (2012). Early fear as a predictor of avoidance in a rat model of post-traumatic stress disorder. *Behavioural Brain Research*, *226*(1), 112–117. https://doi.org/10.1016/j.bbr.2011.09.004

Chen, X., Wang, H., Lin, Z., Li, S., Li, Y., Bergen, H. T., … Kirouac, G. J. (2014). Orexins (hypocretins) contribute to fear and avoidance in rats exposed to a single episode of footshocks. *Brain Structure and Function*, *219*(6), 2103–2118. https://doi.org/10.1007/s00429-013-0626-3

Cheng, J., Wang, J., Ma, X., Ullah, R., Shen, Y., & Zhou, Y.-D. (2018). Anterior Paraventricular Thalamus to Nucleus Accumbens Projection Is Involved in Feeding Behavior in a Novel Environment. *Frontiers in Molecular Neuroscience*, *11*(June), 202. https://doi.org/10.3389/fnmol.2018.00202

Chisholm, A., Iannuzzi, J., Rizzo, D., Gonzalez, N., Fortin, É., Bumbu, A., … Shalev, U. (2019). The role of the paraventricular nucleus of the thalamus in the augmentation of heroin seeking induced by chronic food restriction. *Addiction Biology*, (November 2018), 1–11. https://doi.org/10.1111/adb.12708

Choi, E. A., Jean-Richard-dit-Bressel, P., Clifford, C. W. G., & McNally, G. P. (2019).

Paraventricular Thalamus Controls Behavior during Motivational Conflict. *The Journal of Neuroscience*, *39*(25), 4945–4958. https://doi.org/10.1523/JNEUROSCI.2480-18.2019

Choi, E. A., & McNally, G. P. (2017). Paraventricular Thalamus Balances Danger and Reward. *The Journal of Neuroscience*, *37*(11), 3018–3029. https://doi.org/10.1523/JNEUROSCI.3320-16.2017

Choudhary, A. G., Somalwar, A. R., Sagarkar, S., Rale, A., Sakharkar, A., Subhedar, N. K., & Kokare, D. M. (2018). CART neurons in the lateral hypothalamus communicate with the nucleus accumbens shell via glutamatergic neurons in paraventricular thalamic nucleus to modulate reward behavior. *Brain Structure and Function*, *223*(3), 1313–1328. https://doi.org/10.1007/s00429-017-1544-6

Christie, M. J., Summers, R. J., Stephenson, J. A., Cook, C. J., & Beart, P. M. (1987). Excitatory amino acid projections to the nucleus accumbens septi in the rat: A retrograde transport study utilizingd[3H]aspartate and [3H]GABA. *Neuroscience*, *22*(2), 425–439. https://doi.org/10.1016/0306-4522(87)90345-9

Christoffel, D. J., Golden, S. a, Walsh, J. J., Guise, K. G., Heshmati, M., Friedman, A. K., … Russo, S. J. (2015). Excitatory transmission at thalamo-striatal synapses mediates susceptibility to social stress. *Nature Neuroscience*, *18*(7), 6–11. https://doi.org/10.1038/nn.4034

Ciocchi, S., Herry, C., Grenier, F., Wolff, S. B. E., Letzkus, J. J., Vlachos, I., … Lüthi, A. (2010). Encoding of conditioned fear in central amygdala inhibitory circuits. *Nature*, *468*(7321), 277–282. https://doi.org/10.1038/nature09559

Clark, A., Leroy, F., Martyniuk, K. M., Feng, W., McManus, E., Bailey, M., … Kellendonk, C. (2017). Dopamine D2 Receptors in the Paraventricular Thalamus Attenuate Cocaine Locomotor Sensitization. *Eneuro*, *4*(October), ENEURO.0227-17.2017. https://doi.org/10.1523/ENEURO.0227-17.2017

Conte, W. L., Kamishina, H., Reep, R. L. (2009). Multiple neuroanatomical tract-tracing using fluorescent Alexa Fluor conjugates of cholera toxin subunit B in rats. *Nature Protocols*, *4*(8), 1157–1166. https://doi.org/10.1038/nprot.2009.93

Corcoran, K. A., & Quirk, G. J. (2007). Activity in prelimbic cortex is necessary for the expression of learned, but not innate, fears. *Journal of Neuroscience*, *27*(4), 840–844. https://doi.org/10.1523/JNEUROSCI.5327-06.2007

Couceyro, P. R., Koylu, E. O., & Kuhar, M. J. (1997). Further studies on the anatomical distribution of CART by in situ hybridization. *Journal of Chemical Neuroanatomy*. https://doi.org/10.1016/S0891-0618(97)00212-3

Courtin, J., Bienvenu, T. C. M., Einarsson, E. Ö., & Herry, C. (2013). Medial prefrontal cortex neuronal circuits in fear behavior. *Neuroscience*, *240*(2013), 219–242. https://doi.org/10.1016/j.neuroscience.2013.03.001

Covington, H. E., Lobo, M. K., Maze, I., Vialou, V., Hyman, J. M., Zaman, S., … Nestler, E. J. (2010). Antidepressant Effect of Optogenetic Stimulation of the Medial Prefrontal Cortex. *Journal of Neuroscience*, *30*(48), 16082–16090. https://doi.org/10.1523/JNEUROSCI.1731-

10.2010

Cryan, J. F., & Holmes, A. (2005). The ascent of mouse: advances in modelling human depression and anxiety. *Nature Reviews Drug Discovery*, *4*(9), 775–790. https://doi.org/10.1038/nrd1825

da Cunha, I. C., Lopes, A. P. F., Steffens, S. M., Ferraz, A., Vargas, J. C., de Lima, T. C. M., … Faria, M. S. (2008). The microinjection of AMPA receptor antagonist into the accumbens shell, but not into the accumbens core, induces anxiolysis in an animal model of anxiety. *Behavioural Brain Research*, *188*(1), 91–99. https://doi.org/10.1016/j.bbr.2007.10.023

Danielsen, E. H., Magnuson, D. J., & Gray, T. S. (1989). The central amygdaloid nucleus innervation of the dorsal vagal complex in rat: a Phaseolus vulgaris leucoagglutinin lectin anterograde tracing study. *Brain Research Bulletin*, *22*(4), 705–715. https://doi.org/10.1016/0361-9230(89)90090-7

Davis, M., Walker, D. L., Miles, L., & Grillon, C. (2010). Phasic vs sustained fear in rats and humans: role of the extended amygdala in fear vs anxiety. *Neuropsychopharmacology : Official Publication of the American College of Neuropsychopharmacology*, *35*(1), 105–135. https://doi.org/10.1038/npp.2009.109

de Lecea, L., Kilduff, T. S., Peyron, C., Gao, X. B., Foye, P. E., Danielson, P. E., … Sutcliffe, J. G. (1998). The hypocretins: Hypothalamus-specific peptides with neuroexcitatory activity. *Proceedings of the National Academy of Sciences*, *95*(1), 322–327. https://doi.org/10.1073/pnas.95.1.322

de Olmos, J. S., & Heimer, L. (1999). The concepts of the ventral striatopallidal system and extended amygdala. *Annals of the New York Academy of Sciences*, *877*, 1–32. https://doi.org/10.1111/j.1749-6632.1999.tb09258.x

Deutch, A. Y., Bubser, M., & Young, C. D. (1998). Psychostimulant-Induced Fos Protein Expression in the Thalamic Paraventricular Nucleus. *The Journal of Neuroscience*, *18*(24), 10680–10687. https://doi.org/10.1523/JNEUROSCI.18-24-10680.1998

Do-Monte, F. H., Manzano-Nieves, G., Quiñones-Laracuente, K., Ramos-Medina, L., & Quirk, G. J. (2015). Revisiting the role of infralimbic cortex in fear extinction with optogenetics. *The Journal of Neuroscience : The Official Journal of the Society for Neuroscience*, *35*(8), 3607–3615. https://doi.org/10.1523/JNEUROSCI.3137-14.2015

Do-Monte, F. H., Minier-Toribio, A., Quiñones-Laracuente, K., Medina-Colón, E. M., & Quirk, G. J. (2017). Thalamic Regulation of Sucrose Seeking during Unexpected Reward Omission. *Neuron*, *94*(2), 388-400.e4. https://doi.org/10.1016/j.neuron.2017.03.036

Do-Monte, F. H., Quiñones-Laracuente, K., & Quirk, G. J. (2015). A temporal shift in the circuits mediating retrieval of fear memory. *Nature*, *519*(7544), 460–463. https://doi.org/10.1038/nature14030

Dong, H. W., Petrovich, G. D., & Swanson, L. W. (2000). Organization of projections from the juxtacapsular nucleus of the BST: A PHAL study in the rat. *Brain Research*, *859*(1), 1–14. https://doi.org/10.1016/S0006-8993(99)02246-5

Dong, H. W., Petrovich, G. D., Watts, A. G., & Swanson, L. W. (2001). Basic organization of

projections from the oval and fusiform nuclei of the bed nuclei of the stria terminalis in adult rat brain. *Journal of Comparative Neurology*, *436*(4), 430–455. https://doi.org/10.1002/cne.1079

Dong, H. W., & Swanson, L. W. (2004a). Organization of Axonal Projections from the Anterolateral Area of the Bed Nuclei of the Stria Terminalis. *Journal of Comparative Neurology*, *468*(2), 277–298. https://doi.org/10.1002/cne.10949

Dong, H. W., & Swanson, L. W. (2004b). Projections from Bed Nuclei of the Stria Terminalis, Posterior Division: Implications for Cerebral Hemisphere Regulation of Defensive and Reproductive Behaviors. *Journal of Comparative Neurology*, *474*(4), 603–604. https://doi.org/10.1002/cne.20002

Dong, H. W., & Swanson, L. W. (2006). Projections from bed nuclei of the stria terminalis, anteromedial area: Cerebral hemisphere integration of neuroendocrine, autonomic, and behavioral aspects of energy balance. *Journal of Comparative Neurology*, *494*(1), 142–178. https://doi.org/10.1002/cne.20788

Dong, X., Li, S., & Kirouac, G. J. (2017). Collateralization of projections from the paraventricular nucleus of the thalamus to the nucleus accumbens, bed nucleus of the stria terminalis, and central nucleus of the amygdala. *Brain Structure and Function*, *222*(9), 3927–3943. https://doi.org/10.1007/s00429-017-1445-8

Dong, X., Li, Y., & Kirouac, G. J. (2015). Blocking of orexin receptors in the paraventricular nucleus of the thalamus has no effect on the expression of conditioned fear in rats. *Frontiers in Behavioral Neuroscience*, *9*(June), 161. https://doi.org/10.3389/fnbeh.2015.00161

Dragunow, M., & Faull, R. (1989). The use of cFos as a metabolic marker in neuronal pathway tracing. *Journal of Neuroscience Methods*, *29*(3), 261–265. https://doi.org/10.1016/0165-0270(89)90150-7

Duvarci, S., & Pare, D. (2014). Amygdala microcircuits controlling learned fear. *Neuron*, *82*(5), 966–980. https://doi.org/10.1016/j.neuron.2014.04.042

Ebling, F. J. P., Maywood, E. S., Humby, T., & Hastings, M. H. (1992). Circadian and Photoperiodic Time Measurement in Male Syrian Hamsters Following Lesions of the Melatonin-Binding Sites of the Paraventricular Thalamus. *Journal of Biological Rhythms*, *7*(3), 241–254. https://doi.org/10.1177/074873049200700305

España, R. A., Valentino, R. J., & Berridge, C. W. (2003). Fos immunoreactivity in hypocretin-synthesizing and hypocretin-1 receptor-expressing neurons: Effects of diurnal and nocturnal spontaneous waking, stress and hypocretin-1 administration. *Neuroscience*. https://doi.org/10.1016/S0306-4522(03)00334-8

Etkin, A., & Wager, T. D. (2007). Functional neuroimaging of anxiety: a meta-analysis of emotional processing in PTSD, social anxiety disorder, and specific phobia. *The American Journal of Psychiatry*, *164*(10), 1476–1488. https://doi.org/10.1176/appi.ajp.2007.07030504

Eysenck, M. W., Derakshan, N., Santos, R., & Calvo, M. G. (2007). Anxiety and cognitive performance: Attentional control theory. *Emotion*, *7*(2), 336–353. https://doi.org/10.1037/1528-3542.7.2.336

Fadok, J. P., Krabbe, S., Markovic, M., Courtin, J., Xu, C., Massi, L., … Lüthi, A. (2017). A competitive inhibitory circuit for selection of active and passive fear responses. *Nature*, *542*(7639), 96–100. https://doi.org/10.1038/nature21047

Fadok, J. P., Markovic, M., Tovote, P., & Lüthi, A. (2018). New perspectives on central amygdala function. *Current Opinion in Neurobiology*, *49*, 141–147. https://doi.org/10.1016/j.conb.2018.02.009

Fanselow, M. S. (1980). Conditional and unconditional components of post-shock freezing. *The Pavlovian Journal of Biological Science : Official Journal of the Pavlovian*, *15*(4), 177–182. https://doi.org/10.1007/BF03001163

Fanselow, M. S. (2018). The role of learning in threat imminence and defensive behaviors. *Current Opinion in Behavioral Sciences*, *24*, 44–49. https://doi.org/10.1016/j.cobeha.2018.03.003

Fanselow, M. S., & Dong, H. W. (2010). Are the Dorsal and Ventral Hippocampus Functionally Distinct Structures? *Neuron*, *65*(1), 7–19. https://doi.org/10.1016/j.neuron.2009.11.031

Felix-Ortiz, A. C., Beyeler, A., Seo, C., Leppla, C. A., Wildes, C. P., & Tye, K. M. (2013). BLA to vHPC Inputs Modulate Anxiety-Related Behaviors. *Neuron*, *79*(4), 658–664. https://doi.org/10.1016/j.neuron.2013.06.016

Fendt, M., & Fanselow, M. S. (1999). The neuroanatomical and neurochemical basis of conditioned fear. *Neuroscience and Biobehavioral Reviews*, *23*(5), 743–760. https://doi.org/10.1016/s0149-7634(99)00016-0

Fernando, A. B. P., Murray, J. E., & Milton, A. L. (2013). The amygdala: securing pleasure and avoiding pain. *Frontiers in Behavioral Neuroscience*, *7*, 190. https://doi.org/10.3389/fnbeh.2013.00190

Flores, Á., Saravia, R., Maldonado, R., & Berrendero, F. (2015). Orexins and fear: Implications for the treatment of anxiety disorders. *Trends in Neurosciences*, *38*(9), 550–559. https://doi.org/10.1016/j.tins.2015.06.005

Floresco, S. B. (2015). The Nucleus Accumbens: An Interface Between Cognition, Emotion, and Action. *Annual Review of Psychology*, *66*(1), 25–52. https://doi.org/10.1146/annurev-psych-010213-115159

Furlong, T. M., Vianna, D. M. L., Liu, L., & Carrive, P. (2009). Hypocretin/orexin contributes to the expression of some but not all forms of stress and arousal. *European Journal of Neuroscience*. https://doi.org/10.1111/j.1460-9568.2009.06952.x

Fyer, A. J. (1998). Current approaches to etiology and pathophysiology of specific phobia. *Biological Psychiatry*, *44*(12), 1295–1304. https://doi.org/10.1016/S0006-3223(98)00274-1

Gao, C., Leng, Y., Ma, J., Rooke, V., Rodriguez-Gonzalez, S., Ramakrishnan, C., … Penzo, M. A. (2020). Two genetically, anatomically and functionally distinct cell types segregate across anteroposterior axis of paraventricular thalamus. *Nature Neuroscience*. https://doi.org/10.1038/s41593-019-0572-3

Gehrlach, D. A., Dolensek, N., Klein, A. S., Roy Chowdhury, R., Matthys, A., Junghänel, M., …

Gogolla, N. (2019). Aversive state processing in the posterior insular cortex. *Nature Neuroscience*, *22*(9), 1424–1437. https://doi.org/10.1038/s41593-019-0469-1

Gomez, J. L., Bonaventura, J., Lesniak, W., Mathews, W. B., Sysa-shah, P., Rodriguez, L. A., … Michaelides, M. (2017). Chemogenetics Revealed: Dreadd Occupancy and Activation Via Converted Clozapine. *Science*, *507*(August), 503–507. https://doi.org/10.1126/science.aan2475

Griessner, J., Pasieka, M., Böhm, V., Grössl, F., Kaczanowska, J., Pliota, P., … Haubensak, W. (2018). Central amygdala circuit dynamics underlying the benzodiazepine anxiolytic effect. *Molecular Psychiatry*. https://doi.org/10.1038/s41380-018-0310-3

Groenewegen, H. J., & Berendse, H. W. (1994). The specificity of the "nonspecific" midline and intralaminar thalamic nuclei. *Trends in Neurosciences*, *17*(2), 52–57. https://doi.org/10.1016/0166-2236(94)90074-4

Groenewegen, H. J., der Zee, E. V.-V., te Kortschot, A., & Witter, M. P. (1987). Organization of the projections from the subiculum to the ventral striatum in the rat. A study using anterograde transport of Phaseolus vulgaris leucoagglutinin. *Neuroscience*, *23*(1), 103–120. https://doi.org/10.1016/0306-4522(87)90275-2

Groenewegen, H. J., & Witter, M. P. (2004). Thalamus. In G. Paxinos (Ed.), *The rat nervous system* (3th ed., pp. 407–453). Academic Press.

Groenewegen, H. J., Wright, C. I., Beijer, A. V. J., & Voorn, P. (1999). Convergence and segregation of ventral striatal inputs and outputs. *Annals of the New York Academy of Sciences*, *877*, 49–63. https://doi.org/10.1111/j.1749-6632.1999.tb09260.x

Groenewegen, H. J., Wright, C. I., & Uylings, H. B. M. (1997). The anatomical relationships of the prefrontal cortex with limbic structures and the basal ganglia. *Journal of Psychopharmacology (Oxford, England)*, *11*(2), 99–106. https://doi.org/10.1177/026988119701100202

Gross, C. T., & Canteras, N. S. (2012). The many paths to fear. *Nature Reviews Neuroscience*, *13*(9), 651–658. https://doi.org/10.1038/nrn3301

Gross, J. J., & Muñoz, R. F. (1995). Emotion Regulation and Mental Health. *Clinical Psychology: Science and Practice*, *2*(2), 151–164. https://doi.org/10.1111/j.1468-2850.1995.tb00036.x

Grupe, D. W., & Nitschke, J. B. (2013). Uncertainty and anticipation in anxiety: An integrated neurobiological and psychological perspective. *Nature Reviews Neuroscience*, *14*(7), 488–501. https://doi.org/10.1038/nrn3524

Gunaydin, L. A., Grosenick, L., Finkelstein, J. C., Kauvar, I. V., Fenno, L. E., Adhikari, A., … Deisseroth, K. (2014). Natural neural projection dynamics underlying social behavior. *Cell*, *157*(7), 1535–1551. https://doi.org/10.1016/j.cell.2014.05.017

Gunaydin, L. A., & Kreitzer, A. C. (2016). Cortico–Basal Ganglia Circuit Function in Psychiatric Disease. *Annual Review of Physiology*, *78*(1), 327–350. https://doi.org/10.1146/annurev-physiol-021115-105355

Hale, M. W., Hay-Schmidt, A., Mikkelsen, J. D., Poulsen, B., Shekhar, A., & Lowry, C. A. (2008). Exposure to an open-field arena increases cFos expression in a distributed anxiety-related system projecting to the basolateral amygdaloid complex. *Neuroscience*, *155*(3), 659–672. https://doi.org/10.1016/j.neuroscience.2008.05.054

Haller, J., Bakos, N. (2002). Stress-induced social avoidance: a new model of stress-induced anxiety? *Physiology & Behavior*, *77*(2002), 327–332.

Hasler, G., Fromm, S., Alvarez, R. P., Luckenbaugh, D. A., Drevets, W. C., & Grillon, C. (2007). Cerebral blood flow in immediate and sustained anxiety. *Journal of Neuroscience*, *27*(23), 6313–6319. https://doi.org/10.1523/JNEUROSCI.5369-06.2007

Haubensak, W., Kunwar, P. S., Cai, H., Ciocchi, S., Wall, N. R., Ponnusamy, R., … Anderson, D. J. (2010). Genetic dissection of an amygdala microcircuit that gates conditioned fear. *Nature*, *468*(7321), 270–276. https://doi.org/10.1038/nature09553

Heidbreder, C. A., & Groenewegen, H. J. (2003). The medial prefrontal cortex in the rat: Evidence for a dorso-ventral distinction based upon functional and anatomical characteristics. *Neuroscience and Biobehavioral Reviews*, *27*(6), 555–579. https://doi.org/10.1016/j.neubiorev.2003.09.003

Heimer, L., Alheid, G. F., de Olmos, J. S., Groenewegen, H. J., Suzanne, N. H., Richard, E. H., & Zahm, D. S. (1997). The accumbens: beyond the core-shell dichotomy. *The Journal of Neuropsychiatry and Clinical Neurosciences*, *9*(3), 354–381. https://doi.org/10.1176/jnp.9.3.354

Heimer, L., & Van Hoesen, G. W. (2006). The limbic lobe and its output channels: Implications for emotional functions and adaptive behavior. *Neuroscience and Biobehavioral Reviews*, *30*(2), 126–147. https://doi.org/10.1016/j.neubiorev.2005.06.006

Heimer, L., Van Hoesen, G. W., Trimble, M., & Zahm, D. S. (2008). *Anatomy of Neuropsychiatry*. Elsevier. https://doi.org/10.1016/B978-0-12-374239-1.X5001-5

Herrera, C. G., Cadavieco, M. C., Jego, S., Ponomarenko, A., Korotkova, T., & Adamantidis, A. (2016). Hypothalamic feedforward inhibition of thalamocortical network controls arousal and consciousness. *Nature Neuroscience*, *19*(2), 290–298. https://doi.org/10.1038/nn.4209

Herry, C., & Johansen, J. P. (2014). Encoding of fear learning and memory in distributed neuronal circuits. *Nature Neuroscience*, *17*(12), 1644–1654. https://doi.org/10.1038/nn.3869

Herry, C., & Mons, N. (2004). Resistance to extinction is associated with impaired immediate early gene induction in medial prefrontal cortex and amygdala. *European Journal of Neuroscience*, *20*(3), 781–790. https://doi.org/10.1111/j.1460-9568.2004.03542.x

Heydendael, W., Sharma, K., Iyer, V., Luz, S., Piel, D., Beck, S., & Bhatnagar, S. (2011). Orexins/hypocretins act in the posterior paraventricular thalamic nucleus during repeated stress to regulate facilitation to novel stress. *Endocrinology*, *152*(12), 4738–4752. https://doi.org/10.1210/en.2011-1652

Hofmann, S. G., & Hay, A. C. (2018). Rethinking avoidance: Toward a balanced approach to avoidance in treating anxiety disorders. *Journal of Anxiety Disorders*.

https://doi.org/10.1016/j.janxdis.2018.03.004

Hoover, W. B., & Vertes, R. P. (2007). Anatomical analysis of afferent projections to the medial prefrontal cortex in the rat. *Brain Structure and Function*, *212*(2), 149–179. https://doi.org/10.1007/s00429-007-0150-4

Hopkins, D. A., & Holstege, G. (1978). Amygdaloid projections to the mesencephalon, pons and medulla oblongata in the cat. *Experimental Brain Research*, *32*(4). https://doi.org/10.1007/BF00239551

Hsu, D. T., Kirouac, G. J., Zubieta, J., & Bhatnagar, S. (2014). Contributions of the paraventricular thalamic nucleus in the regulation of stress, motivation, and mood. *Frontiers in Behavioral Neuroscience*, *8*(March), 1–10. https://doi.org/10.3389/fnbeh.2014.00073

Hua, R., Wang, X., Chen, X., Wang, X., Huang, P., Li, P., … Li, H. (2018). Calretinin Neurons in the Midline Thalamus Modulate Starvation-Induced Arousal. *Current Biology*, *28*(24), 3948-3959.e4. https://doi.org/10.1016/j.cub.2018.11.020

Hurley, K. M., Herbert, H., Moga, M. M., & Saper, C. B. (1991). Efferent projections of the infralimbic cortex of the rat. *Journal of Comparative Neurology*. https://doi.org/10.1002/cne.903080210

Ilg, A.-K., Enkel, T., Bartsch, D., & Bähner, F. (2018). Behavioral Effects of Acute Systemic Low-Dose Clozapine in Wild-Type Rats: Implications for the Use of DREADDs in Behavioral Neuroscience. *Frontiers in Behavioral Neuroscience*, *12*(August). https://doi.org/10.3389/fnbeh.2018.00173

Insel, T. R., & Quirion, R. (2005). Psychiatry as a clinical neuroscience discipline. *Journal of the American Medical Association*, *294*(17), 2221–2224. https://doi.org/10.1001/jama.294.17.2221

Isogai, Y., Si, S., Pont-Lezica, L., Tan, T., Kapoor, V., Murthy, V. N., & Dulac, C. (2011). Molecular organization of vomeronasal chemoreception. *Nature*, *478*(7368), 241–245. https://doi.org/10.1038/nature10437

Janak, P. H., & Tye, K. M. (2015). From circuits to behaviour in the amygdala. *Nature*, *517*(7534), 284–292. https://doi.org/10.1038/nature14188

Jasmin, L., Granato, A., & Ohara, P. T. (2004). Rostral agranular insular cortex and pain areas of the central nervous system: A tract-tracing study in the rat. *The Journal of Comparative Neurology*, *468*(3), 425–440. https://doi.org/10.1002/cne.10978

Kask, A., Schiöth, H. B., Mutulis, F., Wikberg, J. E. S., & Rägo, L. (2000). Anorexigenic cocaine- and amphetamine-regulated transcript peptide intensifies fear reactions in rats. *Brain Research*, *857*(1–2), 283–285. https://doi.org/10.1016/S0006-8993(99)02383-5

Kawaguchi, A., Nemoto, K., Nakaaki, S., Kawaguchi, T., Kan, H., Arai, N., … Akechi, T. (2016). Insular volume reduction in patients with social anxiety disorder. *Frontiers in Psychiatry*, *7*(JAN), 1–7. https://doi.org/10.3389/fpsyt.2016.00003

Kawaguchi, Y. (1993). Physiological, morphological, and histochemical characterization of three classes of interneurons in rat neostriatum. *The Journal of Neuroscience*, *13*(11), 4908–4923.

https://doi.org/10.1523/JNEUROSCI.13-11-04908.1993

Kessler, R. C., Berglund, P., Demler, O., Jin, R., Merikangas, K. R., & Walters, E. E. (2005). Lifetime prevalence and age-of-onset distributions of DSM-IV disorders in the national comorbidity survey replication. *Archives of General Psychiatry*, *62*(6), 593–602. https://doi.org/10.1001/archpsyc.62.6.593

Kim, J., Zhang, X., Muralidhar, S., LeBlanc, S. A., & Tonegawa, S. (2017). Basolateral to Central Amygdala Neural Circuits for Appetitive Behaviors. *Neuron*, *93*(6), 1464-1479.e5. https://doi.org/10.1016/j.neuron.2017.02.034

Kim, S. Y., Adhikari, A., Lee, S. Y., Marshel, J. H., Kim, C. K., Mallory, C. S., … Deisseroth, K. (2013). Diverging neural pathways assemble a behavioural state from separable features in anxiety. *Nature*, *496*(7444), 219–223. https://doi.org/10.1038/nature12018

Kirouac, G. J. (2015). Placing the paraventricular nucleus of the thalamus within the brain circuits that control behavior. *Neuroscience & Biobehavioral Reviews*, *56*, 315–329. https://doi.org/10.1016/j.neubiorev.2015.08.005

Kirouac, G. J., Parsons, M. P., & Li, S. (2005). Orexin (hypocretin) innervation of the paraventricular nucleus of the thalamus. *Brain Research*, *1059*(2), 179–188. https://doi.org/10.1016/j.brainres.2005.08.035

Kirouac, G. J., Parsons, M. P., & Li, S. (2006). Innervation of the paraventricular nucleus of the thalamus from cocaine- and amphetamine-regulated transcript (CART) containing neurons of the hypothalamus. *The Journal of Comparative Neurology*, *497*(2), 155–165. https://doi.org/10.1002/cne.20971

Kjelstrup, K. G., Tuvnes, F. A., Steffenach, H.-A., Murison, R., Moser, E. I., & Moser, M.-B. (2002). Reduced fear expression after lesions of the ventral hippocampus. *Proceedings of the National Academy of Sciences*, *99*(16), 10825–10830. https://doi.org/10.1073/pnas.152112399

Klumpers, F., & Kroes, M. C. W. (2019). Roles of the amygdala and basal forebrain in defense: a Reply to Lucyk Et al. and implications for defensive action. *Neuropsychology Review*, 10–13. https://doi.org/10.1007/s11065-019-09401-y

Knapska, E., & Maren, S. (2009). Reciprocal patterns of cFos expression in the medial prefrontal cortex and amygdala after extinction and renewal of conditioned fear. *Learning & Memory*, *16*(8), 486–493. https://doi.org/10.1101/lm.1463909

Kolaj, M., Doroshenko, P., Yan Cao, X., Coderre, E., & Renaud, L. P. (2007). Orexin-induced modulation of state-dependent intrinsic properties in thalamic paraventricular nucleus neurons attenuates action potential patterning and frequency. *Neuroscience*, *147*(4), 1066–1075. https://doi.org/10.1016/j.neuroscience.2007.05.018

Kolaj, Miloslav, Zhang, L., Hermes, M. L. H. J., & Renaud, L. P. (2014). Intrinsic properties and neuropharmacology of midline paraventricular thalamic nucleus neurons. *Frontiers in Behavioral Neuroscience*, *8*(APR), 1–15. https://doi.org/10.3389/fnbeh.2014.00132

Kollack-Walker, Don, Watson, & Akil. (1999). Differential Expression of c- fos mRNA Within Neurocircuits of Male Hamsters Exposed to Acute or Chronic Defeat. *Journal of*

Neuroendocrinology, *11*(7), 547–559. https://doi.org/10.1046/j.1365-2826.1999.00354.x

Kondoh, K., Lu, Z., Ye, X., Olson, D. P., Lowell, B. B., & Buck, L. B. (2016). A specific area of olfactory cortex involved in stress hormone responses to predator odours. *Nature*, *532*(7597), 103–106. https://doi.org/10.1038/nature17156

Koylu, E. O., Couceyro, P. R., Lambert, P. D., & Kuhar, M. J. (1998). Cocaine- and amphetamine-regulated transcript peptide immunohistochemical localization in the rat brain. *Journal of Comparative Neurology*. https://doi.org/10.1002/(SICI)1096-9861(19980202)391:1<115::AID-CNE10>3.0.CO;2-X

Krout, K. E., Belzer, R. E., & Loewy, A. D. (2002). Brainstem projections to midline and intralaminar thalamic nuclei of the rat. *Journal of Comparative Neurology*, *448*(1), 53–101. https://doi.org/10.1002/cne.10236

Krout, K. E., & Loewy, A. D. (2000a). Parabrachial nucleus projections to midline and intralaminar thalamic nuclei of the rat. *Journal of Comparative Neurology*, *428*(3), 475–494. https://doi.org/10.1002/1096-9861(20001218)428:3<475::AID-CNE6>3.0.CO;2-9

Krout, K. E., & Loewy, A. D. (2000b). Periaqueductal gray matter projections to midline and intralaminar thalamic nuclei of the rat. *Journal of Comparative Neurology*, *424*(1), 111–141. https://doi.org/10.1002/1096-9861(20000814)424:1<111::AID-CNE9>3.0.CO;2-3

Kukkonen, J. P., & Leonard, C. S. (2014). Orexin/hypocretin receptor signalling cascades. *British Journal of Pharmacology*, *171*(2), 314‐331. https://doi.org/10.1111/bph.12324

Lacroix, L., Spinelli, S., Heidbreder, C. A., & Feldon, J. (2000). Differential role of the medial and lateral prefrontal cortices in fear and anxiety. *Behavioral Neuroscience*, *114*(6), 1119–1130. https://doi.org/10.1037/0735-7044.114.6.1119

Laird, K. T., Siddarth, P., Krause-Sorio, B., Kilpatrick, L., Milillo, M., Aguilar, Y., … Lavretsky, H. (2019). Anxiety symptoms are associated with smaller insular and orbitofrontal cortex volumes in late-life depression. *Journal of Affective Disorders*, *256*(November 2018), 282–287. https://doi.org/10.1016/j.jad.2019.05.066

LeDoux, J. E. (1998). Fear and the brain: where have we been, and where are we going? *Biological Psychiatry*, *44*(12), 1229–1238. https://doi.org/10.1016/s0006-3223(98)00282-0

LeDoux, J. E. (2000). Emotion Circuits in the Brain. *Annual Review of Neuroscience*, *23*(1), 155–184. https://doi.org/10.1146/annurev.neuro.23.1.155

LeDoux, J. E. (2003). The emotional brain, fear, and the amygdala. *Cellular and Molecular Neurobiology*, *23*(4–5), 727–738. https://doi.org/10.1023/A:1025048802629

LeDoux, J. E. (2012). Rethinking the emotional brain. *Neuron*, *73*(4), 653–676. https://doi.org/10.1016/j.neuron.2012.02.004

LeDoux, J. E., Iwata, J., Cicchetti, P., & Reis, D. J. (1988). Different projections of the central amygdaloid nucleus mediate autonomic and behavioral correlates of conditioned fear. *Journal of Neuroscience*. https://doi.org/10.1523/jneurosci.08-07-02517.1988

Lee, Y., & Davis, M. (1997). Role of the hippocampus, the bed nucleus of the stria terminalis,

and the amygdala in the excitatory effect of corticotropin-releasing hormone on the acoustic startle reflex. *The Journal of Neuroscience : The Official Journal of the Society for Neuroscience*, *17*(16), 6434–6446. https://doi.org/10.1523/jneurosci.4012-11.2012

Levita, L., Hoskin, R., & Champi, S. (2012). Avoidance of harm and anxiety: A role for the nucleus accumbens. *NeuroImage*, *62*(1), 189–198. https://doi.org/10.1016/j.neuroimage.2012.04.059

Li, Haohong, Penzo, M. A., Taniguchi, H., Kopec, C. D., Huang, Z. J., & Li, B. (2013). Experience-dependent modification of a central amygdala fear circuit. *Nature Neuroscience*, *16*(3), 332–339. https://doi.org/10.1038/nn.3322

Li, Hui, Chen, L., Li, P., Wang, X., & Zhai, H. (2014). Insular muscarinic signaling regulates anxiety-like behaviors in rats on the elevated plus-maze. *Behavioural Brain Research*, *270*, 256–260. https://doi.org/10.1016/j.bbr.2014.05.017

Li, S., Dong, X., & Kirouac, G. J. (2019). Extensive divergence of projections from neurons in the paraventricular nucleus of the thalamus to widespread regions of the forebrain. In *2019 Neuroscience Meeting Planner*. Chicago, IL: Society for Neuroscience.

Li, S., & Kirouac, G. J. (2008). Projections from the paraventricular nucleus of the thalamus to the forebrain, with special emphasis on the extended amygdala. *The Journal of Comparative Neurology*, *506*(2), 263–287. https://doi.org/10.1002/cne.21502

Li, S., & Kirouac, G. J. (2012). Sources of inputs to the anterior and posterior aspects of the paraventricular nucleus of the thalamus. *Brain Structure & Function*, *217*(2), 257–273. https://doi.org/10.1007/s00429-011-0360-7

Li, S., Shi, Y., & Kirouac, G. J. (2014). The hypothalamus and periaqueductal gray are the sources of dopamine fibers in the paraventricular nucleus of the thalamus in the rat. *Frontiers in Neuroanatomy*, *8*(November), 136. https://doi.org/10.3389/fnana.2014.00136

Li, X. B., Inoue, T., Nakagawa, S., & Koyama, T. (2004). Effect of mediodorsal thalamic nucleus lesion on contextual fear conditioning in rats. *Brain Research*, *1008*(2), 261–272. https://doi.org/10.1016/j.brainres.2004.02.038

Li, Y., Dong, X., Li, S., & Kirouac, G. J. (2014). Lesions of the posterior paraventricular nucleus of the thalamus attenuate fear expression. *Frontiers in Behavioral Neuroscience*, *8*(March), 94. https://doi.org/10.3389/fnbeh.2014.00094

Li, Y., Li, S., Sui, N., & Kirouac, G. J. (2009). Orexin-A acts on the paraventricular nucleus of the midline thalamus to inhibit locomotor activity in rats. *Pharmacology Biochemistry and Behavior*, *93*(4), 506–514. https://doi.org/10.1016/j.pbb.2009.06.017

Li, Y., Li, S., Wei, C., Wang, H., Sui, N., & Kirouac, G. J. (2010a). Changes in emotional behavior produced by orexin microinjections in the paraventricular nucleus of the thalamus. *Pharmacology, Biochemistry, and Behavior*, *95*(1), 121–128. https://doi.org/10.1016/j.pbb.2009.12.016

Li, Y., Li, S., Wei, C., Wang, H., Sui, N., & Kirouac, G. J. (2010b). Orexins in the paraventricular nucleus of the thalamus mediate anxiety-like responses in rats. *Psychopharmacology*, *212*(2), 251–265. https://doi.org/10.1007/s00213-010-1948-y

Li, Y., Wang, H., Qi, K., Chen, X., Li, S., Sui, N., & Kirouac, G. J. (2011). Orexins in the midline thalamus are involved in the expression of conditioned place aversion to morphine withdrawal. *Physiology & Behavior*, *102*(1), 42–50. https://doi.org/10.1016/j.physbeh.2010.10.006

Ligorio, M., Descarries, L., & Warren, R. A. (2009). Cholinergic innervation and thalamic input in rat nucleus accumbens. *Journal of Chemical Neuroanatomy*, *37*(1), 33–45. https://doi.org/10.1016/j.jchemneu.2008.08.003

Likhtik, E., Stujenske, J. M., Topiwala, M. A., Harris, A. Z., and Gordon, J. A. (2014). Prefrontal entrainment of amygdala activity signals safety in learned fear and innate anxiety. *Nature Neuroscience, 17*(1), 106–113. https://doi.org/10.1038/nn.3582

Litvin, Y., Pentkowski, N. S., Pobbe, R. L.,Blanchard, D. C. & Blanchard, R. J. (2008). Unconditioned models of fear and anxiety in Handbook of Anxiety and Fear (eds Blanchard, R. J.,Blanchard, D. C., Griebel, G. & Nutt, D.) 81–99.

Lopes, A. P. F., Ganzer, L., Borges, A. C., Kochenborger, L., Januário, A. C., Faria, M. S., … Paschoalini, M. A. (2012). Effects of GABA ligands injected into the nucleus accumbens shell on fear/anxiety-like and feeding behaviours in food-deprived rats. *Pharmacology Biochemistry and Behavior*, *101*(1), 41–48. https://doi.org/10.1016/j.pbb.2011.11.013

Luppi, P. H., Fort, P., & Jouvet, M. (1990). Iontophoretic application of unconjugated cholera toxin B subunit (CTb) combined with immunohistochemistry of neurochemical substances: a method for transmitter identification of retrogradely labeled neurons. *Brain Research*. https://doi.org/10.1016/0006-8993(90)90131-T

Maimon, B. E., Sparks, K., Srinivasan, S., Zorzos, A. N., & Herr, H. M. (2018). Spectrally distinct channelrhodopsins for two-colour optogenetic peripheral nerve stimulation. *Nature Biomedical Engineering*, *2*(7), 485–496. https://doi.org/10.1038/s41551-018-0255-5

Marcus, J. N., Aschkenasi, C. J., Lee, C. E., Chemelli, R. M., Saper, C. B., Yanagisawa, M., & Elmquist, J. K. (2001). Differential expression of Orexin receptors 1 and 2 in the rat brain. *Journal of Comparative Neurology*. https://doi.org/10.1002/cne.1190

Marek, R., Jin, J., Goode, T. D., Giustino, T. F., Wang, Q., Acca, G. M., … Sah, P. (2018). Hippocampus-driven feed-forward inhibition of the prefrontal cortex mediates relapse of extinguished fear. *Nature Neuroscience, 21*(3), 384–392. https://doi.org/10.1038/s41593-018-0073-9

Marek, R., Sun, Y., & Sah, P. (2019). Neural circuits for a top-down control of fear and extinction. *Psychopharmacology*, *236*(1), 313–320. https://doi.org/10.1007/s00213-018-5033-2

Maren, S. (2001). Neurobiology of Pavlovian Fear Conditioning. *Annual Review of Neuroscience, 24*(1), 897–931. https://doi.org/10.1146/annurev.neuro.24.1.897

Maren, S., Phan, K. L., & Liberzon, I. (2013). The contextual brain: implications for fear conditioning, extinction and psychopathology. *Nature Reviews. Neuroscience, 14*(6), 417–428. https://doi.org/10.1038/nrn3492

Martinez, R. C., Carvalho-Netto, E. F., Ribeiro-Barbosa, É. R., Baldo, M. V. C., & Canteras, N.

S. (2011). Amygdalar roles during exposure to a live predator and to a predator-associated context. *Neuroscience*, *172*, 314–328. https://doi.org/10.1016/j.neuroscience.2010.10.033

Matzeu, A., Cauvi, G., Kerr, T. M., Weiss, F., & Martin-Fardon, R. (2017). The paraventricular nucleus of the thalamus is differentially recruited by stimuli conditioned to the availability of cocaine versus palatable food. *Addiction Biology*, *22*(1), 70–77. https://doi.org/10.1111/adb.12280

McDonald, A. J. (1991a). Organization of amygdaloid projections to the prefrontal cortex and associated striatum in the rat. *Neuroscience*, *44*(1), 1–14. https://doi.org/10.1016/0306-4522(91)90247-L

McDonald, A. J. (1991b). Topographical organization of amygdaloid projections to the caudatoputamen, nucleus accumbens, and related striatal-like areas of the rat brain. *Neuroscience*, *44*(1), 15–33. https://doi.org/10.1016/0306-4522(91)90248-M

McDonald, A. J. (1998). Cortical pathways to the mammalian amygdala. *Progress in Neurobiology*, *55*(3), 257–332. https://doi.org/10.1016/S0301-0082(98)00003-3

McDonald, A. J. (2006). Is There an Amygdala and How Far Does It Extend? *Annals of the New York Academy of Sciences*, *985*(1), 1–21. https://doi.org/10.1111/j.1749-6632.2003.tb07067.x

Menard, J., & Treit, D. (1996). Lateral and medial septal lesions reduce anxiety in the plus-maze and probe-burying tests. *Physiology & Behavior*, *60*(3), 845–853. https://doi.org/10.1016/S0031-9384(96)00138-2

Méndez-Ruette, M., Linsambarth, S., Moraga-Amaro, R., Quintana-Donoso, D., Méndez, L., Tamburini, G., … Stehberg, J. (2019). The role of the rodent insula in anxiety. *Frontiers in Physiology*, *10*(MAR), 1–10. https://doi.org/10.3389/fphys.2019.00330

Meshul, C. K., & McGinty, J. F. (2000). Kappa opioid receptor immunoreactivity in the nucleus accumbens and caudate-putamen is primarily associated with synaptic vesicles in axons. *Neuroscience*, *96*(1), 91–99. https://doi.org/10.1016/S0306-4522(99)90481-5

Mesulam, M. M. (2000). Behavioral Neuroanatomy. In *Principles of Behavioral and Cognitive Neurology*. Oxford University Press.

Mikkelsen, J. D. D., Larsen, P. J. J., O'Hare, M. M. T. M. T., & Wiegand, S. J. J. (1991). Gastrin releasing peptide in the rat suprachiasmatic nucleus: An immunohistochemical, chromatographic and radioimmunological study. *Neuroscience*, *40*(1), 55–66. https://doi.org/10.1016/0306-4522(91)90174-M

Mikula, S., Trotts, I., Stone, J. M., & Jones, E. G. (2007). Internet-enabled high-resolution brain mapping and virtual microscopy. *NeuroImage*, *35*(1), 9–15. https://doi.org/10.1016/j.neuroimage.2006.11.053

Milad, M. R., & Quirk, G. J. (2002). Neurons in medial prefrontal cortex signal memory for fear extinction. *Nature*, *420*(6911), 70–74. https://doi.org/10.1038/nature01138

Minami, M., Toya, T., Katao, Y., Maekawa, K., Nakamura, S., Onogi, T., … Satoh, M. (1993). Cloning and expression of a cDNA for the rat k -opioid receptor. *FEBS Letters*, *329*(3),

291–295. https://doi.org/10.1016/0014-5793(93)80240-U

Moga, M. M., Weis, R. P., & Moore, R. Y. (1995). Efferent projections of the paraventricular thalamic nucleus in the rat. *Journal of Comparative Neurology*, *359*(2), 221–238. https://doi.org/10.1002/cne.903590204

Morgan, M. A., Romanski, L. M., & LeDoux, J. E. (1993). Extinction of emotional learning: Contribution of medial prefrontal cortex. *Neuroscience Letters*, *163*(1), 109–113. https://doi.org/10.1016/0304-3940(93)90241-C

Morrow, B. A., Elsworth, J. D., Inglis, F. M., & Roth, R. H. (1999). An antisense oligonucleotide reverses the footshock-induced expression of Fos in the rat medial prefrontal cortex and the subsequent expression of conditioned fear-induced immobility. *Journal of Neuroscience*, *19*(13), 5666–5673. https://doi.org/10.1523/jneurosci.19-13-05666.1999

Motta, S. C., Goto, M., Gouveia, F. V., Baldo, M. V. C., Canteras, N. S., & Swanson, L. W. (2009). Dissecting the brain's fear system reveals the hypothalamus is critical for responding in subordinate conspecific intruders. *Proceedings of the National Academy of Sciences*, *106*(12), 4870–4875. https://doi.org/10.1073/pnas.0900939106

Murugan, M., Jang, H. J., Park, M., Miller, E. M., Cox, J., Taliaferro, J. P., … Witten, I. B. (2017). Combined Social and Spatial Coding in a Descending Projection from the Prefrontal Cortex. *Cell*, *171*(7), 1663-1677.e16. https://doi.org/10.1016/j.cell.2017.11.002

Myers, B., Mark Dolgas, C., Kasckow, J., Cullinan, W. E., & Herman, J. P. (2014). Central stress-integrative circuits: forebrain glutamatergic and GABAergic projections to the dorsomedial hypothalamus, medial preoptic area, and bed nucleus of the stria terminalis. Brain Structure and Function, 219(4), 1287–1303. https://doi.org/10.1007/s00429-013-0566-y

Myers, K. M., & Davis, M. (2007). Mechanisms of fear extinction. *Molecular Psychiatry*. https://doi.org/10.1038/sj.mp.4001939

Nakahara, K., Fukui, K., & Murakami, N. (2004). Involvement of thalamic paraventricular nucleus in the anticipatory reaction under food restriction in the rat. *Journal of Veterinary Medical Science*, *66*(10), 1297–1300. https://doi.org/10.1292/jvms.66.1297

Nam, H., Chandra, R., Francis, T. C., Dias, C., Cheer, J. F., & Lobo, M. K. (2019). Reduced nucleus accumbens enkephalins underlie vulnerability to social defeat stress. *Neuropsychopharmacology*, *44*(May), 1876–1885. https://doi.org/10.1038/s41386-019-0422-8

Nambu, T., Sakurai, T., Mizukami, K., Hosoya, Y., Yanagisawa, M., & Goto, K. (1999). Distribution of orexin neurons in the adult rat brain. *Brain Research*, *827*(1-2), 243–260. https://doi.org/10.1016/s0006-8993(99)01336-0

Nardou, R., Lewis, E. M., Rothhaas, R., Xu, R., Yang, A., Boyden, E., & Dölen, G. (2019). Oxytocin-dependent reopening of a social reward learning critical period with MDMA. *Nature*, *569*(7754), 116–120. https://doi.org/10.1038/s41586-019-1075-9

Neugebauer, V., Galhardo, V., Maione, S., & Mackey, S. C. (2009). Forebrain pain mechanisms. *Brain Research Reviews*, *60*(1), 226–242. https://doi.org/10.1016/j.brainresrev.2008.12.014

Neumann, I. D., & Slattery, D. A. (2016). Oxytocin in General Anxiety and Social Fear: A Translational Approach. *Biological Psychiatry*, *79*(3), 213–221. https://doi.org/10.1016/j.biopsych.2015.06.004

Oh, Y., Park, Y., Cho, J. H., Wu, H., Paulk, N. K., Liu, L. X., … Lin, M. Z. (2019). An orange calcium-modulated bioluminescent indicator for non-invasive activity imaging. *Nature Chemical Biology*, *15*(5), 433–436. https://doi.org/10.1038/s41589-019-0256-z

Öhman, A., & Mineka, S. (2001). Fears, phobias, and preparedness: Toward an evolved module of fear and fear learning. *Psychological Review*. https://doi.org/10.1037/0033-295X.108.3.483

Otake, K. (2005). Cholecystokinin and substance P immunoreactive projections to the paraventricular thalamic nucleus in the rat. *Neuroscience Research*, *51*(4), 383–394. https://doi.org/10.1016/j.neures.2004.12.009

Otake, K., & Nakamura, Y. (1998). Single midline thalamic neurons projecting to both the ventral striatum and the prefrontal cortex in the rat. *Neuroscience*. https://doi.org/10.1016/S0306-4522(98)00062-1

Otake, K., & Ruggiero, D. A. (1995). Monoamines and nitric oxide are employed by afferents engaged in midline thalamic regulation. *Journal of Neuroscience*, *15*(3 I), 1891–1911. https://doi.org/10.1523/jneurosci.15-03-01891.1995

Otis, J. M., Namboodiri, V. M. K., Matan, A. M., Voets, E. S., Mohorn, E. P., Kosyk, O., … Stuber, G. D. (2017). Prefrontal cortex output circuits guide reward seeking through divergent cue encoding. *Nature*, *543*(7643), 103–107. https://doi.org/10.1038/nature21376

Otis, J. M., Zhu, M., Namboodiri, V. M. K., Cook, C. A., Kosyk, O., Matan, A. M., … Stuber, G. D. (2019). Paraventricular Thalamus Projection Neurons Integrate Cortical and Hypothalamic Signals for Cue-Reward Processing. *Neuron*, *103*(3), 423-431.e4. https://doi.org/10.1016/j.neuron.2019.05.018

Padilla-Coreano, N., Bolkan, S. S., Pierce, G. M., Blackman, D. R., Hardin, W. D., Garcia-Garcia, A. L., … Gordon, J. A. (2016). Direct Ventral Hippocampal-Prefrontal Input Is Required for Anxiety-Related Neural Activity and Behavior. *Neuron*, *89*(4), 857–866. https://doi.org/10.1016/j.neuron.2016.01.011

Padilla-Coreano, N., Do-Monte, F. H., & Quirk, G. J. (2012). A time-dependent role of midline thalamic nuclei in the retrieval of fear memory. *Neuropharmacology*, *62*(1), 457–463. https://doi.org/10.1016/j.neuropharm.2011.08.037

Panksepp, J. (1998a). *Affective neuroscience: The foundations of human and animal emotions*. Oxford university press.

Panksepp, J. (1998b). The Sources of Fear and Anxiety in the Brain. In Affective Neuroscience. In *Affective neuroscience: The foundations of human and animal emotions* (pp. 206–208). Retrieved from http://ebookcentral.proquest.com/lib/spu/detail.action?docID=431176.

Pape, H. C., & Paré, D. (2010). Plastic Synaptic Networks of the Amygdala for the Acquisition, Expression, and Extinction of Conditioned Fear. *Physiological Reviews*, *90*(2), 419–463. https://doi.org/10.1152/physrev.00037.2009

Papp, E., Borhegyi, Z., Tomioka, R., Rockland, K. S., Mody, I., & Freund, T. F. (2012). Glutamatergic input from specific sources influences the nucleus accumbens-ventral pallidum information flow. Brain Structure and Function, 217(1), 37–48. https://doi.org/10.1007/s00429-011-0331-z

Paré, D., & Smith, Y. (1993). The intercalated cell masses project to the central and medial nuclei of the amygdala in cats. *Neuroscience*, *57*(4), 1077–1090. https://doi.org/10.1016/0306-4522(93)90050-P

Parent, A., Sato, F., Wu, Y., Gauthier, J., Lévesque, M., & Parent, M. (2000). Organization of the basal ganglia: the importance of axonal collateralization. *Trends in Neurosciences*, *23*, S20–S27. https://doi.org/10.1016/S1471-1931(00)00022-7

Parfitt, G. M., Nguyen, R., Bang, J. Y., Aqrabawi, A. J., Tran, M. M., Seo, D. K., … Kim, J. C. (2017). Bidirectional Control of Anxiety-Related Behaviors in Mice: Role of Inputs Arising from the Ventral Hippocampus to the Lateral Septum and Medial Prefrontal Cortex. *Neuropsychopharmacology*, *42*(8), 1715–1728. https://doi.org/10.1038/npp.2017.56

Park, K., & Chung, C. (2019). Systemic Cellular Activation Mapping of an Extinction-Impaired Animal Model. *Frontiers in Cellular Neuroscience*, *13*(March), 1–11. https://doi.org/10.3389/fncel.2019.00099

Parsons, M. P., Li, S., & Kirouac, G. J. (2006). The paraventricular nucleus of the thalamus as an interface between the orexin and CART peptides and the shell of the nucleus accumbens. *Synapse*, *59*(8), 480–490. https://doi.org/10.1002/syn.20264

Pati, S., Sood, A., Mukhopadhyay, S., & Vaidya, V. A. (2018). Acute pharmacogenetic activation of medial prefrontal cortex excitatory neurons regulates anxiety-like behaviour. *Journal of Biosciences*, *43*(1), 85–95. https://doi.org/10.1007/s12038-018-9732-y

Paxinos, G., & Watson, C. (2007). *The Rat Brain in Stereotaxic Coordinates*. *Elsevier Academic Press* (6th ed.). Academic Press. Retrieved from https://www.elsevier.com/books/the-rat-brain-in-stereotaxic-coordinates/paxinos/978-0-12-374121-9

Pearson, C., Janz, T., & Ali, J. (2013). *Mental and substance use disorders in Canada*. *Health Reports* (Vol. 9).

Pellow, S., Chopin, P., File, S. E., and Briley, M. (1985). Validation of open:closed arm entries in an elevated plus-maze as a measure of anxiety in the rat. *Journal of Neuroscience Methods*, *14*, 149–167. https://doi.org/10.1016/0165-0270(85)90031-7

Penzo, M. A., Robert, V., Tucciarone, J., De Bundel, D., Wang, M., Van Aelst, L., … Li, B. (2015). The paraventricular thalamus controls a central amygdala fear circuit. *Nature*, *519*(7544), 455–459. https://doi.org/10.1038/nature13978

Perusini, J. N., & Fanselow, M. S. (2015). Neurobehavioral perspectives on the distinction between fear and anxiety. *Learning and Memory*, *22*(9), 417–425. https://doi.org/10.1101/lm.039180.115

Petrovich, G. D. (2013). Forebrain networks and the control of feeding by environmental learned cues. *Physiology & Behavior*, *121*, 10–18. https://doi.org/10.1016/j.physbeh.2013.03.024

Petrovich, G. D., Risold, P. Y., & Swanson, L. W. (1996). Organization of projections from the basomedial nucleus of the amygdala: A PHAL study in the rat. *The Journal of Comparative Neurology*, *374*(3), 387–420. https://doi.org/10.1002/(SICI)1096-9861(19961021)374:3<387::AID-CNE6>3.0.CO;2-Y

Peyron, C., Tighe, D. K., Van Den Pol, A. N., De Lecea, L., Heller, H. C., Sutcliffe, J. G., & Kilduff, T. S. (1998). Neurons containing hypocretin (orexin) project to multiple neuronal systems. *Journal of Neuroscience*. https://doi.org/10.1523/jneurosci.18-23-09996.1998

Pliota, P., Böhm, V., Grössl, F., Griessner, J., Valenti, O., Kraitsy, K., … Haubensak, W. (2020). Stress peptides sensitize fear circuitry to promote passive coping. *Molecular Psychiatry*, *25*(2), 428–441. https://doi.org/10.1038/s41380-018-0089-2

Pomrenze, M. B., Tovar-Diaz, J., Blasio, A., Maiya, R., Giovanetti, S. M., Lei, K., … Messing, R. O. (2019). A corticotropin releasing factor network in the extended amygdala for anxiety. *Journal of Neuroscience*, *39*(6), 1030–1043. https://doi.org/10.1523/JNEUROSCI.2143-18.2018

Prensa, L., Giménez-Amaya, J. M., Parent, A., Bernácer, J., & Cebrián, C. (2009). The Nigrostriatal Pathway: Axonal Collateralization and Compartmental Specificity. In *Birth, Life and Death of Dopaminergic Neurons in the Substantia Nigra* (pp. 49–58). Vienna: Springer Vienna. https://doi.org/10.1007/978-3-211-92660-4_4

Quirk, G. J., Garcia, R., & González-Lima, F. (2006). Prefrontal Mechanisms in Extinction of Conditioned Fear. *Biological Psychiatry*, *60*(4), 337–343. https://doi.org/10.1016/j.biopsych.2006.03.010

Quirk, G. J., Likhtik, E., Pelletier, J. G., & Paré, D. (2003). Stimulation of medial prefrontal cortex decreases the responsiveness of central amygdala output neurons. *Journal of Neuroscience*, *23*(25), 8800–8807. https://doi.org/10.1523/jneurosci.23-25-08800.2003

Radulovic, J., Rühmann, A., Liepold, T., & Spiess, J. (1999). Modulation of learning and anxiety by corticotropin-releasing factor (CRF) and stress: Differential roles of CRF receptors 1 and 2. *The Journal of Neuroscience*, *19*(12), 5016–5025. https://doi.org/10.1523/JNEUROSCI.19-12-05016.1999

Ranganath, C., & Ritchey, M. (2012). Two cortical systems for memory-guided behaviour. *Nature Reviews Neuroscience*, *13*(10), 713–726. https://doi.org/10.1038/nrn3338

Reed, M. D., Hildebrand, D. G. C., Santangelo, G., Moffa, A., Pira, A. S., Rycyna, L., … Stellar, J. R. (2015). Assessing contributions of nucleus accumbens shell subregions to reward-seeking behavior. *Drug and Alcohol Dependence*, *153*, 369–373. https://doi.org/10.1016/j.drugalcdep.2015.05.001

Reichard, R. A., Subramanian, S., Desta, M. T., Sura, T., Becker, M. L., Ghobadi, C. W., … Zahm, D. S. (2017). Abundant collateralization of temporal lobe projections to the accumbens, bed nucleus of stria terminalis, central amygdala and lateral septum. *Brain Structure and Function*, *222*(4), 1971–1988. https://doi.org/10.1007/s00429-016-1321-y

Ren, S., Wang, Y., Yue, F., Cheng, X., Dang, R., Qiao, Q., … Hu, Z. (2018). The paraventricular thalamus is a critical thalamic area for wakefulness. *Science*, *362*(6413), 429–434.

https://doi.org/10.1126/science.aat2512

Ressler, K. J., & Mayberg, H. S. (2007). Targeting abnormal neural circuits in mood and anxiety disorders: From the laboratory to the clinic. *Nature Neuroscience*, *10*(9), 1116–1124. https://doi.org/10.1038/nn1944

Reynolds, S. M., & Berridge, K. C. (2001). Fear and feeding in the nucleus accumbens shell: Rostrocaudal segregation of GABA-elicited defensive behavior versus eating behavior. *Journal of Neuroscience*, *21*(9), 3261–3270.

Reynolds, S. M., & Berridge, K. C. (2002). Positive and negative motivation in nucleus accumbens shell: Bivalent rostrocaudal gradients for GABA-elicited eating, taste "liking"/"disliking" reactions, place preference/avoidance, and fear. *Journal of Neuroscience*, *22*(16), 7308–7320.

Reynolds, S. M., & Berridge, K. C. (2008). Emotional environments retune the valence of appetitive versus fearful functions in nucleus accumbens. *Nature Neuroscience*, *11*(4), 423–425. https://doi.org/10.1038/nn2061

Richardson, N. R., & Roberts, D. C. S. (1996). Progressive ratio schedules in drug self-administration studies in rats: A method to evaluate reinforcing efficacy. *Journal of Neuroscience Methods*. https://doi.org/10.1016/0165-0270(95)00153-0

Richter, T. A. (2005). Low Voltage-Activated Ca2+ Channels Are Coupled to Ca2+-Induced Ca2+ Release in Rat Thalamic Midline Neurons. *Journal of Neuroscience*, *25*(36), 8267–8271. https://doi.org/10.1523/JNEUROSCI.1942-05.2005

Risold, P. Y., & Swanson, L. W. (1996). Structural Evidence for Functional Domains in the Rat Hippocampus. *Science*, *272*(5267), 1484–1486. https://doi.org/10.1126/science.272.5267.1484

Risold, P. Y., & Swanson, L. W. (1997). Connections of the rat lateral septal complex. *Brain Research Reviews*, *24*(2–3), 115–195. https://doi.org/10.1016/S0165-0173(97)00009-X

Risold, P. Y., Thompson, R. H., & Swanson, L. W. (1997). The structural organization of connections between hypothalamus and cerebral cortex. *Brain Research Reviews*, *24*(2–3), 197–254. https://doi.org/10.1016/S0165-0173(97)00007-6

Rizvi, T. A., Ennis, M., Behbehani, M. M., & Shipley, M. T. (1991). Connections between the central nucleus of the amygdala and the midbrain periaqueductal gray: Topography and reciprocity. *Journal of Comparative Neurology*, *303*(1), 121–131. https://doi.org/10.1002/cne.903030111

Rosen, J. B., Hitchcock, J. M., Miserendino, M. J. D., Falls, W. A., Campeau, S., & Davis, M. (1992). Lesions of the perirhinal cortex but not of the frontal, medial prefrontal, visual, or insular cortex block fear-potentiated startle using a visual conditioned stimulus. *Journal of Neuroscience*. https://doi.org/10.1523/jneurosci.12-12-04624.1992

Roth, B. L. (2016). DREADDs for Neuroscientists. *Neuron*, *89*(4), 683–694. https://doi.org/10.1016/j.neuron.2016.01.040

Royer, S., Martina, M., & Paré, D. (1999). An inhibitory interface gates impulse traffic between

the input and output stations of the amygdala. *The Journal of Neuroscience : The Official Journal of the Society for Neuroscience*, *19*(23), 10575–10583. https://doi.org/10.1523/jneurosci.19-23-10575.1999

Sakurai, T., Amemiya, A., Ishii, M., Matsuzaki, I., Chemelli, R. M., Tanaka, H., … Yanagisawa, M. (1998). Orexins and Orexin Receptors: A Family of Hypothalamic Neuropeptides and G Protein-Coupled Receptors that Regulate Feeding Behavior. *Cell*, *92*(4), 573–585. https://doi.org/10.1016/S0092-8674(00)80949-6

Salamone, J. D., & Correa, M. (2018). Neurobiology and pharmacology of activational and effort-related aspects of motivation: rodent studies. *Current Opinion in Behavioral Sciences*, *22*, 114–120. https://doi.org/10.1016/j.cobeha.2018.01.026

Sanford, C. A., Soden, M. E., Baird, M. A., Miller, S. M., Schulkin, J., Palmiter, R. D., … Zweifel, L. S. (2017). A Central Amygdala CRF Circuit Facilitates Learning about Weak Threats. *Neuron*, *93*(1), 164–178. https://doi.org/10.1016/j.neuron.2016.11.034

Saper, C. B. (1982). Convergence of autonomic and limbic connections in the insular cortex of the rat. *Journal of Comparative Neurology*, *210*(2), 163–173. https://doi.org/10.1002/cne.902100207

Saper, C. B., & Stornetta, R. L. (2015). Central Autonomic System. In *The Rat Nervous System* (pp. 629–673). Elsevier. https://doi.org/10.1016/B978-0-12-374245-2.00023-1

Sarhan, M., Freund-Mercier, M. J., & Veinante, P. (2005). Branching patterns of parabrachial neurons projecting to the central extended amgydala: Single axonal reconstructions. *Journal of Comparative Neurology*, *491*(4), 418–442. https://doi.org/10.1002/cne.20697

Schoenfeld, T. J., Kloth, A. D., Hsueh, B., Runkle, M. B., Kane, G. A., Wang, S. S. H., & Gould, E. (2014). Gap junctions in the ventral hippocampal-medial prefrontal pathway are involved in anxiety regulation. *Journal of Neuroscience*. https://doi.org/10.1523/JNEUROSCI.3234-13.2014

Senn, V., Wolff, S. B. E., Herry, C., Grenier, F., Ehrlich, I., Gründemann, J., … Lüthi, A. (2014). Long-range connectivity defines behavioral specificity of amygdala neurons. *Neuron*, *81*(2), 428–437. https://doi.org/10.1016/j.neuron.2013.11.006

Shah, A. A., Sjovold, T., & Treit, D. (2004). Inactivation of the medial prefrontal cortex with the GABAA receptor agonist muscimol increases open-arm activity in the elevated plus-maze and attenuates shock-probe burying in rats. *Brain Research*, *1028*(1), 112–115. https://doi.org/10.1016/j.brainres.2004.08.061

Shi, T. Y., Feng, S. F., Wei, M. X., Huang, Y., Liu, G., Wu, H. T., … Zhou, W. X. (2018). Kainate receptor mediated presynaptic LTP in agranular insular cortex contributes to fear and anxiety in mice. *Neuropharmacology*, *128*, 388–400. https://doi.org/10.1016/j.neuropharm.2017.10.037

Siegmund, A., & Wotjak, C. T. (2007). Hyperarousal does not depend on trauma-related contextual memory in an animal model of Posttraumatic Stress Disorder. *Physiology and Behavior*, *90*(1), 103–107. https://doi.org/10.1016/j.physbeh.2006.08.032

Sierra-Mercado, D., Padilla-Coreano, N., & Quirk, G. J. (2011). Dissociable roles of prelimbic

and infralimbic cortices, ventral hippocampus, and basolateral amygdala in the expression and extinction of conditioned fear. *Neuropsychopharmacology : Official Publication of the American College of Neuropsychopharmacology*, *36*(2), 529–538. https://doi.org/10.1038/npp.2010.184

Silva, B. A., Gross, C. T., & Gräff, J. (2016). The neural circuits of innate fear: Detection, integration, action, and memorization. *Learning and Memory*, *23*(10), 544–555. https://doi.org/10.1101/lm.042812.116

Silva, B. A., Mattucci, C., Krzywkowski, P., Murana, E., Illarionova, A., Grinevich, V., … Gross, C. T. (2013). Independent hypothalamic circuits for social and predator fear. *Nature Neuroscience*, *16*(12), 1731–1733. https://doi.org/10.1038/nn.3573

Soares-Cunha, C., de Vasconcelos, N. A. P., Coimbra, B., Domingues, A. V., Silva, J. M., Loureiro-Campos, E., … Rodrigues, A. J. (2019). Nucleus accumbens medium spiny neurons subtypes signal both reward and aversion. *Molecular Psychiatry*. https://doi.org/10.1038/s41380-019-0484-3

Sofroniew, M. V., & Weind, A. (1978). Extrahypothalamic neurophysin-containing perikarya, fiber pathways and fiber clusters in the rat brain. *Endocrinology*. https://doi.org/10.1210/endo-102-1-334

Sotres-Bayon, F., & Quirk, G. J. (2010). Prefrontal control of fear: More than just extinction. *Current Opinion in Neurobiology*, *20*(2), 231–235. https://doi.org/10.1016/j.conb.2010.02.005

Steimer, T. (2002). The biology of fear- and anxiety-related behaviors. *Dialogues in Clinical Neuroscience*, *4*(3), 231–249.

Stein, D. J., Scott, K. M., de Jonge, P., & Kessler, R. C. (2017). Epidemiology of anxiety disorders: from surveys to nosology and back. *Dialogues in Clinical Neuroscience*, *19*(2), 127–136. https://doi.org/10.1038/jid.2015.269

Steinman, M. Q., Duque-Wilckens, N., & Trainor, B. C. (2019). Complementary Neural Circuits for Divergent Effects of Oxytocin: Social Approach Versus Social Anxiety. *Biological Psychiatry*, *85*(10), 792–801. https://doi.org/10.1016/j.biopsych.2018.10.008

Su, H.-S., & Bentivoglio, M. (1990). Thalamic midline cell populations projecting to the nucleus accumbens, amygdala, and hippocampus in the rat. *The Journal of Comparative Neurology*, *297*(4), 582–593. https://doi.org/10.1002/cne.902970410

Sukikara, M. H., Mota-Ortiz, S. R., Baldo, M. V., Felicio, L. F., & Canteras, N. S. (2010). The periaqueductal gray and its potential role in maternal behavior inhibition in response to predatory threats. *Behavioural Brain Research*, *209*(2), 226–233. https://doi.org/10.1016/j.bbr.2010.01.048

Suzuki, M., Beuckmann, C. T., Shikata, K., Ogura, H., & Sawai, T. (2005). Orexin-A (hypocretin-1) is possibly involved in generation of anxiety-like behavior. *Brain Research*. https://doi.org/10.1016/j.brainres.2005.03.002

Swanson, L. W. (2000). Cerebral hemisphere regulation of motivated behavior. *Brain Research*, *886*, 113–164.

Swanson, L. W. (2003). The amygdala and its place in the cerebral hemisphere. *Annals of the New York Academy of Sciences*, *985*(1), 174–184. https://doi.org/10.1111/j.1749-6632.2003.tb07081.x

Tepper, J. M., Koós, T., Ibanez-Sandoval, O., Tecuapetla, F., Faust, T. W., & Assous, M. (2018). Heterogeneity and Diversity of Striatal GABAergic Interneurons: Update 2018. *Frontiers in Neuroanatomy*, *12*. https://doi.org/10.3389/fnana.2018.00091

Thompson, B. M., Baratta, M. V., Biedenkapp, J. C., Rudy, J. W., Watkins, L. R., & Maier, S. F. (2010). Activation of the infralimbic cortex in a fear context enhances extinction learning. *Learning & Memory*, *17*(11), 591–599. https://doi.org/10.1101/lm.1920810

Timofeeva, E., & Richard, D. (2001). Activation of the central nervous system in obese Zucker rats during food deprivation. *The Journal of Comparative Neurology*, *441*(1), 71–89. https://doi.org/10.1002/cne.1398

Toth, I., & Neumann, I. D. (2013). Animal models of social avoidance and social fear. *Cell and Tissue Research*. https://doi.org/10.1007/s00441-013-1636-4

Tovote, P., Fadok, J. P., & Lüthi, A. (2015). Neuronal circuits for fear and anxiety. *Nature Reviews. Neuroscience*, *16*(6), 317–331. https://doi.org/10.1038/nrn3945

Trent, N. L., & Menard, J. L. (2010). The ventral hippocampus and the lateral septum work in tandem to regulate rats' open-arm exploration in the elevated plus-maze. *Physiology & Behavior*, *101*(1), 141–152. https://doi.org/10.1016/j.physbeh.2010.04.035

Tripathi, A., Prensa, L., Cebrían, C., & Mengual, E. (2010). Axonal branching patterns of nucleus accumbens neurons in the rat. *Journal of Comparative Neurology*, *518*(22), 4649–4673. https://doi.org/10.1002/cne.22484

Tye, K. M., Prakash, R., Kim, S. Y., Fenno, L. E., Grosenick, L., Zarabi, H., … Deisseroth, K. (2011). Amygdala circuitry mediating reversible and bidirectional control of anxiety. *Nature*, *471*(7338), 358–362. https://doi.org/10.1038/nature09820

Unzai, T., Kuramoto, E., Kaneko, T., & Fujiyama, F. (2017). Quantitative Analyses of the Projection of Individual Neurons from the Midline Thalamic Nuclei to the Striosome and Matrix Compartments of the Rat Striatum. *Cerebral Cortex*, *27*(2), 1164–1181. https://doi.org/10.1093/cercor/bhv295

Urban, D. J., & Roth, B. L. (2015). DREADDs (Designer Receptors Exclusively Activated by Designer Drugs): Chemogenetic Tools with Therapeutic Utility. *Annual Review of Pharmacology and Toxicology*, *55*(1), 399–417. https://doi.org/10.1146/annurev-pharmtox-010814-124803

van den Burg, E. H., & Stoop, R. (2019). Neuropeptide signalling in the central nucleus of the amygdala. *Cell and Tissue Research*, *375*(1), 93–101. https://doi.org/10.1007/s00441-018-2862-6

van der Werf, Y. D., Witter, M. P., & Groenewegen, H. J. (2002). *The intralaminar and midline nuclei of the thalamus. Anatomical and functional evidence for participation in processes of arousal and awareness*. *Brain Research Reviews* (Vol. 39). https://doi.org/10.1016/S0165-0173(02)00181-9

van Strien, N. M., Cappaert, N. L. M., & Witter, M. P. (2009). The anatomy of memory: an interactive overview of the parahippocampal–hippocampal network. *Nature Reviews Neuroscience*, *10*(4), 272–282. https://doi.org/10.1038/nrn2614

Vertes, R. P. (2004). Differential projections of the infralimbic and prelimbic cortex in the rat. *Synapse*, *51*(1), 32–58. https://doi.org/10.1002/syn.10279

Vertes, R. P., & Hoover, W. B. (2008). Projections of the paraventricular and paratenial nuclei of the dorsal midline thalamus in the rat. *The Journal of Comparative Neurology*, *508*(2), 212–237. https://doi.org/10.1002/cne.21679

Vertes, R. P., Linley, S. B., Groenewegen, H. J., & Witter, M. P. (2015). Thalamus. In G. Paxinos (Ed.), *The Rat Nervous System* (4th ed., pp. 335–390). Elsevier. https://doi.org/10.1016/B978-0-12-374245-2.00016-4

Vertes, R. P., Linley, S. B., & Hoover, W. B. (2015). Limbic circuitry of the midline thalamus. *Neuroscience and Biobehavioral Reviews*, *54*, 89–107. https://doi.org/10.1016/j.neubiorev.2015.01.014

Viviani, D., Charlet, A., van den Burg, E., Robinet, C., Hurni, N., Abatis, M., … Stoop, R. (2011). Oxytocin Selectively Gates Fear Responses Through Distinct Outputs from the Central Amygdala. *Science*, *333*(6038), 104–107. https://doi.org/10.1126/science.1201043

Wacker, J., Dillon, D. G., & Pizzagalli, D. A. (2009). The role of the nucleus accumbens and rostral anterior cingulate cortex in anhedonia: integration of resting EEG, fMRI, and volumetric techniques. *NeuroImage*, *46*(1), 327–337. https://doi.org/10.1016/j.neuroimage.2009.01.058

Wang, G.-Q., Cen, C., Li, C., Cao, S., Wang, N., Zhou, Z., … Wang, Y. (2015). Deactivation of excitatory neurons in the prelimbic cortex via Cdk5 promotes pain sensation and anxiety. *Nature Communications*, *6*(1), 7660. https://doi.org/10.1038/ncomms8660

Wang, D. V., Wang, F., Liu, J., Zhang, L., Wang, Z., & Lin, L. (2011). Neurons in the amygdala with response-selectivity for anxiety in two ethologically based tests. *PLoS ONE*, *6*(4), 1–7. https://doi.org/10.1371/journal.pone.0018739

Watts, A. G., & Swanson, L. W. (1987). Efferent projections of the suprachiasmatic nucleus: II. Studies using retrograde transport of fluorescent dyes and simultaneous peptide immunohistochemistry in the rat. *Journal of Comparative Neurology*. https://doi.org/10.1002/cne.902580205

Winrow, C. J., Tanis, K. Q., Reiss, D. R., Rigby, A. M., Uslaner, J. M., Uebele, V. N., … Renger, J. J. (2010). Orexin receptor antagonism prevents transcriptional and behavioral plasticity resulting from stimulant exposure. *Neuropharmacology*. https://doi.org/10.1016/j.neuropharm.2009.07.008

Winsky-Sommerer, R., Yamanaka, A., Diano, S., Borok, E., Roberts, A. J., Sakurai, T., … De Lecea, L. (2004). Interaction between the corticotropin-releasing factor system and hypocretins (orexins): A novel circuit mediating stress response. *Journal of Neuroscience*. https://doi.org/10.1523/JNEUROSCI.3459-04.2004

Witter, M. P., Doan, T. P., Jacobsen, B., Nilssen, E. S., & Ohara, S. (2017). Architecture of the

entorhinal cortex a review of entorhinal anatomy in rodents with some comparative notes. *Frontiers in Systems Neuroscience*, *11*(June), 1–12. https://doi.org/10.3389/fnsys.2017.00046

Wright, C. I., Beijer, A. V. J., & Groenewegen, H. J. (1996). Basal amygdaloid complex afferents to the rat nucleus accumbens are compartmentally organized. *The Journal of Neuroscience*, *16*(5), 1877–1893. https://doi.org/10.1523/JNEUROSCI.16-05-01877.1996

Wright, C. I., & Groenewegen, H. J. (1995). Patterns of convergence and segregation in the medial nucleus accumbens of the rat: Relationships of prefrontal cortical, midline thalamic, and basal amygdaloid afferents. *The Journal of Comparative Neurology*, *361*(3), 383–403. https://doi.org/10.1002/cne.903610304

Wright, C. I., & Groenewegen, H. J. (1996). Patterns of overlap and segregation between insular cortical, intermediodorsal thalamic and basal amygdaloid afferents in the nucleus accumbens of the rat. *Neuroscience*, *73*(2), 359–373. https://doi.org/10.1016/0306-4522(95)00592-7

Wunsch, A. M., Yager, L. M., Donckels, E. A., Le, C. T., Neumaier, J. F., & Ferguson, S. M. (2017). Chemogenetic inhibition reveals midline thalamic nuclei and thalamo-accumbens projections mediate cocaine-seeking in rats. *European Journal of Neuroscience*, *46*(3), 1850–1862. https://doi.org/10.1111/ejn.13631

Xiu, J., Zhang, Q., Zhou, T. T. T. T. T., Zhou, T. T. T. T. T., Chen, Y., & Hu, H. (2014). Visualizing an emotional valence map in the limbic forebrain by TAI-FISH. *Nature Neuroscience*, *17*(11), 1552–1559. https://doi.org/10.1038/nn.3813

Xu, C., Krabbe, S., Gründemann, J., Botta, P., Fadok, J. P., Osakada, F., … Lüthi, A. (2016). Distinct Hippocampal Pathways Mediate Dissociable Roles of Context in Memory Retrieval. *Cell*, *167*(4), 961-972.e16. https://doi.org/10.1016/j.cell.2016.09.051

Yasoshima, Y., Scott, T. R., & Yamamoto, T. (2007). Differential activation of anterior and midline thalamic nuclei following retrieval of aversively motivated learning tasks. *Neuroscience*, *146*(3), 922–930. https://doi.org/10.1016/j.neuroscience.2007.02.044

Ye, J., & Veinante, P. (2019). Cell-type specific parallel circuits in the bed nucleus of the stria terminalis and the central nucleus of the amygdala of the mouse. *Brain Structure and Function*, *224*(3), 1067–1095. https://doi.org/10.1007/s00429-018-01825-1

Yeoh, J. W., James, M. H., Graham, B. A., & Dayas, C. V. (2014). Electrophysiological characteristics of paraventricular thalamic (PVT) neurons in response to cocaine and cocaine- and amphetamine-regulated transcript (CART). *Frontiers in Behavioral Neuroscience*, *8*, 280. https://doi.org/10.3389/fnbeh.2014.00280

Zahm, D. S. (1998). Is the caudomedial shell of the nucleus accumbens part of the extended amygdala? A consideration of connections. *Critical Reviews in Neurobiology*. https://doi.org/10.1615/CritRevNeurobiol.v12.i3.50

Zahm, D. S. (2000). An integrative neuroanatomical perspective on some subcortical substrates of adaptive responding with emphasis on the nucleus accumbens. *Neuroscience and Biobehavioral Reviews*, *24*(1), 85–105. https://doi.org/10.1016/S0149-7634(99)00065-2

Zahm, D. S. (2006). The evolving theory of basal forebrain functional - Anatomical "macrosystems." *Neuroscience and Biobehavioral Reviews*, *30*(2), 148–172. https://doi.org/10.1016/j.neubiorev.2005.06.003

Zahm, D. S., & Brog, J. S. (1992). On the significance of subterritories in the "accumbens" part of the rat ventral striatum. *Neuroscience*, *50*(4), 751–767. https://doi.org/10.1016/0306-4522(92)90202-D

Zahm, D. S., & Heimer, L. (1993). Specificity in the efferent projections of the nucleus accumbens in the rat: Comparison of the rostral pole projection patterns with those of the core and shell. *Journal of Comparative Neurology*, *327*(2), 220–232. https://doi.org/10.1002/cne.903270205

Zhang, L., Renaud, L. P., & Kolaj, M. (2009). Properties of a T-Type Ca 2+ Channel–Activated Slow Afterhyperpolarization in Thalamic Paraventricular Nucleus and Other Thalamic Midline Neurons. *Journal of Neurophysiology*, *101*(6), 2741–2750. https://doi.org/10.1152/jn.91183.2008

Zhang, X., & van den Pol, A. N. (2017). Rapid binge-like eating and body weight gain driven by zona incerta GABA neuron activation. *Science*, *356*(6340), 853–859. https://doi.org/10.1126/science.aam7100

Zhou, L., Furuta, T., & Kaneko, T. (2003). Chemical organization of projection neurons in the rat accumbens nucleus and olfactory tubercle. *Neuroscience*, *120*(3), 783–798. https://doi.org/10.1016/S0306-4522(03)00326-9

Zhu, Y., Nachtrab, G., Keyes, P. C., Allen, W. E., Luo, L., & Chen, X. (2018). Dynamic salience processing in paraventricular thalamus gates associative learning. *Science*, *362*(6413), 423–429. https://doi.org/10.1126/science.aat0481

Zhu, Y., Wienecke, C. F. R., Nachtrab, G., & Chen, X. (2016). A thalamic input to the nucleus accumbens mediates opiate dependence. *Nature*, *530*(7589), 219–222. https://doi.org/10.1038/nature16954